Papers Presented To The

Conference On Luna 24

Houston, Texas
1-3 December 1977

A Lunar Science Institute Topical Conference

Universities Space Research Association
The Lunar Science Institute
3303 NASA Road 1
Houston, Texas 77058

PAPERS PRESENTED TO THE

CONFERENCE ON LUNA 24

A LUNAR SCIENCE INSTITUTE TOPICAL CONFERENCE

1-3 DECEMBER 1977

Compiled by

The Lunar Science Institute

3303 NASA Road 1

Houston, Texas 77058

LSI CONTRIBUTION 304

PREFACE

This volume contains papers which have been accepted for publication by the Program Committee of the Conference on Luna 24. Papers were solicited which address one of the following major topics:

I. Mare Crisium and the Luna 24 landing site: Regional geology, geochemistry, and geophysics

II. Petrology, mineral chemistry, and cooling histories of the lithic fragments in Luna 24 samples

III. Chemistry, isotopic studies and geochronology of Luna 24 samples

IV. Regolith studies of the Luna 24 soil samples

The Program Committee consists of A. L. Albee (*California Institute of Technology*), T. R. McGetchin (*Lunar Science Institute*), D. S. McKay (*Johnson Space Center*), R. B. Merrill (*Lunar Science Institute*), L. E. Nyquist (*Johnson Space Center*), J. J. Papike, Chairman, (*State University of New York*), C. Pieters (*Johnson Space Center*), and P. H. Schultz (*Lunar Science Institute*).

Logistic and administrative support for this conference has been provided by P. P. Jones (*Administrative Assistant, Lunar Science Institute*). This abstract volume has been prepared under the supervision of P. C. Robertson (*Technical Assistant, Lunar Science Institute*).

Papers are arranged alphabetically by the name of the first author. An index lists papers which were submitted to address each of the four topics. Additional indices by author and subject are included.

The Lunar Science Institute is operated by the Universities Space Research Association under contract No. NSR 09-051-001 with the National Aeronautics and Space Administration.

TABLE OF CONTENTS

INDICES

SPECTRAL REFLECTANCE OF LUNA 24 SOILS

John B. Adams and Russell L. Ralph, Department of Geological Sciences, University of Washington, Seattle, Washington, 98195

Visible and near infrared (0.35 μm to 2.5 μm) diffuse reflectance spectra were measured of five samples of lunar soils returned by the Soviet unmanned spacecraft Luna 24. Reflectance measurements were made on <90 μm sieved fractions of samples 24077,27, 24109,21, 24149,23, 24174,18, and 24182,27, each weighing <0.050g. Spectra were obtained with a Beckman DK-2A spectroreflectometer, using an integrating sphere and MgO as a reference. The MgO reference was corrected for water absorption and drift by comparison with Au and Pd standards.

Reflectance spectra of Luna 24 soils are shown in Figure 1 and are compared with spectra of Apollo 11 and Apollo 12 mare soils. The Luna 24 samples have low "albedos", as measured by the intensity of reflectance at 0.56 μm: 24109 (.102); 24174 (.113); 24077 (.130); 24182 (.139); 24149 (.139). These reflectance intensities bracket the values for Apollo 11, 12 and 17 mare soils. Low reflectance is correlated with high FeO in lunar soils, and the Luna 24 samples are consistent with this trend.

Despite their low reflectance the Luna 24 samples show unusually deep absorption bands near 1 μm and 2 μm (Figures 1 and 2). The 1 μm feature is a composite of Fe^{2+} absorption in pyroxene near 0.95 μm and Fe^{2+} absorption in glass (mainly in agglutinates) near 1.0 μm. The 2 μm feature is primarily due to Fe^{2+} in pyroxene. A weaker feature at 1.25 μm is contributed by Fe^{2+} in calcic plagioclase. Below about 0.5 μm, and extending to shorter wavelengths, multiple bands involving titanium and iron charge-transfers coalesce to give a UV absorption feature.

The above absorption bands occur in the spectra of most lunar soils; however, the Luna 24 samples are unique in having the deepest bands yet measured. Such strong spectral contrast has been observed previously only in the spectra of lunar rocks and breccias, which are free of agglutinates. Luna 24 soils, nevertheless, exhibit the steep positive continuum slope and the low integral reflectance that are typical for soils.

The combination of high FeO (which gives low reflectance) and deep absorption bands separates the Luna 24 samples in a plot of FeO vs the depth of the 1 μm band (Figure 2). Other Apollo mare soils have 1 μm band depths <11%, with the exception of the unusually pyroxene-rich soil at the edge of Hadley rille (station 9a) at the Apollo 15 site, which can be distinguished from the Luna samples by its low (7.1) UV slope. In Figure 2 the Apollo 11 and 17 dark mare soils all cluster at low band-depths, and have high FeO and high TiO_2. In Figure 2 the TiO_2 content of the mare soils decreases as band depth increases. A graph similar to Figure 2 occurs for FeO vs the depth of the absorption band near 2 μm.

The strong spectral contrast of Luna 24 soils also produces large values for the slope of the curve between 0.40 μm and 0.56 μm. We define the slope

SPECTRAL REFLECTANCE OF LUNA 24 SOILS

Adams, J.B.

$$M = \frac{I_{.56} - I_{.40}}{.16\mu m\ I_{.56}} \times 10^4$$

Calculated UV slopes for Luna 24 soils range from 11.3 (24077 and 24149) to 14.8 (24182). The lowest slope we have measured is 4.5 for Apollo 17 soil 71061. Other Ti and Fe-rich soils have low slopes (flatter curves) as was pointed out by Charette et al. (1) (It should be noted that UV slopes calculated by Pieters et al. (2) for telescopic relative curves are opposite in sign to slopes presented here.)

Based on other lunar soil samples that we have measured, UV slopes that are >10 occur uniquely for soils with 0.5 to 1.8% TiO_2, in good agreement with the Luna 24 values of about 1% TiO_2. Significantly, the telescopic spectra of the Luna 24 landing area (Pieters et al. (2,3) do not show the unusually steep UV slope that is seen for the samples. The apparent discrepancy between the 2-4% TiO_2 predicted by Pieters et al. (2) for Luna 24 on the basis of the slope of the telescopic curve and the 1% TiO_2 in the returned samples, suggests that the samples are not representative of surface soils at the nominal landing site as observed on a scale of kilometers. Pieters et al. (2), however, noted a very low (<1.5%) TiO_2 mare unit 100 km north of the landing site that corresponds closely in spectral properties (high UV slope, low albedo) to the Luna 24 samples.

In conclusion, the Luna 24 samples are unique in their spectral reflectance properties compared with soils returned by all other missions. Luna 24 samples have unusually low albedos, deep absorption bands, and steep UV slopes. These properties, in combination, apparently are diagnostic of soils with very low TiO_2 and high FeO. Thus, the spectral "signature" of soils formed on low TiO_2 basalts should facilitate mapping by spectral reflectance techniques.

References:

(1) Charette, M.P., T.B. McCord, C. Pieters, and J.B. Adams (1974) J. Geophys. Res., 79, 1605-1613

(2) Pieters, C., T.B. McCord, and J.B. Adams (1976) Geophys. Res. Letters, 3, 697-700.

(3) Pieters, C. and T.B. McCord, This volume.

(4) Blanchard et al., This volume.

SPECTRAL REFLECTANCE OF LUNA 24 SOILS

Adams, J. B.

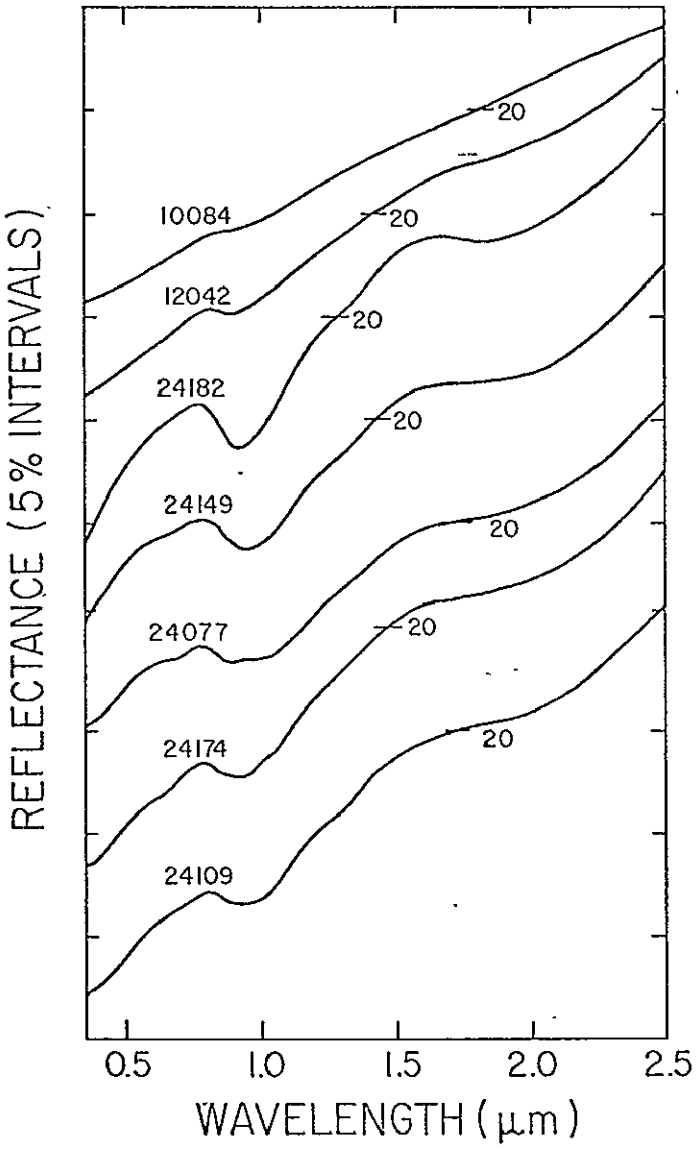

Figure 1.

Diffuse reflectance spectra of Luna 24 soils and representative Apollo soils relative to MgO in the wavelength interval 0.35 μm to 2.50 μm measured in percent. Successive spectra are offset 5% vertically for clarity. Lines labeled 20% define the absolute reflectance scale for each curve. Note the relatively deep absorptions near 1.0 μm and 2.0 μm on the Luna 24 spectra.

SPECTRAL REFLECTANCE OF LUNA 24 SOILS

Adams, J. B.

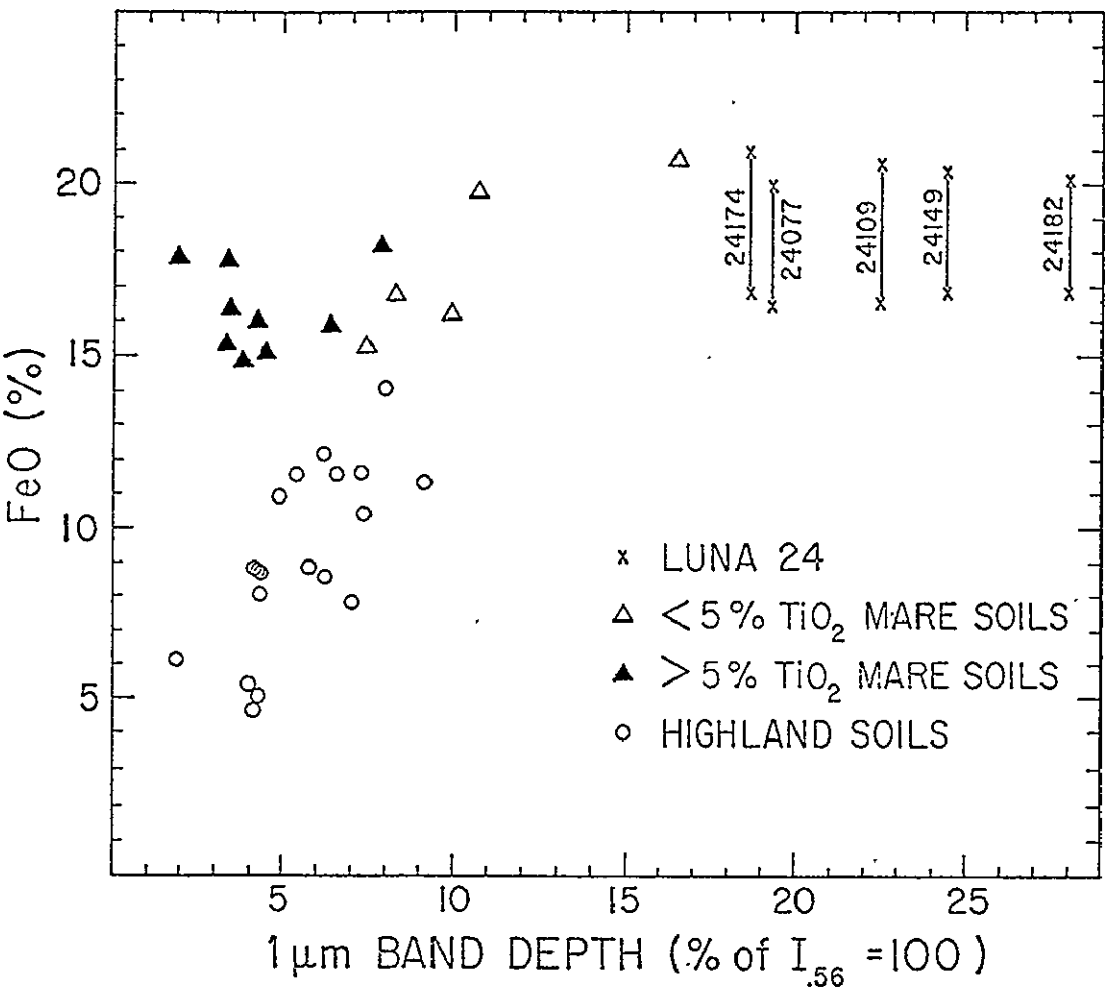

Figure 2.

Depth in percent of the absorption band near 1 μm vs weight percent FeO. Band depths are measured on curves that have intensity values scaled to 1 at 0.56 μm. FeO values for Luna 24 soils are from Blanchard et al (4). The higher Luna 24 FeO values are for <250 μm sieve fractions, whereas the lower values are for <20 μm sieve fractions. Luna 24 samples can be distinguished from other FeO-rich mare soils on the basis of band depth.

PETROGRAPHY OF LUNA 24 SAMPLE 24170. A.L.Albee, A.A.Chodos, R.F. Dymek, Div. of Geol. and Plan. Sci., Calif. Inst. of Tech., Pasadena, Calif. 91125.

Sample 24170 is from the 170-171 cm depth of the regolith core returned from Mare Crisium by the Luna 24 mission. It is a light-colored, 2 cm-thick layer of coarse particles and "...appears to represent a rather-large fragment of coarse-grained gabbro broken up by drilling." (Florensky et al., 1977).

The rock is a relatively coarse-grained subophitic basalt (or microgabbro), comprised of plagioclase, pyroxene, and olivine, together with minor amounts of ilmenite, cristobalite, and troilite. Petrographic and electron microprobe studies have been performed on two polished micro-thin sections (FQM-648, FQM-650), which were prepared from different lithic fragments, and on grain mounts, which were prepared to monitor the mineral separations for isotopic studies. The thin sections have a combined area of ~1.5 mm^2 and are too small for reliable modal estimates, but individual plagioclase-pyroxene-olivine contents are about 50-40-10% and 60-30-10%. Tarasov et al. (1977) report a range in various fragments for plagioclase content of 20-70%, for pyroxene of 20-60% and for olivine of up to 35% and a normative composition of 50 mole % plagioclase, 27% pyroxene, 19% olivine, 1.2% ilmenite, 0.7% chromite, and 0.3% apatite for a chemically-analyzed fragment of cristobalite gabbro. However, the relative yields of mineral separates obtained from several fragments, totaling about 130 mg, indicated a much lower plagioclase content of about 25% (D. Papanastassiou, oral communication).

Plagioclase ranges in composition from $An_{84.4}Ab_{15.1}Or_{0.5}$ to $An_{97.0}Ab_{3.0}Or_{0.0}$ with the most sodic compositions occurring at the edges of grains near cristobalite. Plagioclase occurs as tiny 10-50 μm rounded to tabular inclusions in pyroxene and olivine, in aggregates of interlocking (25-100 μm) tabular grains, and as elongate laths (up to 500 μm) intergrown with pyroxene. Grain boundaries with pyroxene are straight whereas plagioclase-olivine contacts tend to be undulose on a scale of tens of microns. However, the margins of plagioclase inclusions in olivine are straight.

Pyroxene ranges from pale pink to dark pink to yellow-brown in color and occurs as anhedral, angular grains intergrown with plagioclase. Analyses of the pyroxene define a U-shaped trend on the pyroxene quadrilateral (Fig. 1). Pyroxene zones continuously from ~$Wo_{26}En_{46}Fs_{28}$ to less-calcic and thence to more iron-rich compositions. The borders of larger grains, tiny (5-10 μm) grains intergrown with ilmenite, and tiny (5-10 μm) angular grains in the interstices between plagioclase laths fall in the range $Wo_{15}En_{43}Fs_{42}$ to $Wo_{32}En_{18}Fs_{50}$, the dominant trend being an increase in Ca-content. One pyroxene grain displays thin, poorly-defined exsolution lamellae of high-Ca pyroxene.

The contents of Al_2O_3 (0.7-1.9 wt %) and TiO_2 (0.2-1.5 wt %) are low, but the Cr_2O_3-content ranges to relatively high concentrations for lunar pyroxene (up to 0.8 wt %). In some grains the Cr_2O_3-content exceeds that of TiO_2. A plot of relative Al-Ti-Cr contents (Fig. 1) indicates decreasing Al and Cr, and increasing Ti as Fe/(Fe+Mg) increases, consistent with simultaneous crystallization of plagioclase, and late crystallization of ilmenite.

A large grain of pyroxene with a dark-colored overgrowth (FQM-649) has compositions along the U-shaped trend in some sectors, but "hops" across the top of the U in other sectors. Correspondingly the sectors display continuity

PETROGRAPHY OF LUNA 24 SAMPLE 24170

A. L. Albee

or discontinuity in their Al-Ti-Cr trends. Tiny inclusions of ilmenite and spinel are concentrated near the inner margin of the overgrowth.

Olivine occurs as rounded to irregular 10-400 μm grains that locally possess amoeboid apophyses that protrude into adjacent grains of plagioclase. The range in measured composition is Fo_{31} to Fo_9, but individual grains are quite homogenous (<2 mole % Fo zoning). The contents of Al_2O_3 (<0.20 wt %), TiO_2 (<0.14 wt %), Cr_2O (<0.06 wt %), and NiO (<0.09 wt %) are low, but the concentration of CaO (0.4-0.6 wt %) is high. No obvious reaction relation occurs between pyroxene and olivine, but fayalite (Fo_9) is in contact with pyroxene ($\sim Wo_{36}En_{14}Fs_{50}$) at the margin of a large pyroxene grain.

Tiny (<10 μm), angular grains of ilmenite [Fe/(Fe+Mg) = 0.97], together with μm-size blebs of troilite, occur in the interstices between plagioclase laths. Thin plates of ilmenite border euhedral surfaces of both plagioclase and pyroxene. No areas of K-rich mesostasis were found, but electron beam scans and optical examination suggest that a thin film of such mesostasis is associated with ilmenite on some grain surfaces. Electron beam scans also indicate the presence of Ca-phosphate in grains too small to analyse. A single grain of cristobalite (~50 μm) occurs between grains of plagioclase near the edge of a thin section. No reaction relationships with Fe-rich pyroxene or olivine such as described by Tarasov et al. (in press) or Ryder et al. (in press) can be seen.

The textural and compositional features are all consistent with crystallization from a melt with the following sequence: 1) plagioclase 2) pyroxene 3) olivine 4) ilmenite, cristobalite, and troilite.

The high Fe-content of the pyroxene and olivine, the extensive zoning in the pyroxene, the high Ca-content of the olivine, and the low K-content of the plagioclase, taken together, suggest that Luna 24 sample 24170 is analogous to other lunar mare basalts. The extensive early crystallization of plagioclase, the near absence of ilmenite, the low minor element content of the pyroxene, the trend in the relative amounts of Al-Ti-Cr in pyroxene, and the olivine-pyroxene relations are distinctive.

Florensky, C.P., et al. (1977) Luna 24: Geologic setting of landing site and characteristics of sample core (preliminary data): Proc. Lunar Sci. Conf. 8th, in press.

Ryder, G., et al., (1977) Basalts from Mare Crisium. The Moon, in press.

Tarasov, L.S., et al. (1977) Mineralogy and Petrography of Lunar Rocks from Mare Crisium: Proc. Lunar Sci. Conf. 8th, in press.

PETROGRAPHY OF LUNA 24 SAMPLE 24170

A. L. Albee

Figure 1.

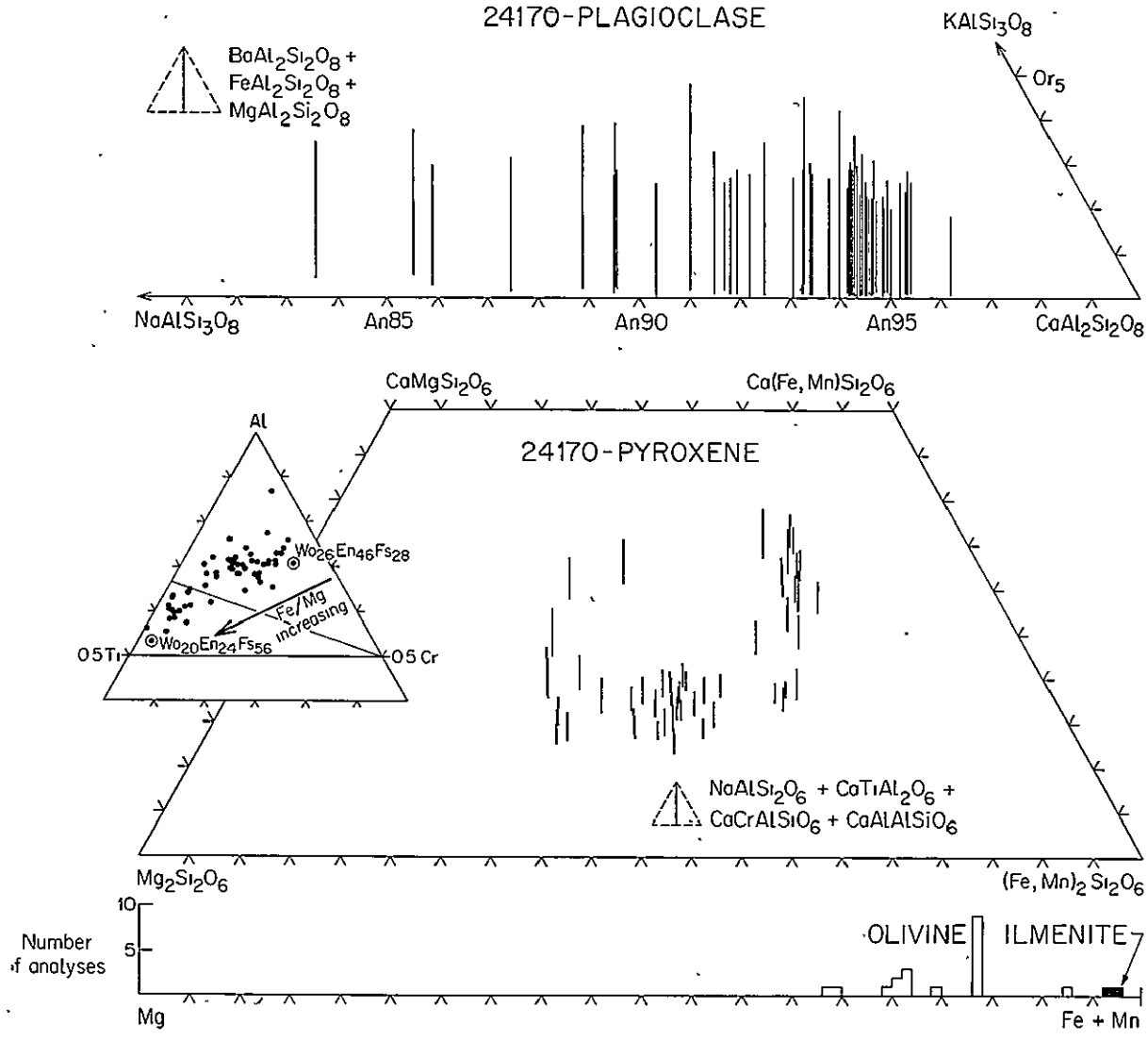

EVIDENCE FOR A HIGH-MAGNESIUM SUBSURFACE BASALT IN MARE CRISIUM FROM ORBITAL X-RAY FLUORESCENCE DATA. C. G. Andre*, R. W. Wolfe**, and I. Adler*. *University of Maryland, College Park, MD 20742. **National Air and Space Museum, Washington, D.C. 20560.

The Apollo 15 X-ray Fluorescence Experiment (XRF) coverage of the southern half of Mare Crisium provides more than 300 data points which measure the aluminum, magnesium, and silicon intensities of surface soils. A weighted filter technique has been applied to Al/Si, Mg/Si, and Mg/Al intensity ratios to obtain optimum resolution and signal-to-noise ratio.[1]

Analysis of these XRF intensity ratios indicates that the regolith of the Luna 24 landing site (62° 12'E, 12° 45'N) is representative of soils in southern Mare Crisium and that these soils are relatively homogeneous with the exception of those near the crater Picard (54° 30'E, 14° 30'N).

The predominant rock types in the Luna 24 drill core are mare basalts with a low content of TiO_2 and MgO, and a high Fe:Mg ratio, plus brown glasses and impact melts of about the same composition. Fragments present in small amounts include cristobalite gabbro and the more magnesium-rich materials green glass and olivine gabbro/vitrophyre.[2-5]

The Al/Si concentration ratio calculated from XRF data for a 2° square area centered at the landing site (Al/Si = 0.39) compares closely with the value for the finest fraction (< 74μm) of the regolith from the core (Al/Si = 0.41)[6]. The Mg/Si concentration ratio for the Luna 24 soil is 0.26, both from XRF and from analysis of the finest fraction. We believe this finest fraction of the core (50% of the regolith sampled) to be most representative of the surface soils. The Luna 24 soil, while dominantly basaltic, is more aluminous and more magnesian than basalt lithic fragments from the core. This suggests that the soil is a mixture of local basalt, terra material, and a third, more magnesian component, possibly with the composition of green glass or olivine gabbro/vitrophyre.

What is the source of the high-MgO material? It has been suggested that the olivine vitrophyre may have been derived from the patches of low albedo material 20 km. to the east of the landing site.[2] However, XRF data show no significant difference between this site and Luna 24. On the other hand, the area near the Eratosthenian crater Picard, 200 km. west of the landing site, is distinctly more magnesian than the average southern Mare Crisium regolith. (It has also been noted from earth-based spectral reflectance studies that Picard may have excavated an anomalously high TiO_2 unit.[7]) Both the Mg/Al intensity ratio (1.69 $\pm$ .08) and the Mg/Si intensity ratio (1.33 $\pm$ .08) are highest near Picard and decrease gradually toward the Luna 24 landing site (Figure 1). To the west and southwest of Picard, the change is more abrupt and the regolith is more aluminous as well as less magnesian. We attribute this to the contribution of terra material from the highlands to the southwest and to rays from the Copernican crater Proclus in the highlands about 170 km. west of Picard.

SUBSURFACE BASALT IN MARE CRISIUM

C. G. Andre, et al.

On an elemental composition diagram (Figure 2) the Al/Si and Mg/Si concentration ratios for the Picard region are seen to lie on a mixing line between the olivine gabbro/vitrophyre and the Luna 24 basalts. It is likely, therefore, that the high Mg XRF measurements associated with Picard represent material excavated from a substratum of basalt with the composition of the olivine gabbro/vitrophyre. Furthermore, Picard may be the source of these components in the Luna 24 drill core. As would be expected, material ejected by this crater would be present in only very minute amounts at a site 200 km. away. Calculations indicate that the amount of Picard ejecta at the Luna 24 site would be equivalent to a layer 2 cm. thick.[8]

Lunar sounder data reveal a radar reflector 1400 m. beneath the surface of Mare Crisium.[9] The floor of Picard lies about 1700 m. beneath the level of the mare. Therefore, material from beneath the discontinuity detected by the sounder has been sampled by Picard (Figure 3). Although Picard is located in the deepest part of the Crisium basin[10], it appears from Figure 3 that the crater may penetrate the basin floor. However, there is no evidence from the XRF data that Picard or any other crater in southern Mare Crisium has excavated any terra (basin floor) material. The Crisium basin is, therefore, probably deeper than indicated by the published isopach and structure maps.

We propose that early mare volcanism in the Crisium basin erupted basaltic lavas with a high MgO content, which filled the deepest parts of the basin. These flows form the layer detected by the lunar sounder and were excavated by Picard. The Luna 24 olivine-rich rocks are representative of these early lavas with the olivine vitrophyre formed at the chilled upper margins and the olivine gabbro crystallized within the flows. Later volcanism erupted low-titanium, low magnesium basalt, such as that found in the Luna 24 drill core.

References

1. Andre, C. G., Bielefeld, M. J., Eliason, E., Soderblom, L. A., Adler, I., and Philpotts, I. A., 1977, Science, 197, p. 986-989.
2. Ryder, G., McSween, H. Y., and Marvin, U. B., 1977, The Moon, in press.
3. Vaniman, D. T., and Papike, J. J., 1977, Geophys. Res. Let., in press.
4. Taylor, G. J., Keil, K., and Warner, R. D., 1977, Geophys. Res. Let., 4, p. 207-210.
5. Tarasov, L. S., Nazarov, M. A., Shevaleyvsky, I. D., Kudryashova, A. F., Gaverdovskaya, A. S., and Horina, M. I., 1977, Proc. Lunar Sci. Conf. 8th, in press.
6. Barsukov, V. L., Tarasov, L. S., Dmitriev, L. V., Kolesov, G. M., Shevaleyevsky, I. D., and Garanin, M. I., 1977, Proc. Lunar Sci. Conf. 8th, in press.
7. Pieters, C., McCord, R. B., and Adams, J. B., 1976, Geophys. Res. Let., 3, p. 697-700.

8. McGetchin, T. R., Settle, M., and Head, J. W., 1973, Earth Planet. Sci. Let., 20, p. 226-236.
9. May, T. W., Peeples, W. J., Maxwell, T., Sill, W. R., Ward, S. H., Phillips, R. J., Jordan, R. L., and Abbott, E. A., 1976, Lunar Sci. VII, p. 540-542.
10. DeHon, R. A. and Waskom, J. D., 1976, Proc. Lunar Sci. Conf. 7th, p. 2729-2746.

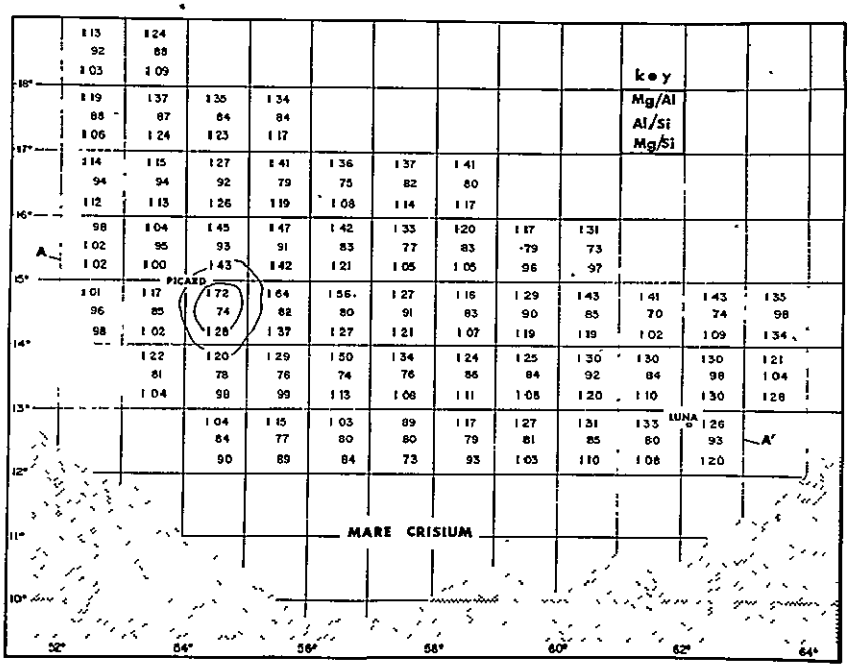

Figure 1. Orbital XRF data for southern Mare Crisium.

SUBSURFACE BASALT IN MARE CRISIUM

C. G. Andre, et al.

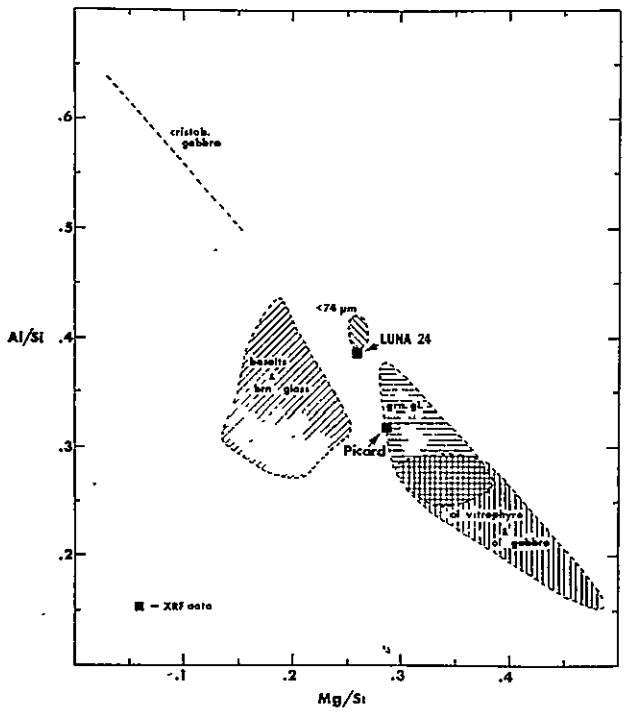

Figure 2. Orbital and sample Al/Si values for the Luna 24 regolith (refs. 1-4 and 6).

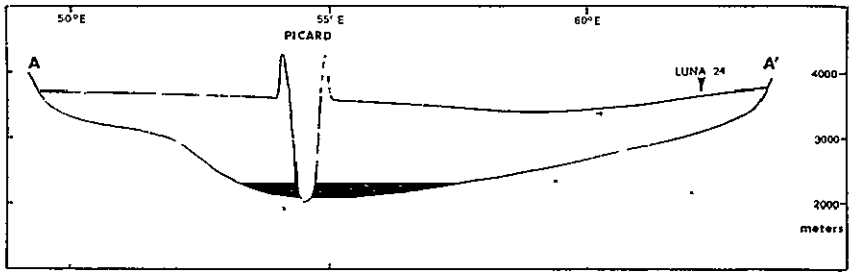

Figure 3. Cross section of southern Mare Crisium. Basin floor from (ref. 10) and 1.4 km. deep discontinuity from (ref. 9). Picard depth from LTO 62A1. Vertical exaggeration ≃ 38.

ELECTRON MICROSCOPY OF RADIATION DAMAGE IN LUNA 24 SOIL

D.J. Barber, Physics Dept., University of Essex, Colchester, Essex, England.

Micron-sized and sub-millimetre sized soil grains have been examined by optical microscopy, high voltage electron microscopy (HVEM) and scanning electron microscopy (SEM) to assess levels of radiation damage, mineralogy and microstructural state. The study of the micron-sized grains has been supplemented by comparison studies on similarly-sized soil fractions returned by the Luna 16 and Luna 20 missions. It should be recalled that Phakey and Price (1973) have concluded that of the returned soil samples the small grains from the Luna 20 site were the least heavily irradiated, while those from the Luna 16 site were by far the most heavily irradiated.

The micron-sized grains were supported on carbon films and examined by HVEM without etching or other treatment. Use of selected area diffraction frequently enables mineralogical species to be identified, while the relative intensities of diffuse-scattered and Bragg-reflected electrons is a sensitive measure of the higher levels of radiation damage (track densities $> 5 \times 10^{11}$ cm^{-2}). The preliminary results suggest that the soil from the Mare Crisium site has suffered only a moderate radiation exposure. Although the amorphous coating produced by solar wind damage (Borg et al., 1970) is present on many grains, the grain interiors are mainly highly crystalline. No tracks are visible when some grains are viewed with high resolution dark field imaging, implying track densities in these instances $\leqslant 10^{8}$ cm^{-2}. Figure 1 shows two dark-field views (at 1 MV) of an olivine grain from specimen 24125 exhibiting slight irradiation effects ('blobs' and a few tracks) only in the top corner. Metamict (very heavily-irradiated grains) are rare and the highest track density so far recorded in micron-sized grains from the Luna-24 site is $< 10^{11}$ cm^{-2}.

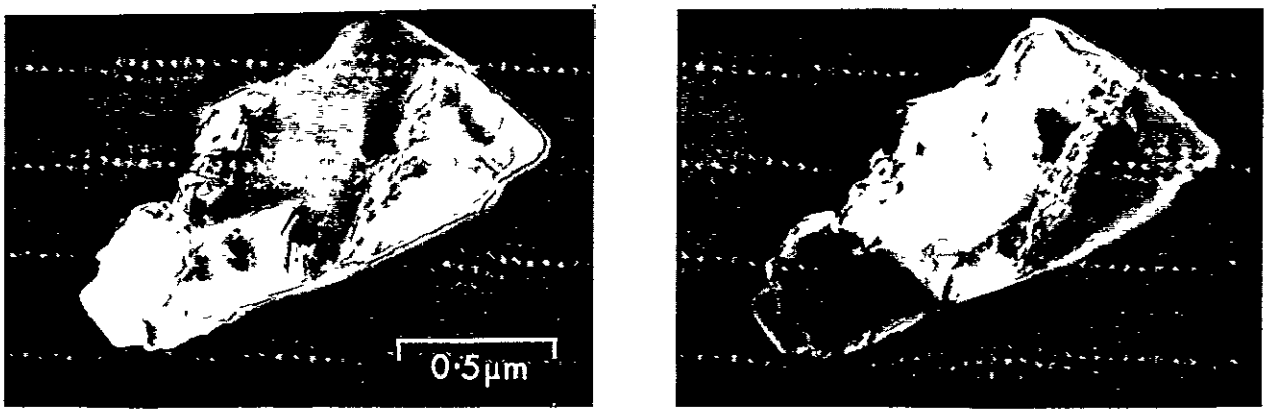

Figure 1

The larger (sub-millimetre) grains were mostly examined for particle tracks before ion-thinning for HVEM. Each grain was potted in epoxy resin and polished to ¼ µm diamond finish prior to chemical etching to establish the track density. The grains were etched lightly, with etchants appropriate

RADIATION DAMAGE IN LUNA 24 SOIL

Barber, D.J.

to their mineral type and examined by optical and SEM methods. Typical track densities in the grain interiors were $\lesssim 10^8$ cm^{-2}. Figure 2 is a SEM picture of part of an etched large pyroxene grain, with diameter 0.98 mm, from specimen 24090, which had a fairly uniform track density of 7 x 10^8 cm^{-2}. A few grains exhibited steep track gradients from one edge, indicative of either little stirring in the regolith or more probably (in view of the generally low level of the irradiation effects) of relatively recent fracture of the soil fragment from the surface of a larger rock. The presence of a crater-like feature at the region of maximum track density on one grain confirms that the region corresponds to an exposed external surface. Using the now reasonably well-established energy spectrum for solar flare Fe particles (Hutcheon et al., 1974) and assuming long-term constancy of particle flux, exposure times can be deduced.

Figure 2

Most of the sub-millimetre grains show macroscopic cracking and some have glass-cemented dust grains, consistent with the impact origin of the regolith. It is anticipated that the HVEM results now being obtained from ground, repolished and ion-thinned sections from the sub-millimetre grains will provide further evidence as to microstructure, possibly including effects of impact and shock. Amongst these large soil grains we have already identified breccia fragments which contain evidence for pre-agglomeration VH-particle irradiation, as already reported by Macdougall et al. (1973) for Apollo 14, 15 and 16 breccias.

Borg, J., Dran, J.C., Durrieu, L., Jouret, C. and Maurette, M. (1970) Earth Planet. Sci. Lett. 8, 379-386
Hutcheon, I.D., Macdougall, D. and Price, P.B. (1974), Proc. Fifth Lunar Sci. Conf., Vol. 3, 2561-2576
Macdougall, D., Rajan, R.S., Hutcheon, I.D. and Price, P.B. (1973), Proc. Fourth Lunar Sci. Conf., Vol. 3, 2319-2336
Phakey, P.P., Hutcheon, I.D., Rajan, R.S. and Price P.B. (1972), Proc. Third Lunar Sci. Conf., Vol. 3, 2905-2915

GLASS PARTICLES IN LUNA 24 DRILL CORE SOILS

Abhijit Basu[1], D. S. McKay[2], U. Clanton[2], G. Waits[3], and R. M. Fruland [2]

[1]The Lunar Science Institute, Houston, TX 77058, USA
[2]NASA Johnson Space Center, Houston, TX 77058, USA
[3]Lockheed Electronic Co., Houston, TX 77058, USA

Investigation of the morphology and composition of lunar non-agglutinitic homogeneous glass particles can provide insights into the processes of their formation, transport and near surface history, as well as the rock types melted by impact. In the case of volcanic glass, the magma composition is reflected by the glass composition. We report the results of a preliminary examination of handpicked glass droplets by Scanning Electron Microscope (SEM), and optical microscope and electron probe studies of homogeneous glass particles, vitrophyres, and clast laden quench-crystallized glass in polished grain mounts. Agglutinitic and soil breccia glasses were excluded from the glass analyses.

SEM Studies. We have handpicked and classified about 300 glass droplets from the 45-150 μm size fraction of 6 Luna 24 soils. Examination of 200 droplets with high resolution (~ 25Å) SEM reveals (Table 1) that nearly half of the black and brown droplets have either vesicles or iron droplet trains or both. These features are common on agglutinates and so an appreciable proportion of the black and brown droplets may be a variety of agglutinate. Only a small percentage of the droplets, mainly brown ones, have microcraters (Table 1). The largest microcrater observed was 2 μm in diameter. Microcraters are perhaps the best criteria for lunar surface exposure and reworking. Therefore few of the droplets, even the agglutinate-like ones, have had a significant exposure at the lunar surface. This observation is particularly important for the light colored droplets which are likely to be highland composition. The complete lack of microcraters on these droplets suggest that they have not been transported from the highlands by multiple impacts in a diffusion-like process which would be expected to maximize their chances of surface exposure. It is therefore likely that they have been transported by single step events, probably from relatively large highland impacts, perhaps as ray ejecta. None of the examined droplets displayed the major morphologic features characteristic of the Apollo 15 green glass and the Apollo 17 orange and black glass. These features, attributable to fire fountaining, include micromound coatings disturbed by scraping, composite droplet-on-droplet structure, and crystals protruding from the interior. If the nearby dark mantle [1,2] consists of Apollo 15 and 17 type droplets, we have not observed them with the SEM in the Luna 24 samples.

Glass in Thin Sections. Glass particles in polished grain mounts were classified according to color and opacity (Table 2). As with the handpicked droplets dark brown and black glasses are dominant over colorless and grey varieties while yellow and green glasses are the least abundant. In general, the abundance of glass particles increases with decreasing grain size. Electron-probe analyses (12 elements) of these glass particles (90-250 μm) indicate a variety of chemical compositions a few of which are represented by only two or three particles. The average of 71 homogeneous glass compositions (Table 3) is considerably different from the composition of the bulk soil [3]. A simple

cluster analysis indicates three broad groups (Table 3). The largest group approximates the major element chemistry of Luna 24 soils [3] which is dominated by basaltic rock types [4]. The next cluster is equivalent to anorthositic gabbro composition [5,6] and the third is very nearly the anorthosite glass of the highlands [5,6]. These three clusters can also be inferred from visual inspection of simple binary variation diagrams. In plots of Mg/Mg+Fe (Mg value) vs. TiO_2 or Al_2O_3 the group which approximates the average soil composition is represented by a very tight cluster at $\sim$ 0.35 Mg value and with some additional scattered points at $\sim$ 0.45 Mg value. Both the subgroups of this cluster have approximately 1% TiO_2 and 12% Al_2O_3 (fig. 1). These are also apparent in oxide variation diagrams (fig. 2) and have approximately 6% and 10% MgO, but with a fairly constant 12% Al_2O_3, 1% TiO_2, and $\sim$ 21% FeO.

The other two groups, anorthositic gabbro and anorthosite glass compositions, overlap in their Mg values (0.71 and 0.69) but show (fig. 2) a trend and small clusters with respect to their TiO_2% (0.37 & 0.13), Al_2O_3 (25.1 & 32.1), FeO% (5.9 & 1.65), and MgO% (7.5 & 2.3). In view of the extreme rarity ($\sim$ 1.5%) of anorthosites and anorthositic gabbros among the crystalline rock fragments [7] the high proportion ($\sim$ 42%) of highland glasses in the homogeneous glass population is remarkable. Despite the abundance of highland glass, those with LKFM affinity are extremely rare. So far, we have found only one LKFM droplet with high alumina ($\sim$ 23%), low K (0.17%), and low P (0.12%), and a primitive Mg value (0.74). The latter is comparable to the most primitive KREEP basalt reported so far [8,9].

An important occurrence of glass in the Luna 24 core soils is in two types of fragments: olivine vitrophyre and glass fragments with feathery quenched crystals of olivine and clasts. The relatively rare olivine vitrophyre consists of fairly large ($\sim$ 40 x 60 μm) nearly euhedral but skeletal olivine phenocrysts and small euhedral spinel crystals set in a clast-free yellow-green groundmass which has flow structures. The Fe/Mg K_D value is $\sim$ 0.26 between olivine phenocrysts and the glass. The glassy fragments with feathery olivine crystals are dominant and contain clasts of olivine, pyroxene, and rarely of plagioclase and cristobalite. Spinel is absent and there are no euhedral olivine phenocrysts. Instead, feathery quenched crystals of olivine ($\sim$ 5 x 20 μm) occur in the pale yellow-green groundmass ($K_D \sim 0.17$). Many of the fragments of clast-laden olivine vitrophyre display rounded external outlines in thin sections. These surfaces suggest that the fragments may have been droplets or related forms. While not texturally similar to the green and orange glasses from Apollo 15 and 17, the clast-laden variety may possibly represent another kind of pyroclastic ash. The compositions of the olivine phenocrysts and clasts in the vitrophyre with a strong unimodal peak around Fo_{75} are similar to those of the proposed cumulate body under Mare Crisium [7]. Perhaps the clast-laden vitrophyre is a pyroclastic equivalent of the coarse grained ultramafic cumulate which may have been excavated by the Farenheit event. Alternatively, the olivine vitrophyre may be an impact melt of the cumulate, and was distributed as impact-produced glassy droplets and related forms. Some of the clast-laden fragments resemble the ropy glasses thought to be impact-produced [10]. The clast-free vitrophyre fragments may be a quenched flow related to the pyroclastic unit mentioned above.

GLASS PARTICLES IN LUNA 24

Basu, A. et al.

Table 1 SEM features on 200 glass droplets. All numbers in percent.

FEATURES	COLOR: BLACK (46)	BROWN TO AMBER (41)	GREEN (3)	CLEAR (10)	PERCENTAGE OF TOTAL GRAINS WITH FEATURES
Glass splashes	100	100	100	100	100
Vesicles	48	27	0	34	40
Chips and fractures	96	92	80	95	94
Iron droplets and trains	54	40	0	15	44
Accretionary features (pancakes, spheres)	91	88	80	100	89
Microcraters	1	10	0	0	5

Table2 Modal Abundance of Homogeneous Glass Particles in Size Fractions of Luna Soils (number percent of the bulk size fraction)

Sample #	-077, 9	-109, 13	-149, 15	-174, 10	-182, 15	-210, 9
150-250μm						
Black, brown, etc	3 9	1 7	1 3	1 7	1 6	2 0
Green, yellow, etc	1 6	0 7	1 0	0 7	0.6	1 0
Colorless, grey, etc	0 6	0 3	1 9	0 7	2 0	2 0
Total	*6 1*	*2 7*	*4 2*	*3 1*	*4 2*	*5.0*
90-150μm						
Black, brown, etc	2 0	2 7	1 0	3 2	2 6	1.3
Green, yellow, etc	0 7	1 0	0 0	0 3	0 0	1 0
Colorless, grey, etc	2 6	0 3	1 0	2 2	2 3	1 3
Total	*5 3*	*4 0*	*2 0*	*5 7*	*4.9*	*3 6*
45-90μm						
Black, brown, etc	1 6	1 9	1 6	0 6	2 6	2 3
Green, yellow, etc	0 3	1 0	0 6	0 6	0 3	2 0
Colorless, grey, etc	0 7	2 6	2 8	1 3	2 9	2 6
Total	*2 6*	*5.5*	*5 0*	*2 5*	*5 8*	*6.9*
20-45μm						
Black, brown, etc	4.5	4 5	4 5	-	4 5	1 9
Green, yellow, etc	2 3	1 6	3 8	-	1 3	1 3
Colorless, grey, etc	0 3	5 2	2 2	-	2 6	4 8
Total	*7 1*	*11 3*	*10 5*	-	*8 4*	*8 0*

Table 3 Compositions of Glass in Luna 24 Soils

	Homogeneous Glass				Olivine-vitrophyric & clast-laden glass
	Anorthosite	Anorthositic gabbro	Mare basalt soil	Average	Average
Number of analysis	11	19	41	71	32
SiO_2	44 5	44 7	45 1	44 9 ± 1 4	45 2 ± 3 6
TiO_2	0 13	0 37	1 05	0 73 ± 0 53	1 03 ± 0 52
Al_2O_3	32 1	25 1	12 3	18 8 ± 8 2	10 3 ± 2 6
Cr_2O_3	0 04	0.14	0 30	0·22 ± 0 14	0 42 ± 0 18
P_2O_5	0 02	0 04	0 04	0 04 ± 0 03	0 04 ± 0 02
MgO	2.3	7 5	8 1	7 0 ± 3 0	7 5 ± 2 9
CaO	18 5	15 0	12 0	13 8 ± 2 8	12.1 ± 1.7
MnO	0.03	0 05	0 28	0 18 ± 0 12	0 29 ± 0.07
FeO	1.65	5 9	21 2	14 05 ± 8 8	22 7 ± 5 6
NiO	0.0	0 0	0 01	-	-
Na_2O	0.36	0 34	0 25	0 29 ± 0 18	0 25 ± 0 08
K_2O	0.03	0 07	0 04	0 05 ± 0 03	0 04 ± 0 01
Total	99.7	99 2	100 7	99 87	99 35
Mg/Mg+Fe	0 71	0 69	0 40	0 47	0 37
			CIPW NORMS		
Or	0.18	0 41	0 24	0 30	0 24
Ab	3.0	2 9	2.1	2 5	2 1
An	85.8	66 9	32 2	49 8	26 9
Wo	2.5	3 0	11.3	7 7	13 6
Di	2 2	2 6	10 9	7 3	13 6
Hy	3 3	11 7	21.4	16 7	24 1
Fo	1 4	6 6	5.9	5 3	4.7
Fa	0 76	4.1	11 9	8 2	11.1
Il	0 25	0 70	1 99	1 39	1 96
Ap	0 05	0 09	0.09	0 09	0 09

GLASS PARTICLES IN LUNA 24 DRILL CORE SOILS

Basu, A. et al.

References. 1. Butler, P. and Morrison, D., 1977, PLC 8. 2. Pieters, C. et al., 1976, GRL, v.3, p.697. 3. Blanchard, D.P. et al., 1977: this volume. 4. Barsukov, V.L. et al., 1977, PLC 8. 5. Reid, A.M. et al., 1973, GC Acta, v.73, p.1011. 6. Taylor, S.R., 1975, Lunar Science, Pergamon, 372 p. 7. Basu, A. et al., 1977: this volume. 8. Basu, A. and Bower, J.F., 1976, PLC 7, p.659. 9. Irving, A.J., 1977, PLC 8. 10. Fruland, R.M. et al., 1977, PLC 8.

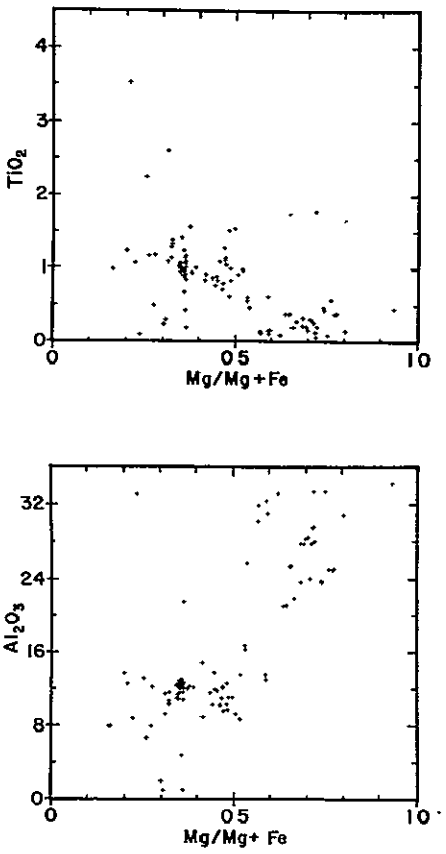

Fig.1

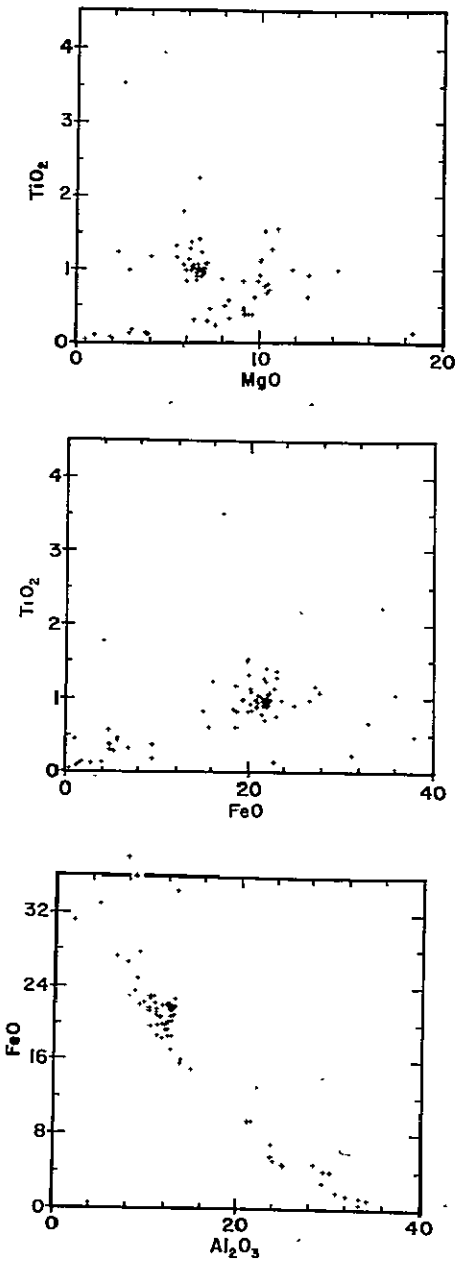

Fig. 2

PETROGRAPHY, MINERALOGY AND SOURCE ROCKS OF LUNA 24 DRILL CORE SOILS

Abhijit Basu[1], David S. McKay[2], and Ruth M. Fruland[2]

[1]The Lunar Science Institute, Houston, TX 77058, USA
[2]NASA Johnson Space Center, Houston, TX 77058, USA

Introduction. We have carried out petrographic modal analysis on grain size separates of 6 Luna 24 core samples. Polished grain mounts were made of the 150-250 μm, 90-150 μm, 45-90 μm, and 20-45 μm for samples 24077,9; 24109,13; 24149,15; 24174,10; 24182,15; and 24210,9. Approximately 300 grains were identified and described in each section except for the 20-45 μm section of 24174,10 which was ground away during thin sectioning. In addition to tabulating the petrographic data from each grain size we have recombined the grain size data weighted according to the weight percent of each grain size fraction [1] in order to present a modal analysis closer to that of the bulk soil (Table 1).

Mineral Fragments. The most striking feature of the modal data is the very high (~ 52%) abundance of monomineralic fragments which makes this regolith unique among all the lunar regolith sampled so far. These monomineralic fragments are abundant in the coarsest grain size studied (250-150 μm) and are prominent even in the 250-500 μm, 500 μm-1 mm and > 1 mm fractions [2]. The abundance of coarse fragments of pyroxene, plagioclase, and olivine implies that the lithic fragments from which they are derived are very coarse grained and may not be well represented, if even present, in the lithic fragments found in the Luna 24 samples.

The population of monomineralic fragments is dominated by pyroxene (~ 66%), plagioclase (~ 22%), and olivine (~ 8%). Opaques and cristobalite (?) make up the rest. Two kinds of pyroxene can be recognized in thin sections optically. The dominant variety is reddish brown, contains a large number of inclusions, and has a characteristic pitted surface; these are obviously derived from the ferrobasalts and ferrogabbros [3,4,5]. The other type is relatively clear, or rarely, pale green to pale pink in color, generally free of inclusions, and has a smooth surface. These may be related to other types of basalts and gabbros.

We have performed a limited number of electron probe microanalysis on olivine and pyroxene fragments in the 150-250 μm size range. We find a bimodal distribution of olivine composition (Fe,Mg) with the stronger mode at ~ Fo_{75}, a subsidiary mode at ~ Fo_{50} and a tail towards fayalite (fig. 1). The iron-rich olivines ($Mg/Fe+Mg \leq 0.5$) can be related to the basalts and gabbros from Luna 24 reported so far [3,4,5,6]. However, the high magnesian variety of olivine has not been observed in any of the rock fragments from Luna 24 except for the olivine vitrophyres which we describe elsewhere [7]. Tarasov et al. [5] report ~ Fo_{77} also for a coarse monomineralic olivine. We believe that the parent of these monomineralic high magnesian olivine particles is a coarse grained cumulate rock which has not yet been observed as discrete rock fragments, but which has contributed significantly to the regolith at the Luna 24 site. The average CaO content of these magnesium-rich olivine particles is about 0.22%. An important feature of the olivine compositions is that the CaO content increases from ~ 0.20 to ~ 0.90 systematically with decreasing Fo content (fig. 2; also see [5]).

SOURCE ROCKS OF LUNA 24 SOILS

Basu, A.et al

Table 1. Weighted modal analysis of 20 μm-250 μm grain size fractions of Luna 24 drill core soils.

Sample No.	-077,9	-109,13	-149,15	-174,10	-182,15	-210,9
wt % of < 250 μm fraction	73.52%	80.22%	82.95%	57.54%*	77.01%	84.47%
Monomineralic fragments	47.53	48.42	51.22	53.79	58.24	50.04
Plagioclase	9.78	9.95	9.95	12.22	15.82	12.71
Pyroxene	32.49	33.64	36.14	36.84	36.20	31.87
Olivine	4.44	3.81	3.42	3.84	5.03	4.49
Opaques	0.68	0.82	1.00	0.49	0.69	0.45
Ilmenite, Chromite, etc.	0.00	0.50	0.40	0.14	0.06	0.07
Troilite	0.05	0.17	0.08	0.14	0.06	0.00
Fe metal	0.63	0.17	0.80	0.23	0.55	0.38
SiO_2 phases	0.14	0.21	0.45	0.43	0.56	0.52
Xlline Lithics	10.99	11.52	11.43	14.42	13.57	13.24
ANT	0.45	0.36	0.47	1.58	0.53	0.94
Anorthositic	0.31	0.36	0.16	1.01	0.40	0.63
Gabbroic	0.14	0.00	0.31	0.57	0.14	0.31
Mare basalts	5.52	5.78	5.30	5.70	5.71	4.76
Olivine-bearing	1.56	1.57	1.82	1.20	1.45	1.10
Olivine-free	3.97	4.25	3.48	4.52	4.26	3.66
Non-mare basalts	0.0	0.06	0.00	0.00	0.00	0.13
Feldspathic	0.0	0.06	0.00	0.00	0.00	0.13
KREEPy	0.0	0.00	0.00	0.00	0.00	0.00
Indeterminate	5.02	5.31	5.64	7.13	7.31	7.41
Plagioclase rich	0.53	1.75	1.27	2.87	2.39	1.82
Pyroxene rich	3.52	2.78	3.81	3.82	4.10	4.91
Olivine rich	0.24	0.52	0.34	0.33	0.64	0.53
Opaque rich	0.10	0.09	0.24	0.14	0.17	0.08
SiO_2 rich	0.04	0.17	0.00	0.00	0.06	0.09
Breccia & Rexllzd Lithics	10.32	9.94	17.43	11.00	9.19	13.32
Low grade, vitric	8.43	7.03	15.19	9.01	6.64	11.33
Dark matrix	7.86	6.83	14.80	8.92	6.09	10.57
Light matrix	0.57	0.20	0.40	0.09	0.60	0.63
High grade, rexllzed	1.89	2.89	2.24	2.00	2.53	2.14
Poikilitic	0.20	0.62	0.42	0.50	0.29	0.08
Melt-matrix	0.97	1.00	0.84	0.68	1.04	0.97
Other	0.72	1.27	0.96	0.78	1.23	0.73
Agglutinates	26.05	23.68	14.64	17.17	12.70	18.02
Glass	5.03	6.27	5.66	3.67	6.05	6.06
Black, brown, etc.	2.90	2.76	4.14	1.69	3.00	1.93
Green, yellow, etc.	1.18	1.12	1.41	0.52	0.56	1.40
Colorless, grey, etc.	0.97	2.39	2.05	1.44	2.55	2.77
Miscellaneous	0.00	0.09	0.24	.07	0.00	0.00
Total %	99.92	99.92	100.62	100.12	99.75	100.68
Total # of grains	1229	1219	1245	914	1236	1221

*Does not include data for the 20-45 μm fraction which was ground away during thin sectioning.

Source Rocks of Luna 24 Soils

Basu, A. et al.

Pyroxene compositions show a typical zoning pattern (fig. 3) consistent with derivation from mare basalts analyzed by others [3,4,5]. The minor element zoning patterns of monomineralic pyroxene generally confirm the low-Ti high-Al nature of their parent rocks (Al is mostly tetrahedral in the pyroxene). In addition to the usual strongly zoned pyroxene we also find a bronzitic variety of monomineralic pyroxene which does not show any major element zoning from core to margin. Because there is no complementary diopsidic augite cluster we believe that the bronzitic variety is not highland derived [cf. 8] but are related to the cumulate that supplied the coarse monomineralic olivine particles. The Mg/Mg+Fe ratio of $\sim$ 0.75 for both olivine and pyroxene lend support to such a hypothesis. On the basis of the abundance of very coarse grained magnesian monomineralic olivine and pyroxene, presence of unzoned bronzitic pyroxene, and the absence of such mineral compositions from the lithic fragments in Luna 24 samples, we speculate that a body of ultramafic cumulate rocks occur at or near the base of Mare Crisium, which may help to explain the associated mascon.

Rock Fragments. Identifiable rock fragments ($\sim$ 6% of the core) are dominated by mare basalts ($\sim$ 90%) of which about 25% are olivine-bearing. This latter category includes both crystalline fragments and olivine vitrophyres. The rest of the identifiable rock fragments are made up of dominantly anorthositic and some gabbroic rocks from the highlands. These fragments make up about 1.5% of the soils. Feldspathic basalts are rare and KREEP basalts are totally absent. Indeterminate rock fragments (Table 1) probably are mostly mare basalt varieties.

As in all other mare sites, the breccia population at this site is dominated by the low grade dark vitric variety which shows an increase in abundance at a depth of 149 cm. Such an increase has been also observed in the > 500 μm sizes at this depth [2]. Perhaps a large soil breccia near this level has been crushed and incorporated in the drill core tube. High grade and recrystallized breccia and lithic fragments including the metabasalts [3] constitute a little more than 2% of the core soils.

An interesting and unusual lithic type is the melt matrix breccia, fragments of which are extremely vuggy ($\sim$ 20% vugs) and contain micron sized globules and crystals of Fe metal. The groundmass has a quench-crystalline texture and its crystallinity is gradational from micron sized crystallites to $\sim$ 10 μm x 2 μm plagioclase laths and pyroxene. The proportion of pyroxene to plagioclase in the groundmass is approximately 60:40 and is consistent with a possible mare source. Lithic clasts in these breccias are very rare and about 90% of the mineral clasts are mafic. Electronprobe analyses of some of the clasts show that both olivine and pyroxene are fairly Mg-rich (Mg/Fe+Mg $\geq$ 0.5) and a mafic source is indicated. We conclude that a medium sized impact on a mare regolith, perhaps not far from the Luna 24 site, generated a gas-rich (from the irradiated regolith particles) melt sheet. The melt-matrix breccias observed in thin section may be represented in the > 1 mm fragments by the high FeO, high metallic iron particles observed by Morris [9] who suggested that these particles were derived from mare regolith.

We have also observed fragments of olivine vitrophyre in the soil samples

Source Rocks of Luna 24 Soils

Basu, A. et al.

[3]. Two varieties are seen and are described elsewhere [7]. These particles may represent the volcanic equivalent or the impact product of the ultramafic cumulate body that we have proposed above.

Summary. The Luna 24 soils contain high abundances of pyroxene, olivine, and plagioclase fragments. While many of these fragments are derived from the ferrobasalts found in the soils, others, particularly the Mg-rich pyroxene and olivine may be derived from a coarse-grained cumulate not observed as lithic fragments in the soil. This coarse-grained cumulate may be related to both the olivine vitrophyre and the vuggy melt-matrix breccia. The vuggy melt matrix breccia correlates well with the monomineralic olivine grains in the twenty-three modal analyses (r = 0.8 at a 99% confidence level). Butler and Morrison [10] suggest that up to 1 meter of ejecta from the crater Farenheit may be present at the Luna 24 site. The cumulate-derived minerals, the vuggy melt-matrix breccia and the olivine vitrophyre may all be part of a spectrum of impact products from the Farenheit event which have been mixed into the local soil which consists primarily of locally derived ferrobasalts and their related products. Our modal data indicate that of these 3 possible exotic additions to the soil, the cumulate derived mineral fragments are volumetrically the most important.

References. 1. McKay, D.S. et al., 1977: this vol. 2. Nagle, J.S. and Walton, W.J.A., 1977. Luna 24 Catalog and Preliminary Description, NASA-JSC, 85 p. 3. Ryder, G. et al., 1977. CFA Preprint 775. 4. Vaniman, D. and Papike, J.J., 1977, GRL (in press). 5. Tarasov, L.S. et al., 1977. Proc. Lunar Sci. Conf. 8th. 6. Barsukov, V.L. et al., 1977. Proc. Lunar Sci. Conf. 8th. 7. Basu, A. et al., 1977: this vol. 8. Irving, A.J., 1975. Proc. Lunar Sci. Conf. 6th, p. 363. 9. Morris, R.V., 1977: this vol. 10. Butler, P. and Morrison, D., 1977. Proc. Lunar Sci. Conf. 8th.

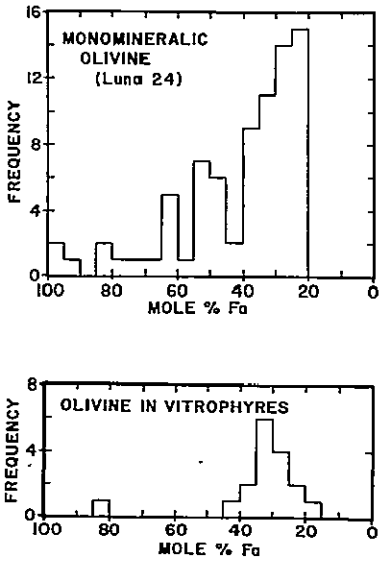

Fig.1

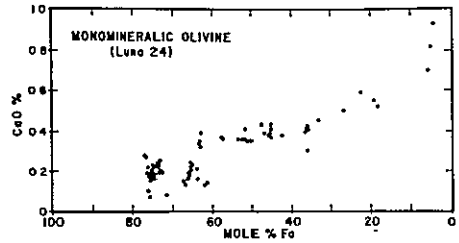

Fig.2

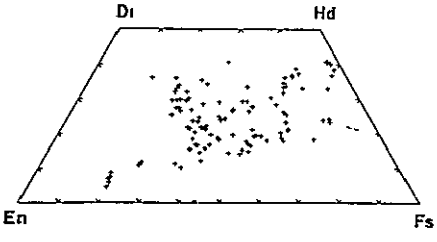

Fig.3

THE HIGHLAND COMPONENT IN THE LUNA 24 CORE; A. E. Bence and T. L. Grove, Dept. of Earth and Space Sciences, State Univ. of New York, Stony Brook, N. Y. 11794

The highland component is a volumetrically insignificant fraction of the LUNA 24 core [1]. We have examined 18 thin sections of the 0.15-0.50 mm size fraction from seven levels in the core. One of the objectives of this study has been to characterize the highland component and to compare it with highland components from other sites. In the Luna 24 core, highland lithologies are represented by melt rocks, glasses, annealed breccias, single mineral grains, and possible plutonic fragments. Their overall abundance in our total sample is less than about 2%. However, this ranges from a maximum of about 8% at the 109 cm level to 0% at the 170 cm.

Melt rocks and glasses dominate the highland population. However, their recognition is complicated by the high Al_2O_3 and low TiO_2 character of the local mare component. The highlands affinity of these fragments can be determined only by electron microprobe analysis and the chemical criteria we have used to separate the highlands component from the abundant ferrobasalts [2] and ferrogabbros [3] are CaO/Al_2O (wt.) $\lesssim$ 0.8 and Fe/(Fe+Mg) (molar) < 0.45.

The melt rocks are fine-to-very-fine-grained, are clast laden, and have textures ranging from vitrophyric to subophitic with the majority having intersertal textures. They are characterized by: Al_2O_3 = 20-30%, K_2O < 0.15%, Fe/(Fe+Mg) = 0.25-0.4, and CaO/Al_2O_3 (wt.) < 0.8. Their compositions, plotted on the Ol-An-Qtz pseudoquaternary [4], fall in the plagioclase field, generally along the olivine-plagioclase cotectic, but extending well over to the anorthite apex (Fig. 1). On the basis of their ranges of Al_2O_3 and K_2O abundances and Fe/(Fe+Mg) ratios, these melt rocks are either anorthositic basalts or VHA basalts (low-K members) according to Irving's [5] breakdown. It is important to note that the KREEP component in all of the melt rocks we examined is extremely low. We believe that all of these melt rocks were generated within the crust through impact processes.

Several types of glasses occur in our sample. The majority of these appear to have mare affinities when the chemical criteria given above are used. Representative glass compositions are plotted on Fig. 1 where, in addition to the highland components, we have plotted the brown glass representative of the LUNA 24 mare ferrogabbro, an aluminous, Mg-rich green glass that may be a fused soil mixture of highlands and mare material or of mare origin, and an Mg-rich green-glass. Several criteria disqualify these chemistries as highlands. The brown glass is distinguished by its very low Ti content (< 1.0 wt.%) and Fe/(Fe+Mg) ratio of 0.6 to 0.7. The aluminous green glass bears a deceptive similarity to aluminous mare basalt [6,7], but contains much less TiO_2 (0.45-0.55 wt.%, as compared to 1.5 to 7 wt.%). The green glass bears some similarity to other mafic green glasses (CaO/Al_2O_3 = 1.03, Fe/(Fe+Mg) = 0.49), but has higher TiO_2 (1.4 wt.%) and Al_2O_3 (15.0 wt.%) contents. The glasses, whose compositions range from anorthositic through noritic, like the melt rocks are very low in K_2O. A unique glass type that consists of a mixture of olivine and plagioclase components (Fe/(Fe+Mg) = 0.11) has been identified. Its high MgO and Al_2O_3 contents, low CaO/Al_2O_3 (0.65) and low Ni ($\lesssim$ 25 ppm) concentrations are consistent with its origin in the lunar highlands crust through mixing of the plagioclase and high-Mg primitive components [8]. Alternatively, it

LUNA 24 HIGHLAND COMPONENT

Bence, A. E. *et al.*

may represent a shock melt of residuum remaining after partial melting within the crust.

Lithic fragments (annealed breccias and possible plutonic fragments) are exceedingly rare. Two fragments with coexisting low and high Ca pyroxenes occur in our samples. These pyroxenes are clearly more magnesian than the most magnesian of the local mare pyroxenes (Fig. 2) and fall near the Mg end of the field of pyroxenes from other highland localities. One of the fragments contains coexisting orthopyroxene ($Wo_{1.5}En_{68.0}Fs_{30.5}$) and calcic clinopyroxene ($Wo_{41}En_{45}Fs_{14}$). The coefficient for Fe/Mg partitioning between these phases is 0.68 (K_d as defined by Lindsley *et al.* [9]). This is consistent with an equilibration temperature of $\sim 810^{o}C$ [9]. Both lithic fragments contain plagioclase (An_{94-96}) and the minor element contents of both pyroxenes and the plagioclases have been used as aids in the recognition of highland monomineralic fragments. The highland pyroxenes are, in addition to higher Mg/(Mg+Fe), characterized by higher Cr and lower Ti than the local mare pyroxenes (Fig. 3). The dominant others components are $Cr\text{-}Al^{IV}$ and $Al^{VI}\text{-}Al^{IV}$ (Fig. 4). Highland plagioclases can be distinguished from the local mare plagioclases by the combination of high An content (An_{94}), low Fe and negligible Mg [10].

Although our sampling is extremely small and our statistics poor, we can make two important observations concerning the highland component at the LUNA 24 drill site. It has (1) a very low KREEP content and (2) a strong chemical similarity to the highland material returned by LUNA 20.

References

[1] *Florensky, C. P., et al., PLSC 8th, in press, 1977;* [2] *Vaniman, D. T. and J. J. Papike, GRL, in press, 1977;* [3] *Bence, A. E., et al., GRL, in press, 1977;* [4] *Walker, D., et al., EPSL, 20, 325-336;* [5] *Irving, A. J., PLSC 6th, 363-394, 1975;* [6] *Ridley, W. I., PLSC 6th, 131-145, 1975;* [7] *Walker, D., et al., PLSC 3rd, 797-817, 1972;* [8] *Taylor, S. R., and A. E. Bence, PLSC 6th, 1121-1141, 1975;* [9] *Lindsley, D. H., et al., GRL, 134-136, 1974;* [10] *Grove, T. L. and A. E. Bence, this volume, 1977.*

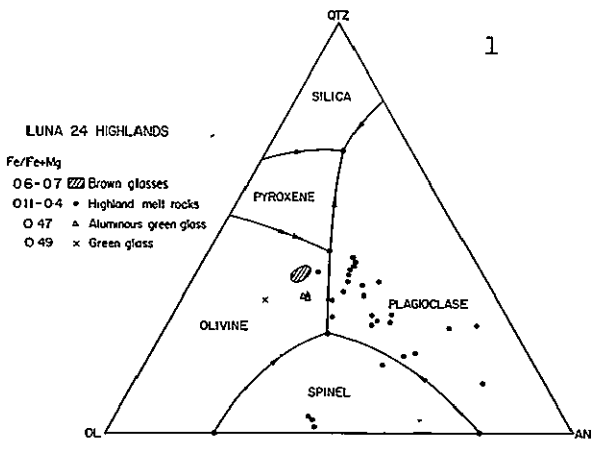

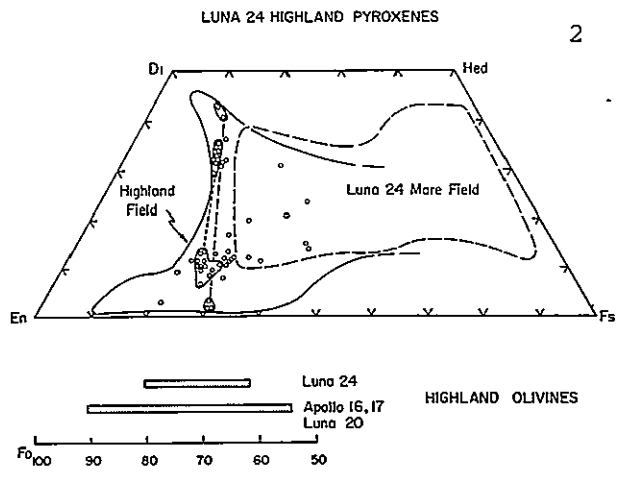

LUNA 24 HIGHLAND COMPONENT

Bence, A. E. et al.

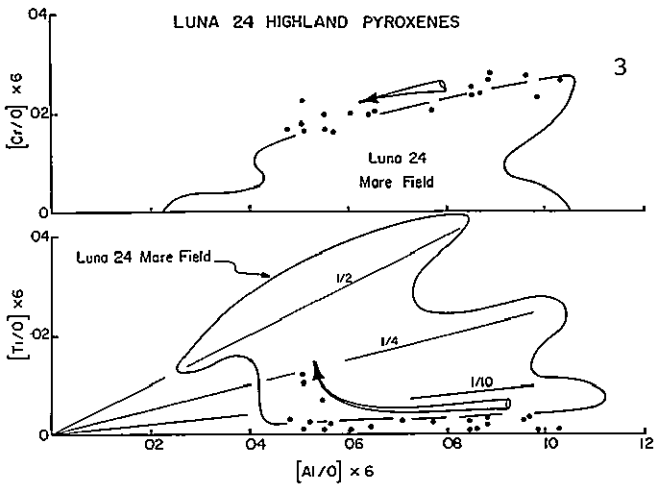

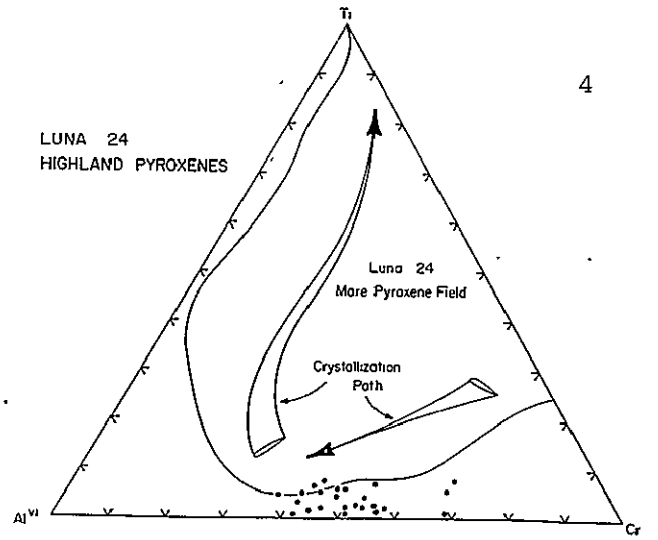

RADIOACTIVITY AND MORPHOLOGY OF LUNA 24 SAMPLES.
N. Bhandari, J.T.Padia, M.B.Potdar and V.G.Shah, Physical Research Laboratory, Ahmedabad 380 009, India.

Cosmic ray induced ^{26}Al and natural ^{232}Th have been measured in the 87 cm layer taken from the Luna 24 core. In addition grains from six 1cm thick strata taken from 87,123,148,163,179 and 190 cms have been examined under a scanning electron microscope for their morphology and chemistry. For a comparative study grains from Luna 16 and 20 samples have also been examined. The preliminary results are presented here.

24087, a sample taken from 86-87 cm depth of the Luna 24 core has been analysed for ^{26}Al and ^{208}Tl. The measurement was performed by direct counting of 162 mg sample on a β-γ coincidence spectrometer following the technique described earlier(3). The counting details and results are given in Table 1 for 24087 and Apollo 16 scoop 67481. The positron(.511 MeV) peak, after due correction for U,Th daughter products, is attributed to (^{26}Al + ^{22}Na) whereas .580 MeV peak is due to ^{208}Tl, the daughter product of ^{232}Th. Since Apollo 16 soil was collected 5 years ago, the ^{22}Na contribution to the positron peak is mostly (96%) due to ^{26}Al, whereas in Luna 24 collected on 18th August, 1976, the ^{22}Na contribution to positron peak is about 11% if the following compositions are assumed : Apollo 16: Mg = 3.9%, Al = 13.9%, Na = 0.32%, Si = 21.2%; Luna 24: Mg = 6.25%, Al = 8%, Na= 0.25%, Si = 19.7%. The Apollo 16 composition was taken from an analysis of similar soils, whereas Luna 24 is somewhat arbitrary and based on available descriptions of the sample(1). The chemical analysis is in progress and actual composition should shortly become available. Using these compositions and solar and galactic cosmic ray fluxes, given by Bhandari et al(3) and Reedy and Arnold(5) respectively, we have calculated the depth profile of ^{26}Al and ^{22}Na. Figure 1 shows (^{26}Al + ^{22}Na) as expected at the (mean) time of counting. The observed activity is also shown in this figure. Although the statistical errors so far are large, they lead to the inference that the average depth on lunar surface was 3 ± 1.5 cms for the scoop sample 67481 and >35 cms for 24087, assuming the core density of 1.8 g cm^{-2}. Since the upper 60 cms of the Luna 24 core was empty(2), the actual depth of the core on the moon is debatable. The 86-87 cm strata could either refer to about 26-27 cms on the moon if the soil top in the core is the lunar top or 87 cm if the upper 60 cms of the lunar top is not contained in the tube. Our results indicate that atleast the upper 12 cm has been lost. ^{232}Th in this soil is estimated to be $1.5\pm.4$ ppm.

Other studies in the core relate to morphological and chemical studies using SEM and X-ray techniques. For a comparative study we have also examined Luna 16 and 20 soils. In Luna 20 we

RADIOACTIVITY AND MORPHOLOGY

Bhandari, N. et al.

TABLE-1 : COUNTING DATA

Soil	Depth (cms)	Sample weight (mg)	Deposited area (cm^2)	Total counting time (Minutes)	GROSS COUNTS CPT 0.511 MeV	GROSS COUNTS CPT 0.580 MeV	$^{26}Al + ^{22}Na$ Net CPT	$^{26}Al + ^{22}Na$ dpm/kg
24087,1	86-87 In core	162	2.35	30,056	4.2±0.4	2.1±0.3	0.59±0.48	57±45
67481,7	Scoop	228	2.35	8,870	6.2±0.8	1.6±0.4	3.1±0.95	245±75
BACKGROUND	-	-	5.25	15,840	2.3±0.3	0.9±0.2	-	-

CPT = Counts per thousand minutes.

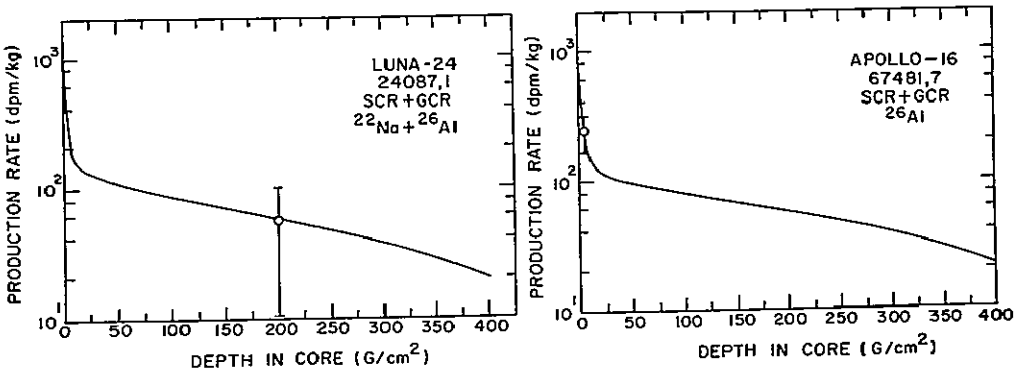

Fig. 1

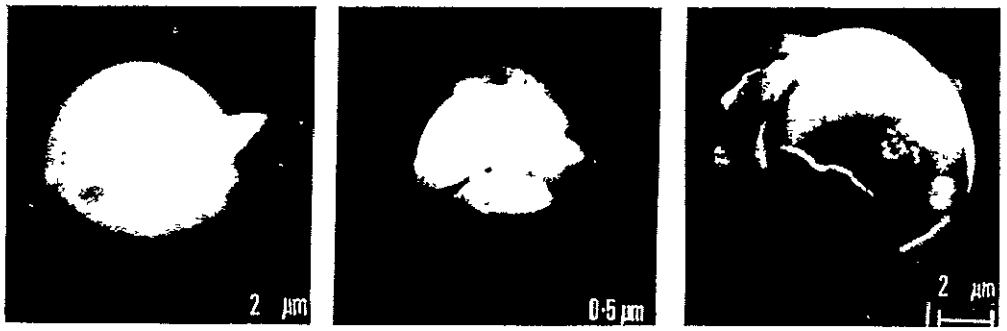

Fig.2

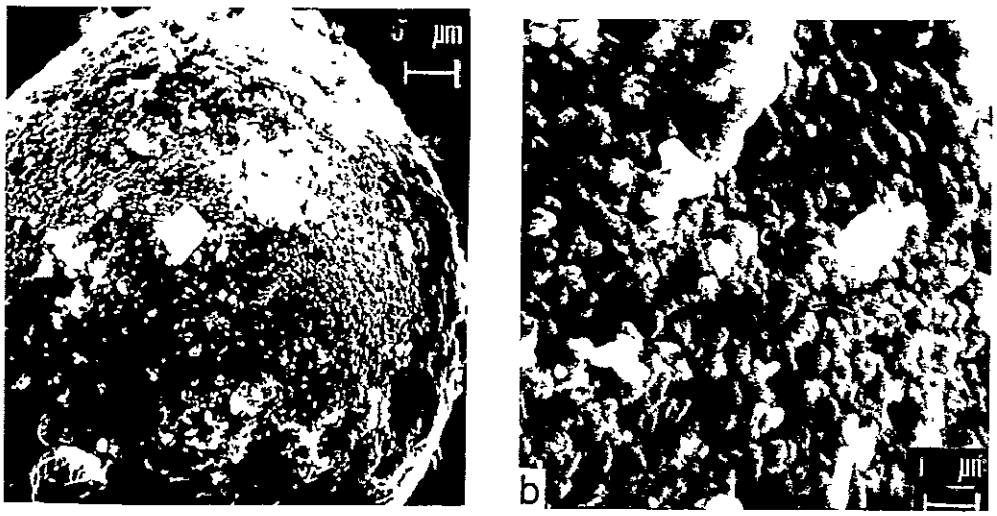

Fig.3

have found some microspheres, cenospheres (hollow spheres) and platelets, a few microns in size, which are extremely rich in potassium. These are shown in Fig.2. No element other than potassium with $Z \gtrsim 11$ has been detected. Since the detection technique is insensitive to lighter elements ($Z < 11$), exact chemical nature of the spheres could not be ascertained so far. Carter(4) has reported growth of K-rich globules on Apollo 15 lunar samples, but they appear to be different from spherules observed here. So far none of the Luna 24 or Luna 16 samples have shown presence of such K-rich spherules. Morphological studies reveal several silicate spherules in Luna 24. A typical case from 24179 is shown in Fig.3, with a peculiar surface texture. These studies are currently in progress.

We are grateful to the U.S.S.R. Academy of Sciences for kindly providing us with Luna 24 samples.

References

1. Barsukov, V.L. and Florensky, C.P. (1977a) Lunar Science VIII, p.59.

2. Barsukov, V.L., Ivanov, A.V., Nasarova, M.A., Rode, O.D., Stakeev, V.I., Tarasov, L.S., Tobelko, K.I. and Florensky, C.P. (1977b) Lunar Science VIII, p.67.

3. Bhandari, N., Bhattacharya, S.K. and Padia, J.T. (1975) Proc. Lunar Sci. Conf. 6th, p.1913.

4. Carter, J.L. (1973) Proc. Lunar Sci. Conf. 4th, p.413.

5. Reedy, R.C. and Arnold, J.R. (1972) J. Geophys. Res. 77, p.537.

Captions

Fig.1 Depth profiles of (^{26}Al + ^{22}Na) in Luna 24 and Apollo 16 soil, corrected for decay to the time of measurement. For solar flare particles $(J, R_o) = (140, 150)$ are assumed(3) and for galactic cosmic rays the flux of 1.7 $P/cm^2.sec$ 4π, >1 GeV is taken from Reedy and Arnold(5).

Fig.2 Potassium-rich microspheres and platelets in Luna 20 sample. The middle micrograph shows a possible cenosphere.

Fig.3 A silicate spherule in Luna 24 sample taken from 179 cms depth(a). The surface structure is shown with high resolution in (b).

CORRELATION OF CHEMISTRY WITH NORMAL ALBEDO IN THE CRISIUM REGION. Michael J. Bielefeld, Computer Sciences Corp., Silver Spring, MD 20910, Robert L. Wildey, Dept. of Physics and Astronomy, Northern Arizona University, and U. S. Geological Survey, Flagstaff, AZ 86001 and Jacob I. Trombka, Goddard Space Flight Center, Greenbelt, MD 20771

The correlation between normal albedo as measured from earth and the Al/Si fluorescent X-ray intensity ratio as measured by the orbital Apollo experiments has been noted by Adler (1,2) and treated recently in detail by Clark (3) for the Tranquillity/Serenity region. However, recent advances by the La Jolla Consortium in conjunction with the U. S. Geological Survey, Flagstaff in the standardization of multiple lunar data sets have made correlation among parameters much easier. We present here the correlation of normal albedo with the geochemical parameters of Al/Si and Mg/Al from X-ray for the vicinity of the LUNA 24 landing site, viz., 40-70°E, 0-20°N. A description of the preparation of the albedo data set is given by Wildey (4) and of the X-ray data set is presented by Bielefeld (5) and Andre(6).

Figure 1 depicts the area of comparison along with false color images of the areal differentiation of albedo and the chemical parameters of Mg/Al and Al/Si ratios by weight. The colors were chosen to accentuate the correlation between albedo and chemistry under the constraints of the color Xerox technology. The reader is reminded of the caveat that false color can over-emphasize the contrast between small variations in gray levels at color boundaries while dampening small changes in gray levels within the boundaries. Note that red corresponds to high values for albedo and Al/Si, but low, for Mg/Al. If Si is assummed to have a constant concentration, the Crisium basin can be seen to have a uniform albedo and a relatively uniform Al concentration. A major deviation from the low-albedo-low-Al rule of thumb is in thePeirce region of the basin where the high Al of the adjacent highland ring extends far into the basin. There is much more variation in the Mg content of the basin. Maria Crisium, Fecunditatis, Undarum and Spumans are colored sea blue. Note the difference between the Al content the craters Firmicus and its neighbor Apollonius near the LUNA 20 site.

Figures 2 and 3 exemplify one method of intercomparison of the multiple data sets in the La Jolla Consortium. They are a two component frequency distribution of the gray level values within an image of common coverage. Some 7000 $\frac{1}{4}^{o} \times \frac{1}{4}^{o}$ regional units, which comprise the image in Figure 1 where there is common coverage, are positioned on the arrays in Figures 2 and 3 according to the intensity value of each of the components. The frequency of occurrence of the same values is reflected in the height of the 3-D plot. For example, in the Crisium region there are no areas with very high albedo but low Al/Si ratio, whereas,

there is a major component of low albedo, low Al/Si material. The plots along the axes are not projections but frequency histograms of all the values of each component considered separately.

Figure 2 clearly depicts the strong correlation between albedo and Al content of the surface material. In terms of linear regression analysis, the correlation coefficient for over 7000 points is 0.70. Quantitatively, the points following the regression line can be related by the expression:

$$(Al/Si) = -0.51 + 8.34\ (albedo).$$

The frequency histogram for the Al/Si values in the Crisium does not show the clear bimodality for the complete Al/Si data set (5,6) mainly because the eastern maria, Crisium and Fecunditatis, are more aluminous. Deviations from the correlation are more interesting than the correlation itself. Some of the reasons for these deviations are discussed by Clark (3).

Figure 3 shows an anti-correlation between albedo and the Mg/Al ratio with a correlation coefficient of 0.77. The anti-correlation is dominated by the 1/Al factor. However, the effect of Mg content is seen in the shift in the Mg/Al frequency histogram to lower values with a peak around 0.40. This peak corresponds to the yellow in the Mg/Al image in Figure 1.

The next step in this analysis which will hopefully extract the deviations from the correlations in a meaningful manner will follow the lines of unsupervised multi-component classification.

Acknowledgement: We are please to acknowledge Walter C. Shoup for many helpful discussions concerning data presentation. This work was entirely supported by NASA.

References:

(1) Adler, I., et al., (1972) Proc. Lunar Sci. Conf. 3rd, p.2157-78.
(2) Adler, I., et al., (1973) Proc. Lunar Sci. Conf. 4th, p.2783-91.
(3) Clark, P. E., et al., (1976) Geophys. Res. Letters, 3, p.421-24.
(4) Wildey, R. L. (1977) The Moon, 16, p.231-77.
(5) Bielefeld, M. J., et al., (1977) Proc. Lunar Sci. Conf. 8th, in press.
(6) Andre, C. G., et al., (1977) Science, 197, p.986-89.

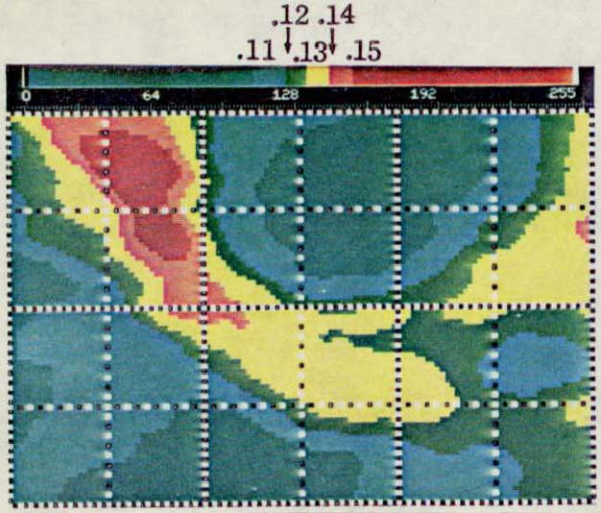

NORMAL ALBEDO
(Wildey, La Jolla Consortium)

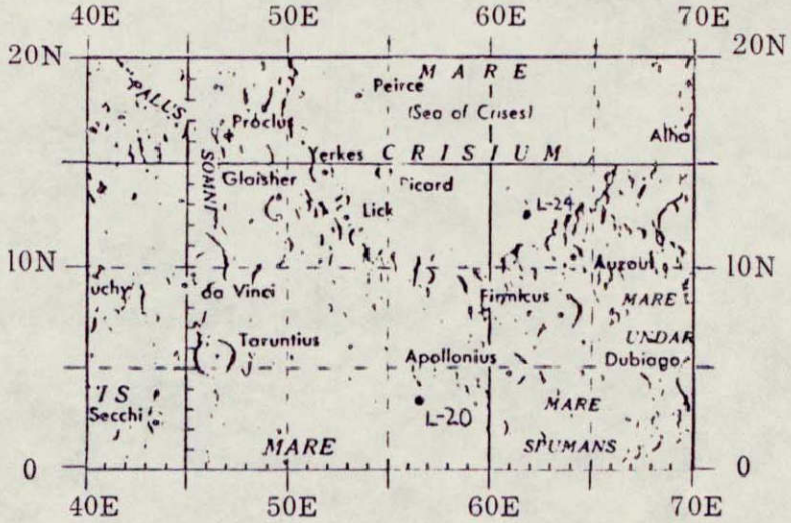

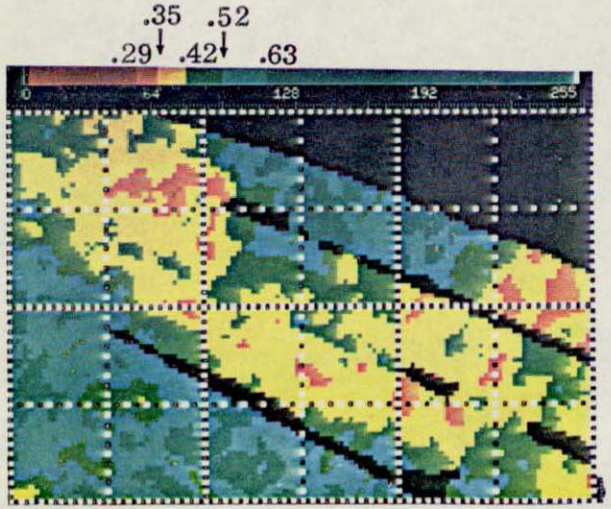

X-RAY Mg/Al CONCENTRATION RATIO
(Bielefeld et al., La Jolla Consortium)

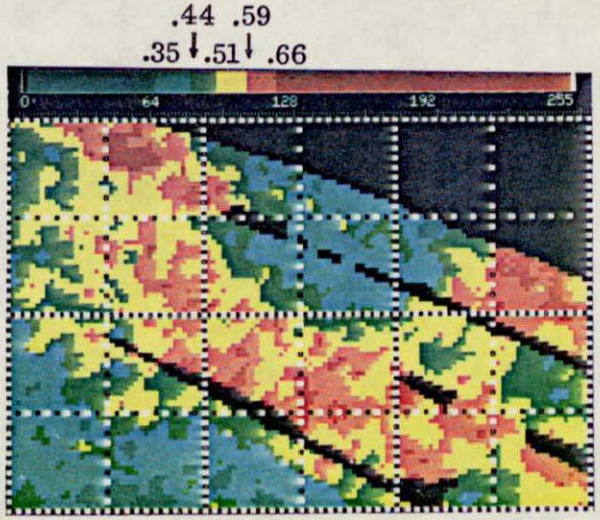

X-RAY Al/Si CONCENTRATION RATIO
(Bielefeld et al., La Jolla Consortium)

Fig. 1. MARE CRISIUM REGION

CORRELATION OF CHEMISTRY WITH NORMAL ALBEDO

Bielefeld, M. J., et al.

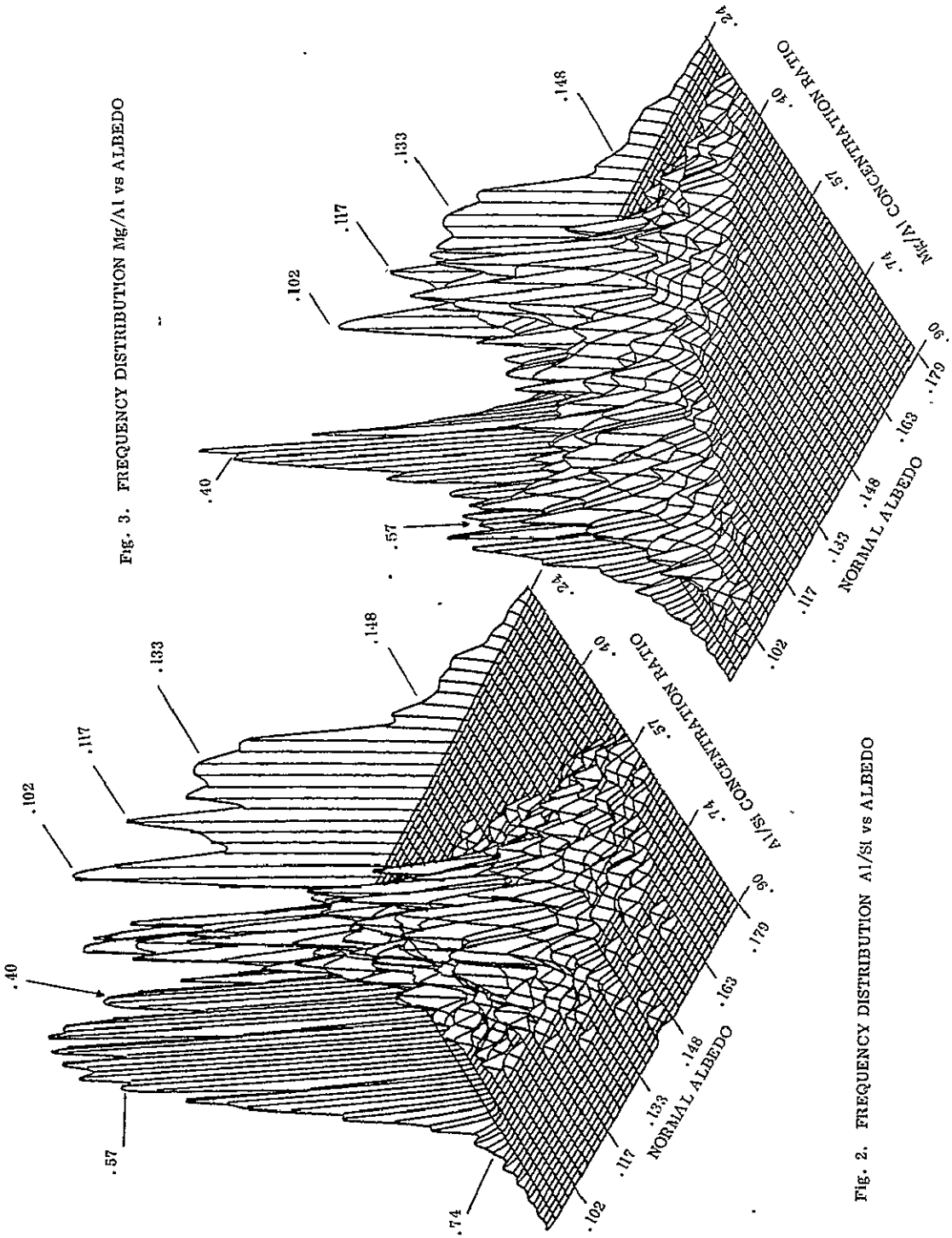

Fig. 3. FREQUENCY DISTRIBUTION Mg/Al vs ALBEDO

Fig. 2. FREQUENCY DISTRIBUTION Al/Si vs ALBEDO

$^{87}Rb/^{87}Sr$ AGE OF LUNA 24 MICROGABBROS, AND ISOTOPIC AND TRACE ELEMENT STUDY OF SOIL 24096.

Birck J.L. Manhes G., Richard P., Joron J.L., Treuil M., Allegre C.J.
Lab. Geochimie et Cosmochimie, Univ. P VI et PVII, 75005 Paris France.

We have analyzed two soils from Luna 24 mission at levels 96 and 154, and microgabbros pieces from level 171.

Sample 24171 is believed to be a crushed rock from the bed rock of Mare Crisium (1). An $^{87}Rb/^{87}Sr$ isochron of 30 mg. of this sample has been obtained. It includes both hand picked and heavy liquid (methylene iodide) separates of plagioclase and pyroxene, and gives an age of 3.74 $\pm$ 0.28 ($\lambda = 1.39\ 10^{-11} y^{-1}$), and $^{87}Sr/^{86}Sr = 0.69909 \pm 3$ (1σ errors).

This age is in good agreement with the $^{39}Ar^{40}Ar$ age at 3.66 $\pm$ 0.12 by. of a 10 mg. microdolerite sample (a probable impact melt) from soil 24096 (2). These results place the age of formation of Mare Crisium well within the range of ages of lunar Mare basalts. If the 3.7 by. value is correct, this age is older than the late Imbrium age which was expected (3). The precisely defined initial ratio, similar to Luna 16 value (4), is amongst the lowest Mare basalt initial ratio. This indicates both a low Rb/Sr ratio of the source of these basalts and a low contamination by a more radiogenic crust.

A lead, strontium, neodymium and potassium isotopic analysis and trace element study of soil 24096 have been achieved. This soil is expected to more or less represent the 2nd unit of Luna 24 core (5).

$^{87}Sr/^{86}Sr$ isotopic composition has been measured twice at 0.70042 $\pm$ 7 and 0.70032 $\pm$ 5. This value places 24096 amongst the least radiogenic lunar soils, and well on teh 4.6 by. isochron of lunar soils. This soil is however more radiogenic than 24171 and indicates the presence of a radiogenic component in the soil.

The corrected values of lead isotopic compositions of soils 24096 and 154 are given in table 1. They are similar to the one of Luna 16 and 20 soils (6). The identical discordance of these two Luna 24 soils suggests a perturbation of the U-Pb system anterior to the setting up of these levels, although they

$^{87}Rb/^{87}Sr$ AGE OF LUNA 24 MICROGABBROS.

Birck J.L. et al.

are situated in different units of the core (unit II and III respectively ,5).

The Nd isotopic composition and Sm and Nd concentrations have been measured in 24096 (table 2). The nearly chondritic Sm/Nd ratio prevents any study of two stage models such as described in (7). The model age of 24096, relative to $^{143}Nd/^{144}Nd_{Juvinas} = 0.50598$ is 4.55 10^9y. As for the Rb/Sr system, this result is believed to date the early lunar differentiation. It seems possible to obtain a Sm/Nd isochron of Lunar soils to date this event. Such an analysis would palliate the possible Rb volatilization effects.

Trace element concentrations have been obtained by isotope dilution (K, Rb, Sr, U, Pb, Sm, Nd) and INAA in 24096. This soil is amongst the poorest lunar soil in LIL elemnts, similar to A 67460 (8). The REE pattern is flat (9x chondritic) and presents a small positive Eu anomaly. If this composition is discussed in terms of components, as compared to Luna 16 and 20 soils (9), this soil can be described qualitatively by a larger amount of the anorthositic component. In order to satisfy the similitude of lead and strontium isotopic compositions of these soils, the amount of the radiogenic KREEP component cannot be much smaller in 24096. The siderophile element concentrations of 24096 and Luna 16 soils are similar and indicate a same amount of the meteoritic component.

Finally the potassium isotopic composition of 24096 has been analyzed. Whereas the $^{39}K/^{41}K$ ratio is close to the terrestrial value (13.857), the $^{40}K/^{41}K$ ratio is significantly lower than the terrestrial value of 576.3 $\pm$ 0.8. Assuming that this is due to secondary neutron effects on ^{40}Ca, one can correct against mass discrimination through the $^{39}K/^{41}K$ ratio, and obtain a value of $^{40}K/^{41}K = 557.2 \pm 2.2$. Assuming a ^{40}K production rate half of the one of Norton County (10) (due to shielding effect at the surface of the moon), and an exposure age of this meteorite of 72 My., one can calculate an exposure age of 24096 of 475 $\pm$ 75 My., in good agreement with the value at 660 My. obtained by rare gas measurements (2).

$^{87}Rb/^{87}Sr$ AGE OF LUNA 24 MICROGABBROS

Birck J.L. et al.

Table 1	Weight mg.	Concentrations Pb	U ppm	Corrected Comp. α	β	γ	206/238	207/235
24096	37	0.507	0.126	75.3	57.9	90.2	1.369	136.1
24154	38	0.320	0.088	120.9	90.5	131.5	1.353	133.9

Table 2	Weight mg.	$^{147}Sm/^{144}Nd$	$^{143}Nd/^{144}Nd$	Sm(ppm)	Nd(ppm)
24096	29.3	0.1883	0.51166 ± 14	1.89	6.06

Table 3	K	Rb	Sr	Ba	La	Eu	Tb	Hf	Zr	Ta	U	Th
24096	440.	1.04	142.	37.	2.7	0.68	0.41	1.49	54.	0.19	0.13	0.43

Sc	Cr	Co	Ni
40.2	2494.	52.9	195.

1) Ryder G., MsSween H.Y., Marvin U.B., (1977) Submitted to Moon. 2) Stettler A. Albarede F., (1977) preprint. 3) Wilhelms D.E. (1973) Nasa special Pub. SP 330, 29. 4) Papanastassiou D.A., Wasserburg G.J. (1972) E.P.S.L. 13,368 5) Barsukov V.L., Ivanov A.V., Nazarov M.A., Rode O.D., SKakeev I., Tarasov L.S Tobelko K.I., Florensky C.P. (1977) Lunar Sci. VIII Lunar SCience Inst. 67, 69. 6) Tera F. Wasserburg G.J. (1972) E.P.S.L. 13,467.. Manhes G. unpublished res. 7) Lungmair G.W., Marti K., Kurtz J.P., Scheinin N.B. (1976) Proc. Lunar Sci. Conf 7th, 2009. 8) Boynton W.V. Chen C.L., Robinson K.L., Warren P.H. Wasson J. (1976) Proc. Lunar Sci. Conf. 7th, 727. 9) Loubet M., Birck J.L., Manhes G. Allegre C.J. (1972) C R Acad Sci. Paris 274, 158. Loubet M. Birck J.L. Allegre C.J. (1972) E.P.S.L. 17,19. 10) Burnett D.S. Lippolt H.J. Wasserburg G.J. (1966) J.G.R. 71, 1249.

CHEMISTRY OF SOILS AND PARTICLES FROM LUNA 24. Douglas P. Blanchard[1], Larry A. Haskin[2], Joyce C. Brannon[2,3], and Erik Aaboe[4]. ([1]NASA Johnson Space Ctr., Houston, TX; [2]Washington Univ., St. Louis, MO; [3]Lockheed Electronics Co., Houston, TX; [4]Lunar Science Institute, Houston, TX 77058)

We have analyzed 6 soils and 5 small particles from Luna 24. Major element compositions were determined by atomic absorption spectrophotometry; trace element compositions by instrumental neutron activation analysis (1). Results are given in tables 1 and 2. The same soil fractions and particles were also studied by other investigators (2-8).

Our 6 samples of Luna 24 soils have very similar compositions, with respect to both bulk compositions and compositions of corresponding size fractions. However, within any single soil there is rather severe elemental fractionation among the size separates. The clear implication is that the soils in the core are well mixed with each other, although not internally homogeneous. Average compositions and sample standard deviations given in tables 1 and 2 indicate that variations between soils are usually less than 10%. Only soil 24210 shows any discernible compositional variation. The soils have low TiO_2 compared to our expectations based on their otherwise basaltic composition (FeO=20-21%).

The particles we have analyzed have a wide range of compositions. Samples 24077,21 and 24149,5 are described as an agglutinate and a soil breccia respectively (9) and in most respects their compositions closely approximate those of the bulk soils. 24077,19 is a plagioclase grain with mare basalt affinity (6). 24174,5 is a pyroxene-rich gabbro (9); this fragment has basalt affinity but is most likely not a representative sample of the parent rock. 24077,17 is a recrystallized breccia (9). Its composition is remarkably identical to that of the gray matrix of breccia 73215 (11). Materials of this composition are widely interpreted as impact-generated, clast-laden melts from a large basin-forming event, presumably the Serenitatis event. Such an impact event could have easily transported this type of material to the Luna 24 site.

We have investigated the details of the compositional make-up of the Luna 24 soil by analyzing the 90-150 μm and <20 μm size fractions. There are large differences in composition between these two size fractions. Two of the more probable mechanisms which could result in elemental partitioning of this magnitude among grain sizes are differential comminution and mixing of materials which are compositionally distinct and also have different grain size distributions. Korotev and Haskin (10,12) have shown that simple crushing of a lunar basalt (70135) will produce grain size fractions (especially the <20 fraction) with compositions quite unlike that of the parent material. Appropriate comparisons of their data and the averaged Luna 24 soils are given in Table 3. Within the considerable uncertainties of comparing these two materials, the resemblance of the elemental partitioning is quite striking. Thus, while there is strong evidence that mixing of components with different compositions and grain size distributions is essential to produce the partitioning observed in Luna 24 soils, comminution causes partitioning in the same direction so that estimating the quantitative proportions of mixing is complicated by the possible effects of differential comminution. With this caveat we discuss mixing relationships in the Luna 24 soils.

Several lines of evidence lead us to the conclusion that the Luna 24 soils are mixes of two or more components. The soils have bimodal size distributions

CHEMISTRY OF SOILS AND PARTICLES FROM LUNA 24

Blanchard, D.P. et al.

(4) quite unlike that predicted for a single component soil. The bulk soils have surface exposure indices typical of an immature to submature soil (3,4,5), however, a plagioclase component in the soils is saturated by particle tracks (2). Apparently an old, mature component has been diluted by fresh immature material. The <20 μm soil fraction probably did not derive directly from the bulk soil. Comminution by meteorite bombardment adds meteoritic metal preferentially to the finest fractions; when Co and Ni are subtracted from the <20 fraction in meteoritic proportions, the resultant composition does not coincide with the bulk soil (Fig. 1). We note that extrapolation to low Ni values would pass within analytical uncertainty through a component with Ni-Co like that of 24174,5. The finest fractions (<20 μm) should be enriched in the more mature component because it should have a smaller mean grain size. Similarly, the fresh, coarse material should be somewhat enriched in 90-150 μm fraction. The 90-150 μm fractions are very similar to the bulk soils, thus by the above reasoning the major component of the soil is probably the relatively fresh component. If the composition of the 90-150 μm fraction is typical of the local basalt, then this basalt is richer in FeO than any of the Luna 24 soil components (clusters of glass analyses) identified by (13). If the local basalt has lower FeO than the bulk soil, then an additional high FeO component is required to complete the mass balance. The <20 fractions are enriched in REE relative to the bulk soils (Fig. 3). Small amounts (3-5%) of material like recrystallized breccia 24077,17 added to the composition of the 90-150 fraction can easily account for the REE abundances in the bulk soil. We note that the <20 fractions do not lie on simple mixing lines between bulk soils and 24077,77 type material, thus an additional component low in both REE and FeO is also required. We have little evidence to identify this component other than the tenuous relationship between the <20 μm fractions and the pyroxene gabbro chip (Fig. 1) which has been discussed above.

We have used the composition of 24077,19 and distribution coefficients from (10) to model possible parent liquids for this basaltic plagioclase grain. Calculated pattern A on Fig. 3 is the simple equilibrium liquid. Pattern B is the other extreme of totally closed system crystallization. Patterns C and D represent closed system models that allow for 0.2% and 2.0% mesostasis, the range of mesostasis normally found in mare basalts. We conclude that in no way is it possible to derive this plagioclase from a liquid with a positive Eu anomaly (even using extreme values for D^{Eu}). Secondly, the liquid is clearly mare basalt-like in its relative REE abundances. We note that if plagioclase were a late crystallizing phase, the original magma may have had lower absolute abundances than suggested by C and D.

Table 3. Size fraction composition ratios.

	70135 <20/<500	Luna 24 <20/<250	70135 90-150/<500	Luna 24 90-150/<250
	Ref. 12		Ref. 12	
FeO	0.88	0.80	1.02	1.01
Na_2O	1.38	1.36	0.90	0.93
Cr_2O_3	0.96	0.87	0.96	0.81
Sc	0.79	0.70	1.02	1.03
Co	1.06	0.89	0.92	1.02
Hf	1.03	1.25	0.96	0.69
Th	>2.3	2.03	1.0	--
Ta	1.12	--	0.88	--
La	1.92	1.67	0.98	0.97
Ce	1.70	1.47	0.95	0.74
Sm	1.59	1.42	0.98	0.81
Eu	1.45	1.32	0.94	0.87
Tb	1.37	1.33	0.96	0.88
Yb	1.07	1.22	0.99	0.92
Lu	1.00	1.14	1.00	0.89

CHEMISTRY OF SOILS AND PARTICLES FROM LUNA 24

Blanchard, D.P. et al.

REFERENCES: 1) Jacobs et al. (1977) J. Radioanal. Chem., in press. 2) Blanford and Wood (1977) this volume. 3) Bogard and Hirsch (1977) ibid. 4) McKay et al. (1977) ibid. 5) Morris (1977) ibid. 6) Keil et al. (1977) ibid. 7) Nyquist et al. (1977) ibid. 8) Taylor et al. (1977) ibid. 9) Luna 24 Catalog. 10) Haskin and Korotev (1977) GCA 41, 921-939. 11) Blanchard et al. (1976) PLSC 7th, 2179-2187. 12) Korotev (1976) PLSC 7th, 695-726. 13) Simonds et al. (1977) this volume.

Table 1. Luna 24 Regolith Major Element Chemistry

	SiO_2	TiO_2	Al_2O_3	FeO	MgO	CaO	Na_2O	K_2O	Cr_2O_3	Total
24077	45.9	0.9	11.8	19.9	9.7	11.2	0.29	0.03	0.56	100.3
24109	44.1	1.0	11.3	20.6	10.3	11.0	0.27	0.02	0.62	99.2
24149	44.6	1.3	11.0	20.3	10.1	10.8	0.28	0.03	0.48	98.9
24174	45.5	0.9	11.1	20.9	9.7	10.8	0.29	0.03	0.49	99.7
24182	44.5	1.3	11.5	20.2	10.0	11.1	0.29	0.04	0.50	99.4
24210	47.6	1.0	9.7	21.1	11.3	10.8	0.25	--	0.45	102.2
Average ± S	45.4 1.3	1.1 0.2	11.1 0.7	20.5 0.5	10.2 0.6	11.0 0.2	0.28 0.02	0.03 0.01	0.52 0.06	100.1

Table 2. Luna 24 regolith and particle trace element chemistry.

		FeO	Na_2O	Cr_2O_3	Sc	Co	Ni	Hf	Th	Ta	La	Ce	Sm	Eu	Tb	Yb	Lu
24077	bulk	19.9	.290	.56	41.1	50.9	160	1.5	.41	---	3.10	8.9	2.00	.66	.49	1.76	.273
	90-150	20.1	.321	.52	43.2	61.0	230	1.0	---	---	2.51	7.0	1.66	.61	---	1.8	.25
	<20	16.3	.57	.46	30.5	47.0	430	2.1	.66	---	4.35	10.3	2.57	.83	.64	2.04	.31
24109	bulk	20.6	.272	.62	43.4	52.5	230	1.36	.25	---	3.22	9.7	2.04	.65	.49	1.78	.272
	90-150	20.7	.234	.41	45.8	51.0	---	1.0	---	---	2.38	6.9	1.69	.54	.36	1.55	.22
	<20	16.5	.341	.46	31.5	46.7	400	1.8	.53	---	5.2	11.9	2.73	.81	.65	2.24	.31
24149	bulk	20.3	.282	.48	43 0	50.7	100	1.9	.26	---	2.32	7.3	1.73	.60	.40	1.63	.263
	90-150	19.5	.250	.39	42.4	47.0	---	1.0	---	---	2.05	6.4	1.45	.53	.6	1.61	.23
	<20	16.8	.359	.45	30.6	44.2	380	2.2	.57	---	4.43	12.0	2.64	.81	.63	2.21	.31
24174	bulk	20.9	.287	.49	43.9	50.4	130	1.47	.24	---	2.74	8.5	1.95	.63	.46	1.85	.299
	90-150	20.9	.255	.39	45.4	48.0	---	1.2	---	---	2.10	6.5	1.49	.52	.40	1.56	.26
	<20	16.8	.352	.46	31.4	45.6	430	2.1	.7	.29	5.0	13.0	2.90	.89	.65	2.26	.35
24182	bulk	20.2	.295	.50	42.3	48.4	90	1.6	.40	---	3.24	9.9	2.09	.70	.56	1.93	.296
	90-150	20.8	.262	.38	45.8	50.0	90	1.2	---	---	2.07	6.0	1.58	.55	.45	1.80	.28
	<20	16.7	.377	.45	30.4	46.0	350	2.3	.67	.27	5.8	17.3	3.35	.92	.75	2.55	.367
24210	bulk	21.1	.252	.45	44.6	53.0	---	1.5	.3	---	2.64	6.8	1.74	.54	.51	1.81	.27
	90-150	22.2	.237	.44	44.6	56.0	140	1.3	---	---	2.14	5.8	1.48	.54	.36	1.56	.24
	<20	15.0	.310	.44	27.3	42.3	270	1.7	---	---	3.95	10.3	2.23	.69	.58	1.85	.29
Average	bulk	20.5	0.28	0.52	43.1	51.0	140	1.6	0.31	---	2.55	8.53	1.93	0.63	0.49	1.80	0.26
	± S	0.5	0.02	0.06	1.2	1.6	60	0.2	0.08	---	0.37	1.26	0.15	0.06	0.05	0.11	0.02
Average	90-150	20.7	0.26	0.42	44.5	52.1	150	1.1	----	---	2.27	6.30	1.56	0.55	0.43	1.65	0.25
	± S	0.9	0.03	0.05	1.4	5.3	70	0.1	----	---	0.19	3.75	0.10	0.03	0.10	0.12	0.02
Average	<20	16 4	0 38	0.45	30.3	45.3	380	2.0	0.63	---	4.80	12.5	2.74	0.85	0.65	2.19	0.32
	± S	0.7	0.09	0.01	4.2	1.8	60	0.2	0.07	---	0.66	2.6	0.37	0.08	0.06	0.23	0.03
24077,19 Plag-rich gabbro		0.77	0.63	0.018	1.76	2.04	20	0.79	---	----	0.45	1.30	0.21	0.84	---	0.10	>0.009
24077,17 Recryst. Breccia		7.60	0.66	0.184	13.3	20.2	180	9.9	1.4	4.8	24.9	68	12.1	1.74	2.9	9.7	1.40
24077,21 Agglutinate		16.3	0.31	0.46	36.4	46	160	1.0	---	---	2.6	7.0	1.6	0.58	0.38	1.4	0.22
24149,5 Soil Breccia		20.3	0.27	0.51	47	50.7	150	1.3	---	0.3	2.8	9.2	2.0	0.59	0.43	1.75	0.29
24174,5 Px-rich gabbro		16.6	0.38	0.20	35.8	29.7	n.d.	0.88	---	---	0.86	2.33	0.80	0.70	0.20	0.96	0.17

CHEMISTRY OF SOILS AND PARTICLES FROM LUNA 24

Blanchard, D.P. et al.

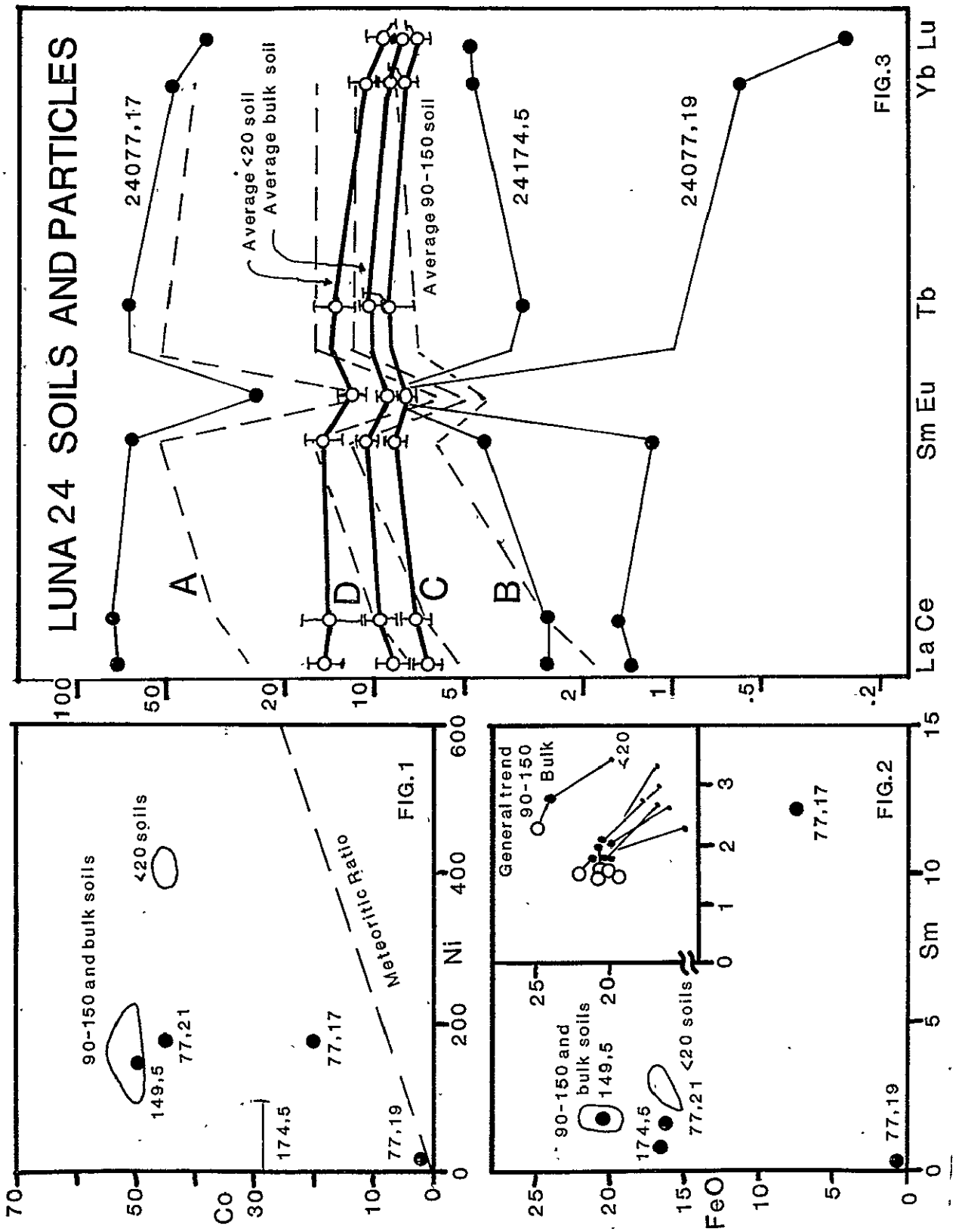

PARTICLE TRACK DENSITIES IN THE LUNA 24 CORE. G. E. Blanford and G. C. Wood, University of Houston at Clear Lake City, Houston, TX 77058

Correlated studies have been made on a set of six Luna 24 core samples (24077,9; 24109,13; 24149,15; 24174,10; 24182,15; 24210,9). Blanchard et al. (1) have determined trace element and some major element abundances, Bogard and Hirsch (2) have measured solar wind and cosmogenic rare gas contents, McKay et al. (3) have determined grain-size distributions, Basu et al. (4) have made petrographic modal analyses, and Morris (5) has measured magnetic free iron contents and ferromagnetic resonance intensities. We have contributed measurements of particle track densities in plagioclase-bearing grains in the 45-90 μm fraction of these samples.

We etch polished grain mounts for 3h in boiling 1N NaOH to reveal the tracks. By counting tracks and measuring areas on scanning electron micrographs we can calculate track densities. We show the results of our measurements in Fig. 1.

Particle track density distributions provide information on the origin and the duration of solar and galactic cosmic ray bombardment of the soil and consequently on its maturity and its age. The upper four samples (24077, 24109, 24149, and 24174) are mature because the grains have track densities almost exclusively > 10^9 cm^{-2} (Fig. 1). Tracks in these grains must be primarily of solar flare origin and therefore these grains have been exposed and reworked into the soil many times within millimeters of the lunar surface. The lower two samples (24182 and 24210) have a significant component of grains whose tracks are cosmogenic (Fig. 1). Since the two groups are sharply divided, we would conclude that the soil is a mixture of a mature and an immature component although others would dispute the basis for this conclusion and would conclude that the soil may be reworked (6). However, measurements of ferromagnetic resonance intensities (Is/FeO) (5) and agglutinate contents (4) indicate that these soils have not been reworked for more than a few million years. Cosmogenic particle track densities in the lower two samples are too high to have been irradiated in situ and consequently these soils have a preirradiation history at shallower depths which is also verified by ^{21}Ne abundances (2).

As far as we can determine from track density distributions in the upper four samples the soil could be reworked down to a depth of 175 cm in the core (~142 cm from the lunar surface (2)). Such a large reworking depth is very improbable and in addition measurements of Is/FeO (5) and agglutinate contents (4) indicate that these soils are immature to submature. Because plagioclase mineral fragments constitute only from 10-15% of the 45-90 μm fraction for these soils (4), it is reasonable to conclude that the Luna 24 soils are a mixture of soils in which the feldspathic component is mostly mature. Chemical (1) and petrographic (4) data also indicate that the Luna 24 soils are mixtures, but without any indication that a plagioclase-rich component may be mature. In order to determine the maturity of a more significant component of these soils, we intend to measure track density distributions in the pyroxene-bearing grains and report on them at the conference.

PARTICLE TRACK DENSITIES IN THE LUNA 24 CORE

Blanford, G. E. and Wood, G. C.

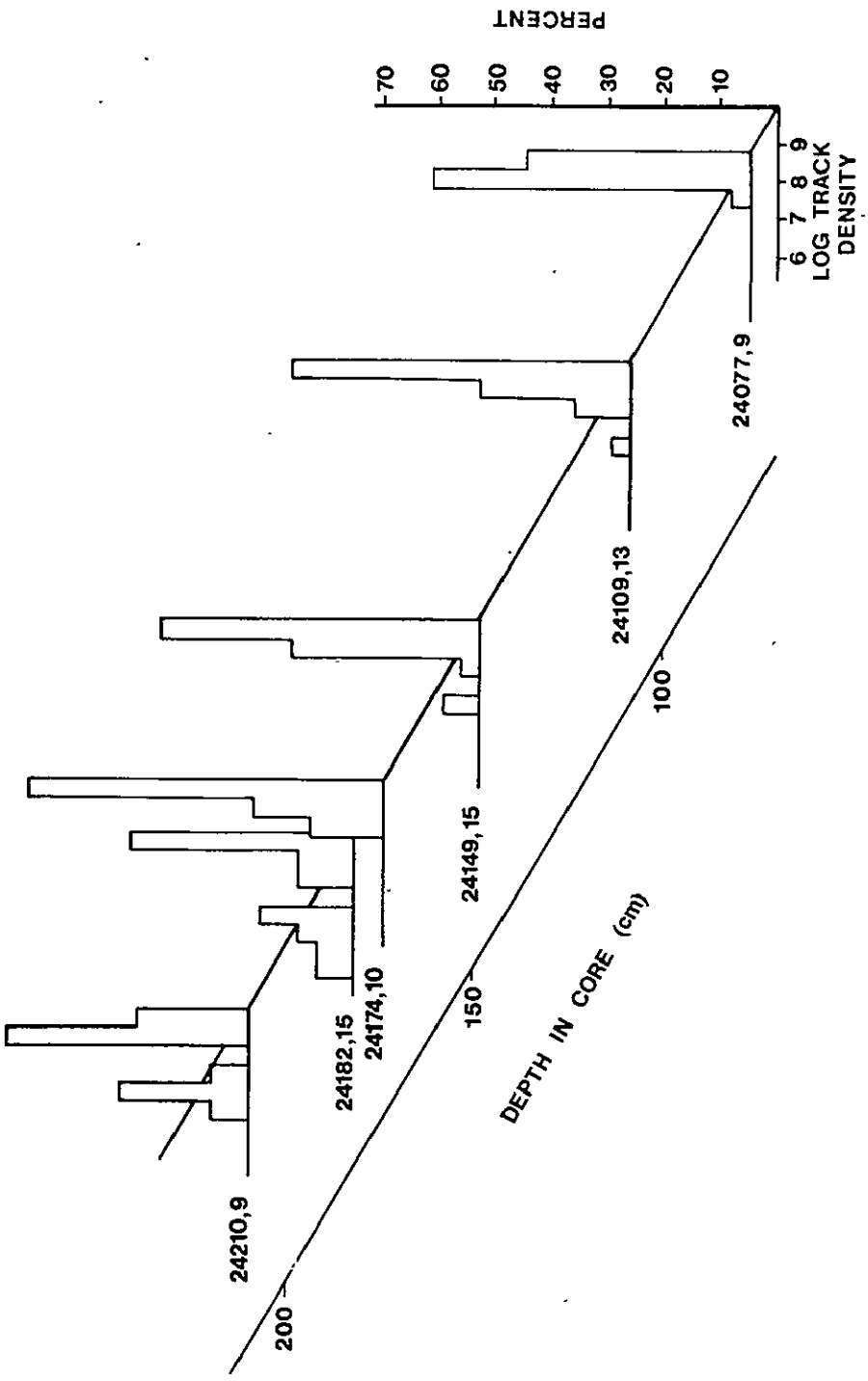

Fig. 1. Histograms of particle track densities measured in plagioclase-bearing grains in the 45-90 μm fraction of Luna 24 core samples. Each histogram is based on the measurement of 30 soil grains. Correlations of core depths with depths from the lunar surface are discussed by Bogard and Hirsch (2).

PARTICLE TRACK DENSITIES IN THE LUNA 24 CORE

Blanford, G. E. and Wood, G. C.

REFERENCES

(1) Blanchard D. P. et al., this volume.
(2) Bogard D. D. and Hirsch W. C., this volume.
(3) McKay D. S. et al., this volume.
(4) Basu A. et al., this volume.
(5) Morris R. V., this volume.
(6) Bibring J. P., et al. (1975), Proc. Lunar Sci. Conf. 6th, 3471.
(7) Blanford G. E., et al. (1977), Proc. Lunar Sci. Conf. 8th, in press.
(8) Morris R. V. (1976), Proc. Lunar Sci. Conf. 7th, 315.

NOBLE GASES IN LUNA 24 CORE SOILS. D.D. Bogard and W. C. Hirsch[1], NASA Johnson Space Center, Houston, TX 77058 ([1]Also, Northrop Services Inc.).

We have determined by mass spectrometry abundances of the 23 stable isotopes of the noble gases (He, Ne, Ar, Kr, and Xe) in 90-45 μm and <20 μm size separates of six soils from the Luna 24 core. These separates are aliquants of samples for which data on petrography, chemistry, magnetic properties, and particle tracks are reported elsewhere in this volume (Basu et al.; McKay et al.; Blanchard et al.; Morris; and Blanford et al.). Most of the measured noble gases (Table 1) have an origin from the solar wind and occur in concentrations typical of lunar soils. For a given grain size, concentrations vary among the six Luna 24 soils by a factor of ∿2 and are proportional to the surface maturity index of each soil as measured by agglutinates (McKay et al., 1977) and I_S/FeO (Morris, 1977). We have applied the ordinate-intercept technique to the data on each pair of grain sizes of each soil to determine the isotopic composition of the trapped solar component. These trapped ratios are similar to other lunar soils and show ranges of 31.0-32.0 for $^{22}Ne/^{21}Ne$, 5.22-5.26 for $^{36}Ar/^{38}Ar$, and 2700-2800 for $^{4}He/^{3}He$, except for one value at 2975. Trapped Xe and Kr typically show only small variations in isotopic composition among soils ($\leq$0.5% per mass unit for Xe), which generally are consistent with a mass fractionation relationship (e.g., Bogard et al., 1974). Trapped $^{40}Ar/^{36}Ar$ in these soils are in the range 0.62-0.72, except for the two deepest soils, where this ratio is less well determined, but appears to be 0.9-1.

In an effort to elucidate the irradiation history of the Luna 24 core, we have calculated the cosmic ray-produced ^{21}Ne in the 45-90 μm size separates using the trapped Ne compositions determined from the ordinate-intercept plots. Unfortunately, large ratios of trapped gas/cosmogenic gas make the equivalent calculations for cosmogenic ^{3}He and ^{38}Ar highly uncertain. (By the time of the Luna 24 Conference we anticipate that we shall have data on coarser grain size fractions, which will enable us to more accurately determine cosmogenic ^{3}He and ^{38}Ar in these soils.) Small corrections were made to cosmogenic ^{21}Ne for differences in abundances of target elements, utilizing the technique reported by Bogard and Hirsch (1976) and bulk soil compositions given by Blanchard et al. (1977). These corrections were <2%, except for soil 24210,9, for which the correction was 6%. We expect that any additional correction uncertainties due to measured differences in composition as a function of grain size (Blanchard et al., 1977) would not be large because the 45-90 μm separate represents the mean grain size below 250 μm, and consequently the compositions of the 45-90 μm fractions and the bulk soil below 250 μm can be expected to be similar.

The subsurface depths of the soils must be known to utilize cosmogenic ^{21}Ne to determine irradiation history. Unfortunately, considerable ambiguity exists in these depths. From descriptions given by Florensky et al. (1977) and Barsukov et al. (1977) and from discussions with C. Simonds (pers. comm., 1977), who observed the core under dissection in Moscow, we have attempted to deduce depth relationships in the core (Fig. 1). The right hand side of the Figure represents the 260 cm core tube which penetrated the surface at an angle of 30 degrees. Regolith filled the core below the 73 cm level indicated, except for an 11 cm void near the bottom. A few grams of soil and coarse fines were distributed between the 47 and 73 cm levels, and only traces of

NOBLE GASES IN LUNA 24 CORE SOILS

Bogard D. D. and Hirsch W. C.

soil were observed between the 47 cm level and the indicated surface. Soil numbers assigned by the Soviets represent distances measured along the core from the point of surface penetration, which the Soviets assume to be that point on the core where traces of soil are first found. To explain the greater depth of core tube penetration compared to recovered core length (approx. 220 cm and 140 cm, respectively) the Soviets offer several possibilities: 1) uppermost parts of the regolith could have been incompletely sampled, 2) the soil column may have shortened after entering the core due to compaction, or 3) the soil may have expanded to fill the greater diameter of the core (∿11-12 mm) compared to the bit (8 mm). Considering the small bit diameter, temporary blockage by coarse fragments conceiveably could have occurred at several points. Rolling of the core and its cloth container onto a drum for return conceiveably could have distorted depth relationships as well.

On the left hand side of Fig. 1 we have rotated the core into a verticle orientation and have indicated two extreme, but possible cases of subsurface depth relationships among our Luna 24 soils. One interpretation assumes that all void spaces in the ∿223 cm of core tube which presumably penetrated the regolith were caused by expansion of the core in cross-section to fill the tube. This interpretation indicates that ∿191 cm of regolith were sampled and that sample 24077 and the coarse fragments located above it were located on or near the lunar surface. The second interpretation is that no expansion of the core occurred and that the void spaces are due to incomplete recovery during coring. This interpretation results in a vertical section only ∿121 cm deep, which in Fig. 1 we indicate to have been taken from the surface down to a depth of ∿121 cm. It is also conceiveable that this ∿121 cm core was taken from various levels along the cored section or from the bottom ∿121 cm of the cored section. Only with the last interpretation would the 24077 sample have had a depth greater than ∿10 cm, and possibly up to ∿70 cm.

Our cosmogenic ^{21}Ne data are plotted as a function of depth in Fig. 2 with the assumption that the cored section was ∿191 cm deep. The curve indicates the approximate production profile with depth (Reedy and Arnold, 1972), and is arbitrarily normalized on the vertical scale. The data are grossly inconsistent with in situ production of ^{21}Ne in a static regolith, as the $[^{21}Ne]_c$ below ∿110 cm depth are too high relative to $[^{21}Ne]_c$ above ∿60 cm. If we plot $[^{21}Ne]_c$ versus a core depth of ∿121 cm, the uppermost three soils would be roughly consistent with an in situ production profile, but $[^{21}Ne]_c$ in the lowermost three soils would still be too large. Therefore, at least part, and probably all of the soils were substantially pre-irradiated before deposition in the core, in spite of the low surface maturity of most of these soils (Morris, 1977). A cosmogenic Ne content of 60 x 10^{-8} cm^3/g and a near-surface production rate of 0.2 x 10^{-8} cm^3/g-my indicate a minimum cosmic ray exposure time of ∿3 x 10^8 years for all soils. In this period of time the surface maturity of 24077,9 should have become much higher than that observed if this soil were within ∿20 cm of the surface. One possible explanation is that these soils are comprised of various mixtures of soils, one with high $[^{21}Ne]_c$ and high surface maturity, and another with low surface maturity. Grain size distributions (McKay et al., 1977) and differences in chemical composition among different grain sizes (Blanchard et al., 1977) also indicate that these Luna 24 samples are soil mixtures. Such an origin by mixing was demonstrated for

NOBLE GASES IN LUNA 24 CORE SOILS

Bogard D. D. and Hirsch W. C.

60009-60010 drive tube soils (McKay et al., 1976; Bogard and Hirsch, 1976). Hopefully, additional data on cosmogenic products in coarser grain sizes will permit a more definitive model of the irradiational and depositional history of the Luna 24 core.

Noble Gases in Grain-size separates of Luna 24 soils. Abundances are in units of cm^3 STP/g and have estimated uncertainties of ± 5-10% for He, Ne, Ar, and ± 10-15% for Kr. Ratios of $^{40}Ar/^{36}Ar$ are also given.

Soil and Grain size	^{3}He 10^{-6}	^{4}He 10^{-2}	^{22}Ne 10^{-5}	^{36}Ar 10^{-5}	^{84}Kr 10^{-8}	^{132}Xe 10^{-8}	$^{40}Ar/^{36}Ar$
24077,9							
45-90μm	14.6	3.35	6.72	14.4	10.1	1.33	0.79
<20μm	58.1	16.5	29.4	68.9	38.5	5.69	0.67
24109,13							
45-90μm	14.3	3.32	6.64	14.6	10.2	1.35	0.71
<20μm	70.6	18.7	30.2	68.3	41.6	5.26	0.72
24149,15							
45-90μm	12.3	2.76	5.68	10.3	5.03	0.93	0.81
<20μm	52.3	14.1	23.6	48.1	30.5	3.68	0.74
24174,10							
45-90μm	12.7	3.03	6.18	11.7	7.18	0.93	0.72
<20μm	76.8	20.5	32.7	65.6	43.4	5.41	0.66
24182,15							
45-90μm	7.83	1.49	3.35	6.10	4.61	0.78	1.11
<20μm	42.3	11.3	20.3	40.8	25.8	3.41	1.03
24210,9							
45-90μm	11.1	2.50	5.15	10.9	7.52	1.06	0.84
<20μm	43.6	11.7	18.1	>31	-	-	0.90

Barsukov V.L., Tarasov L.S., Dmitriev L.V., Kalesov G.M., Shevaleyevsky I.D., and Garanin A.V. (1977) Proc. Lunar Sci. Conf. 8th, in press.
Blanchard D.P., Haskin L.A., Brannon J.C., and Aaboe E. This Volume.
Bogard D.D., Hirsch W.C., and Nyquist L.E. (1974) Proc. Lunar Sci. Conf. 5th, 1975-2003.
Bogard D.D. and Hirsch W.C. (1976) Proc. Lunar Sci. Conf. 7th, 259-279.
Bogard D.D. and Hirsch W.C. (1977) Proc. Lunar Sci. Conf. 8th, in press.
Florensky C.P., Basilensky A.T., Ivanov A.V., Pronin A.A., and Rode O.D. (1977) Proc. Lunar Sci. Conf. 8th, in press.
McKay D.S., Dungan M.A., Morris R.V., and Fruland R.M. (1977) Proc. Lunar Sci. Conf. 8th, in press.
McKay D.S., Basu A., Clanton U.S., Fruland R.M., and Waits G. This Volume.
Morris R.V. This Volume.
Reedy R.C. and Arnold J.R. (1972) J. Geophys. Res 77, 537-555.

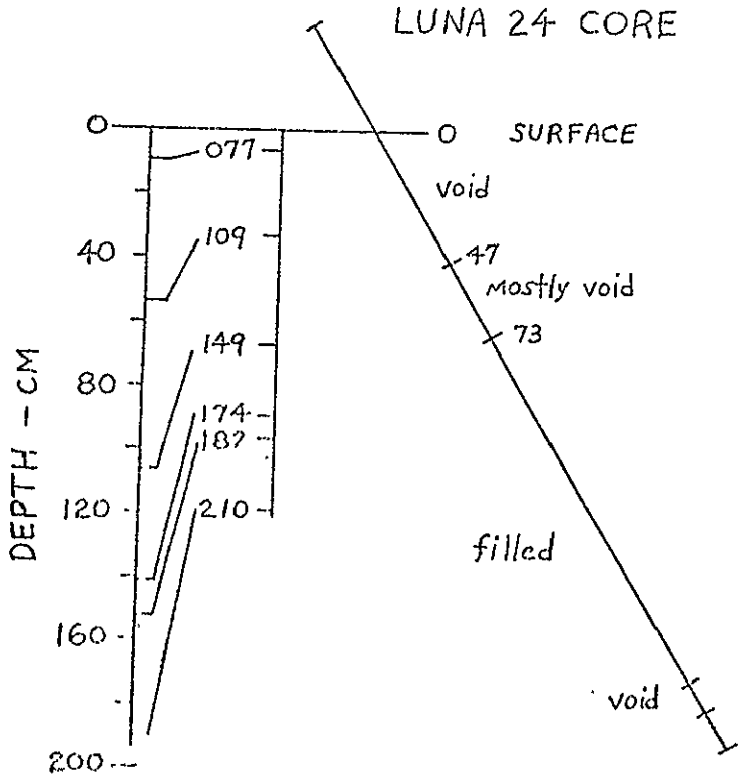

Fig.1: Schematic of the Luna 24 core showing possible subsurface depth relationships among the six analyzed soils.

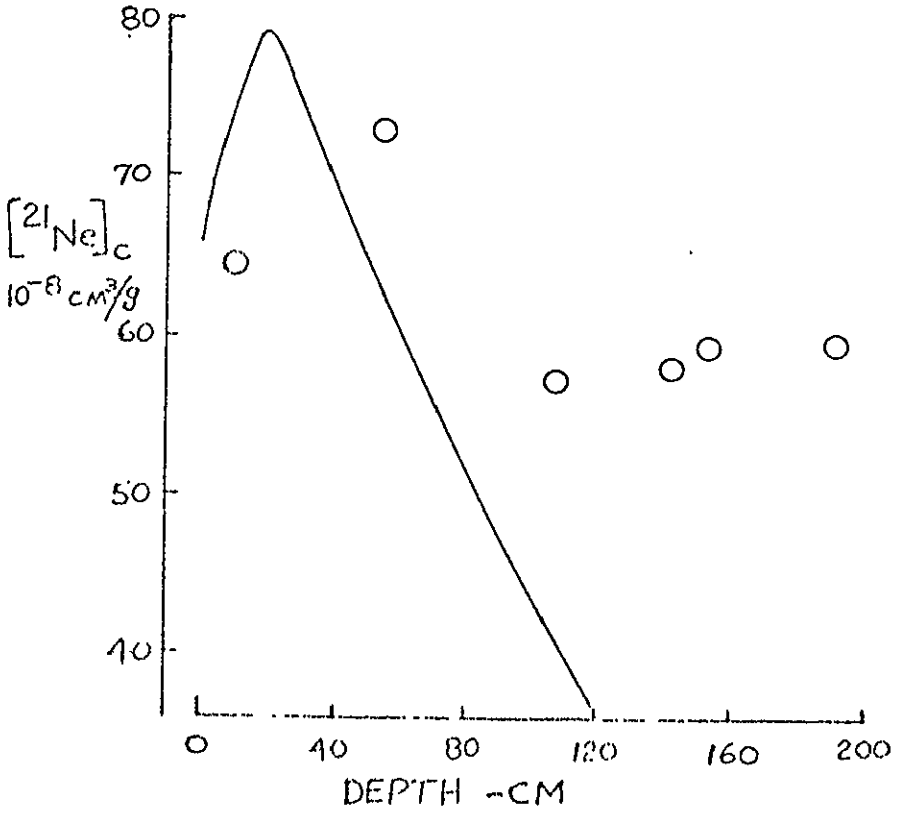

Fig. 2: Concentrations of cosmogenic Ne as a function of core depth assuming a total subsurface sampling depth of ~191 cm. The approximate production-rate profile is also indicated.

IGNEOUS ROCKS FROM MARE CRISIUM: MINERALOGY AND PETROLOGY

R.A. Coish and Lawrence A. Taylor, Department of Geological Sciences, The University of Tennessee, Knoxville, Tennessee 37916.

The Luna 24 drill core from Mare Crisium comprises up to 50% mineral and rock fragments. Most of these particles have been broken down from low-Ti, aluminous Mare Crisium basalt flows (1,2,3,4,) ; a few may have a highlands origin. The purpose of this paper is to describe the petrography and geochemistry of the rock types at the Luna 24 site and to present a petrogenetic model for Mare Crisium magmatism.

The principal rock types (textural classification) are subophitic basalts, metabasalts, olivine vitrophyres and cumulate material. In the 150-250 um grain size fraction which we studied, subophitic and metabasalt fragments are by far the most abundant; olivine vitrophyres and cumulates occur in minor quantities. Mineral fragments in this grain size greatly outnumber rock fragments suggesting that the parent rocks at Mare Crisium were mostly coarse-grained basalts or fine-grained gabbros.

Subophitic basalts, the most prominent rock type, comprise plagioclase laths embedded in pyroxenes; often these basalts also have phenocrysts of olivine and pyroxene and minor amounts of chromite-ulvospinel, ilmenite, troilite and native Fe. Some late stage fragments contain silica patches coexisting with Fe-rich olivines and pyroxenes. Subophitic basalts (open circles in Fig. 1) have low TiO2 and high Al2O3 contents compared with most other mare basalts; however, Luna 16 soils contain a few rock fragments with similar chemistry (5) and Apollo 17 VLT basalts (6,7) have comparable TiO2 contents but are richer in MgO (Fig. 1). High Fe/Fe+Mg ratios also characterize these rock fragments. Pyroxene crystallization begins with Mg-pigeonite and augite/sub-calcic augite and trends toward Fe-rich compositions - ferrohedenbergite and rarely pyroxferroite (Fig. 2). Cr decreases, Ti and Ti/Al increase with increasing Fe/Fe+Mg ratio in the pyroxenes (Fig. 3). These minor element relationships suggest that chromite was an early crystallizing phase; ilmenite appeared late in the cooling history; and plagioclase began to crystallize after pyroxenes had already started precipitating. Olivines in these basalts range from Fo59 to Fo3. Thus, even the most magnesian olivines in the subophitic basalts were in equilibrium with relatively Fe-rich liquids. Plagioclase has compositions from An78 to An96 but the majority lie between An90 and An96 (Fig. 2). The spinels are members of the chromite-ulvospinel-hercynite solid solution series. Their textures are reminiscent of Apollo 12 and 15 spinels in as much as these are Ti-chromite rimmed by Cr-ulvöspinels. Their chemistry is somewhat unusual in having high Al (up to 14.2%) and low Mg (0.6 to

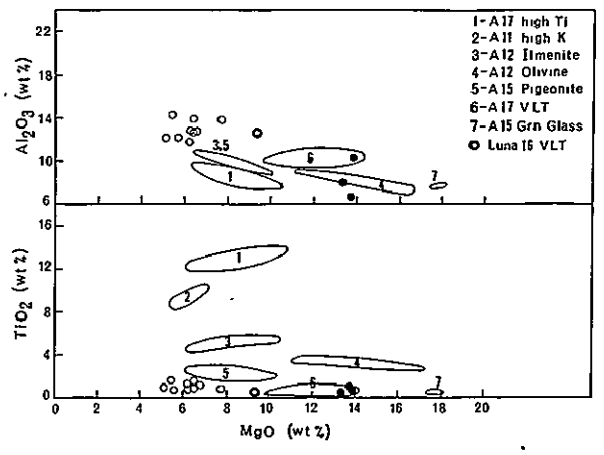

Fig. 1 Major element variations in subophitic basalts (o) & olivine vitrophyres (●). Data from (1), (6), & this study.

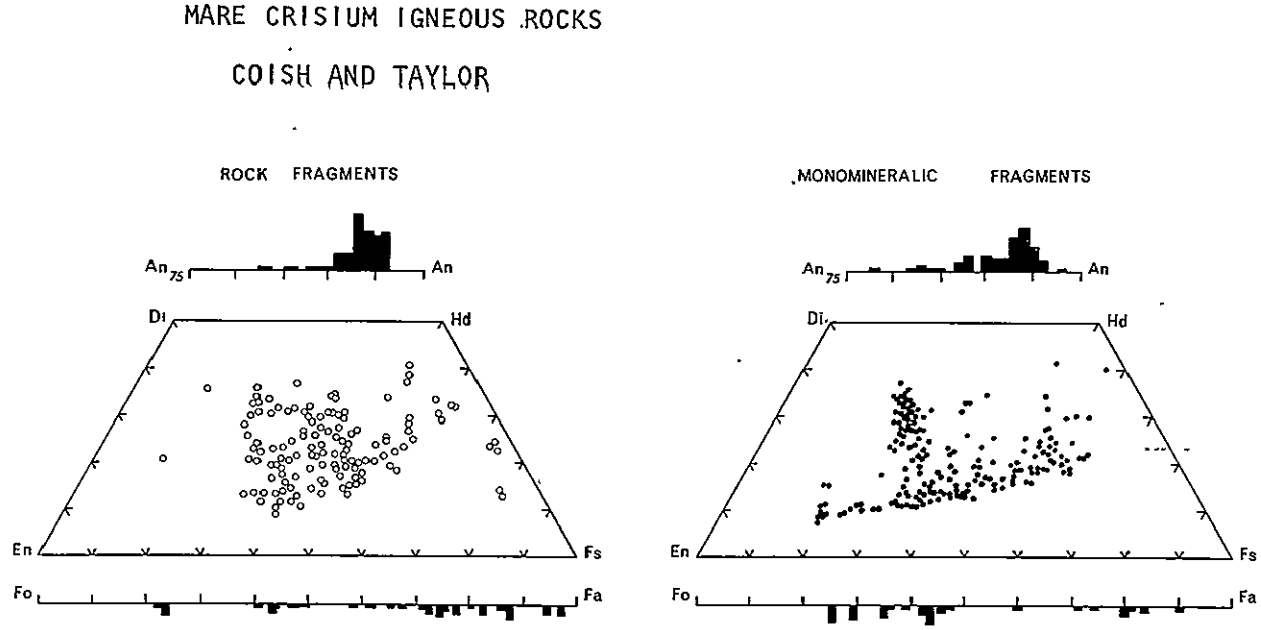

Fig. 2 Mineral compositions for Luna 24 rock and mineral fragments.

1.6%). As deduced from textural considerations and pyroxene chemistry, the order of crystallization of minerals in the subophitic basalts was olivine with chromite, pigeonite, sub-calcic augite/augite, plagioclase, ilmenite and silica + fayalite.

Metabasalts are considered to be metamorphosed tops of basalt flows. Their petrology is described in an accompanying paper (8) and will not be discussed further.

Olivine vitrophyres are a minor component of the Luna 24 soils. They are composed of thin, skeletal olivine quench crystals in a matrix of glass or partially devitrified glass. The olivines are Fo75-Fo78 indicating the rock is from a primitive magma. Compared with the subophitic basalts, the olivine vitrophyres (Fig. 1) are lower in TiO2, Al2 03 and richer in MgO. Some Apollo 17 VLT basalts have similar compositions.

One rock fragment has been tentatively identified as cumulate in origin. This conclusion is based on the following observations: 1) the texture of subrounded olivines and pyroxenes with interstitial plagioclase contrasts greatly with the other basaltic textures and is similar to terrestrial cumulates. 2) the composition of the olivines is uniform at around Fo75. This is expected if the rock fragment is a small portion of an early formed cumulate; in contrast, rocks formed by cooling a liquid contain olivines with a wide range of compositions. Plagioclase is very calcic (An94-96) and has low Fe contents - similar to Fe values in plagioclase from highlands rocks. This cumulate then may be from a highlands area.

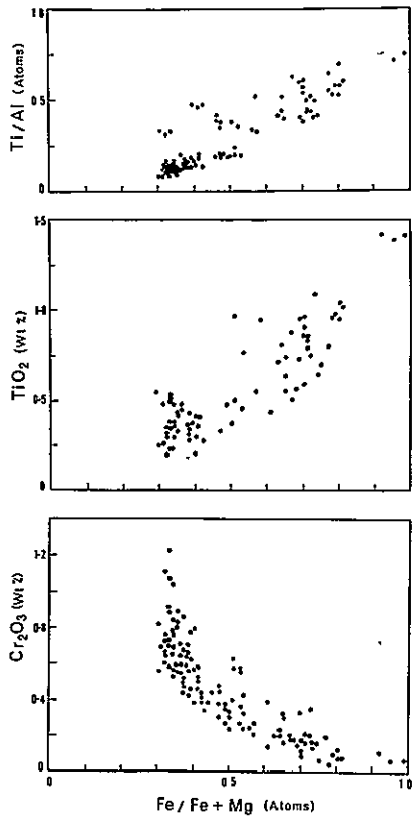

Fig. 3 Minor element variations in Luna 24 pyroxenes.

MARE CRISIUM IGNEOUS ROCKS

COISH & TAYLOR

The two rock types (subophitic basalts and olivine vitrophyres) representing liquid compositions at Mare Crisium exhibit chemical variations that may be related by fractionation processes (Fig. 1). The more primitive olivine vitrophyre could be the parent magma for the subophitic basalts because of the low Ti and Al, and high Mg of the former. Using Wright and Doherty's 1970 mixing program (9), it is possible to quantitatively derive the subophitic basalts from an olivine vitrophyre magma by fractionating 16-18% pigeonite ($Wo_{11}En_{64}Fs_{25}$) 7% augite ($Wo_{29}En_{48}Fs_{23}$), 1% chromite and 15-16% olivine (Fo_{62}). These mineral compositions are reasonable as they are actual analyses from the basaltic rock fragments. The question now arises: what is the ultimate source of the olivine vitrophyre magma? There are two possible scenarios to explain its origin: 1) It represents a direct partial melt of a lunar source depleted in TiO_2 and enriched in Al_2O_3. In this case, the source is directly beneath Mare Crisium so that the magma produced from it has little chance to undergo any changes from the time of its formation to extrusion at the surface. 2) The olivine vitrophyre magma underwent limited crystal fractionation prior to its shallow level emplacement beneath Mare Crisium and is, therefore, a derivative from a more primitive magma. The Apollo 15 green glass (10) may represent such a primary magma. Simple fractionation of 15% olivine(Fo_{79}) from Apollo 15 green glass composition can give rise to the Luna 24 olivine vitrophyre liquid (11). At the present time, it is not possible to choose between the above two alternatives because of the lack of information on the nature of source regions within the moon's interior.

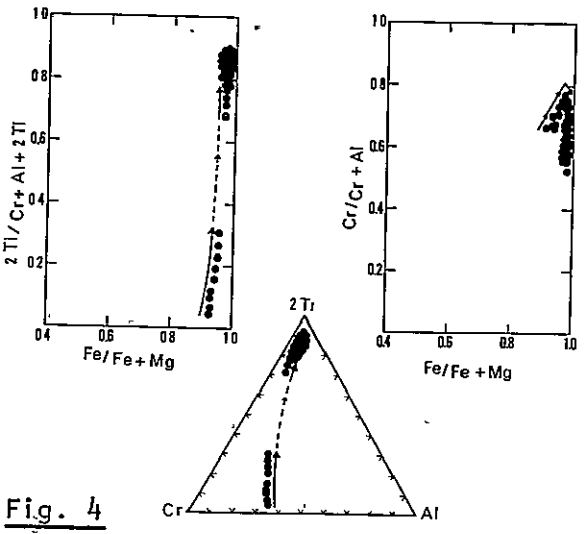

Fig. 4

REFERENCES: (1) Ryder, McSween and Marvin, 1977. The Moon, in press; (2) Vaniman and Papike, 1977. Geophys. Res. Lett., in press; (3) Coish, Hu and Taylor, 1977. (abstr.) Am. Geophys. Union Midwest Mtg.; (4) Ryder, McSween and Marvin, 1977. (abstr.) Meteoritical Soc. Mtg.; (5) Kurat, Kracher, Keil, Warner and Prinz, 1976. Proc. Lunar Sci. Conf. 7th., 1301; (6) Taylor, Keil and Warner, 1977. Geophys. Res. Lett. 4, 207; (7) Vaniman and Papike, 1977. Proc. Lunar Sci. Conf. 8th., in press; (8) McSween, Taylor and Clark, 1977. Luna 24 Conf., this volume; (9) Wright and Doherty, 1970. Geol. Soc. Am. Bull 81, 1995; (10) Reid, Warner, Ridley and Brown, 1972. Meteoritics 7, 395; (11) Norman, Coish and Taylor, 1977. (abstr.) Am. Geophys. Union Midwest Mtg.

THICKNESS OF MARE BASALT: LUNA 24 LANDING SITE,
R. A. De Hon, Department of Geosciences, Northeast Louisiana University, Monroe, LA 71203.

Luna 24 landed on the mare basalt surface of southeastern Mare Crisium approximately 50 km from the contact with basin rim materials. Within the basin, buried craters suitable for estimates of basalt thickness (1) are sparse, but a generalized setting may be constructed as a frame of reference for the interpretation of the Luna 24 samples. Crisium is a 475 km diameter multi-ringed basin (2) in which the mare basalts occupy a deep central basin and flood the surrounding shelf region. The flooding extends eastward beyond the second raised ring giving an overall elliptical outline to the mare surface. The surface is terraced, stepping down toward a relatively flat interior. Mare ridges mark the boundary of each level (Fig. 1). A large crescent-shaped shelf forms an intermediate level (60° to 65°E) between the basin interior and the higher eastern extension of the mare surface.

The Luna 24 landing site lies near Dorsum Harker within the southern tip of the crescent shelf (Fig. 1). Buried craters along the southern edge of the basin indicate 500 m of mare basalt in the area of the landing site (1). Inclusion of data from less certain crater remnants (30 km southwest and 45 km northwest of the landing site) tend to support the 500 m estimate. In contrast, the Apollo 17 sounder profile indicates a subsurface reflecting horizon at a depth of 1400 m in this area (3). One means of verifying the proper interpretation of thickness is by remote geochemical or mineralogical characterization of ejecta from the nearby crater Fahrenheit (Fig. 1). This 6.5 km diameter crater, 19 km from the landing site, excavates 1200-1300 m below the surface. Identification of highland components in the crater ejecta would imply penetration below the mare basalts; hence, the basalts would be less than 1200 m thick. On the other hand, a basalt signature for the rim materials would imply that the basalts are at least as thick as the crater depth.

Candidate sources for highland materials in the Luna 24 cores include ejecta from the craters Auzout, Fahrenheit, Langrenus and Giordano Bruno. The late Imbrian crater Auzout, 90 km southeast of the landing site (Fig. 1), excavates Crisium rim material and pre-Crisium highland material. Ray materials produced by the Giordano Bruno impact into pre-Nectarian highland material as well as small amounts of ejecta from Langrenus derived from maria and highland materials may be present in the regolith. Contributions to the sample from either Giordano Bruno

THICKNESS OF MARE BASALT

R. A. De Hon

(4) or Langrenus are expected to be quite small due to the large distances to these craters. Samples from any of these sources are expected to record a highly complex history of multiple shock events.

References

(1) De Hon, R. A. and Waskom, J. D. (1976) Proc. Lunar Sci. Conf. 7th, 2729.
(2) Olson, A. B. and Wilhelms, D. E. (1974) Geologic Map of the Undarum Quadrangle of the Moon, U.S. Geol. Survey.
(3) May et al. (1976) Lunar Sci. 7, 540.
(4) Butler, P. and Morrison, D. A. (1977) Lunar Sci. 8, 151.

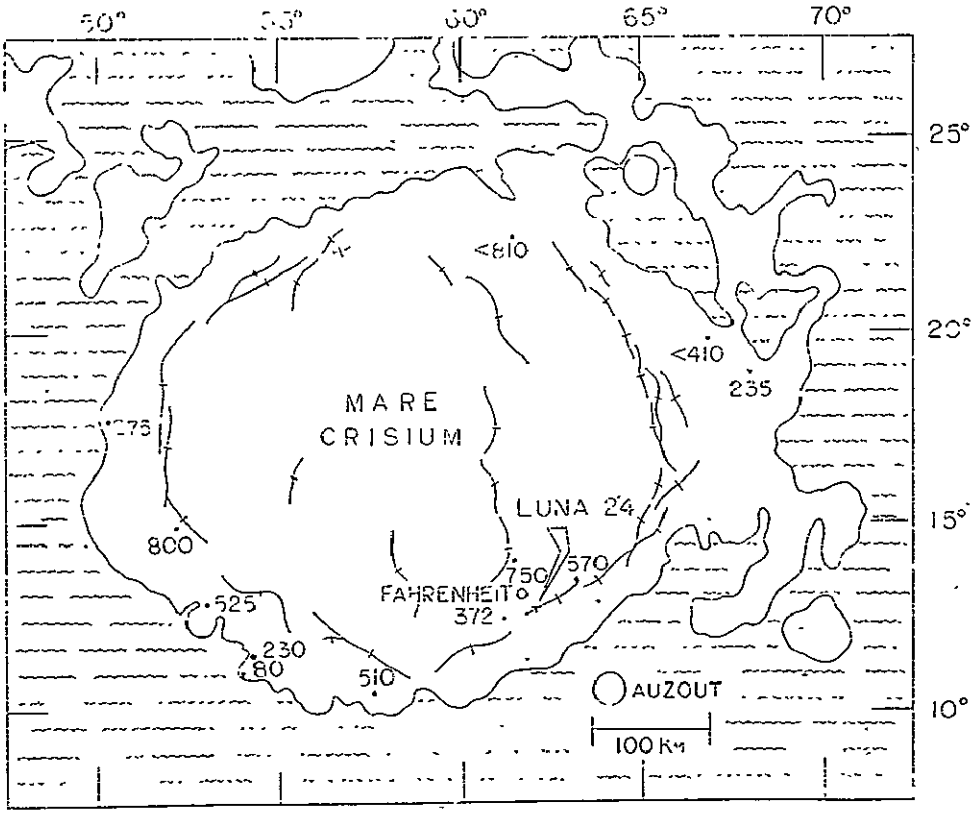

Figure 1. Sketch map of Mare Crisium. Location of craters used to estimate thickness of mare basalt shown by dots. Thickness in meters. Mare ridges potrayed by crestline and crossbar symbol.

PARTICLE TRACK RECORD AND THERMOLUMINESCENCE STUDIES OF LUNA 24 DRILL CORE SAMPLES. S.A. Durrani, R.K. Bull, and S.W.S. McKeever, Department of Physics, University of Birmingham, Birmingham B15 2TT, England.

INTRODUCTION. The purpose of charged-particle track analysis and thermoluminescence (TL) studies is to interpret the radiation and thermal histories of the lunar samples in their natural environment on the Moon. As the Luna 24 samples have come from known depths below the lunar surface (down to ~2m), it is of particular interest to study the radiation and temperature effects as a function of depth. Whereas TL studies are particularly valuable in delineating the temperature profile of the 'deep core' samples, track analysis can throw light on the exposure history and soil-mixing properties of the regolith material over geological time-periods. The cooling-down histories and the solidification ages of the lunar rocks can also be determined by track-analysis methods. The following samples have been analysed in the preliminary studies reported hereunder: 24090, 1 (from a depth of 89-90cm below the lunar surface); 24125, 1 (124-125cm); and 24196, 1 (195-196cm).

PARTICLE-TRACK RECORD. Approximately 20 mineral grains of size 150-250 μm from a high-density fraction were made available to us from the core samples 24090,1 (9302); 24125,1 (9302); and 24196,1 (9302) for the purposes of charged-particle track studies. The crystals were mounted, usually singly, in epoxy resin; ground; and then polished. The mineral type was identified on the basis of examination under a low-power microscope as well as of etching characteristics and elemental analysis using the X-ray analyser attached to a scanning electron microscope (SEM). Olivines were etched for 0.5 to 1 hr using the WN etchant[1]; feldspars, in boiling 40% NaOH for 5-10 min; and pyroxenes, in 60% NaOH for 20-30 min.

Track counts were made from SEM photographs at magnifications of 2-5K, but occasionally at 10K. Where variations in track density by more than a factor of ~2 from the rim to the centre of a grain were evident, a strip of the grain was scanned at ~5K and the track density vs depth profile measured. Less than half of the grains have as yet been analysed. The data obtained so far are summarized in Table 1. In a few cases, detailed measurements on the track density have not been made but rough estimates from optical-microscope observations have been made.

Track-density vs depth profiles for four grains are shown in Fig.1. Figure 2 shows a photograph of one of these 'gradient' grains, 24090,1; grain 3. In only two out of 13 cases are track densities of less than $\sim 10^8$ tracks.cm^{-2} obtained. Grains showing track-density gradients are apparent in all three samples. The nature of the gradient is somewhat variable. Thus 24090,1, grain 3, has a gradient at two edges only, which falls within ~20μm to a fairly constant track density. Other grains show more smoothly-falling track densities; but again in all but one of the five grains so far found to exhibit track density gradients, it is observed that high track densities exist around only some of the grain edges (i.e., the gradient is anisotropic). Clearly no firm conclusions can be drawn from such a limited number of crystals; but the data obtained so far present no conflict with the picture of a regolith made up of a number of layers, each having had a surface

exposure of a few million years. Such a model has emerged from a number of other experimental studies and computer simulations[2].

THERMOLUMINESCENCE (TL) STUDIES. About 4mg of the sieved fraction below 75μm from each of the three locations mentioned above were made available to us, bearing the numbers: 24090,1(9601); 24125,1(9601); and 24196,1(9601). The apparatus used for TL analysis has been described elsewhere[3]; essentially, the samples were heated to ~500°C at a rate of 3.6 $^{o}C.s^{-1}$ in an inert atmosphere and the signal monitored with a photomultiplier (PM) tube in a cooled housing. Both the natural glow and that induced in a drained sample after β-irradiation were examined.

Figure 3 shows the glow curves obtained: the natural TL from all three samples as well as that resulting from irradiating sample 24196,1 with 50 krad of ^{90}Sr β-particles is displayed. The arbitrary units are a measure of the current output from the PM tube; the black-body radiation has not been subtracted.

Attention is drawn in this figure to the starting temperature of the natural glow from the three samples rather than to the intensity, because each sample has a different TL sensitivity. The starting temperature in each case is between 160 and 170°C. This is in strong contrast to the starting temperature (~65°C) of the artificially induced glow. It is clear that the early part of the natural glow (corresponding to the 135°C peak in the induced-glow curve) has been lost because of the storage and subsequent treatment of these samples during the past one year. Our earlier studies have given a starting temperature of ~60°C for the natural TL glow from a soil sample obtained from the deep shadow of an Apollo 17 boulder and kept refrigerated by NASA Lunar Receiving Laboratory and by ourselves[3]. The Luna 24 samples, coming as they do from a cold environment well below the lunar surface, should have displayed some well-preserved low-temperature glow. The high-temperature part of the natural TL has, of course, survived and corresponds to a natural dose well in excess of 50 krad β-equivalent.

It must, however, be pointed out that the sieved fraction received by us (<75μm) had been washed in acetone and dried for ~15 min at a temperature of ~50-100°C at Cambridge. This treatment must have contributed to the fading that would result from a room-temperature storage of the samples for one full year (August 1976 - September 1977) both in the USSR and in the UK. We plan to repeat our experiments on other fractions (106-150μm) that have not been subjected to the heat-drying treatment. There is no doubt however that, as amply demonstrated in the case of Apollo-17 shaded samples[3], it would be highly desirable to refrigerate a part of the material from any future Luna missions by placing it in a deep-freeze unit, or by packing it in CO_2 snow or liquid nitrogen. Such a procedure was recommended to[4], and accepted by, NASA and resulted in much valuable information on the thermal and radiation history of lunar samples being preserved.

REFERENCES. 1. Krishnaswami S. et al. (1971). Science, 174, 287-91. 2. Langevin Y. and Arnold J.R. (1977). Ann. Rev. Earth Planet. Sci., 5, 449-89. 3. Durrani S.A., Khazal K.A.R., and Ali A. (1976). Proc. Lunar Sci. Conf. 7th, 1157-77 (Pergamon, N.Y.). 4. Durrani S.A. (1972). Nature, 240, 96-97.

TRACK AND TL STUDIES

Durrani, S.A., et al.

Table 1 Charged-particle track analysis of mineral grains

Sample and Grain No.	Mineral	Mean Track Density (cm^{-2})	Gradient ?
Sample 24090,1			
Grain 1	calcic pyroxene	2×10^8	No
2	pyroxene	-	-
3	olivine	3×10^8	Yes; anisotropic
4	feldspar + calcic pyroxene	2×10^7	Very slight
5	feldspar	2×10^8	No
6	olivine	1×10^8	Yes; anisotropic
7	olivine	5×10^8	No
8	pyroxene	2×10^8	No
Sample 24125,1			
Grain 1	olivine	$\sim 10^8$	Yes; isotropic
2	olivine	1×10^8	slight
3	olivine	3×10^8	Yes; anisotropic
5	pyroxene	4×10^8	No
Sample 24196,1			
Grain 1	olivine	4×10^8	Yes; anisotropic
2	olivine	9×10^8	No
3	feldspar	$\sim 2 \times 10^7$	No
4	feldspar	$\gtrsim 10^8$	No

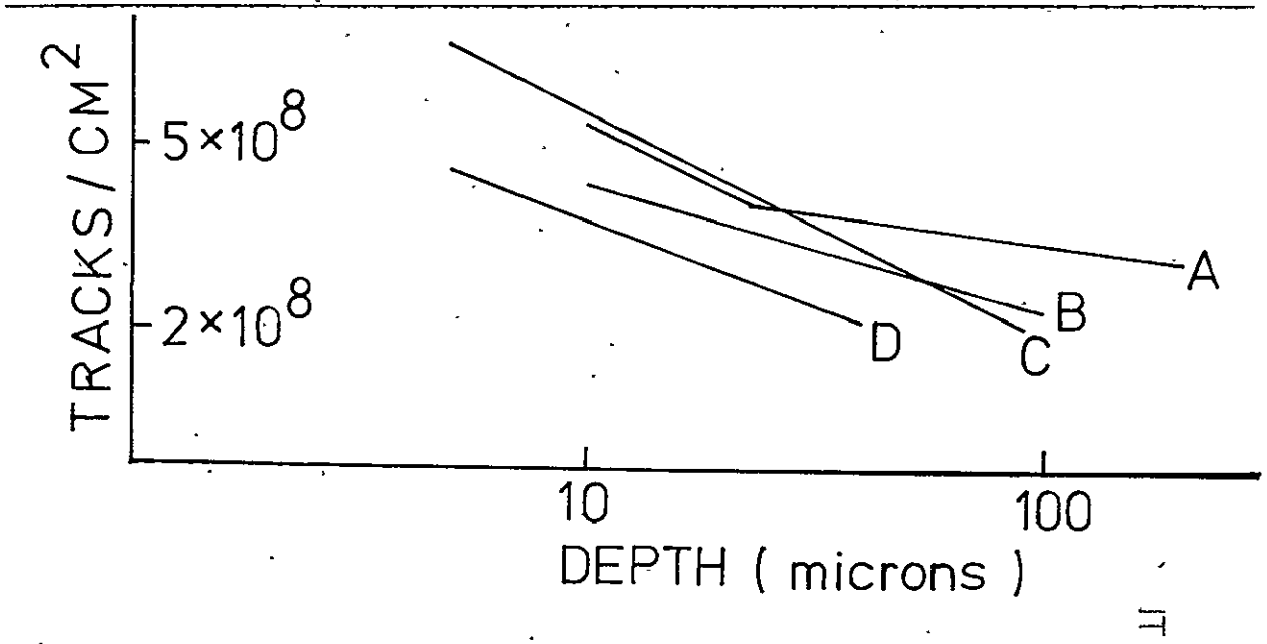

Fig.1. Track density vs depth profiles for: (A) 24090,1,9303 (grain 3); (B) 24090,1,9303(grain 6); (C) 24196,1,9303 (grain 1); and (D) 24125,1,9303 (grain 3).

TRACK AND TL STUDIES

Durrani, S.A.,et al.

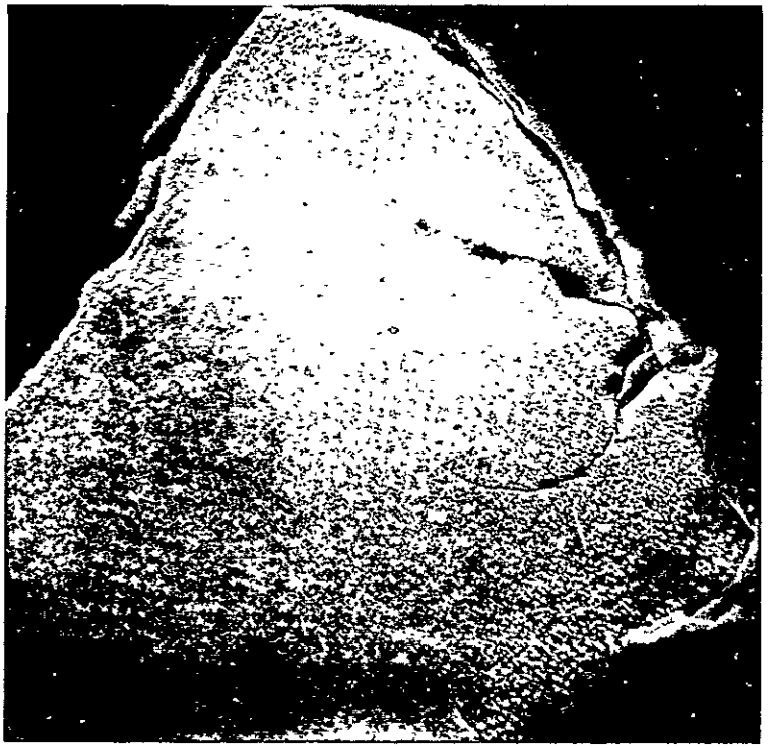

Fig.2. Olivine grain, magnification 530x, etched for 30 minutes in WN solution[1]. Note gradient in track density in bottom RH corner. Sample 24090,1,9303 (grain 3).

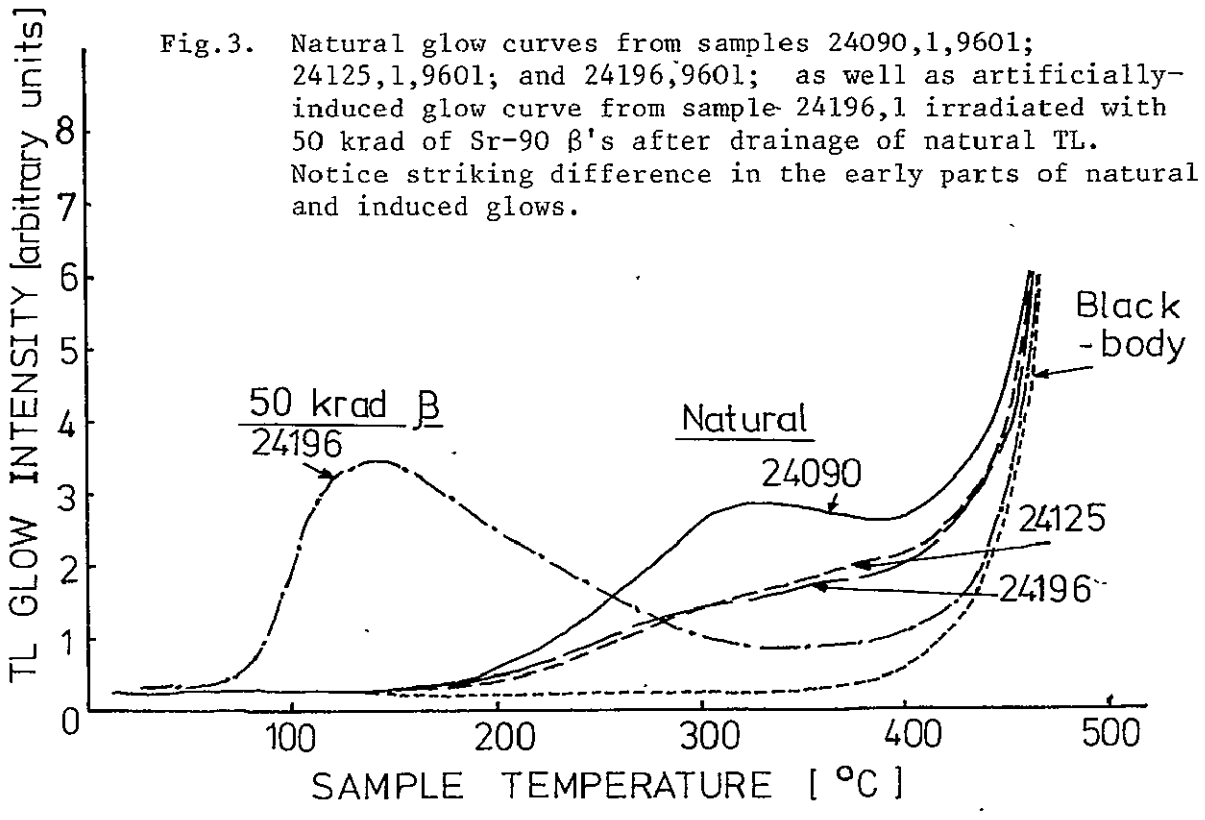

Fig.3. Natural glow curves from samples 24090,1,9601; 24125,1,9601; and 24196,9601; as well as artificially-induced glow curve from sample 24196,1 irradiated with 50 krad of Sr-90 β's after drainage of natural TL. Notice striking difference in the early parts of natural and induced glows.

METAL PARTICLES IN THE LUNA 24 SOIL. J. J. Friel and J. I. Goldstein, Metallurgy & Materials Science Dept., Lehigh University, Bethlehem, PA

The metal particles from 18 Luna 24 polished grain mounts were studied with the optical microscope and the electron microprobe. Less than 3% of the grains in these sections contained any metal and many of the metal particles were $\leq 5\,\mu m$ in diameter. Seventeen metal particles were found, however, which were large enough to analyze with the microprobe. These metals are found mainly in agglutinates and glass fragments. Metal was rarely observed in the abundant basalts and gabbro fragments and then mainly as blebs within sulfide grains.

The chemical analyses of the metal grains were reported by Friel and Goldstein (1) and the Ni-Co contents of the Luna 24 metals are shown in Fig.1. The two particles which fall in the meteoritic range (2) are the largest metal grains found, each $>50\,\mu m$ in their longest dimension. The larger of these metal particles (Section 24170,8) is approximately 100 x 125 μm. The structure as shown in Fig. 2 consists of a matrix of blocky massive-martensite (α_2) with inclusions of FeS at some of the grain boundaries. The bulk composition as determined using a 40 x 50 μm^2 area scan is 8.43 wt% Ni, 0.37 wt% Co, 0.79 wt% P, 89.3 wt% Fe and ~0.8 wt% S. The Ni and Co content of the matrix metal varies from 7.87 to 8.55 wt% and 0.34 to 0.43 wt%, respectively while the P content is relatively constant at 0.79 $\pm$ 0.03 wt%. This metal particle is not enclosed within a silicate matrix but is surrounded in part by a plagioclase glass plus sulfide. The same plagioclase glass also occurs at some of the grain boundaries within the metal particle. No detectable phosphorus was found in the glass. This metal grain is probably a meteorite fragment which was shock melted in the presence of sulfide. A second possibility is a shock remelted highlands metal particle. The metal grain must have cooled quickly ($> 1^{\circ}C$/day) to 500°C or below to prevent phosphide exsolution and to maintain a homogeneous phosphorus distribution. The presence of metal matrix martensite (α_2) and the glassy rim coating also argues for rapid cooling. This cooling history represents the last major reheating of the particle on the lunar surface.

The second metal particle (Section 24210,40) of meteoritic composition is approximately 40 x 60 μm in size. The structure as shown in Fig. 3 consists of a taenite core approximately 30 μm in diameter (~ 14.8 wt% Ni, 0.6 wt% Co, 0.02 wt% P, remainder Fe) which grades into a kamacite rim (~ 5.1 wt% Ni, 0.5 wt% Co, 0.03 wt% P, remainder Fe) over a broad diffusion zone of about 6 μm. The metal contains several FeS inclusions and one of a silicate glass. The host silicate is a melt rock consisting of clinopyroxene, plagioclase, and olivine in order of abundance. This particle was probably originally a two-phase (kamacite plus taenite) meteorite fragment, which was reheated and then cooled slowly enough to allow the Ni at the kamacite-taenite interface to diffuse over a broad diffusion zone. It is possible that the broad diffusion zone formed during the melting event which produced the host melt rock.

Most of the other metals analyzed fall in a group with compositions just

METAL PARTICLES IN THE LUNA 24 SOIL

J. J. Friel et al.

below the meteoritic range (Fig. 1). These particles are most often found in glass fragments or within the glass phase of agglutinates. The lesser Ni and Co contents may result from the addition of iron from reduction of silicates and oxides on impact. Most of the grains in this group did not contain any significant phosphorus, but this is probably due to the low overall phosphorus in the Luna 24 soil. Very few phosphate minerals were found, and none of these were associated with the metals.

A third group of metal compositions with Co contents greater than the meteoritic range (high-Co metal) probably also represents a mixture of lunar and meteoritic metal. It appears that high-Co metals are most common in the soils associated with mare basalts, specifically those of the low-Ti basalts (3). The Ni content of the low-Ti basalt soils is also higher (4), but the original Ni content is obscured by the meteoritic component of the soil. The Apollo 12 and 15 low-Ti basalts contain discrete Ni-rich metal grains, which apparently formed throughout the crystallization sequence. In contrast, the Apollo 11 and 17 basalts contain a greater overall abundance of metal, but almost all of it is associated with sulfides and is Ni-poor (4).

Since the Luna 24 soil contains some very low titanium (VLT) mare basalt fragments (5), it is possible that the high-Co metal had its origin in this rock type. In order to investigate this association, two large ($\sim$ 2 mm) VLT fragments from the Apollo 17 core, 70008 were analyzed. Only three metal grains large enough to analyze with the microprobe were found. Their compositions are given in Table I.

TABLE I

	Fe(wt%)	Ni(wt%)	Co(wt%)	P(wt%)	Total
70008,356 #516	97.01	0.95	1.00	<.02	98.96
70008,370 #512	97.56	0.69	1.23	.05	99.53
70008,370 #528	97.34	0.53	0.96	.07	98.90

It appears that metal in both the low-Ti basalts and also the VLT basalts have Ni/Co ratios ≤ 1. In addition, both Ni and Co are more abundant in the metals of low-Ti and VLT basalts than in the metals of high-Ti basalts. This may reflect different concentrations of these elements in the magmas or it may be due to the fractional crystallization of metal and silicates (6). The latter implies that the Co-rich metal crystallizes from a later stage liquid. Also contributing to the observed effect is the greater abundance of Fe^{o} in the high-Ti basalts thus diluting the available cobalt.

Perhaps the simplest explanation, however, is a more primitive source area for the low-Ti and VLT basalts. This does not require a common source for these two rock types, nor does it imply that one derived from the other. It merely suggests a more olivine-rich source area for these rocks than for the high-Ti basalts.

METAL PARTICLES IN THE LUNA 24 SOIL

J. J. Friel et al.

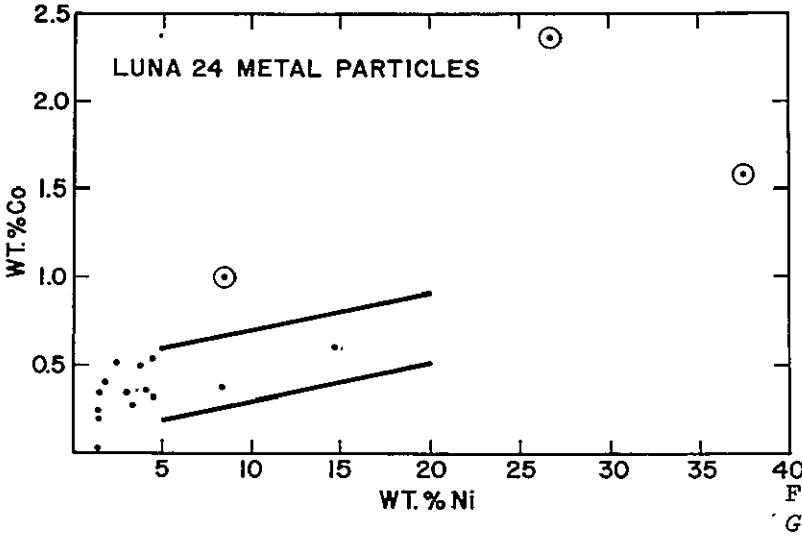

Fig. 1:
Ni-Co compositions of Luna 24 metal particles. Lines indicate field of meteoritic composition(2). High Co particles are circled.

Fig. 1 reproduced courtesy of *Geophys. Res. Lett.*

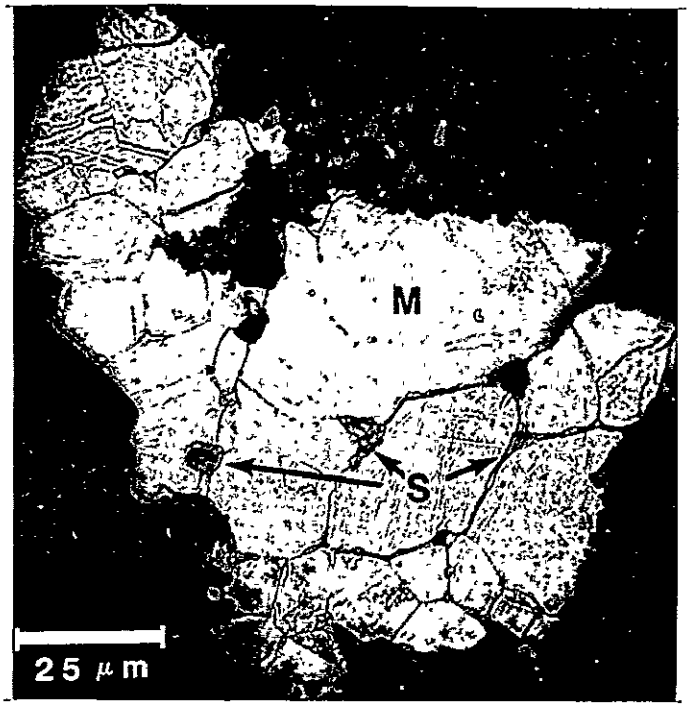

Fig. 2: Microstructure of metal particle from Section 24170,8. The FeS at the grain boundaries is designated by S.

Fig. 3: Microstructure of metal particle from Section 24210,40. The field of view is 95 x 75 μm.

References: 1. Friel,J.J. and Goldstein,J.I. (1977) Geophysical Research Letters, in press; 2. Goldstein,J.I. and Yakowitz,H. (1971) Proc. Lunar Sci.Conf. 2nd, p.177-191; 3. Goldstein,J.I.,Hewins,R.H. and Axon,H.J.(1974) Proc.Lunar Sci. Conf.5th, p.653-671; 4. Brett,R.(1976) Geochim.Cosmochim.Acta, p.997-1004; 5. Vaniman,D.T. and Papike,J.J. (1977) Geophysical Research Letters,in press; 6. Hewins,R.H. and Goldstein,J.I. (1975) Proc. Lunar Sci. Conf.6th,p.343-362.

CARBON CHEMISTRY AND METALLIC IRON CONTENT OF SOME LUNA 24 CORE SAMPLES. L. R. Gardiner, A. J. T. Jull, M. R. Woodcock, C. T. Pillinger, Planetary Sciences Unit, Dept. of Mineralogy and Petrology, University of Cambridge, England and A. Stephenson, Institute of Lunar and Planetary Physics, School of Physics, Univeristy of Newcastle-upon-Tyne, England.

As part of our studies concerning the carbon systematics of lunar soils, three Luna 24 core samples: 24090, 24125, 24196. have been investigated to give a variety of information relative to carbon chemistry. All three soils were wet sieved through stainless steel meshes (500, 250, 150, 106 and 75 μm) using spectroscopic grade methanol as the liquid phase. The >500μm fraction was further dry sieved through a 1mm nylon screen. The distribution of particle sizes obtained during sieving and all sample manipulation procedures are reported elsewhere (1). Aliquots (1mg or less) of the 75-106, 106-150 and 150-250μm fractions of each soil have been dissolved in 38% DCl and in all cases the CD_4, CH_4, He, Ne and Ar released were analysed by static mass spectrometry. Separate aliquots (ca 1mg) were investigated by XRF for FeO, TiO_2, MgO, CaO and Al_2O_3. Three single "agglutinates" (selected on their appearance as weakly sintered particles with evidence of glass splash), one from each >1mm fraction, have also been studied by the acid dissolution technique. Prior to destruction, the magnetic susceptibility (χ) and isothermal remanent magnetisation (IRM_s) measurements were performed on the agglutinates. The same non-destructive magnetic techniques were also applied to large aliquots (5-10mgs) of all sieve fractions. The results of all investigations carried out are summarised in the table.

In order to use χ (the abundance of finely-divided or superparamagnetic iron metal) or CD_4 (a measure of hydrolysable carbon (C_{hyd}) associated with the metal) as indicators of relative lunar soil maturity, the bulk iron FeO content of the samples being compared must be known (2,3). Our partial major element analysis clearly indicates that all the soil samples investigated in this study are Mare type; the data strongly suggest that they are composed predominently of material derived from the very low titanium Crisium type basalts recognised by Ryder et al. (4). All the samples under study here have FeO contents which are higher (with the exception of 15601) than any soil we have previously investigated. Sieved fractions from the sample taken from the greatest depth within the core (L24196) exhibit the highest FeO contents. However, even L24196 must contain exotic fragments of highland origin, as a smoke-sized fraction (material sub-

CARBON CHEMISTRY AND METALLIC IRON CONTENT

Gardiner, L. R., et al

stantially <1μm in size, not yet investigated by magnetic methods or acid dissolution) collected from the methanol washings(1) gave a chemical analysis of FeO:13.5%, TiO_2:0.91%, MgO:8.2 %, Al_2O_3:18.7% and CaO:14.6%. Allowing for the bulk iron content of the samples, χ and CD_4 data demonstrate that for the three depths studied, maturity decreases with depth as indicated by particle type distribution (4). On the scale established by Morris (3), L24090 would be considered as mature, with L24196 submature rather than immature. L24125 appears to be border line between mature and submature.

For the limited number of size fractions studied both χ and CD_4 in L24125 and L24196 exhibit a clear inverse dependence on particle size. The solar wind derived rare gases in both samples follow the same trend (all rare gas data cited in this paper are calibrated relative to the CD_4 standard but are uncorrected for relative sensitivity; absolute calibrations for individual species are in progress). Magnetic susceptibility also increases relative to 1/r for L24090, but CD_4, ^{20}Ne and ^{36}Ar are more constant for the three size fractions studied. This may be a function of the higher maturity of L24090. Although coarse (>250μm) particles have not yet been studied by acid dissolution, χ data (not in the table) suggest that there is no tendency towards an excess of solar wind derived species in these fractions. It appears that the concentration of complex grains into coarse fractions had not taken place before the L24090, L24125, or L24196 layers were buried by deposition.

The CD_4/CH_4 ratios for most of the sieved fractions studied are relatively low for Mare type soils. This would suggest that the samples are not highly agglutinated and that the temperatures involved during agglutination are comparatively low (5) as might be expected in view of the high FeO content of the parent rocks. The $^4He/^{20}Ne$ and $^{20}Ne/^{36}Ar$ ratios are also fairly constant for the samples studied with the exception that the L24196 soil seems to have a slightly increased ^{20}Ne content. All three hand-picked "agglutinates" have CD_4/CH_4 and rare gas ratios which are similar to the bulk material; preferential fractionation of volatile species is not apparent. On such grounds, these "agglutinates" are more probably glass-splashed weakly-sintered micro-breccias.

In fig. 1. we have plotted χ against CD_4 values for the twelve Luna 24 samples so far studied. The data define a line of slope 0.04 and χ intercept 0.13, $10^{-3}Gcm^3\ g^{-1}\ Oe^{-1}$ suggesting that the concentration of carbon in finely-divided iron at the Mare Crisium site is extremely constant. However, the slope of

CARBON CHEMISTRY AND METALLIC IRON CONTENT

Gardiner, L. R., et al

Fig. 1 Magnetic Susceptibility vs CD_4.

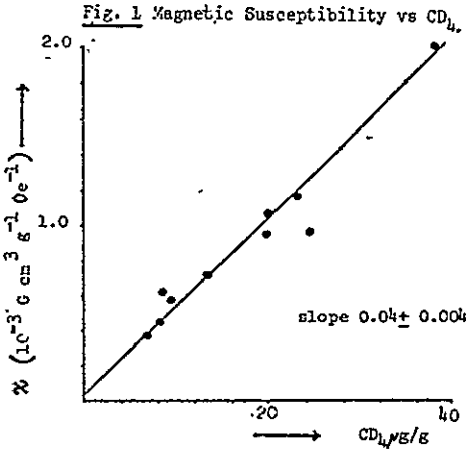

Fig. 2 Magnetic Susceptibility versus saturation isothermal remanent magnetisation

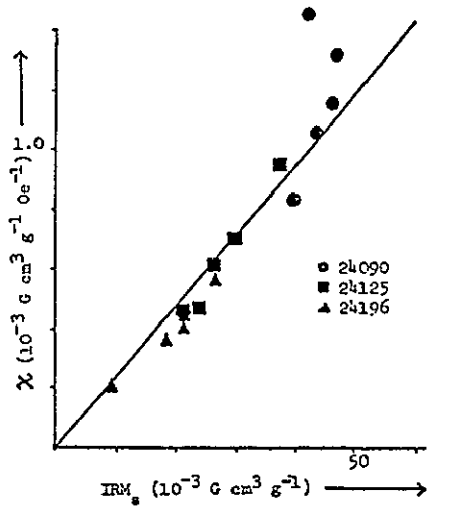

the line is a factor 5 less than a similar line obtained for twenty-nine 15601 soil fractions (6), and 2.9 less than a line fitted to data from 62 bulk lunar soils(7). Even allowing for a systematic error of 1.4, which currently exists between quantitation of samples by our static mass spectrometric method compared to data obtained previously by gas chromatography, the Luna 24 iron must have a carbon concentration of 0.7% by wt, which is 3.6 times greater than iron in 15601 and 2 times greater than the majority of lunar soils.

At present, we are unable to account for the variations observed for carbon in iron concentrations. It would seem that the chemical composition of bulk soils is not involved since 15601 and Luna 24 samples all have similar very high FeO contents. An understanding of such large changes should help to define the mechanism leading to the formation of finely-divided iron in lunar soil. Although the amount of finely-divided iron in the Luna 24 samples shows a considerable spread, a significant correlation between χ and IRM_s is observed (Fig. 2) suggesting that the particle size distribution of iron droplets is constant(8). Because the static mass spectrometric method of analysis does not appreciably degrade the CD_4 released from lunar soils, we have continued our efforts to obtain directly from this gas, a measure of the $^{13}C/^{12}C$ isotopic ratio of very small amounts of C_{hyd} (6). Since sample gases have to be compared with standards on a before-and-after basis (rather than by beam switching) the precision of the measurements obtained depend ultimately on the stability of the mass spectrometer. During the course of the analysis of the Luna 24 samples, over thirty standard CD_4 aliquots have been measured. For each standard,

CARBON CHEMISTRY AND METALLIC IRON CONTENT

Gardiner, L. R., et al

twenty comparisons of the $^{12}CD_4$ (m/e 20) and $^{13}CD_4$ (m/e 21) peak height have been made. The overall variation of $^{13}C/^{12}C$ isotopic ratio observed was 0.010469 ± 0.45%. The fluctuations observed in the measurements of single standards were typically considerably less. The CD_4 released from all samples is considerably enriched in ^{13}C relative to the standard gas (Table). We are still trying to establish the observed enrichments in absolute terms (relative to PDB). Preliminary measurements performed on our standard CD_4 by the Indiana group suggest that this gas is -28‰ relative to PDB. We are experiencing inconsistent quantitation with respect to the samples exchanged and further aliquots are under study. Assuming a value of -28‰ for the standard, the CD_4 released from C_{hyd} in Luna 24 soils is +6 to +20‰ relative to PDB. In order to determine whether the internal variations in the measurements are real, increased precision will be required. We are hoping that modifications our system will provide improved stability during the analysis of future samples.

References 1) Pillinger, C. T., Fabian, D. M. (1977), Preliminary separation of Luna 24 samples presented to the Royal Society by the Soviet Academy of Sciences, (copies available on request). 2) Pillinger, C. T., et al (1974) P4L.S.C. 1493-1508. 3) Morris, R. V. (1976)P.7.L.S.C.,315-335. 4) Ryder, G. et al (1977) The Moon (in press). 5) Pillinger, C. T., et al (1977) Phil. Trans. 284, 145-150. 6) Gardiner, L. R. et al (1977)P.8.L.S.C., in press. 7) Jull, A.J.T. et al (1977) Meteoritics, in press 8) Stephenson, A., et al (1977) Phil. Trans. 284,151-156.

Table 1: Results of acid dissolution, elemental and magnetic analyses on LUNA 24 samples.

Depth in L24 core (cm)	Size Fraction (μm)	Bulk chemistry (wt%) FeO	TiO_2	MgO	Al_2O_3	CaO	Magnetic measurements susceptibility χ	IRM_8	Carbon measurements CD_4 μgc/g	^{13}C (‰ rel to std. CD_4)	Rare gas data+ CD_4/CH_4	^4He	^{20}Ne	^{36}Ar
0	75-106	16.1	0.46	8.6	10.9	11.5	1.32	46.9	22.7	+46 ± 8	2.8	198	9.7	47.6
9	106-150	18.0	0.63	10.7	11.7	14.3	1.16	46.1	23.1	+34 ± 5	2.3	nm	nm	nm
0	150-250	19.2	1.24	9.1	12.8	14.2	1.06	43.4	20.1	+40 ± 5	4.5	163	8.9	43.0
	>1cm*	nm	nm	nm	nm	nm	2.00	102	38.2	+40 ± 5	2.1	508	28.5	129
1	75-106	18.2	0.70	9.5	11.4	11.6	0.96	37.3	24.4	+39 ± 6	2.1	248	13.9	62.9
2	106-150	18.8	0.61	9.0	11.5	11.9	0.71	29.8	13.5	+43 ± 5	4.4	173	9.5	50.0
5	150-250	17.7	0.53	9.7	11.0	12.7	0.62	26.2	8.6	+48 ± 6	7.8	85	4.6	29.8
	>1cm*	nm	nm	nm	nm	nm	1.68	102	39.2	+35 ± 4	3.1	411	26.0	129
1	75-106	19.9	1.03	10.2	9.4	10.6	0.57	26.5	9.6	+37 ± 5	3.2	165	9.5	20.2
9	106-150	20.7	1.99	9.9	8.9	10.6	0.45	21.2	8.4	+37 ± 5	3.1	116	6.1	21.0
6	150-250	20.7	0.55	14.3	8.2	10.1	0.37	18.2	7.0	+46 ± 6	2.1	109	5.8	19.5
	>1cm*	nm	nm	nm	nm	nm	0.95	20.1	19.9	+37 ± 5	1.7	398	-22.1	53.7

Units: χ, 10^{-3} G cm^3 g^{-1} Oe^{-1}, IRM_8 10^{-3} G cm^3 g^{-1}; +rare gas arbitrary units (uncorrected for relative sensitivity)

*single "agglutinate" grain nm not measured

Errors (1σ) FeO, CaO ± 0.3%, TiO_2 ± 0.1%, Al_2O_3, MgO ± 0.5%; CD_4 ± 3.0%

PETROGENESIS OF GABBROS FROM MARE CRISIUM; T. L. Grove and A. E. Bence, Dept. of Earth and Space Sciences, State Univ. of New York, Stony Brook, N. Y. 11794

Ferrogabbro lithic and monomineralic fragments dominate the 0.15-0.50 mm fraction of the seven levels of the Luna 24 core made available to NASA P.I.'s through a USSR-USA sample exchange. Modal abundances range from 30-40% in the upper portions to nearly 100% at 170 cm (Fig. 1). Mare basalt fragments constitute a minor component which suggests that a relatively thick cooling unit (or units) was sampled at the drill site [1]. The relatively low proportions of regolith breccia and agglutinate fragments indicate that the soils are immature and Florensky et al. [2] conclude that the core sampled ejecta from Fahrenheit Crater (18 km to the southwest). This ejecta experienced only limited reworking prior to sampling. The thickness of Fahrenheit ejecta at the site is estimated to be 0.5-1.0 m [2,3].

Five major categories of fragments are present in the sections studied. These are, in approximate decreasing order of abundance: monomineralic fragments, gabbro (grain size > 0.1 mm) lithic fragments, agglutinates and soil breccias, basalts, and highland melt rocks ($CaO/Al_2O_3 \lesssim 0.8$). Miscellaneous types include metal grains and glass fragments and spheres having both mare and highland affinities. The percentage of highland components appears to be quite low. However, since the mare component at the Luna 24 landing site is high in Al_2O_3 and very low in TiO_2 [4,5], it is extremely difficult to distinguish between highland crystalline fragments and coarse-grained mare gabbros in our size fraction using petrographic techniques. The number of highland lithic fragments in the melt rock population, as determined by microprobe analysis, is very low; hence, it is believed that a monomineralic highlands component in the coarse-grained fragments (0.25-0.50 mm) is correspondingly low.

At the 170-cm level, mare gabbroic (lithic and monomineralic) fragments comprise more than 98% of our sample (Fig. 1). This sample may represent a crushed rock whose fragments remained unmixed with other soil material or it may represent a detrital layer (Nagle, pers. comm.). A mode of the sieved and hand-picked fraction (0.15-0.50 mm) from this level is given in Table 1. From considerations of the size range studied and the inter- and intra-grain compositional variations, we conclude that the grain size of the gabbro parent was in excess of one mm. Its textural characteristics are, however, not decipherable from the few grain boundaries present in our samples. A paragenetic model, worked out from detailed analysis of the phase zoning, is described below.

Ferrogabbro Phase Chemistry

Clinopyroxene. The gabbroic component contains in excess of 50% complexly zoned, occasionally exsolved, clinopyroxene. The range of quadrilateral components (Wo-En-Fs) (Fig. 2a) in these pyroxenes is identical to that of the pyroxenes from Luna 24 basalts [6]. This major element zoning trend is similar to the one obtained for Apollo 14 rock 14053 and for a few mare pyroxene fragments found in the Luna 20 sample [7]. The Ti-Al and Ti-Cr-Al^{VI} relationships (Fig. 2b,c) are also similar to 14053 and Luna 20 mare pyroxenes.

Several distinct trends can be seen, and we believe that in addition to the ferrogabbro another chemically distinct (but much rarer) unit characterized

by lower Fe/(Fe+Mg) ratios, was sampled. The ferrogabbro followed a crystallization sequence that involved an early, relatively high-Mg pigeonite ($Wo_{12}En_{56}$) containing low Al^{VI} and Ti and high Cr. This low Ca-pyroxene may have preceded or co-crystallized with an aluminous and Cr-rich calcic pyroxene ($Wo_{36}En_{43}$). With cooling, a more iron-rich pigeonite crystallized. As crystallization proceeded, a trend of iron enrichment at varying levels of Wo content was followed (Fig. 2a). The Ti-Cr-Al^{VI} trend is to one of extreme Ti enrichment and Cr and Al^{VI} depletion. In the late stages hedenbergite and/or pyroxferroite crystallized. The hedenbergite is titaniferous. The dominant Ti-component is $R^{2+}Ti^{4+}Al_2O_6$; however, some $R^{2+}Ti^{3+}SiAlO_6$ is indicated. The pyroxferroite contains no detectable trivalent Ti. Observed pyroxene compositional variations in fragments from the gabbro layer can be achieved through crystallization in different regions of a single flow.

The second distinctive gabbro composition is represented by several lithic fragments containing two magnesian clinopyroxenes ($Wo_{10}En_{64}$) and ($Wo_{35}En_{50}$) with forsteritic olivine (Fo_{68}) (Fig. 2). Both pyroxenes contain high Cr_2O_3 and negligible TiO_2. Approximately one half of the aluminum is octahedrally coordinated. These pyroxenes appear to have crystallized from a low-Ti magma having a Fe/(Fe+Mg) ratio (< 0.6) less than the ferrogabbro and ferrobasalt parental liquids.

Olivine. Olivine compositions range from Fo_{90} to Fo_4 (Fig. 2a); however, only those with forsterite contents less than about Fo_{58} are associated with the ferrogabbro. The rarer, low-Fe gabbro contains olivine of Fo_{67-68} composition. More magnesian olivines (> Fo_{70}) probably have a highland provenance.

Plagioclase. Plagioclase has a relatively restricted compositional range (An_{80}-An_{96}) (Fig. 3a). Abundances of Fe and Mg are quite variable and can be used to distinguish some highland plutonic plagioclase from mare gabbro plagioclase. Highland plagioclases (An_{94-96} and associated with Fo_{80} olivine) contain no Mg and very little iron (Fig. 3b).

Oxide Phases. Oxide phases in the Luna 24 ferrogabbro consist of aluminian chromite, chromian ulvöspinel, ulvöspinel, and ilmenite [8]. Compared to the basalts, the spinels have restricted compositional ranges.

By combining the phase compositional and rare textural information, we have observed in the Luna 24 ferrogabbro, and by applying experimentally determined silicate-liquid partition coefficients, we can reconstruct its paragenetic sequence and the approximate composition of the liquid from which it crystallized. The parental liquid appears to have been nearly multiply saturated at the lunar surface with olivine, two clinopyroxenes, and plagioclase. The evidence for cosaturation at near-surface conditions is that Fe/(Fe+Mg) of the cores of olivine, low-Ca pyroxene, and high-Ca pyroxene indicate that all these phases were in equilibrium with the same liquid (Fe/(Fe+Mg) = 0.68-0.70). The $K_D^{ol\text{-}liq}$ of Roeder and Emslie [9] and Longhi et al. [10] was used for olivine and the $K_D^{pyx\text{-}liq}$ of Grove and Bence [11] was used to estimate Fe/(Fe+Mg) of the liquid in equilibrium with the first pyroxenes.

Minor element data from pyroxene allows us to infer the paragenetic sequence. Early low-Ca pyroxene (Fig. 2b) contains no octahedrally coordinated Al, suggesting that it crystallized at relatively slow cooling rates. This low-Ca pyroxene, a high-Ca pyroxene, olivine, and plagioclase appear nearly simultaneously in the crystallization sequence. Continued crystallization

GABBROS FROM MARE CRISIUM

Grove, T. L., et al.

with resulting Fe enrichment produces a low-Ca trend approaching pyroxferroite and a high-Ca trend that approaches hedenbergite. The mare olivine compositional range (Fig. 2a) is consistent with initial co-crystallization with low Ca pyroxene. Only those olivines associated with unequivocally mare pyroxenes are designated as of mare origin in Fig. 2a, and some of the more magnesian monomineralic olivines designated as highlands could be of mare origin. Throughout much of the crystallization history, olivine, spinel, two pyroxenes and plagioclase appear to have crystallized simultaneously.

A crude estimate of the bulk composition of the liquid from which the Luna 24 ferrogabbro crystallized can be obtained from the chemistry of the pyroxenes. It is assumed that the very low-Ti liquid was multiply saturated at near surface conditions with olivine and two pyroxenes and that the bulk partition coefficients [11] for CaO, MgO, FeO, Al_2O_3, TiO_2 and Cr_2O_3 are applicable for this bulk composition. Since partitioning of CaO between high-Ca pyroxene and liquid is nearly temperature and rate independent, the molar CaO content of the liquid can be estimated from the Wo content of the high-Ca pyroxene. This, in turn, allows calculation of the appearance temperature (1165-1135°C) of the low-Ca pyroxene and the use of the experimentally determined bulk D's to estimate molar abundances of FeO, MgO, Al_2O_3, Cr_2O_3 and TiO_2 of the liquid. Because the paragenetic sequence of the Luna 24 gabbro is similar to that of the Apollo 15 quartz normative basalts on which the experimental bulk D's were determined we feel that the comparison is warranted. The estimated molar abundances are presented in Table 2 along with a representative analysis of the brown glass found in the Luna 24 core. The mineral chemistries of the Luna 24 ferrogabbro and ferrobasalt [6] are nearly identical, suggesting that both crystallized from essentially the same liquid. Comparison of a brown glass chemistry, also present at the site, with that estimated for the gabbro parent liquid (Table 2) indicates that the brown glass may be a representative liquid composition of both the gabbro and basalt. Low-pressure melting studies on the brown glass composition [12] reveal that it has plagioclase on the liquidus quickly followed by olivine, but that it is nearly multiply saturated. Our calculated bulk composition for the ferrogabbro lies near the experimentally determined multiple saturation point (1150°C) olivine-plagioclase-pyroxene ($En_{43}Wo_{33}$). In the vicinity of this point very slight changes in magma composition will dramatically affect the early paragenesis, and representatives of several basalts related by differentiation of plagioclase and olivine in lava flows at Mare Crisium may be mixed together in our soil sample.

References

[1] *Bence, A. E., et al., GRL, in press, 1977;* [2] *Florensky, C. P., et al., PLSC 8th, in press, 1977;* [3] *Barsukov, V. L., PLSC, 8th, in press, 1977;* [4] *Barsukov, V. L. and C. P. Florensky, Proc. L.S.C. VIII 61-63, 1977;* [5] *Tarasov, L. S., et al., in press, 1977;* [6] *Vaniman, D. T. and J. J. Papike, GRL, in press, 1977;* [7] *Cameron, K. L., et al., GCA, 37, 775-795, 1973;* [8] *Haggerty, S. E., GRL, in press, 1977;* [9] *Roeder, P. L. and R. F. Emslie, Contr. Min. Pet., 29, 275-289, 1970;* [10] *Longhi, J., et al., EOS, 56, 471, 1975;* [11] *Grove, T. L. and A. E. Bence, PLSC 8th, in press, 1977;* [12] *Grove, T. L. and D. T. Vaniman, this volume, 1977.*

GABBROS FROM MARE CRISIUM

Grove, T. L., et al.

Table 1. Modal Mineralogy of the Gabbro Layer at 170 cm

Clinopyroxene	52 2
Plagioclase	33.7
Olivine	9 5
Cristobalite	3 0
Ilmenite	0.6
Spinel	Trace
Metal	Trace
Non-gabbro	1.0

Table 2 Comparison of brown glass and estimated Luna 24 gabbro bulk composition from pyroxene minor element chemistry

	a	b	c
SiO_2	47.0	50 0	---
Al_2O_3	12.7	8.0	5.5-7 0
TiO_2	0.80	0 64	0.55
FeO	20 0	17 8	19.0
MnO	0 25	0 23	---
MgO	5 5	8.7	8.8
CaO	12.7	14 5	15 0-16 0
Cr_2O_3	0.3	0 13	0.1
Σ	99 25	100 00	---

(a) Representative brown glass analysis (wt.%).

(b) Brown glass analysis in mole %

(c) Oxide abundances (mole %) estimated from pyroxene chemistry.

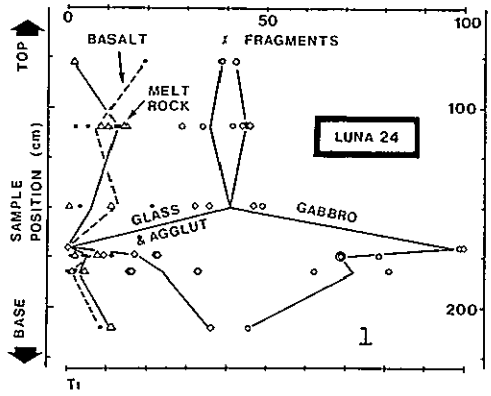

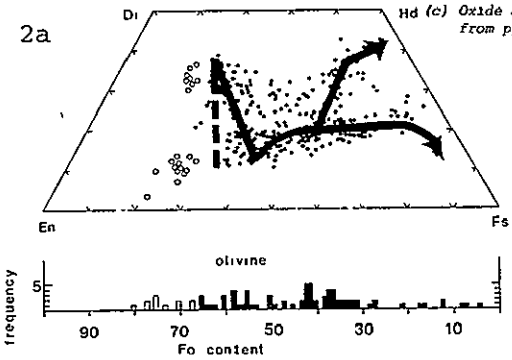

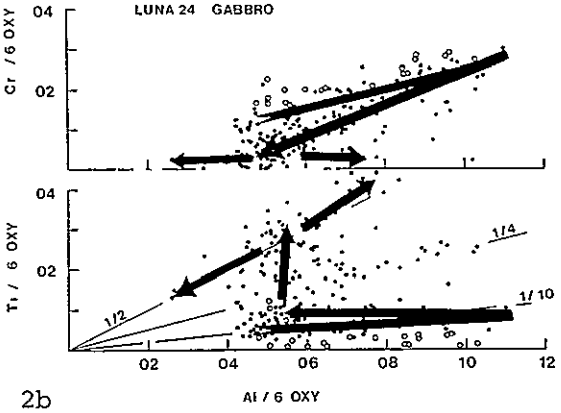

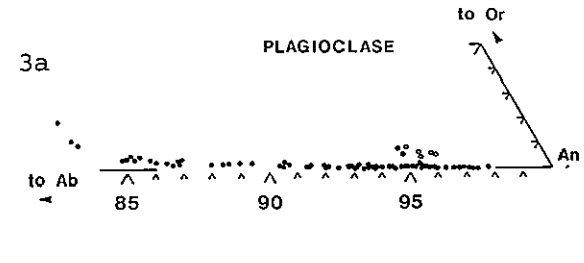

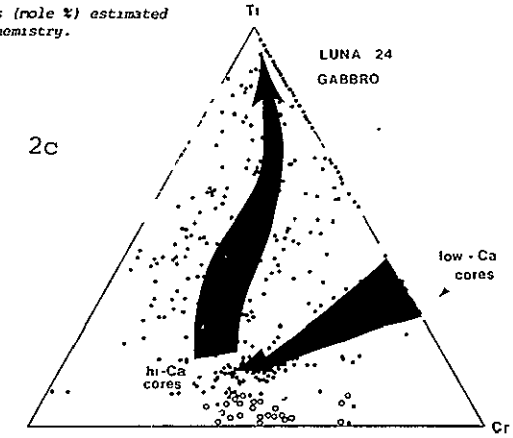

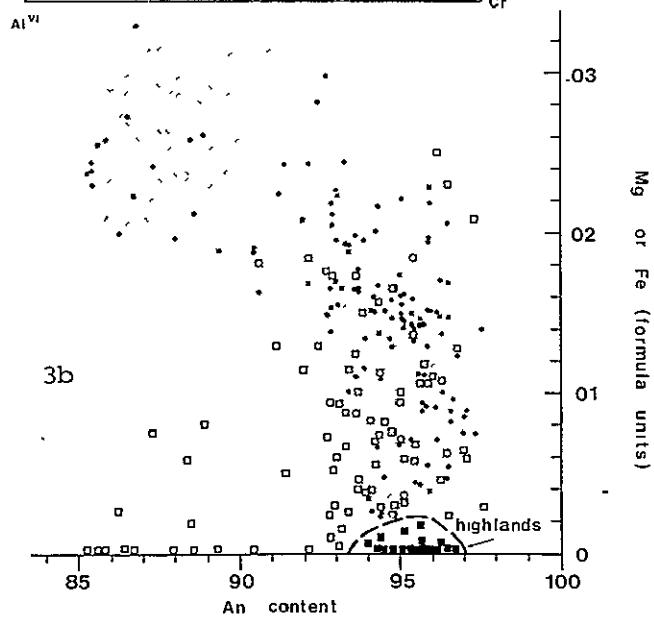

Figure Captions: (1) Lithologic abundances in 0.15-0.50 mm fraction. (2a,b,c) Mare compositions; solid symbols, highland compositions; open symbols. (3a) Mare plagioclase; solid symbols, highland plagioclase; open symbols. (3b) Mare plagioclase; Fe dots, Mg open squares. Highland plagioclase; Fe solid squares, Mg below detectability limits.

EXPERIMENTAL PETROLOGY OF VERY LOW TI BASALTS AND ORIGIN OF LUNA 24 FERROBASALT; T. L. Grove and D. T. Vaniman, Dept. of Earth and Space Sciences, State Univ. of New York, Stony Brook, N. Y. 11794

Introduction. Low-pressure equilibrium experiments in iron capsules have been performed on synthetic analogs of Apollo 15 green glass and LUNA 24 brown glass to determine whether crystal fractionation of the mafic Apollo 15 green glass could generate Apollo 17 very low Ti (VLT) basalts [1] and LUNA 24 ferrobasalt. The results indicate that Apollo 17 VLT's can be derived by low-pressure crystal-liquid fractionation from an Apollo 15 green glass parent but that LUNA 24 ferrobasalts cannot.

Mare basalt compositions in the LUNA 24 drill core. Estimates of LUNA 24 mare basalt compositions have been obtained in four ways: (1) Recombination of modal and microprobe analyses of basalt fragments to yield bulk-rock compositions (Table 1; #4). (2) Modal recombination of recrystallized basalts (Table 1; #3). Although texturally (and perhaps chemically) altered by impact metamorphism, the recrystallized basalts give a more accurate estimate of composition because the minerals involved in modal recombination have requilibrated and are not strongly zoned. (3) Analysis of brown mare glass fragments (Table 1; #2). Brown glass fragments may be brecciated and slightly vesicular; some fragments contain relict crystals and have a patchy micropoikilitic texture. The brown glass is apparently an impact melt of LUNA 24 ferrobasalt flows or soils. (4) Estimates using partition coefficients determined for low and high-Ca clinopyroxenes from the ferrogabbro [2]. The four techniques yield slightly different bulk compositions and we note that the ferrobasalt estimates are slightly more plagioclase rich, the ferrogabbro estimates are plagioclase depleted and the brown glasses and recrystallized ferrobasalts are intermediate. We hesitate to attach any significance to these differences at this time, because the estimation techniques may not have sufficient accuracy.

Experiments. Low-pressure experiments on synthetic analogs of Apollo 15 green glass and LUNA 24 brown glass (Table 1; #1,2) were carried out in iron metal capsules sealed in silica glass tubes. The green glass composition is an average of microprobe analyses compiled by Stolper [3] and the LUNA 24 glass is an average of 10 brown glass analyses from the LUNA 24 soil sample. Phase appearance and chemistry are summarized in Fig. 1 and the liquid line of descent for green glass is depicted in Fig. 2 using the projection scheme of Walker *et al.* [4]. Residual liquid compositions for the experiments are recalculated into the system Mg_2SiO_4(Fo)-Fe_2SiO_4(Fa)-$CaAl_2Si_2O_8$(An)-SiO_2 (molar units). Three subprojections are used; Ol-An-SiO_2, Fo-Fa-An and Fo-Fa-SiO_2. Control by crystal fractionation must be confirmed in all subprojections. Also plotted in Fig. 2 are the compositional estimates for Apollo 17 VLT basalts, LUNA 24 ferrobasalt, ferrogabbro, brown glass and other glass types present in the LUNA 24 sample.

Results: Apollo 17 VLT. The bulk compositional estimates for Apollo 17 VLT basalts lie along the olivine fractionation lines for the green glass experiments, suggesting that approximately 5% to 25% olivine fractionation of an Apollo 15 green glass parent is sufficient to produce the Apollo 17 VLT basalts.

LUNA 24 ferrobasalts. LUNA 24 ferrobasalts and brown glass cannot be

derived from an Apollo 15 green glass parent by any type of low-pressure liquid-crystal fractionation. Ferrobasalt compositions lie below the green glass olivine-pyroxene cotectic and, therefore, can't be derived by near surface fractionation of olivine and pyroxene (± spinel) as suggested by [5,6]. Experiments on the LUNA 24 glass indicate that it lies within the plagioclase primary phase volume close to the olivine-plagioclase cotectic. At present we cannot rule out a genetic relation to other green glass parent material. It is well known that compositional variability exists between green glass groups. However, we have attempted to estimate the liquid line of descent for Apollo 14 green glasses [2,7] and have found that LUNA 24 ferrobasalt cannot be generated from this green glass material.

Origin of LUNA 24 basalts. We will consider three alternative possibilities for the origin of LUNA 24 ferrobasalts: (1) origin by a complex fractionation process at depth in the lunar interior; (2) derivation from other aluminous basalt types; and (3) derivation from other glass chemistries in the LUNA 24 core. (1) It might be possible to generate LUNA 24 basalt from a green glass parent material by fractional crystallization at depth in the lunar interior. A possible scenario would involve the crystallization of a magma at depth with removal of olivine and pyroxene (± spinel) followed by separation of the residual liquid and eruption on the lunar surface. A test of this hypothesis is presently being carried out in the laboratory. (2) LUNA 24 basalts have CaO/Al_2O_3 ratios characteristic of aluminous mare basalts (e.g., 14053, 14072, Luna 16). However, these aluminous basalts contain substantial amounts of TiO_2 (from 2 to 7 wt.% compared with <1% for LUNA 24) and TiO_2 removal through crystallization of a near liquidus Ti-rich oxide phase is unlikely. The near liquidus phases in aluminous basalts are olivine, plagioclase and a Cr-Al rich spinel [8,9] and only in the late stages does the oxide phase approach ulvöspinel in composition. (3) There are several glasses in the LUNA 24 soil sample that might represent parental material for LUNA 24 ferrobasalt and gabbro. There is a mafic green glass that is high in TiO_2 (Table 1; #5) and, therefore, cannot be fractionated to give the low Ti LUNA 24 basalt. An aluminous green glass (Table 1; #6) does not appear to be related to the LUNA 24 ferrobasalts by any reasonable scheme of fractionation of near-liquidus phases.

Conclusions. The LUNA 24 ferrobasalt and ferrogabbro are unique lunar mare rock types. No other mare basalt has so high an Fe/(Fe+Mg) ratio (∿ 0.65, atomic) with low TiO_2 content (∿ 1.0%) and high $CaO+Al_2O_3$ content. Of all lunar and meteoritic rock types, the eucrite meteorites [10] are closest to the LUNA 24 ferrobasalt in major and trace element composition. However, the CaO/Al_2O_3 ratio of comparable eucrites is ∿ 15% lower. The LUNA 24 ferrobasalt has rare earth enrichments similar to eucrites, with REE enrichments ∿ 5-10x chondritic (data of Barsukov et al. [11] on 24170.1-006; and data of J. C. Laul for 24174,7; 24077,4; 24077,62 and 24182,12, pers. comm.).

Low-pressure experiments on an Apollo 15 green glass analog indicate that the Apollo 17 VLT can be generated by near-surface olivine fractionation. Low Ti LUNA 24 ferrobasalts, however, cannot be derived from green glass by near-surface fractional crystallization of Apollo 15 green glass. At present we have no satisfactory means of deriving LUNA 24 basalt from the only other known Ti-poor mare chemistry found on the Moon (green glass). The possibility

that fractional crystallization of green glass at high pressures may be involved is presently being tested in our laboratory. Other glass chemistries at LUNA 24 do not appear to be related to the iron-rich, low-Ti basalt. LUNA 24 ferrobasalts are an evolved mare type that has not been sampled by previous Apollo and LUNA missions.

References

[1] *Vaniman, D. T. and J. J. Papike, PLSC 8th, in press, 1977;* [2] *Bence, A. E. et al., GRL, in press, 1977;* [3] *Stolper, E. M., A. B. thesis, Harvard Univ., 1973;* [4] *Walker, D., et al., Earth Planet. Sci. Lett. 20, 325-336, 1973;* [5] *Vaniman, D. T. and J. J. Papike, GRL, in press, 1977;* [6] *Taylor, G. J., et al., GRL 4, 207-210, 1977;* [7] *Chao, E. C. T., et al., PLSC 3rd, 907-925, 1977;* [8] *Walker, D., et al., PLSC 3rd, 797-817, 1972;* [9] *Haggerty, S. E., PLSC 3rd, 305-322, 1972;* [10] *Stolper, E. M., Geochim Cosmochim. Acta 41, 587-611, 1977;* [11] *Barsukov, V. L., PLSC 8th, in press, 1977.*

Table 1: Analyses of Luna 24 Ferrobasalt Compositions, Magnesian Luna 24 Glasses, and Synthetic Apollo 15 Green Glass.

	1	2	3	4	5	6
SiO_2	45.86	47.10	46.7	45.7	45.15	46.10
TiO_2	0.43	0.88	0.83	0.86	1.35	0.51
Al_2O_3	7.94	12.60	12.9	13.8	10.12	15.20
Cr_2O_3	0.36	0.23	0.26	0.25	0.42	0.38
FeO	19.29	20.20	21.0	19.0	20.55	15.50
MnO	0.22	0.25	0.29	0.28	0.29	0.19
MgO	17.45	6.31	6 90	7.06	11.87	9.69
CaO	8.43	12.80	11.5	13.0	10.47	11.42
Na_2O	0.00	0.20	0.27	0.22	0.09	0.04
K_2O	0.01	0.02	0.01	0.01	0.01	0.02
Σ	99.99	100.59	100.7	100.2	100.32	99.05
Fe/(Fe+Mg)	0.38	0.64	0.63	0.60	0.49	0.47
CaO/Al_2O_3	1.06	1.02	0.89	0.94	1.03	0.75

1: Synthetic Apollo 15 green glass; 2: Average of 10 Luna 24 brown ferrobasalt glasses; 3: Average of two recrystallized ferrobasalt compositions obtained by modal recombination; 4: Average of two unrecrystallized ferrobasalt compositions obtained by modal recombination; 5: Luna 24 green glass; 6: Luna 24 Mg, Al-rich green glass.

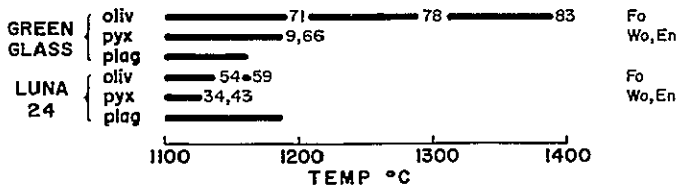

Fig. 1. Summary of phase appearance temperature and chemistry for Apollo 15 green glass and LUNA 24 brown glass experiments.

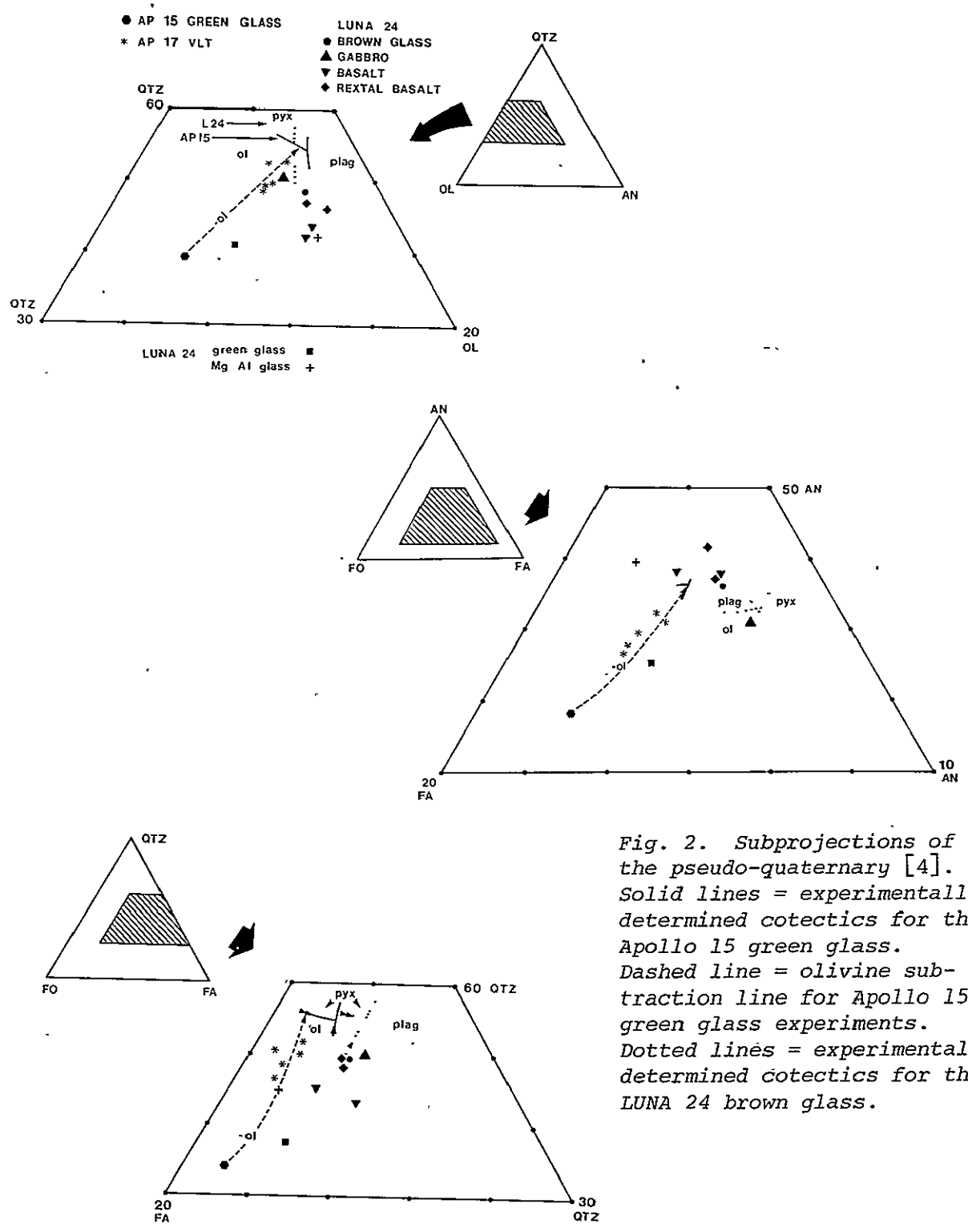

Fig. 2. Subprojections of the pseudo-quaternary [4]. Solid lines = experimentally determined cotectics for the Apollo 15 green glass. Dashed line = olivine subtraction line for Apollo 15 green glass experiments. Dotted lines = experimentally determined cotectics for the LUNA 24 brown glass.

LUNA 24: SYSTEMATICS IN SPINEL MINERAL CHEMISTRY.

Stephen E. Haggerty, Dept. of Geology, Univ. of Mass., Amherst, Ma. 01003.

Basalts and gabbros from the Luna 24 drill string provide a unique opportunity in comparative studies of cooling rates for an isochemical system. Mineral chemistry, bulk compositions and crystallization trends for the Luna 24 ferrobasalts and the ferrogabbro suggest that both rock types are probably derived from a closely similar low titanium source region and that the differences in grain size are the result of contrasting cooling histories (1, 2, 3). Although the opaque mineral constituents of the rocks are in low modal abundances ($\leq$ 1%), the trends in mineral chemistry for the spinel mineral group are significant in the context of the depths from which these phases were initially nucleated.

Electron microprobe data for spinels in 15 basalt fragments (0.09-0.50 mm) from core locations between 77 and 174 cms, and for spinels from the gabbroic horizon at 170 cms are summarized in Fig 1. These data show that spinels in both rock types are highly aluminous and maximum concentrations of 19.8 wt% Al_2O_3 have been determined. The gabbroic spinels are of two types, aluminian chromites (11.5-16.9 wt%) which form a tight cluster at the base of the prism, and ulvöspinels with Al_2O_3 = 1.2-1.5 wt% and MgO = 0.1-0.5 wt% at the prism Fe-apex. In contrast to these two populations, spinels in the basalts form a continuous range of compositions which include Al-Mg-chromites (7 wt% MgO, 19.8 wt% Al_2O_3), Al-chromites (10-13 wt% Al_2O_3), Al-Ti-chromites (6 wt% TiO_2, 13 wt% Al_2O_3), Ti-Al-chromites (18 wt% TiO_2, 6 wt% Al_2O_3), Cr-Al-ulvöspinels (11 wt% Cr_2O_3, 3 wt% Al_2O_3) and ulvöspinel (1 wt% Al_2O_3). This trend is typical of the crystallization sequence which is observed in many mare basalts and although no single Luna 24 basalt spans the entire spinel range, there are three basalts which do span approximately 75% of the solid solution series in crystals with zoned core-mantle relationships. The systematics of Fe-Mg and of Cr-Al (Figs 2-3) variations provide a more detailed clarification of these distributions for ions in tetrahedral and in octahedral coordination respectively. The bimodality of gabbroic spinels is once again well defined and so too are the distributions for spinels in the basalts. For Fe-Mg variations the basaltic spinels fall along two distinctly different linear slopes. The first is defined as the low-Mg slope which is steep and is characterized by Ti-rich spinels; the second is an intermediate-Mg trend which has a gentle slope and is typical of chromites. Early formed chromian spinels in the gabbro occupy the pivotal region in which these changes in slope digress, and this value is Fe = 9 cats/32 O_2, Mg = 1 cat/32 O_2. Comparable changes in slope for Cr-Al relationships are less pronounced and the overall trend is relatively smooth. However, on closer examination the low and intermediate Mg trends are duplicated. High Cr (8-10 cats/ 32 O_2) spinels form one group with variable Al contents, whereas the low Cr group decreases systematically with decreasing Al. These trends are equivalent, respectively, to chromites (on the base of the prism and in the gently sloping Fe-Mg trend) and to Cr-Al-ulvöspinels (which are between the prism base and Fe_2TiO_4, and are also represented by the steep Fe-Mg slope). Two noteworthy points for Cr-Al variations are: (a) that the gabbroic spinels overlap the range in Al contents of the basalts; and (b) that the more aluminous basaltic spinels exhibit a

LUNA 24: SYSTEMATICS IN SPINEL MINERAL CHEMISTRY

Stephen E. Haggerty

depletion in Cr and the resultant trend is partially parabolic; there is a large intervening gap between these spinels and chromian pleonastes from Apollo 14 and Luna 20 (Fig 3).

A comparison of the Luna 24 spinels with spinels from other lunar sites show that the limits of Al-enrichment are comparable to those from Apollo 14 and Luna 16. Chromium concentrations are lower than those of Apollo 17 for chromian spinels, and the inclusive range of Cr contents as a function of Al for titanian spinels is between Cr/Al ratios of 2:1 and 3:1 (Fig 3). Apollo 14 and Luna 16 Fe-Mg variations are also similar to Luna 24 (Fig 2) although neither of those spinel groups exactly duplicate the crystallization trends of Luna 24. It is of interest to note, however, that the Luna 24 gabbroic spinels lie in paths which closely parallel those of spinels in basalts from other low Ti source regions.

Data for spinels from other lunar intrusive suites (3) are included in Figs 1-3. Variations in Fe and Mg show that the discontinuities in slope profiles are confirmed, and that a well defined curve now results with the Luna 24 gabbroic spinels falling at one end of an Fe-enrichment and Mg-depletion trend. With increasing Mg contents the curve is defined by the Luna 24 gabbro, by two Apollo 16 anorthosites, a suite of troctolites, and the Apollo 17 dunite (74215). A large proportion of the Luna 24 basaltic spinels, primary spinels in sample 14053, and spinels in Luna 16 are in close proximity to the curve but do not lie on it. For Cr-Al relationships (Fig 3) there is a remarkable constancy in Cr contents for variable Al concentrations. The Luna 24 gabbro is lower in Cr but the Al variation is otherwise paralleled. A comparison of the lunar spinel trends with those in terrestrial layered intrusive suites (Figs 4-5) are in agreement with the Fe-Mg relationship and these show, furthermore, that for Cr and Al that the trend is indeed parabolic as is suggested by Fig 3. The implication of this comparison is that there are now clear indications that a large proportion of mare basaltic spinels did not nucleate at the surface but are derived instead at some depth. This is supported, in part, by the observation that Cr-rich spinels are the earliest constituents of basalts and that the Ti-enrichment trend which yields ulvö-spinel is a late stage crystallization product. If these two distinct generations are assumed to be depth dependent then the changes in slope discontinuities for Fe and Mg are adequately explained. It is emphasized that the Luna 24 gabbro is at the very extreme of the Fe-Mg intrusive trend, that the basaltic spinels do not lie precisely on this curve, and that this proposed spinel P-T grid is not, therefore, in conflict with the multiple saturation model (1, 2) for the Luna 24 suite under near surface conditions.

Refs: (1) Bence et al. (1977). Gabbros from Mare Crisium: An analysis of the Luna 24 soil. Geophys. Res. Lett. (in press). (2) Vaniman and Papike (1977). Ferrobasalts from Mare Crisium: Luna 24. ibid. (3) Haggerty (1977). Luna 24: Opaque mineral chemistry of gabbroic and basaltic fragments from Mare Crisium. ibid.

LUNA 24: SYSTEMATICS IN SPINEL MINERAL CHEMISTRY

Stephen E. Haggerty

Figs. 1, 2, and 3 reproduced courtesy of *Amer. Geophys. Union.*

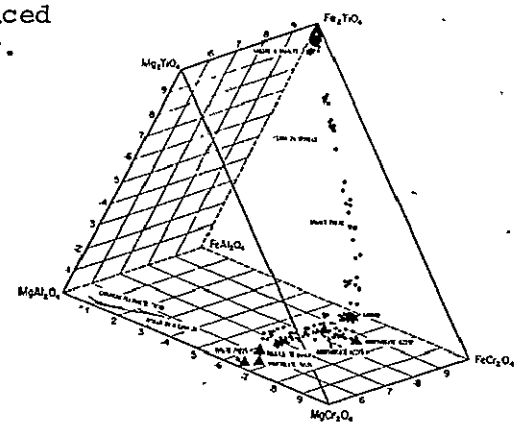

Fig. 1

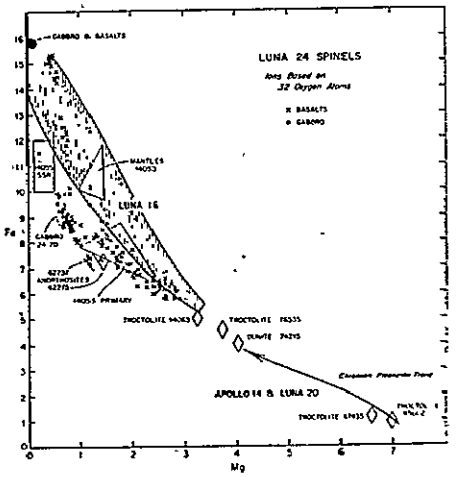

Fig. 2

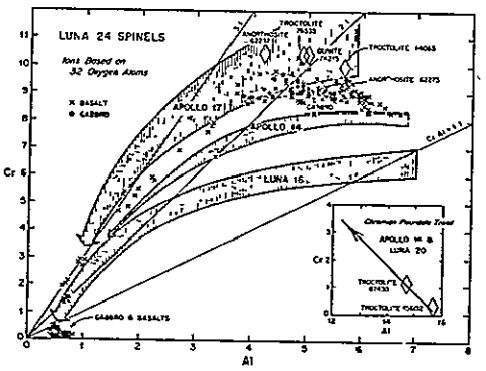

Fig. 3

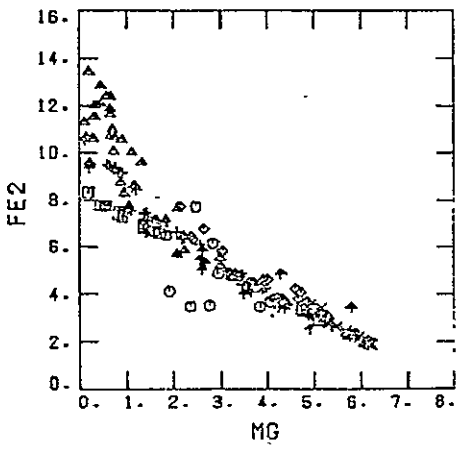

Fig. 4

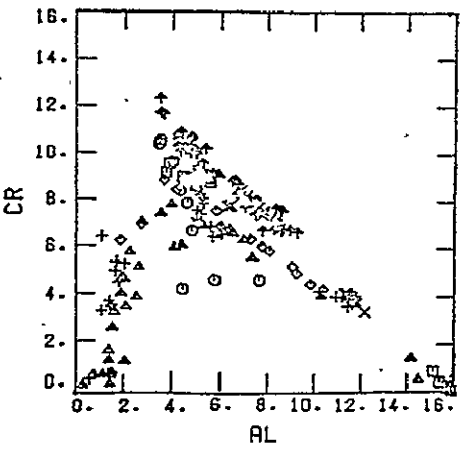

Fig. 5

VISCOUS FLOW, CRYSTAL GROWTH, AND GLASS FORMATION OF HIGHLAND AND MARE BASALTS FROM LUNA 24. C. A. Handwerker, P. I. K. Onorato, and D. R. Uhlmann, Department of Materials Science and Engineering, Massachusetts Institute of Technology, Cambridge, Mass. 02139.

A kinetic treatment of glass formation has been shown to have significant promise for elucidating the conditions of formation of lunar glasses. This approach has previously been applied to a variety of both highly vitric and highly crystalline Apollo 14, 15, 16, and 17 breccias, such as 14259, 14310, 15286, 65016, 67975, 70019, and 79155 (Uhlmann et al., 1975).

This treatment is now applied to two LUNA 24 compositions. From measurements of crystal growth rates and viscous flow behavior over wide ranges of temperatures, the critical conditions for glass formation of these compositions have been calculated. The results, notably the minimum critical cooling rates, have been combined with heat flow analyses to estimate the dimensions of the largest body which can be formed with the degree of crystallinity seen in the LUNA 24 samples.

The two LUNA 24 compositions chosen for the present study are basaltic clusters identified by Simonds et al., 1977. Composition 1 is a highly devitrified mare basalt cluster with low Mg content. The LUNA 24 sample shows a spherulitic devitrification microstructure. Composition 2 is a highly vitric highland basalt cluster comprised of heterogeneous glass fragments. This composition is close to the average composition of the highlands. Glasses of this composition are abundant; but crystalline rocks are almost never found.

The compositions of the two clusters were obtained using electron microprobe analysis by Simonds et al., 1977. They are shown in the Table below.

Table I
Compositions Investigated (wt.pct.)

Composition 1		Composition 2
46.26	SiO_2	44.97
0.98	TiO_2	0.30
12.98	Al_2O_3	26.74
20.00	FeO	4.89
6.47	MgO	6.86
12.73	CaO	15.64
0.29	Na_2O	0.23
0.04	K_2O	0.05

The kinetic analysis requires detailed information about the viscous flow and crystallization behavior of the materials. In the present study, data on viscous flow and crystallization behavior were obtained over wide ranges of temperature on synthetic glasses prepared from reagant grade raw material powders using the compositions listed above. The techniques of

GLASS FORMATION OF LUNA 24 BASALTS

Handwerker, C. A. et al.

preparing the samples and measuring the viscosity have been described in detail elsewhere (Cukierman et al., 1972). The measurements of the crystal growth rates over wide ranges of temperatures were performed using techniques similar to those employed in previous studies of other lunar compositions (Scherer et al., 1972, e.g.). The furnace used for the crystallization runs was equipped with a gas-mixing system, using CO-CO_2 mixtures, and an electrolytic cell similar to those used previously by Lofgren et al., 1974. The use of a controlled atmosphere in the crystallization furnace was considerd important because of the possible effects of Fe-oxidation state on the rates of nucleation and crystal growth. Such effects, reflected in changes of observed textures in crystallized bodies with changes in oxygen fugacity, were noted by Lofgren et al..

It was considered sufficient to provide an atmosphere of low oxygen activity rather than one of closely-controlled oxygen fugacity for the measurements of liquid viscosity, because of the results obtained by Cukierman and Uhlmann, 1974, on Lunar Composition 15555. Even for the composition containing 22.5 wt.pct. FeO, it was found that small changes in the oxidation state from one of low Fe^{3+} concentration (for Fe^{3+}/total Fe ratios of 0.26 or less) has a negligible effect on the measured viscosity. Since the two compositions investigated in the present study have smaller iron concentrations (20.0 wt.pct. for Composition 1 and 4.89 wt.pct for Composition 2) than 15555, no significant effect of variations in oxygen activity on the measured viscosity was anticipated.

The data on growth rate and viscosity have been combined to construct time-temperature-transformation (TTT) curves corresponding to various degrees of crystallinity, and in particular to the degrees of crystallinity observed in the two LUNA 24 sample clusters (greater than 90 volume percent crystallized for Composition 1 and less than 5 volume percent for Composition 2. In both cases, the nucleation frequencies required in the kinetic treatment were calculated from the measured viscosities using the classical theory of homogeneous nucleation. In these calculations, a nucleation barrier of 60kT at a relative undercooling, ΔT_r, of 0.2 was assumed. Here $\Delta T_r = \Delta T/T_E$, where ΔT is the undercooling and T_E is the liquidus temperature. The use of classical nucleation theory and the range of assumed nucleation barrier are in agreement with the results obtained by Klein and Uhlmann, 1976, on Lunar Composition 70019.

In treating the process of crystallization, continuous cooling (CT) curves for both constant-rate and logarithmic cooling conditions were constructed from TTT curves following the procedure described previously (Uhlmann et al., 1975). From the CT curves corresponding to the degrees of crystallinity in the LUNA 24 sample clusters, it has been possible to set limits on the rates at which the lunar samples cooled.

As a complement to the analysis of glass formation described above, a more detailed kinetic description of the development of partial crystallinity in glass bodies has been carried out. By using a crystal distribution function essentially complete statistical information on the state of crystallinity of the two LUNA 24 samples has been obtained. The minimum critical cooling

GLASS FORMATION OF LUNA 24 BASALTS

Handwerker, C. A. et al.

rate has also been estimated from the analysis of crystallization statistics. A comparison of the cooling rate results obtained from the construction of CT curves and from crystallization statistics indicates that the volume fraction crystallized at the critical cooling rate calculated from the CT analysis represents an overestimate of the actual volume fraction crystallized.

Heat flow analyses for a variety of geometries have also been carried out, and have been used to estimate the dimensions of the largest possible body of each composition which can be obtained as a glass.

References

Cukierman, M. et al., 1972. Proc. Lunar Sci. Conf. 3rd, pp. 2619-2626.
Cukierman, M. and Uhlmann, D. R., 1974. J. Geophys. Res. 79, pp. 1594-1598.
Klein, L.C. and Uhlmann, D. R., 1976. Proc. Lunar Sci. Conf. 7th, pp. 1113-1121.
Lofgren, G. et al., 1974. Proc. Lunar Sci. Conf. 5th, pp. 549-567.
Scherer, G. W. et al., 1972. Proc. Lunar Sci. Conf. 3rd, pp. 2627-2637.
Simonds, C. H. et al., 1977. this volume.
Uhlmann, D. R. et al., 1975. Proc. Lunar Sci. Conf. 6th, pp. 641-672.

GEOLOGIC SETTING AND TOPOGRAPHY OF THE CRISIUM BASIN AND THE LUNA 24 LANDING REGION. J. W. Head, Dept. of Geological Sciences, Brown Univ., Providence, RI 02912, S. Zisk, Haystack Observatory, Westford, MA 01886, J. Adams, Dept. of Geological Sciences, Univ. of Washington, Seattle, WA 98195, T. McCord, Inst. for Astronomy, Univ. of Hawaii, Honolulu, HA 96822, C. Pieters, Johnson Space Center, Houston, TX 77058.

The regional geology of the Crisium Basin provides an important framework for the interpretation of contributions to the sample collected by Luna 24. In this paper we report preliminary findings based on examinations of the geology, topography, and multispectral imagery.

Mare Crisium may occupy the site of two major impact basins. The presence of a second large, but degraded, impact basin to the northeast of the main Crisium Basin (Fig. 1) is suggested by: a) irregular development and absence of massifs in the northeast and east (Fig. 2, 3); b) low-lying topography flooded by maria in the region to the northeast. If further analysis establishes the presence of this basin, it is possible that the Crisium projectile may have encountered earlier basin rim materials at the target site, thus enhancing the possible inclusion of deeper crustal materials in Crisium Basin rim deposits. The massifs adjacent to the Luna 24 site lie close to the junction of the two major basin rings.

The regional topography of Mare Crisium has a distinctive annular appearance. Previous topographic profiles over portions of Mare Crisium have shown shelf topography around the central and southern margins of Mare Crisium (1). Radar topography (Fig. 2, 3) shows the shelf area to extend around the basin to the north and east. The outer shelf is about 50 km wide and is distinctive around almost the entire circumference of the basin except in the southwest, where the margin is topographically lower. The inner margin of the shelf generally corresponds to the location of the mare ridge system (Fig. 1). Basinward of the shelf is an annular topographic depression ranging up to 100 km in width. The central part of the basin is a broad topographic high over 150 km in diameter (Fig. 2, 3). Topograph and multispectral imaging (2) suggest a complex filling history for the mare, with several major units reflecting the general topographic trends of Figures 2 and 3. A detailed unit map is presently in preparation.

(References: 1) Phillips, R. J. et al. (1973) Apollo Lunar Sounder Experiment: NASA SP-330, Section 22; Kaula, W. M. et al. (1974) Apollo Laser Altimetry and Inferences as to Lunar Structure: Proc. Lun. Sci. Conf. 5, p. 3049; Roth, L. E. et al. (1977) Equipotential Doming in Flooded Circular Basins on the Moon: Proc. Lun. Sci. Conf. 8, in press. 2) Pieters, C. et al. (1976) Geophys. Res. Lett., 3, p. 697.)

CRISIUM BASIN: SETTING AND TOPOGRAPHY

Head, J. W. et al.

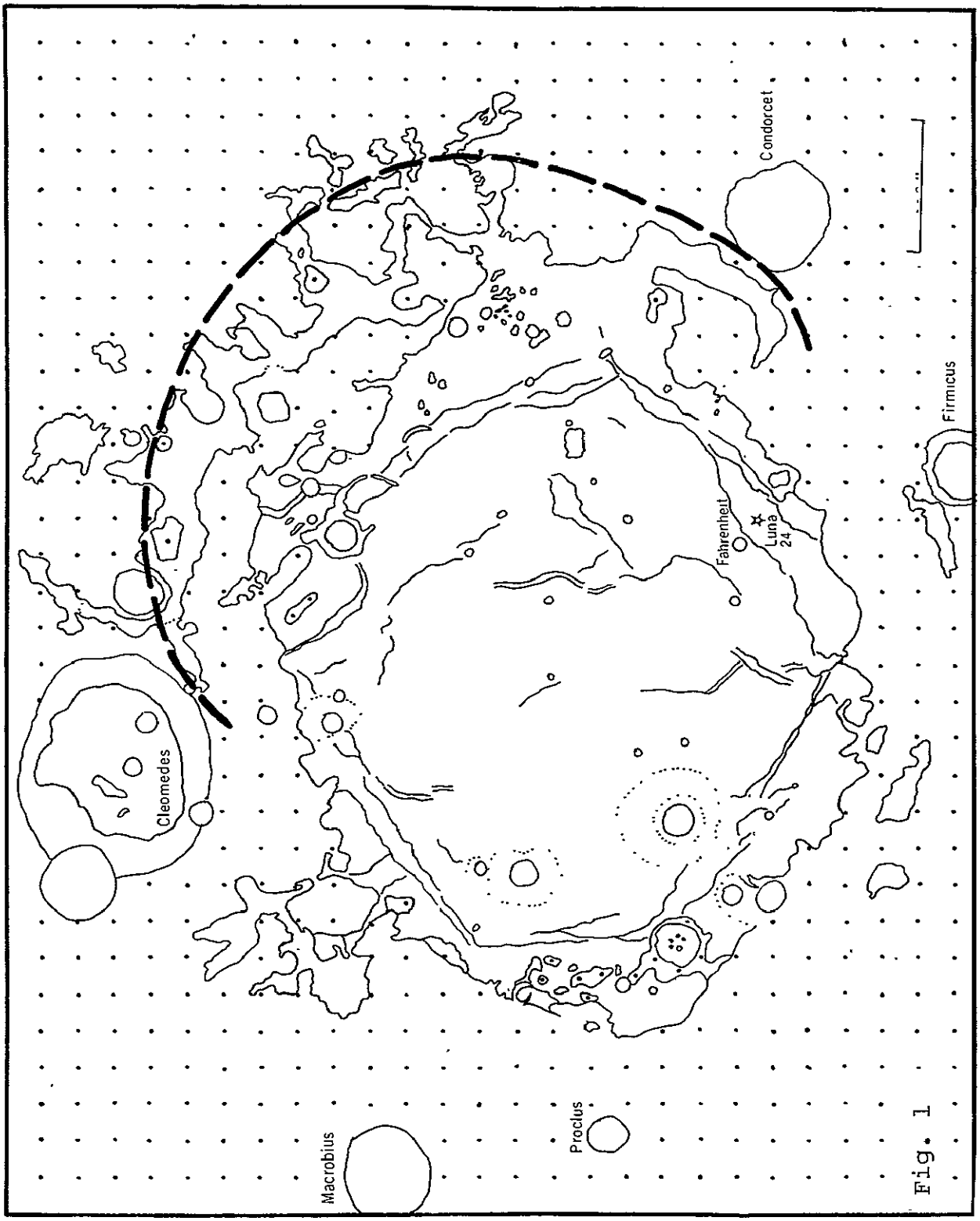

Fig. 1

CRISIUM BASIN: SETTING AND TOPOGRAPHY

Head, J. W. et al.

Fig. 1. Crisium Basin region. Lines within maria show positions of mare ridges. Dashed line shows site of possible pre-Crisium basin. Bar is 100 km.

Fig. 2. Radar topographic map of the Crisium basin. Contour interval 200 meters.

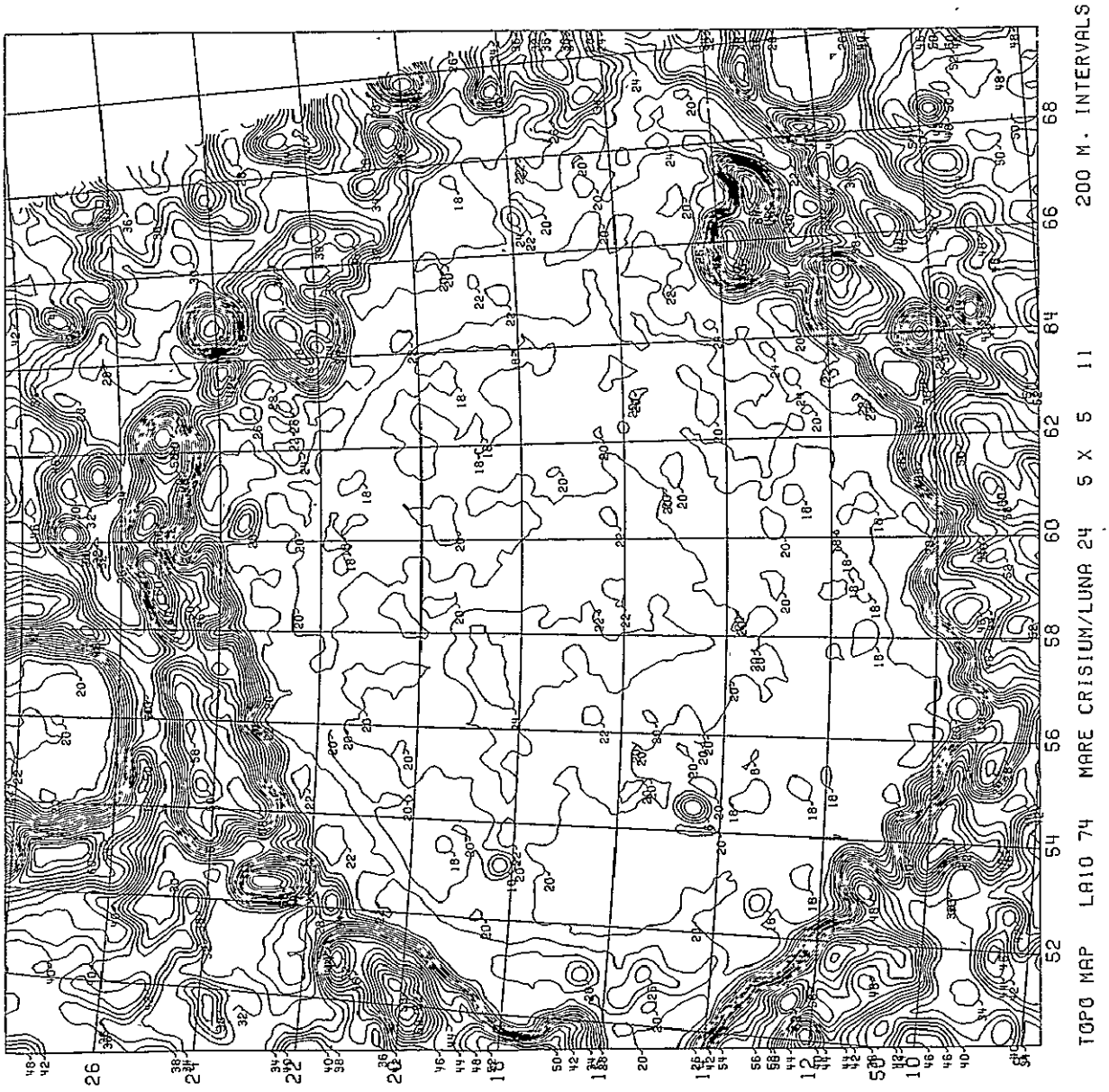

Fig. 2

CRISIUM BASIN: SETTING AND TOPOGRAPHY

Head, J. W. et al.

Fig. 3. Radar hypsographic map of the Crisium region. Gray scale interval is 400 meters.

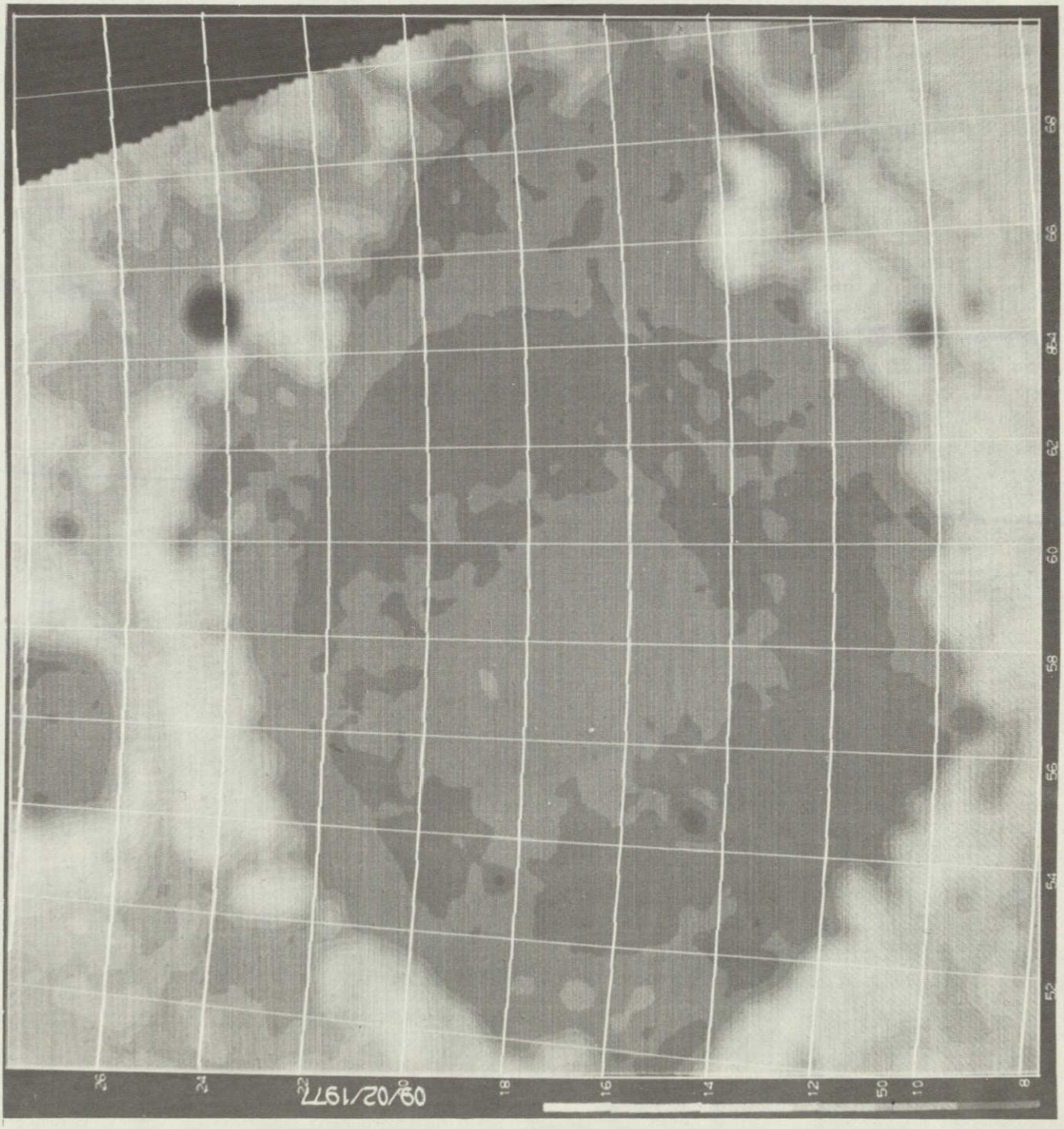

LUNA 24 SOILS FROM MARE CRISIUM: AGGLUTINATE CHEMISTRY

Hsien-Neng Hu and Lawrence A. Taylor, Department of Geological Sciences, The University of Tennessee, Knoxville, TN 37916.

The drill core returned from the Southeast edge of Mare Crisium by the U.S.S.R. unmanned space probe Luna 24 has provided us with materials from a previously unsampled portion of the Moon. The detailed analyses of these soils can form the basis for advanced understanding of regolith and rock-forming processes. In fact, the chemical processes accompanying soil formation on the lunar surface should be reflected in the chemistry of the impact-produced glasses which bond mineral and lithic fragments together into aggregates called agglutinates. The present study was performed in order to characterize the Luna 24 agglutinates and associated glasses and to thereby determine the main source materials for the soils, as well as the core stratigraphy reflected in the agglutinitic glass contents and chemistry (1).

Numerous polished-thin sections of grain mounts were examined from the 90-150 μm (11 PTS), 150-250 μm (11 PTS), and >500 μm (7 PTS) portions of six samples: 24077, 24109, 24149, 24174, 24182, and 24210. A detailed modal analysis of the 90-150 and 150-250 μm grain mounts was performed (Fig. 1; Table 1). It is apparent that the agglutinate contents of the 6 horizons show a general decrease with depth, and the 90-150 μm fraction contains a greater % of agglutinates than the 150-250 μm fraction, a not unexpected finding. Sample 24149 has a unique high microbreccia content (25%) in the 90-150 μm fraction, and as discussed below, this sample also contains an appreciable highland component.

Approximately 135 agglutinate particles were carefully selected, according to the criteria of Hu & Taylor (2), for electron microprobe analyses of the glass. Defocussed beam analyses (30-40 μm beam dia.) were performed on 5 to 10 representative portions in each particle. Glass compositions for 126 agglutinate particles in the 90-250 μm size range are plotted in Fig. 2. The axes of FeO + MgO + TiO_2 versus CaO + Al_2O_3 + Na_2O were used because these are the components that are reportedly (3)

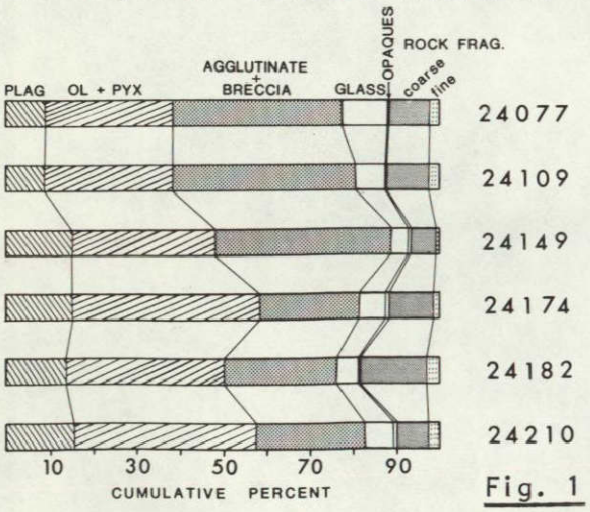

Fig. 1

Table 1. Modal Analyses of Agglutinates in the 90-150 and 150-250 μm fractions of Luna 24

	24077				24109				24149			
	90-150 μm		150-250 μm		90-150 μm		150-250 μm		90-150 μm		150-250 μm	
	grains	%	grains	%	grains	%	grains	%	grains	%	grains	%
Aggluts + Brec.	181	37.8	238	39.2	185	48.5	193	42.3	247	45.8	109	40.7
Agglutinates	154	32.2	---	---	141	37.0	---	---	110	20.4	---	---
Breccias	27	5.6	---	---	44	11.5	---	---	137	25.4	---	---
Others	297	62.2	369	60.8	196	51.5	263	57.7	293	54.2	159	59.3
Totals	478	100.0	607	100.0	381	100.0	456	100.0	540	100.0	268	100.0

	24174				24182				24210			
	90-150 μm		150-250 μm		90-150 μm		150-250 μm		90-150 μm		150-250 μm	
	grains	%	grains	%	grains	%	grains	%	grains	%	grains	%
Aggluts + Brec.	113	26.0	131	23.1	83	20.2	69	26.1	146	32.9	38	25.0
Agglutinates	91	20.9	---	---	55	13.4	---	---	117	26.4	---	---
Breccias	22	5.1	---	---	28	6.8	---	---	29	6.5	---	---
Others	322	74.0	436	76.9	328	79.8	195	73.9	297	67.1	114	75.0
Totals	435	100.0	567	100.0	411	100.0	264	100.0	443	100.0	152	100.0

Table 2. Chemical Compositions of Luna 24 Agglutinitic Glasses in the 90-250 μm size fractions.

No. of Analyses	24077 102	24109 100	24149 98	24174 105	24182 89	24210 102	Average 596
FeO	17.16	18.54	15.71	17.64	15.69	16.34	16.86
MgO	9.14	9.61	8.65	8.91	9.50	8.52	9.05
TiO_2	0.94	0.96	0.84	0.94	0.93	0.88	0.92
CaO	11.84	11.49	12.37	12.04	11.86	12.17	11.96
K_2O	0.05	0.05	0.05	0.05	0.05	0.04	0.05
Na_2O	0.43	0.42	0.43	0.38	0.49	0.47	0.44
Al_2O_3	14.47	13.21	16.27	13.79	15.29	15.34	14.73
SiO_2	44.44	44.34	44.37	44.78	44.78	44.27	44.49
Totals	98.47	98.62	98.69	98.53	98.59	98.03	98.50

AGGLUTINATE CHEMISTRY

Hu and Taylor

enriched and depleted, resp., in the agglutinate fraction versus the bulk soil. The symbol "a" represents the average glass composition of all of the agglutinate particles studied in the Luna 24 samples. Two distinct populations, one with higher ferromagnesian (FeO + MgO + TiO_2 ≈ 27.5%) and the other with a lower (≈12%) ferromagnesian content, can readily be distinguished. Figure 3 presents the glass compositions from the individual layers; the average glass compositions of each sample is compared with the bulk compositions of the medium-sized fractions of layers which are stratigraphically relatively close, as reported by Barsukov et al. (4). It should be noted that the average agglutinate glass composition appears to be in an opposite sense from that predicted by the chemical fractionation theory (3). Table 2 contains the average agglutinitic glass composition for the 6 horizons. Table 3 gives the compositions of 9 of the >500 μm particles. These have higher ferromagnesian contents than the average 90-250 μm glass.

DISCUSSION - The two populations in the glass compositions (e.g., 24149) imply that Luna 24 soils were formed by a mixing process involving at least 2 different source materials. The larger mode with higher ferromagnesian content was derived in situ from the VLT Mare basalt which underlies the soils, whereas the smaller population was derived from some highland source, carried in as ejecta material. We have demonstrated

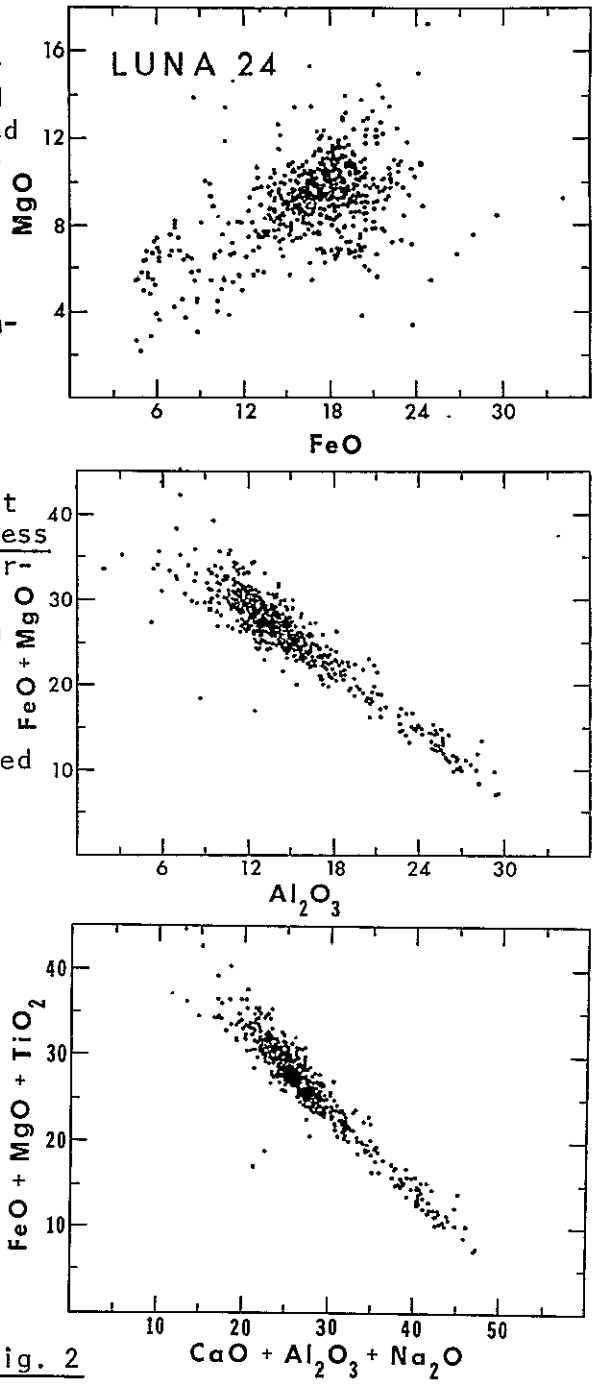

Fig. 2

Table 3 Chemical Compositions of Agglutinitic Glass in Particles Larger than 500 Microns

	24077, 71a	24077, 71b	24109, 68	24109, 70	24149, 60	24149, 72	24174, 69	24182, 29a	24182, 29b
No of Analyses	8	9	6	6	7	8	8	8	8
FeO	17.88	17.83	18 53	15 27	18 52	20.37	19.31	17.47	19 68
MgO	10.29	9.99	10.29	10.22	9.82	12.91	11.72	6 51	11.91
TiO_2	0 95	0 94	0.91	0.76	1.01	1.10	1.06	1 20	1.16
CaO	11 46	11.50	11.27	11.96	11.37	10.23	10.61	13 05	10.46
K_2O	0.03	0.03	0 04	0 05	0.03	0 05	0 08	0 04	0.03
Na_2O	0 39	0 45	0.36	0.46	0.50	0.54	0.44	0 36	0.38
Al_2O_3	13 64	13.90	13.15	15.42	13.05	9.66	11.28	13.67	11.24
SiO_2	44.49	44.60	44.07	46.10	44.29	44.25	44.75	46.57	44.54
Totals	99.17	99.24	98 62	100.24	98 59	99.11	99.25	98.87	99.40

Table 4 Chemical Compositions of Highland Versus Mare Plagioclase

	Mare Plagioclase				Highland Plagioclase				Luna 24
	10024*	12021*	15555*	70035*	15415†	15415@	15415@	61241$	24182,48$
FeO	0 55	0 69	0.74	0.55	0.08	0.16	0.09	0 09	0 07
MgO	0.22	0 17	0.20	0.13	0 07	---	---	0 08	0 04
CaO	15.8	17.7	17 8	16 3	19 34	19.66	19 49	19 50	19 89
Na_2O	2 23	1.06	1 06	1.77	0.32	0 22	0.26	0.28	0 39
K_2O	0.28	0.13	0.16	0.29	0.05	---	---	0 01	0.03
TiO_2	0.13	0.09	0.04	0.08	0.04	0.01	0 01	0 02	0.01
Al_2O_3	31.5	33.0	33.6	31 7	36 04	35.77	36 24	35 27	35.34
SiO_2	49 4	47.1	46.8	49.4	43.36	44.19	43 92	43.59	43.20
Total	100 11	99.94	100.40	100.17	99.30	100.01	100.01	98.84	98.97

* = Crawford (1973); † = Stewart et al. (1972); @ = Hargraves & Hollister (1972); $ = this study.

AGGLUTINATE CHEMISTRY

Hu and Taylor

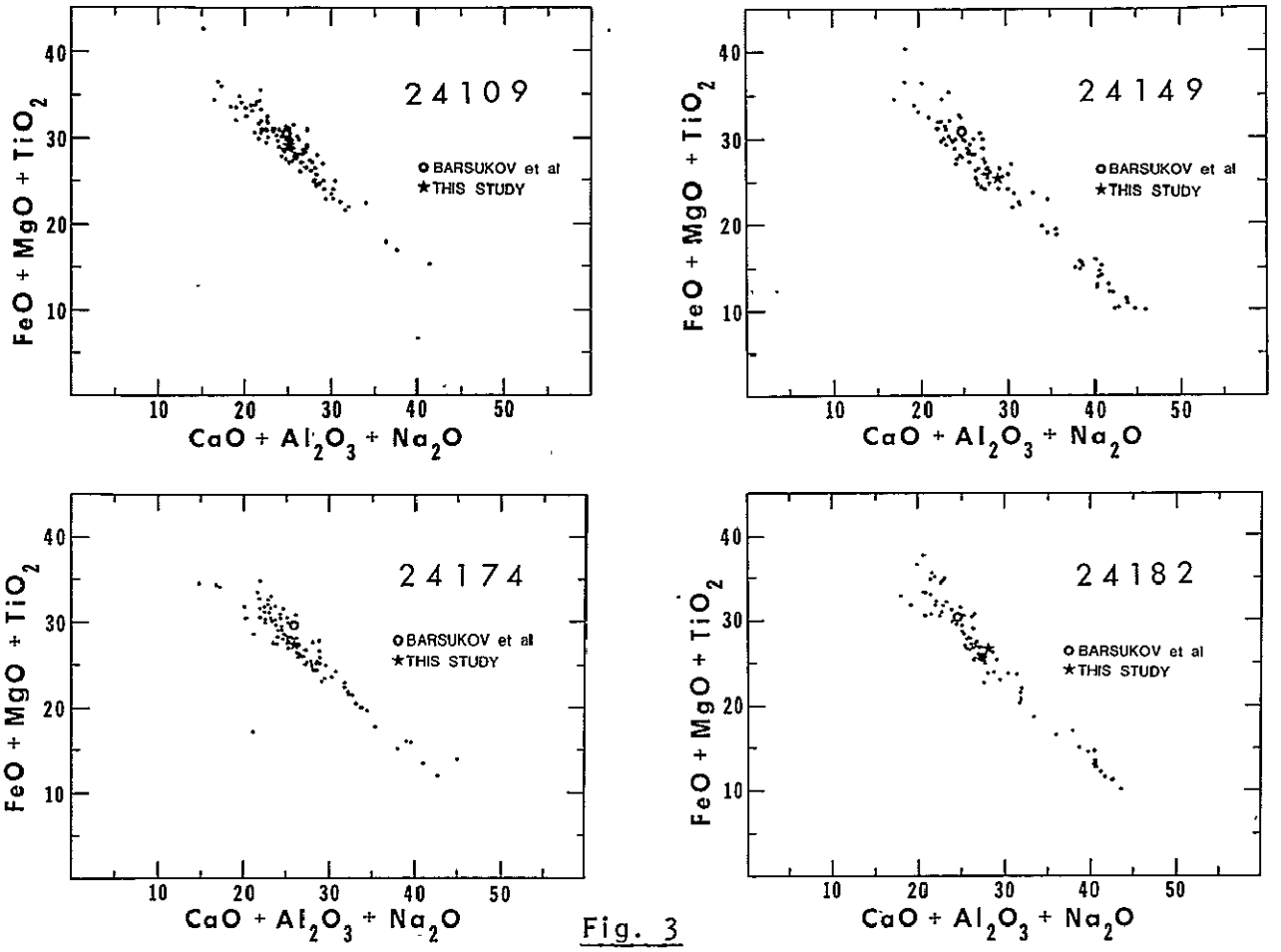

Fig. 3

previously (2), from a similar type of analysis, that certain Apollo 16 soils represent mixtures of 2 different source materials, supporting the mixing model of McKay et al. (5). Our conclusions on the Luna 24 soils are also supported by some agglutinates in 24182, 48 whose glass compositions are similar to the Luna 24 highland glasses reported by Norman et al. (6, 7) and whose included plagioclase crystals have compositions reflective of a highland source (Table 4). This suggested highland component is supported by the 30% homogeneous glass with highlands compositions (7).

However, no matter how confident we may be about our conclusions, we are reminded of a statement by Nagle & Walton (8), "interpretive conclusions based on study of particles of one lithology may not directly apply to the soil as a whole".

REFERENCES: (1) Coish, Hu, & Taylor, 1977, Abstr. A.G.U. Midwest Mtg.; (2) Hu & Taylor, 1977, Proc. Lunar Sci. Conf. 8th; (3) Rhodes et al., 1975, Proc. Lunar Sci. Conf. 6th; (4) Barsukov et al., 1977, Proc. Lunar Sci. Conf. 8th; (5) McKay et al., 1976, Proc. Lunar Sci. Conf. 7th; (6) Norman, Coish, & Taylor, 1977, Abstr. A.G.U. Midwest Mtg.; (7) Norman, Coish, & Taylor, 1977, this volume; (8) Nagle & Walton, 1977, Luna 24 Catalog, J.S.C.

FROM SERENITY TO LANGEMAK: A REGIONAL CHEMICAL SETTING FOR CRISIUM. Norman J. Hubbard, SN7/NASA Johnson Space Center, Houston, TX 77058 and Faith Vilas, Lockheed Electronics Co., Houston, TX 77058.

Orbital X-ray fluorescence data from Apollo 15 are used to describe the chemical relationships of Mare Crisium to Mare Serenitatis, Mare Smythii and to adjacent intermare areas. The chemical variations among these mare are correlated with chemical variations across the adjacent intermare areas and the eastern highlands. We will describe the chemical variations seen in the Apollo 15 orbital X-ray data for orbits 16, 20, 27, 34, and 38 extending from the Apennine mountains west of Mare Serenitatis, across southern Mare Crisium (orbits 16 and 20) and its southern basin rim (orbits 34 and 38), across Mare Smythii and into the eastern highlands over an area of basaltic chemical composition 5°-10° northwest of the highland crater Langemak. The orbital X-ray data used in this study have been re-reduced by us at the Johnson Space Center using a new intercalibration of the three detectors, a restricted number of channels of data in the data reduction, and individual background values for each orbit. These improvements have been made in collaboration with Jacob Trombka at Goddard Space Flight Center and Michael Bielefeld at Computer Sci. Corp. The new intercalibration of the three detectors has resulted in different numerical values for the Al/Mg, Al/Si and Mg/Si intensity ratios from those previously reported. The reduction in the number of channels summed and the use of individual backgrounds for each orbit have resulted in up to 2-fold improvements in signal to noise ratios, in about a 30% increase in the range of Mg signal levels and in improved orbit-to-orbit reproducibility of intensity ratios. The orbit-to-orbit reproducibility of the Mg/Si data now approaches that of the Al/Si data. The Mg/Si data can now be used for lunar studies at a similar spacial resolution as for the Al/Si data. Two orbits of Mg/Si data (orbits 20 and 27) required simple adjustments for level to bring them into close agreement with Mg/Si data for the other three orbits.

The improved orbital X-ray data are presented in Figures 1, 2 and 3. The major features seen in the Al/Si plot (figure 1) are the well-known decrease in Al/Si ratios over maria, relative to adjacent non-mare areas, and the progressive decrease in Al/Si ratios for the maria as one moves westward. Less well-known is the fact that the southern basin rim of Crisium (orbits 34 & 38) has lower Al/Si than the highlands east of Smythii and higher Al/Si ratios than the Apennine and Haemus mountains to the west of Serenitatis (Andre et al. 1977). The Mg/Si data for Mare Crisium and Mare Serenitatis show that they are not distinct from surrounding intermare areas, whereas the data for Mare Smythii show consistent increases in Mg/Si relative to surrounding areas. However, the measured Mg/Si ratios for Smythii and Serenitatis are nearly identical, and those for Crisium are only somewhat lower. In general, the Mg/Si ratios increase from east to west. The major features of the Al/Mg data (fig. 3) are similar to those of the Al/Si data, but with much more pronounced variations in signal levels and a much clearer view of chemical variations across the lunar surface. The features at 110-120° long. will be discussed later.

The progressive decrease of Al/Si ratios from east to west for both mare and intermare areas suggests a genetic link between the chemical composition of the mare surface soils and the adjacent intermare areas. This link could be via normal petrogenetic parameters (source materials, for example), or via

FROM SERENITY TO LANGEMAK

Hubbard N. J. and Vilas F.

pervasive lateral transport of nonmare material onto mare surfaces (as opposed to local lateral transport at mare boundaries). The increases in Mg/Si ratios associated with Smythii demonstrate that lateral transport of adjacent nonmare material onto the mare surfaces cannot be an adequate explanation of the intermare chemical differences because Smythii is an optimal place for this to occur due to its partially flooded floor and the relatively small size of its mare basalt patches (Andre et al., 1977). A further check on the efficiency of lateral transport can be made using the data on orbit 20, which passes over the northern rim of the post-mare crater Picard in Mare Crisium. Picard is a dark, haloed crater that has exposed only low albedo material, and thus is presumed not to have punched through the basaltic fill of Mare Crisium (P. Shultz, pers. comm.). Over this crater, two 40 sec. data points (at ∿54° long.) show a sharp increase in Mg/Si, whereas the Al/Si data show little or no variation at this point. From the chemical and photogeological information we can conclude: 1) that the admixture of any nonmare material, of high Al/Si ratio, into the surface layers of Mare Crisium is not appreciably greater than that at depth in the mare basalt fill, and 2) that the mare basalt fill at depth has a higher Mg concentration than the common surficial material. There is an area in the highlands east of Smythii and northwest of the crater Langemak at about 110-120° long. that is relevant in this study of mare chemical compositions and the extent to which they are obfusticated by cratering processes. In this area, the Mg/Si data show a broad increase, and some orbits of Al/Si data show a decrease in this ratio; these variations are much more prominent in the Al/Mg data. The Mg/Si values are low for any analyzed frontside mare areas and this area is not mapped by Wilhelms and El Baz (1977) as an area of mare flooding. There is nothing obvious to distinguish this area from adjacent highland areas on photographs (P. Schultz, pers. comm.). The simple fact that this highland area of less anorthositic chemical composition has survived the enhanced cratering rate of premare time is further evidence that the reduced rate of post-mare cratering should not have caused extensive lateral transport of intermare materials from circummare areas onto the mare surface.

Further conclusions can be made. If we take the area to the northwest of Langemak as a clear demonstration that the chemical evidence of indigeneous pre-mare petrogenetic activity has been preserved on the lunar surface and that this evidence can be readily studied by chemical analyses made from orbiting spacecraft, and if we can also ignore or avoid the possible blanketing effects of extra-basin volcanism, we can now conclude that the chemical signatures of the basin rim of Mare Crisium and the Apennine-Haemus mountains are those of largely intact samples of excavated basin material. From this we proceed to the suggestion that the westerly decrease in Al/Si and Al/Mg ratios and the corresponding increase in Mg/Si ratios in the intermare and highland areas is evidence of an increasingly non-anorthositic crustal composition as the Imbrium basin is approached. This suggested westward decrease in crustal and/or mantle Al concentrations is apparently also reflected in the westward decrease in Al/Si ratios for the eastern maria and the area near Langemak. If this inference of laterally varying source materials for mare basalts is true, then orbital chemical data have much to tell us about the lunar interior, crustal evolution and the generation of lunar magmas.

FROM SERENITY TO LANGEMAK

Hubbard N. J. and Vilas F.

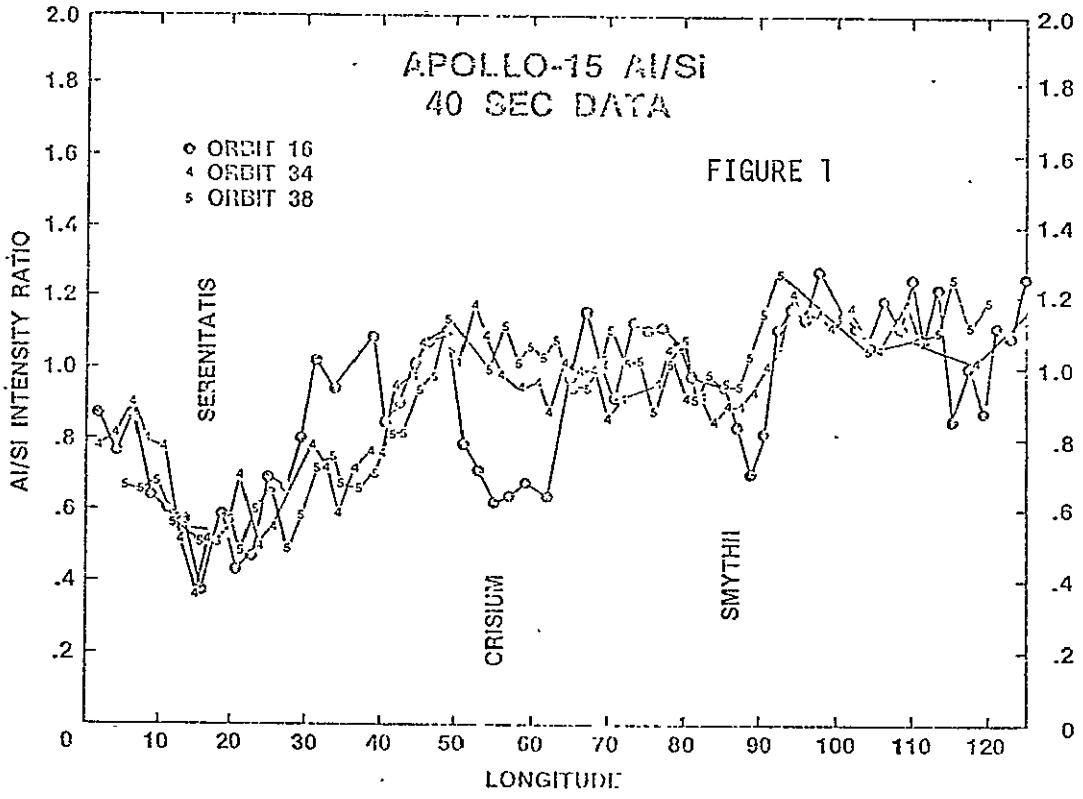

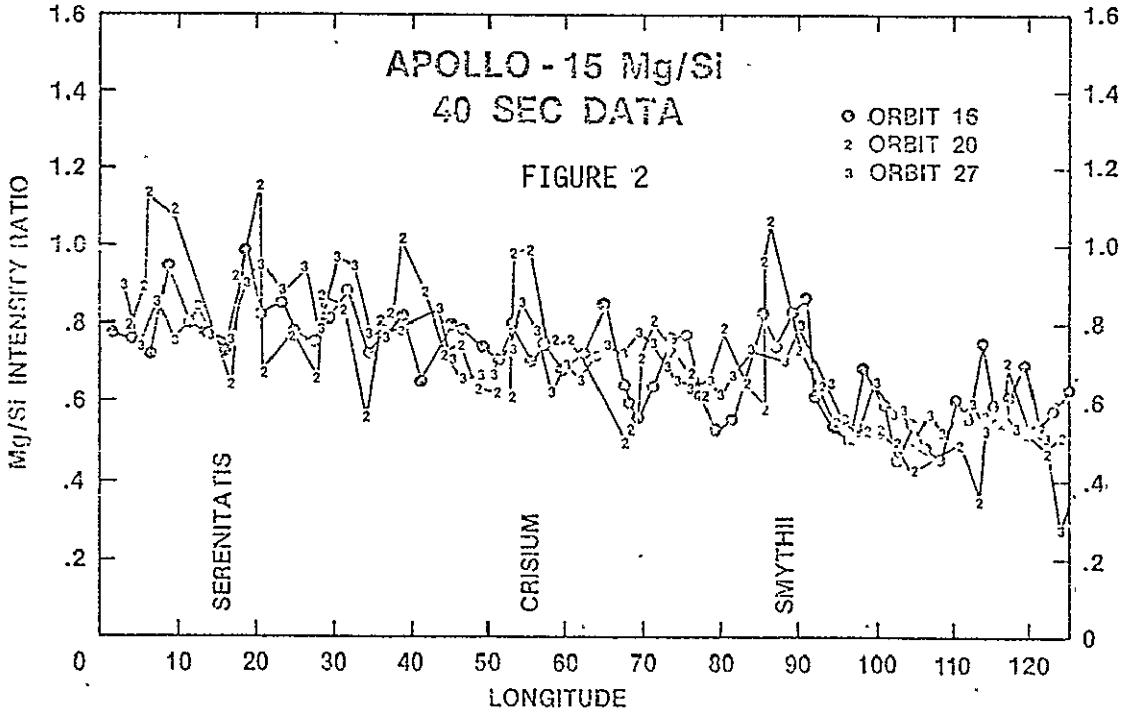

FROM SERENITY TO LANGEMAK

Hubbard N. J. and Vilas F.

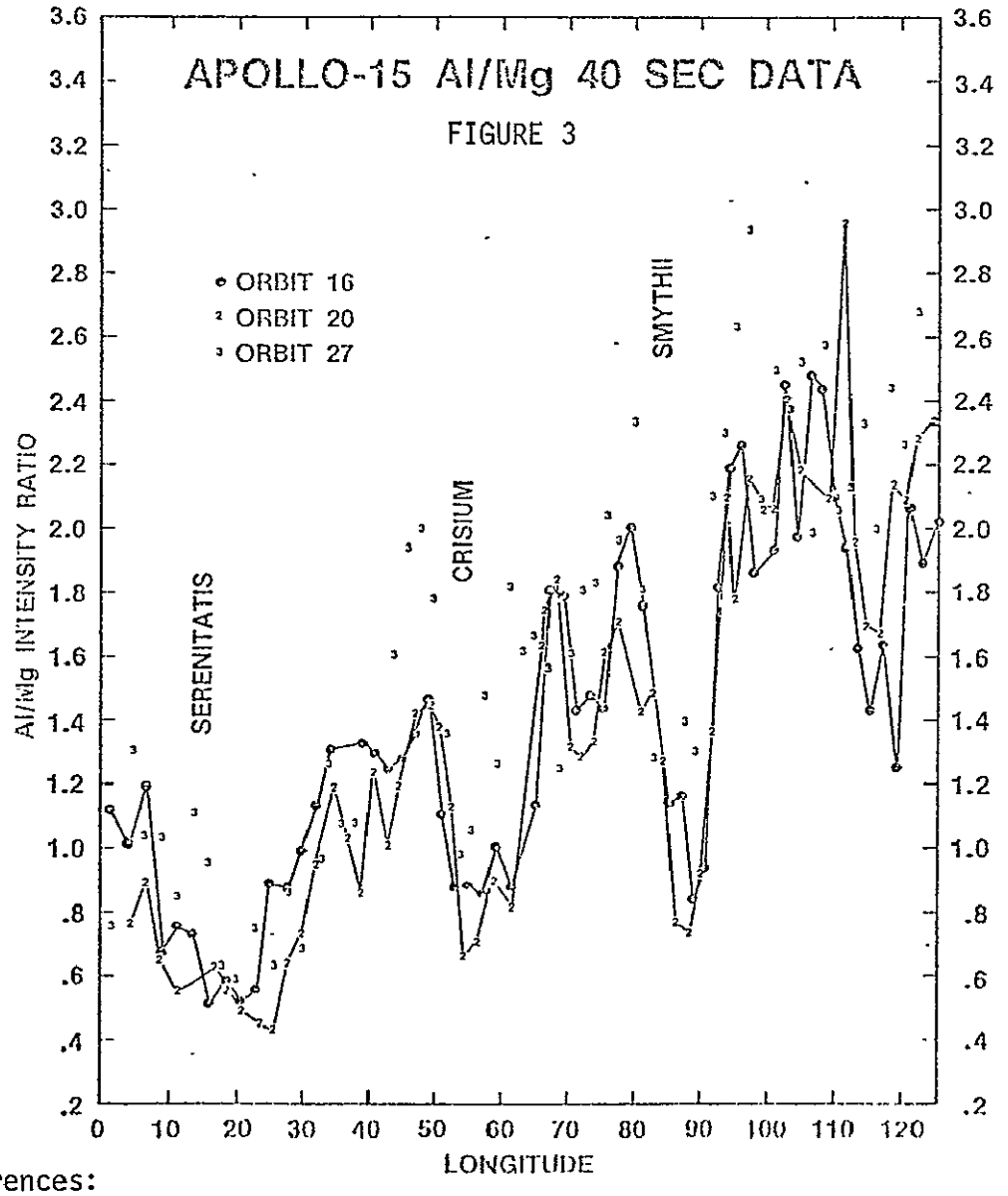

References:

Andre, C. et al. (1977) Lunar surface chemistry: A new imaging technique. Science 197, pp. 986-989.

Andre, C. et al. (1977) Chemical character of the partially-flood Mare Smythii basin from orbital X-ray data. Proc. Lunar Sci. Conf. 8th, in press.

BASALT AND BRECCIAS FROM THE LUNA 24 CORE. R. Hutchison, and A.L. Graham, Dept. of Mineralogy British Museum (Natural History), Cromwell Road, London SW7 5BD.

Microprobe analyses were made of the components of 1 mm-sized grains. Two specimens from the 90 cm level are a basalt and a shocked pyroxenite. The basalt has an ophitic texture, with 100 x 25 μm plagioclases ($An_{94-96}Or_0$), enclosed in larger pyroxenes of variable composition (e.g. $Wo_{34}En_{26}$ - $Wo_{27}En_{15}$). Olivine (Fo_{37-34}) occurs in sub-hedral grains, one of which is associated with pyroxene ($Wo_{14}En_{49}$). Some interstitial cristobalite is present as 10-15 μm sized grains. Ilmenite and chromium ulvospinel occur. This rock is a low-Ti mare basalt. The pyroxenite appears to be free from impurities; grain-size is similar to the basalt, and there is overlap in composition ($Wo_{40}En_{40}$ - $Wo_{21}En_{20}$, average about $Wo_{32}En_{44}$) although it extends to more diopsidic values in the pyroxenite.

Three specimens from the 196 cm level are a friable basalt, a glass-rich breccia and a fine-grained breccia which contains a 20 μm grain of meteoritic metal (6.4%Ni, 0.49% Co). One part of the basalt has pyroxene only ($Wo_{26}En_{48}$), but in another, zoned pyroxene ($Wo_{29}En_{30}$ - $Wo_{20}En_{35}$) co-exists with feldspar ($An_{96}Or_0$). In the glass-rich breccia 3 glasses have basaltic normative mineralogies in the range of the basalt clast described above (e.g. 35% plag. An_{95}, 60% pyroxene $Wo_{24}En_{29}$, 4% olivine Fo_{38} and 1% ilmenite). One glass fragment, 100 x 60 μm, has 65% normative plagioclase (An_{99}), 24% pyroxene (Wo_6En_{70}), 9% olivine (Fo_{75}) and 0.6% ilmenite (all molecular); this is probably an olivine-norite from the lunar highlands.

ORIGINS OF LUNA 24 BASALTS: A GEOCHEMICAL PERSPECTIVE.*

S. Jovanovic, K. J. Jensen, and G. W. Reed, Jr., Argonne National Laboratory, Argonne, Illinois 60439

The 160 cm long core returned from Mare Crisium by the Soviet Union Luna 24 mission provides samples of regolith from the mare farthest east on the near side of the moon. Other mare material from near this region was returned by Luna 16 from Mare Fecunditatis. Samples were requested in the expectation that we may further test our proposal that lunar samples which cluster into one of three major residual Cl_r/P_2O_5 ratio groups are related to a differentiating but isolated magma, possibly in a convection cell, in the early lunar surface ocean (Jovanovic and Reed, 1977). We have measured Cl, Br, I, Li and U by radiochemical activation analysis and, in the case of the halogens, have separated a labile hot water-leachable and a residual fraction. In addition Fe, Cr, Na, Co, Sc, Sm, and Eu were measured in order to relate our samples to those measured by other groups. P_2O_5 was determined by colorimetry. In this discussion we will also use results on Ru-Os by Tarasov et al. (1977) to examine the stratigraphic relationship of Luna 24 basaltic material to other basalts.

The data are given in Tables 1 and 2. Luna 24, <0.250 mm, fines have Cl contents comparable to the low concentrations in Apollo 12 and 15 basalts. About one half of the Cl and Br are present as surface deposits and in relative amounts comparable to those found at other sites (Jovanovic and Reed, 1975). Li and U are among the lowest found in mare soils. Our residual Cl_r is near the soil values reported by Tarasov et al. (1977) and our total Cls are near those for basalts. Our residual Br_r is similar in amount to their total Br; our U and P_2O_5 results are lower. Within the uncertainties noted in the footnotes to Table 2, our data for the other elements listed above overlap results reported for a variety of samples, Table 2. That the data from basalts, melts and soil are comparable supports arguments by others (Ryder et al., 1977; Butler and Morrison, 1977; Florensky et al., 1977) that Luna 24 sampled almost exclusively local basalts and suggests that our samples are representative of local material.

The Cl_r/P_2O_5 ratios for the three samples, 24077, 24174 and 24186 are 0.0097, ≥0.0062, and 0.0078, respectively, placing Luna 24 in Cell II with a mean Cl_r/P_2O_5 ratio of 0.009 ± 0.002 (Jovanovic and Reed, 1976) which includes Apollo 11 basalts, many soils and breccias from the Apennine front, Fra Mauro and the Taurus-Littrow massifs. Many of these samples are KREEP rich in contrast to Luna 24. Sampling of Cell II is unique in that now very low titanium (VLT), KREEPy and high Ti basaltic materials

*Work supported under the auspices of NASA.

ORIGINS OF LUNA 24 BASALTS

Jovanovic, S. et al.

have been returned. Element patterns and trends other than Cl_r/P_2O_5 ratios are useful in placing the Luna 24 VLT basaltic material in perspective. a) Barsukov et al., (1977) note that Cr_2O_3 in L-24 is comparable to low-K Apollo 11 but lower than basalts of other areas. b) Ryder et al., (1977) note that L-24 is distinct from both Ap. 17 VLT and Ap. 16 VLT in TiO_2 and MgO in the former and alkalies in the latter. c) When L-24 samples are plotted on the MgO-FeO diagram of Kurat et al., (1976), the field of these samples [data from, Tarasov et al., (1977); Vaniman and Papike (1977) and Taylor et al., (1977)] overlaps that of L-16 basalts and includes both low and high-K Ap. 11 basalts.

The presence of L-24 basalts in Cell II requires that either the suggested north eastern boundary of the cell presently set by Ap. 17 and L-16 basaltic material (Jovanovic and Reed, 1976) be moved north or the fissure that tapped the lavas that filled Crisium originated in the Fecunditatis or Tranquillitatis region.

The Ru-Os data of Tarasov et al. (1977) can be used to extend our proposed stratigraphic trends. $^{39}Ar/^{40}Ar$ ages reflect the basalt magma sources as melting occurred at progressively greater depths with time. The Ru/Os ratios of Ap. 11 and 17 (<0.2), 15 (~ 2.5) and 12 (~ 25) basalts are correlated with the age (Jovanovic and Reed, 1977). The L-24 Ru/Os ratio of $\gtrsim 0.5$ lies between those of Ap. 11 and 17 and Ap. 15 basalts and the ages of 3.5 and 3.66 by crater counting (Boyce et al., 1977) and by $^{39}Ar/^{40}Ar$ dating (Allègre et al., 1977) lie between the ~ 3.8 and ~ 3.3 by ages of the respective basalts.

Thus, L-24 basalts are from the same Cell (II) as Ap. 11 basalts and from a greater depth. The two basalt types could be derivatives of primary cumulates formed in the original lunar surface ocean in which trace elements (Ti, as well) tended to concentrate in the near surface layers, Ap. 11, and to be relatively depleted at depth, L-24. This interpretation is consistent with but extends the statement of Ryder et al., (1977) that L-24 VLT basalts are the products of an independently derived liquid from a source material which was itself VLT. We have previously linked Ap. 12 and 15 basalts (Jovanovic and Reed,1976), between which differences are not so striking as between L-24 and Ap. 11, as being derived from separate cumulate layers that evolved in Cell III.

C-2

ORIGINS OF LUNA 24 BASALTS

Jovanovic, S. et al.

REFERENCES

Allègre, C. J., et al. (1977), Meteoritical Soc. (Abst).
Barsukov, V. L., et al. (1977), Proc. Lunar Sci. Conf. 8th, in press.
Boyce, J. M., et al. (1977), Nature 265, 38-39.
Butler, P, Jr., and Morrison, D. A. (1977), Proc. Lunar Sci. Conf. 8th, in press.
Florensky, C. P., et al. (1977), Proc. Lunar Sci. Conf. 8th, in press.
Jovanovic, S. and Reed, G. W., Jr. (1975) Proc. Lunar Sci. Conf. 6th, p. 1753-59.
Jovanovic, S. and Reed, G. W., Jr. (1977) Proc. Lunar Sci. Conf. 8th, in press.
Kurat, G., et al. (1976), Proc. Lunar Sci. Conf. 7th, 1301-21.
Ryder, G., et al. (1977), The Moon, in press.
Taylor, G. J., et al. (1977), Geophys. Res. Letts. 4, 207-10.
Tarasov, L. S., et al. (1977), Proc. Lunar Sci. Conf. 8th, in press.
Vaniman, D. T. and Papike, J. J. (1977), Geophys. Res. Letts., in press.

TABLE 1. Halogens, Li, U and P_2O_5 in Lunar Samples Returned by USSR Lunar 24 Mission. Samples are <0.250 mm bulk fines.*

Sample	wt mg	Cl r+ ppm	Cl ℓ+	Br* r ppb	Br* ℓ	I ppb	Li ppm	U ppb	P_2O_5 wt%	P_2O_5 (mg)++
24077,6	28.2	3.2	4.2	39	≤38	4.2		89	0.033	(5.0)
24174,11	21.4	3.6	2.6	24	41	1.7	1.7±0.3	56±10	≤0.058	(7.7)
24182,16	17.7	3.8	4.1	≤20	≤36	1.8	3.6	140±20	0.049	(6.9)

*Counting statistical errors are 10% or less, or as indicated; except 20% or less for Br.

+r = residue after leach; ℓ = 10 min. hot water leach; I observed in leach only; ++ = weight of sample used for P_2O_5 measurement.

TABLE 2. Major, Minor and Trace Element Data for Characterization of Luna 24 Samples.*

Sample	FeO wt%	Cr_2O_3 wt%	Na_2O wt%	Co ppm	Sc ppm	Sm ppm	Eu* ppm
24077,6	19.3	0.496	0.22	54.1	53.2	2.8	0.97
24174,11	17.0	0.345	0.15	39.9	37.2	1.8	0.60
24182,16	18.3	0.448	0.20	57.1	44.1	2.7	0.92
Literature	19[a],20.9[b],18.9[c] 18.5[d],20.55[e], 20.46[f]	0.35[a],0.36[b], 0.37[c],0.18[d], 0.42[e],0.16[f], 0.3639[g]	0.35[a],0.26[b], 0.34[c],0.26[d] 0.09[e],0.10[f]	43[a] 44[b] 52.9[g]	35[a] 37[b] 40.2[g]	2.5[a] 2.7[b]	0.58[a] 0.65[b]

*Counting statistical errors are 4% or less, except 10% for Eu. Absolute errors may be greater due to weighing and to pipetting of aliquants. These elements are determined in aliquants of solutions of irradiated samples.

[a,b]Tarasov et al. (1977): a = 24175, 1-0, b = 24183, 1-0 basalts. [c,d]Ryder et al. (1977): c,d = 24077, 42-35, 12 impact melt. [e,f]Vaniman and Papike (1977): e = 24182 green glass, f = 24182 brown glass. [g]Allègre et al. (1977): 300 mg unspecified soil.

CHEMICAL COMPOSITION OF LUNA 24 MELT ROCKS (24077,4; 24077,62; 24174,7; 24182,12; 24210,50) AND GABBRO (24182,8). J. C. Laul, Physical Sciences Department, Battelle-Northwest, Richland, Washington 99352

Six individual fragments (2 - 7 mg) of Luna 24 are currently being analyzed for some 30 major and trace elements by sequential INAA. Following the completion of INAA, these fragments will be examined petrographically by Papike's group and subsequently age dated by Schaeffer's group. The integrated interpretations of our consortium efforts on these samples will be discussed at a later stage.

The preliminary results of 20 elements (SiO_2, TiO_2, Al_2O_3, FeO, MnO, MgO, CaO, Na_2O, K_2O, Cr_2O_3, Sc, V, Co, La, Sm, Eu, Dy, Ho, Yb and Lu) in samples 24077,4; 24077,62; 24174,7; 24182,8; 24182,12 and 24210,50 along with the Apollo 17 control soils 71501 and 75081 are listed in Table 1. The chondritic normalized REE patterns of the Lunar 24 samples are shown in Fig. 1. The element Ho is reported for the first time by INAA using coincidence-non-coincidence counting.

24077,4; 24077,62; 24174,7 and 24182,12: Based on the bulk chemical composition, these samples are characterized by 43.5% SiO_2, 1.0% TiO_2, 12% Al_2O_3, 22% FeO, 0.27% MnO, 8.0% MgO, 12% CaO, 0.25% Na_2O, 0.020% K_2O and 0.34% Cr_2O_3, which fall in the range of very low K_2O and TiO_2 mare type ferrobasalts from Luna 24 and Apollo 17 sites (1-3). This is also supported by the chronditic normalized negative slope of La-Sm and positive slope of Gd-Lu patterns (Fig. 1) with the exception that their absolute concentrations are lower by a factor of 2-3 relative to the Apollo 17 low Ti mare basalts (LTMB). In addition, unlike LTMB, the Luna 24 fragments exhibit a positive Eu anomaly of varying degree. The sample 24077,4 and 24182,12 are described as melt breccias, whereas, 24077, 62 (sub sample of 24077,14) and 24174,7 are described as recrystallized breccias (4). This suggests that the ferrobasalt melt rocks are probably recrystallized with Plagioclase rich (highland) material to explain the observed positive Eu anomalies. Some Luna 24 very low TiO_2 ferrobasalt fragments do show a negative Eu anomaly (R. A. Schmitt, Private Comm.).

The chondritic normalized REE patterns with the positive Eu anomaly features like in Luna 24 fragments have also been observed previously in Apollo 15 mare basalt rake samples such as 15643 and 15388 (5). Such types of growing examples suggest either recrystallization with plagioclase rich component or assimilation of basaltic magma with plagioclase rich component on its way to the surface. Alternatively, the positive Eu anomaly features may be due to the unique conditions of partial melting of the source material. Based on the REE patterns, the samples 24077,4; 24077,62 and 24182,12 were derived from one lava flow, whereas, the sample 24174,7 was derived from a different lava flow.

24182,8: This sample contains 94% plagioclase based on the Al_2O_3 abundance and its REE pattern including a strong positive Eu anomaly is typical of anorthosites such as 15415, 60015,63 and 64435,44 (5). The 24182,8 has been described as gabbro and its original weight was about 9 mg (4). We received

CHEMICAL COMPOSITION OF LUNA 24 MELT ROCKS AND GABBRO

J. C. Laul

part (2.3 mg) of the bulk sample, which may not be representative of its bulk. The chemical data suggests that our sample is a plagioclase rich component of the bulk gabbro.

24210,50: This sample contains high Al_2O_3 (15.4%) and low FeO (16.4%) relative to the other Luna 24 low Ti ferrobasalts. Probably, the sample 24210,50 is a felspathic basalt. This sample is unique in the sense that its chondritic normalized REFF pattern is essentially flat at 10X (chondrites). Our tentative Eu value suggests a slight (5%) negative Eu anomaly relative to the other REE. We will confirm the Eu anomaly in our later measurements. Our 7.2 mg sample is a subsample of the 25 mg sample of 24120,5 (Pat Butler, Private Comm.). The sample 24120,5 has been described as melt breccia or aphanitic basalt with scattered gabbro clasts, small vesicles, and layered soil inclusions. Some Luna 24 soils do show a flat REE pattern at 10X with a slight negative Eu anomaly (D. P. Blanchard, Private Comm.). This suggests that our fragment is either a soil breccia or has a unique chemistry of its own. Papike's group plan to characterize this and the other above mentioned samples petrographically. The chemical and petrographic studies of these fragments will be discussed at the conference.

References:

(1) Barsukov V. L., Tarosov L. S., Dmitriev L. V., Kolesov G. M., Shevaleyevsky I. D. and Garanin A. V. (1977), Proc. Lunar Sci. Conf. 8th, in Press.

(2) Ryder G., McSween Jr., M. Y., and Marvin U. B. (1977). The Moon, in Press.

(3) Vaniman D. T. and Papike J. J. (1977). Geophysical Research Letters, in Press.

(4) Nagle J. S. and Walton, W. J. A. (1977). Luna 24 Catalog and Preliminary Description.

(5) Laul J. C. and Schmitt R. A. (1972). The Apollo 15 Lunar Sample (abstract), P. 225-227, The Lunar Science Institute, Houston.

CHEMICAL COMPOSITION OF LUNA 24 MELT ROCKS AND GABBRO

J. C. Laul

TABLE 1. ELEMENTAL ABUNDANCES VIA INAA*

	LUNA 24						AP. 17 CONTROL	
SAMPLE NO.	24077	24077	24174	24182	24182	24210	71501	75081
SUB. NO.	4	62	7	8	12	50	18	21
WT. (mg)	1.99	3.61	2.00	2.30	2.23	7.17	4.14	7.09
DESCRIPTION	MELT BREC.	RECRY. BREC.	RECRY. BREC.	PLAG.RICH GABBRO.	MELT BREC.	MELT BREC.	SOIL	SOIL
(%)								
SiO_2	43.9	43.1	44.0	43.5	43.0	41.8	41.0	40.9
TiO_2	0.75	0.98	1.1	<0.14	1.1	0.65	8.6	9.0
Al_2O_3	10.1	12.5	11.8	34.4	12.5	15.4	11.3	11.0
FeO	22.4	21.5	22.9	1.0	22.6	16.4	17.5	17.0
MnO	0.260	0.278	0.272	0.015	0.284	0.235	0.232	0.229
MgO	10.5	7.0	5.8	0.5	7.4	10.3	9.0	9.6
CaO	10.8	12.2	11.5	19.2	12.3	12.3	10.7	10.9
Na_2O	0.210	0.260	0.265	0.693	0.260	0.250	0.350	0.386
K_2O	0.016	0.014	0.022	0.013	0.020	0.037	0.072	0.066
Cr_2O_3	0.468	0.296	0.300	0.0094	0.315	0.430	0.458	0.440
(ppm)								
Sc	43.6	45.0	57.0	1.8	47.0	42.0	66.2	67.0
V	150	160	140	<10	170	120	90	94
Co	59.3	42.0	42.0	1.9	43.4	40.3	30.0	29.0
La	1.80	1.62	2.87	0.18	1.80	3.60	7.47	7.60
Sm	1.39	1.34	2.00	0.092	1.41	2.10	9.00	8.60
Eu	0.61	0.76	1.0	1.2	0.88	0.73	1.6	1.8
Dy	1.7	1.6	2.8	<0.13	1.9	3.2	14	13
Ho	0.45	0.4 2	0.71	<0.04	0.48	0.78	3.2	3.0
Yb	1.22	1.10	2.03	0.045	1.24	2.20	7.70	7.40
Lu	0.18	0.16	0.31	0.007	0.18	0.33	1.10	1.03

*ESTIMATED ERRORS BASED ON COUNTING STATISTICS ARE: ± 0.5-3% FOR SiO_2, Al_2O_3, FeO, MnO, Na_2O, Cr_2O_3, Sc, Co, La, Sm and Yb; ± 5% FOR CaO, K_2O, V and Lu; ± 5-10% FOR TiO_2, MgO, Eu, Dy and Ho.

CHEMICAL COMPOSITION OF LUNA 24 MELT ROCKS AND GABBRO

J. C. Laul

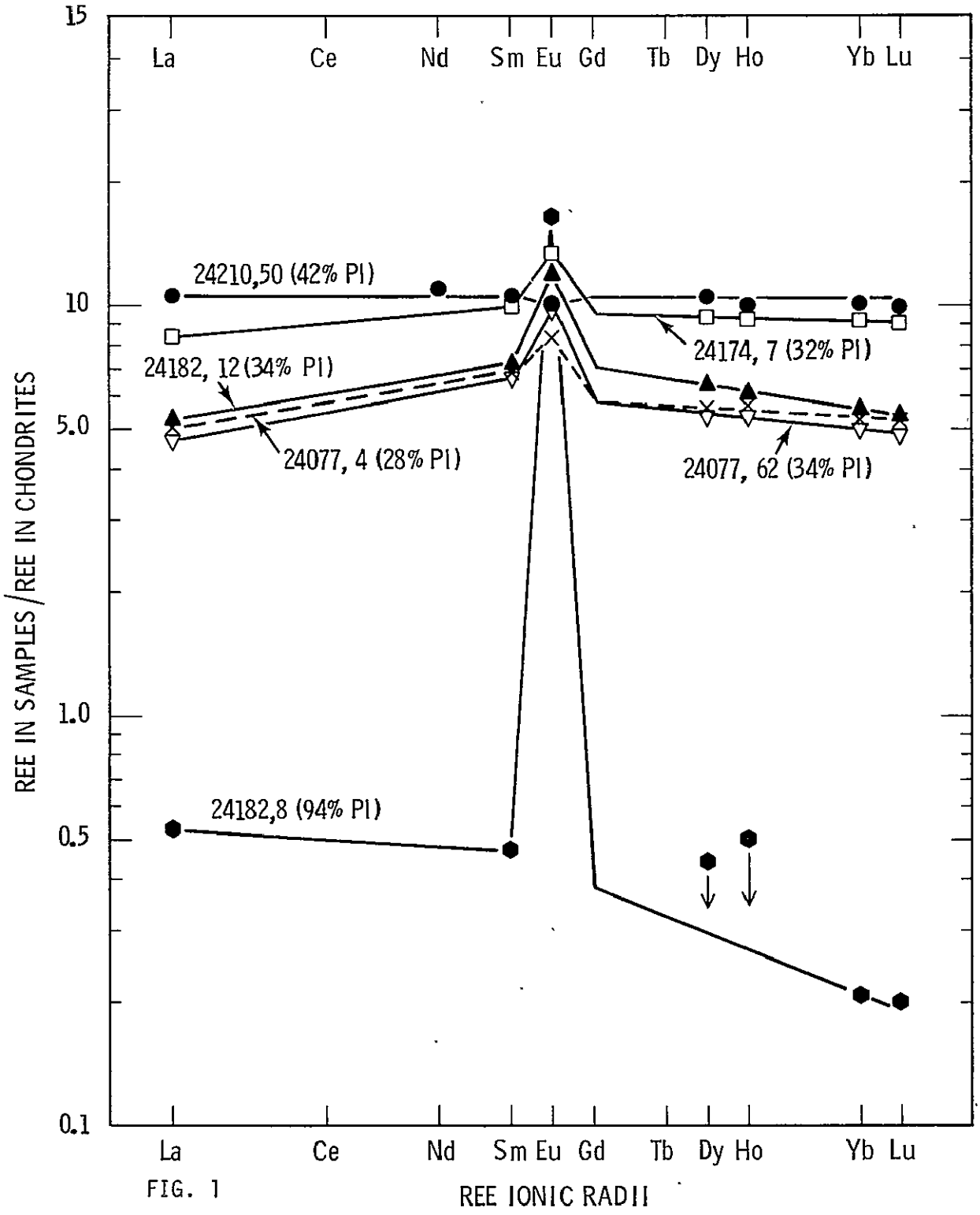

FIG. 1

LUNA 24 SOILS: A CHEMICAL STUDY. M.-S. Ma and R.A. Schmitt, Department of Chemistry and the Radiation Center, Oregon State University, Corvallis, OR 97331.

Five L 24 soils (<125μm) at five different stratigraphic levels of the L 24 core were allocated to us (Wasserburg consortium) for major, minor and trace element determination. In Table 1 are listed the 28 major, minor and trace elements determined in these soils by sequential INAA (instumental neutron activation analysis). The chondritic normalized LIL (large-ion-lithophile) elements (K, Sr, Ba, REE, Hf, Ta and Th) patterns are shown in Fig. 1.

The major, minor and trace element abundances are surprisingly similar in these soils regardless of their core locations. The same is also observed for the <74μm fines (1). The REE (rare earth element) patterns show a bow-shaped fractionation with a negative Eu anomaly, and the light REE are slightly higher than the heavy REE. Our REE abundances are consistently lower with smaller Eu anomalies than those reported by (1) for the <74μm fines. Similarities in major, minor and trace element abundances in L 24 soils throughout the core have been interpreted as the results of repeatedly mixing of fine materials during the formation of the regolith from the inferred similarities in chemical compositions of the basaltic rocks at different stratigraphic levels (1). Ryder et. al. (2) have also concluded that the L 24 core is dominated by a single group of VLT (very low Ti) basalts at the different levels sampled which also contain metabasalts and impact melts with similar composition.

The L 24 VLT soils are the lowest in LIL trace elements relative to all eight other lunar sites; e.g., the relative REE abundance patterns in soils at the L 16 site (3) in Mare Fecunditatis, which is ∿400 km south of the L 24 site, are 4x those found at the L 24 site.

In this study, we have used the unconstrained, weighted multi-linear regression mixing calculation(4) on the available chemical data of L 24 soils, fine-grained basalt, coarse-grained basalt and other possible end-member components to seek for the best combination of components which would be responsible for the L 24 soils. The details of the mixing calculation have been given by (4). We also use the χ^2 test and the sum of the components to judge the degree of fitness for various combinations of different components.

Seven possible end-member components are considered in our calculation. They are L 24 fine-grained basalt, L 24 pyroxene-rich gabbro (coarse), L 24 plagioclase-rich gabbro (coarse), KREEP, lunar dunite 72417, L 20 highland soil (and breccia) and meteoritic components. The use of a fine-grained basalt, coarse-grained pyroxene-rich gabbro and plagioclase-rich gabbro as possible end-member components might present a problem due to the coherent similarity in the chemistry between the fine-grained basalt and the combination of the coarse-grained pyroxene-rich gabbro and plagioclase-rich gabbro. However, because of the abundance of the coarse-grained gabbros in the L 24 core, we feel the incorporation of them in our trial calculation is necessary even though we might not be able to distinguish between the fine- and the coarse-grained components due to the expected large uncertainties associated with the regression coefficients (fractions of components). The amounts of KREEP in the soils might be trivial in view of the relative low LIL abundances in the soils. Most of the LIL abundances in the soils might be contibuted from the fine-grained basalt and Luna 20 soils, if they are indeed present. The adoption of a lunar dunite as one end-

member is justified by the appearance of vitrophyric basalt with olivine phenocripts in the L 24 core (e.g. 2,5). These vitrophyric basalts might be mantle material brought to the L 24 landing site by the cratering events nearby (2). We have included L 20 soil (presumed to represent largely pulverized L 20 breccias) as one possible end-member because it may represent highland material which was ejected from the nearby highlands onto the L 24 landing site. The L 20 soil (6) has a very similar chemical composition to the breccia 22004,1 (6) and might be an important fine material in the L 24 soils. Due to the limited siderophile element data for L 24 soils of this work, we have neglected the use of a meteoritic component in our calculation.

In our calculations, the following chemical data are adopted for the end-member components: L 24 fine-grained basalt from data on 24109,78 (7); L 24 pyroxene-rich gabbro from the weighted average of element abundances in samples 24182,35, 24182,74, 24182,75 and 24210,20 (7); L 24 plagioclase-rich gabbro from the weighted average of element abundances in samples 24077,83 and 24149,63 (7); KREEP from data of KREEP-norite (8); and lunar dunite from data reported for 72417 by (9) and L 20 soils from data for 22001,9 (6).

We have used twenty major, minor and trace elements (Ti, Al, Fe, Mg, Ca, Na, Mn, Cr, Sc, V, Co, La, Sm, Eu, Tb, Dy, Yb, Lu, Hf, and Ta) in our calculations. The first mixing calculation contained pyroxene-rich gabbro, plagioclase-rich gabbro, L 20 soil and dunite as end-member components. Various combinations of selected values of the four components, e.g. combination of pyroxene-rich gabbro + plagioclase-rich gabbro; combination of pyroxene-rich gabbro + plagioclase-rich gabbro + dunite, etc., gave poor fits for the observed soil data. The χ^2's ranged from 7.3 to 17.5 for the five soils for these four different combinations.

In the second trial L 24 fine-grained basalts and KREEP were added as end-member components and L 20 soil was dropped. Reasonable results were obtained in the combination of fine-grained basalt + dunite + pyroxene-rich gabbro + plagioclase-rich gabbro + KREEP. The χ^2's are generally less than 2 except for soil 24174,9003 where the χ^2 is 2.7. The sums of the components range from 101 to 105%. The fractions of KREEP component were $\leq$1% associated with large uncertainties. The uncertainties associated with the regression coefficients, i.e. the fractions of components of the fine-grained basalt, pyroxene-rich gabbro and plagioclase-rich gabbro are large which is indicative of their chemical coherence. In two soil samples, 24182,9003 and 24210,9003, the calculated fractions of pyroxene-rich gabbro are negative (3-8%). When the dunite component was dropped in the second trial, the χ^2's increased to 2.3-3.7 and the sums decreased to 92-95%. This could indicated that dunite is an important component in L 24 soils.

In our third trial, we considered all six components discussed before as end-member components. Again, we did calculations with different combinations of selected numbers of components which were not performed previously. The results from the combination of only a fine-grained basalt + L 20 soil yield χ^2's of 1.5-2.8 and sums range from 91-96%. The combinations of fine-grained basalt + L 20 soil + pyroxene-rich gabbro + plagioclase-rich gabbro + dunite and/or KREEP yield χ^2's range from 1.1-2.7 with a negative fraction for plagioclase-rich gabbro (2-9%). The sums are $\sim$103% for the combinations with dunite

and 93-95% for the combinations without dunite.

The best results obtained from this trial are the combinations of fine-grained basalt + L 20 soil + dunite ± KREEP. The χ^2 for these combinations are very close to unity (0.9-1.2, except 1.8-1.9 for soil 24174) and the sums ranged from 101-105% for the five soils. The fractions of KREEP, when included as one of the components, were <0.6± 0.3%. The component fractions for the five soils of the above mentioned combinations are listed in Table 2. Another possible solution is the addition of the pyroxene-rich gabbro to the fine-grained basalt + L 20 soil + dunite combination; the χ^2's are also close to unity (1.0-1.6). It is clear in this case that the fine-grained basalt fractions generally decrease in proportion to the increases of pyroxene-rich gabbro fractions and the uncertainties for both components increase. However, we did obtain negative fractions of pyroxene-rich gabbro for the two soil samples 24182,9003 and 24210,9003.

From considerations of these calculations, we conclude that the composition of <125 μm L 24 soils are dominated by the L 24 fine-grained basaltic composition (<70%) with the addition of components with compositions similar to lunar dunite and L 20 soil. Pyroxene-rich gabbro and KREEP might contribute some minor contributions to the L 24 soil composition; however, their presence can not be clearly determined by our calculations. Finally, since the observed Co abundances in L 24 soils are always higher (∿15-30%) than the calculated abundances, the presence of small amounts of meteoritic components (<1%) in these soils cannot be ruled out. Assuming that the preponderance of Ni is due to a meteoritic component, ∿1.5% C1 chondrites or equivalent has been added to the L 24 soil, which is comparable to the meteoritic additions at the L 16 and Apollo 11 sites (10).

References: (1) Barsukov V.L., Tarasov L.S., Dmitriev L.V., Kolesov G.M., Schevaleyevsky I.D. and Garanin A.V. (1977) Proc. Lunar Sci. Conf., 8th, in press. (2) Ryder G., McSween Jr. H.Y. and Marvin U.B. (1977) Basalts from Mare Crisium. Submitted to the Moon. (3) Gillum D.E., Ehmann W.D., Wakita H. and Schmitt R.A. (1972) Earth and Planet Sci. Letts. 13, 444-449. (4) Boynton W.V., Baedecker P.A., Chou C.-L., Robinson K.L. and Wasson J.T. (1975) Proc. Lunar Sci. Conf., 6th, 2 pp. 2241-2259. (5) Tarasov L.S., Nazarov, Shevaleevsky I.D., Kudryashova A.F., Gaverdovskaya A.S. and Korina M.I. (1977) Proc. Lunar Sci. Conf., 8th, in press. (6) Laul J.C. and Schmitt R.A. (1973) Geochim Cosmochim. Acta, 37 927-942. (7) Ma M.-S., Schmitt R.A., Taylor J.G., Warner R.D., Lange D.E. and Keil K. (1977) This volume. (8) Laul J.C. and Schmitt R.A. (1973) Proc. Lunar Sci. Conf., 4th, pp. 1349-1367. (9) Laul J.C. and Schmitt R.A. (1975) Proc. Lunar Sci. Conf., 6th, pp. 1231-1254. (10) Laul J.C., Ganapathy R., Morgan J.W. and Anders E. (1972) Earth & Planet Sci. Letts. 13, 450-454.

LUNA 24 SOILS

Ma M.-S. and Schmitt, R.A.

Table 1. Element abundances in Luna 24 core soils, <125μm at five levels

Element	24109,9003 (23 8 mg)	24149,9003 (24.1 mg)	24174,9003 (25.1 mg)	24182,9003 (25.1 mg)	24210,9003 (14.1 mg)
TiO_2 (%)	1.0	1.1	0.8	1.2	0 1
Al_2O_3	12.1	12.1	12.1	12.3	12.0
FeO	18.7	19.6	19.1	19.6	19.8
MgO	10	10	9	10	10
CaO	10 8	11.1	11.3	11.4	10.8
Na_2O	0.27	0.28	0.28	0.30	0.28
K_2O	0.027	0.027	0.029	0.030	0 028
MnO	0.267	0.257	0.245	0.245	0.254
Cr_2O_3	0.380	0.384	0.388	0.390	0.446
Sc (ppm)	40	43	41	41	40
V	155	159	139	147	159
Co	46	60	46	50	42
Ni	155	175	125	145	145
Zr	70	60	50	50	50
Hf	1.3	1.3	1 3	1.5	1.4
Sr	81	109	108	93	103
Ba	25	30	-----	45	45
La	2.9	2.7	2.8	3.2	3.0
Ce	7.8	7.5	7.6	8 6	8.1
Nd	6 3	6.0	6.3	7.0	6.6
Sm	1.96	1.83	1.87	2.14	2.05
Eu	0.59	0.63	0.67	0 67	0.66
Tb	0 42	0.41	0.41	0.46	0.44
Dy	2.9	2 8	2.8	3.2	3.0
Yb	1.6	1.7	1.6	1.7	1.7
Lu	0 23	0.25	0.24	0.25	0.25
Ta	0.2	0.3	-----	0.2	(0.5)
Th	0.5	0.4	0.3	0.5	0.4

*Estimated errors due to counting statistics are: Al_2O_3, FeO, Na_2O, MnO, Cr_2O_3, Sc, Co, La and Sm, ±1-5%, CaO, V, Ce, Eu, Yb, Lu and Ni, ±5-10%; TiO_2 and K_2O, ±8-15%, MgO, Hf, Th, Sr, Nd, Tb, Dy and Ta, ±10-25%, Ba and Zr, ±30-50%. The abundances of Ni, Zr, Sr, Ba, Ce, Nd and Th were obtained by Dr. J.C Laul, using the coincidence-anticoincidence Ge(Li) counting facility at the Battelle Northwest Laboratory.

Table 2. Selected weighted multi-linear regression estimates of component fractions (%) in Luna 24 soils.

Sample	Luna 24 fine-grained basalt	Luna 20 soil	Dunite	KREEP	Sum	χ^2
24109	75.6±3.6	13.6±3.0	12.8±3.4		102	1.0
	76.1±3.7	12.2±3.5	13.0±3.4	0.3±0.3	102	1.0
24149	80.9±4.1	11.3±3.3	12.6±3.8		105	1.2
	81.3±4.2	10.1±3.9	12.7±3.9	0.2±0.3	104	1.2
24174	68.9±4.4	18.5±3.9	14.0±4.2		101	1.8
	69.0±4.6	18.2±4.6	14.0±4.3	0.0±0.4	101	1.9
24182	80.5±3.8	14.3±2.2	10.6±3.5		105	1.0
	81.4±3.5	11.3±3.3	11.0±3.2	0.6±0.3	104	0.9
24210	78.1±3.8	12.9±3.2	13.8±3.5		105	1.1
	79.0±3.6	10.1±3.4	14.2±3.3	0.5±0.3	104	1.0

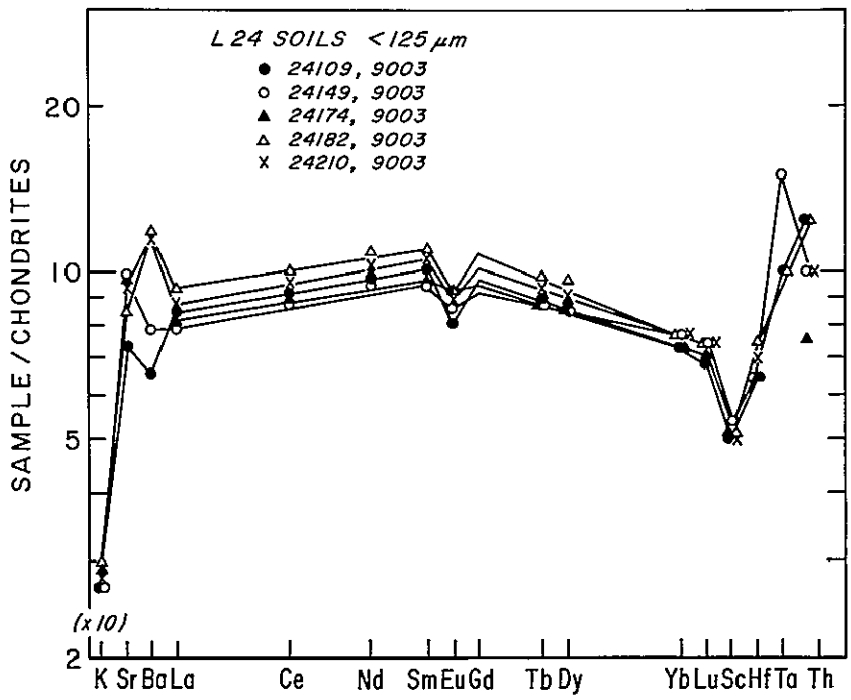

CHEMICAL AND PETROGRAPHIC STUDIES OF 18 LUNA 24 LITHIC FRAGMENTS. M.-S. Ma and R.A. Schmitt, Department of Chemistry and the Radiation Center, Oregon State University, Corvallis, OR 97331 and G.J. Taylor, R.D. Warner, D.E. Lange and K. Keil, Department of Geology and Institute of Meteoritics, University of New Mexico, Albuquerque, NM 87131.

Element abundances of twenty-three major, minor and trace elements have been determined by INAA in 17 fragments (0.5-1.0 mm) and in one recrytallized breccia (1) of 9 mg (0. Schaeffer consortium) of L 24 core samples (Table 1). The min-pet work is still in progress at the time of writing this abstract. We have classified the 18 samples into four groups.

BASALTS: The first group consists of eight samples and is characterized by similar chemical compositions for seven of these samples to a well identified L 24 fine-grained basalt 24109,78. These eight VLT (very low-Ti) basaltic fragments are similar to those reported for other L 24 mare basalts(1-4). The reflected light studies show that 24109,78 is a fine-grained basalt; 24109,76 and 24149,29 are metabasalts; 24077,81 is a breccia; 24149,61 is either a shocked melt or a very fine-grained basalt and 24149,69 and 24174,75 are coarse-grained basalts. Sample 24077,63 is described by (5) as a recrystalized breccia.

Similar bulk abundances were observed for the fine-grained basalt and the metabasalts as well as among their mineral phases. About 65% mafic minerals, in which clinopyroxene is much more abundant than olivine, and ∿35% plagioclase is estimated for these basalts. The REE (rare earth elements) show differences between the fine-grained basalt and the metabasalts (Fig. 1). The bow-shaped REE pattern for the fine-grained basalt 24109,78 has a negative Eu anomaly and the light REE are more fractionated and depleted compared to the heavy REE. This pattern indicates that clinopyroxene is the major REE carrier for the L 24 fine-grained basalt. The REE patterns for the two metabasalts have positive Eu anomalies and both the light and the heavy REE are fractionated to similar degrees. From electron microprobe data on other L 24 coarse-grained basalts (6), we suggest that the observed REE patterns for the metabasalts were inherited from their parent basalts which have different patterns compared to the fine-grained basalt.

The REE patterns and the Sc, V, Hf and Ta contents of the metabasalts are similar to two Apollo 15 rake basalts 15643(7,8) and 15388(8,9) which are olivine microgabbro and feldspathic microgabbro (10), respectively. Difference in the bulk chemistry among the L 24 metabasalts and the basalts 15643 and 15388 could be explained by different amounts of plagioclase and olivine. Except for the anomalously high TiO_2 (5.1%) in one of the two 15388 fragments (9), which could be attributed to a high ilmenite content, the chemistries of these two Apollo 15 rake basalts are the closest to the L 24 metabasalts and the recrystallized breccia 24077,63. Therefore, we speculate that the composition of parent rocks of these metabasalts was very similar to the two Apollo 15 rake basalts discussed above.

Comparisons of the bulk chemistry for the two coarse-grained basaltic fragments 24149,69 and 24174,75 show differences in their plagioclase and pyroxene contents. The ∿39% normative plagioclase in 24149,69 is very sodic (1.1% Na_2O) which reflects in the higher bulk Na_2O content (0.55%) in this fragment compared to 24174,75 even though the latter has a higher normative plagioclase content of ∿47%. The pyroxenes in these two samples are fairly homogeneous but are different in compositions. Average pyroxene compositions in 24149,69 and 24174,75 are

$En_{44.0}$ $Fs_{37.8}$ $Wo_{16.4}$ (5 analyses) and $En_{23.4}$ $Fs_{53.0}$ $Wo_{23.6}$ (12 analyses), respectively. Also observed is the abnormal association of sodic plagioclase with high magnesian pyroxenes in 24149,69. The Cr_2O_3 content in the 24169,69 pyroxenes is lower (0.26%) compared to the Cr_2O_3 content (0.51%) in the pyroxenes of another coarse-grained basalt 24182,71 (mixed mineral fragment group) despite the observation that both pyroxenes have similar end member compositions. The high TiO_2 content (2.3%) in 24149,69 could be due to the heterogeneous presence of ilmenite in the 0.22 mg fragment because the average TiO_2 in Luna pyroxenes is ∿1.0%. Differences in the REE patterns between 24149,69 and 24174,75 are attributed to the differences in plagioclase contents and the differences in the pyroxenes between these samples.

No detailed petrographic work has been completed for samples 24077,81 and 24149,61; they are preliminarily identified as breccia and shocked melt samples, respectively. Their high siderophile element contents might be from ∿1% Cl type chondritic material or equivalent; chemistries of these two samples are similar and resemble that of fine-grained basalts. Both samples have negative Eu anomalies and bow-shaped fractionated REE patterns (Fig. 1).

The recrystallized breccia 24077,63 has a similar bulk composition to the fine-grained basalt and the metabasalts. Its REE pattern with a positive Eu anomaly is similar to the metabasalts.

Taylor et al. (2) have suggested that a typical L 24 mare basalt such as 24077,43-19 could be derived from green glass material such as 78526 by fractional crystallization of ∿20% olivine, ∿14% low Ca pyroxene and ∿1.7% chromite. Using the trace element data for two fragments of 78526 (11,12), and partition coefficients for olivine, high and low Ca clinopyroxenes, we find that the trace element fractionation for La, Sm, Lu and Sc are consistent with the Taylor et al. hypothesis. However, the ratio of 1.6 for the observed Eu in L 24 basalts to the calculated Eu abundance questions the validity of the Taylor et al. hypothesis. The L 24 fine-grained basalt has similar chondrite normalized La and Sc abundances of ∿6x. This is unique compared to the basalts from other lunar missions. Due to the large difference in partition coefficients for La and Sc in pyroxenes, we suggest that L 24 fine-grained basalts could not be derived from the partial melting of chondritic-like matter with appreciable amounts of pyroxenes in the residue. The bow-shaped REE patterns may be interpreted in terms of reasonable degrees of partial melting of cumulates. From the many possible flows sampled at the L 24 site, some presumably emplaced by Fahrenheit ejecta, the mare basalt data suggest that flows with at least two different chemical compositions were sampled. This conclusion is based on considerations of Cr and V data; i.e. fragment 24174,75, with a low V content, is from a different flow relative to the other seven basaltic fragments.

Pyroxene-Rich Fragments: Four samples belong to this group and they are characterized by low Al_2O_3 (2.3-3.3%), high FeO (24.9-28.5%) and high Sc (79-91 ppm) contents. The TiO_2 contents in these samples are comparable with the average TiO_2 contents observed in the pyroxenes. The pyroxenes in all samples are fairly zoned. For example, the pyroxene compositions of sample 24182,74 vary from $En_{43.3}$ $Fs_{30.4}$ $Wo_{26.3}$ to $En_{11.9}$ $Fs_{65.7}$ $Wo_{22.3}$. Average pyroxene compositions for these samples are: 24182,35, $En_{37.1}$ $Fs_{44.3}$ $Wo_{18.6}$ (10 analyses); 24182,74, $En_{28.8}$ $Fs_{45.4}$ $Wo_{25.8}$ (11 analyses); 24182,75, $En_{20.7}$ $Fs_{56.8}$ $Wo_{22.5}$ (21 analyses); and 24210,20, $En_{23.0}$ $Fs_{46.7}$ $Wo_{30.3}$ (10 analyses). The REE, Sc and Hf patterns for 24182,35 and 24182,74 (Fig. 2) are similar to the high-Ca pyroxenes.

Chemical and Petrographic Studies

Ma, M.-S. et al.

Sample 24182,75 has a diabasic texture and contains < 25% (vol.) of mesostasis with a little sodic plagioclase (1.9%Na_2O) and Fe-rich olivine (64.4% FeO). The Fe-rich olivines are found both in and out of the mesostasis, which is fairly homogeneous and are characterized by high FeO (∿42%) and low MgO (∿1.4%) contents. They are mainly composed of Fe-rich olivine, Ca and Fe rich pyroxene and silica. The high FeO of 28.5% in the bulk sample indicates a large amount of mesostasis. The REE abundances in this sample are ∿2.5 times higher than those in 24182,74 and the patterns are almost parallel to each other (Fig. 2). Again, the REE pattern is dominated by the characteristics of high-Ca pyroxene. These data suggest that 24182,75 is derived from a late-stage differentiate.

Sample 24210,20, which is similar to 24182,75, contains very sodic plagioclase (∿7.6% normative plagioclase that has 2.5% Na_2O) and fairly zoned pyroxenes. No mesostasis is exposed on the surface of this fragment. The light REE abundances are higher than 24182,75; however, the heavy REE abundances are slightly lower (Fig. 2). These could have resulted from the differences in the amount of mesostasis and the nature of the pyroxenes between them. Again, this fragment could represent some late-stage material from its mineralogy and trace element data.

Plagioclase Fragments: Samples 24077,83 and 24149,63 are nearly pure plagioclase crystals with very small amounts(<1%) of fine-grained mesostasis which is Fe-rich and contains opaque minerals. Plagioclases are homogenous and very similar in composition. The low REE abundances and patterns are typical of low K (<0.02%) lunar plagioclases (Fig. 2).

Mixed Mineral Fragments: The first three samples, 24109,74, 24182,74 and 24182,71 in this group are characterized by high Al_2O_3 (21.5-24.9%), high CaO (14.5-16.6%) and low FeO (3.9-9.0%) contents. Petrographically, these fragments contain large amounts of plagioclase and minor amounts of pyroxene. The plagioclase compositions are fairly similar among samples. The pyroxenes in 24109,74 and 24182,71 are Mg-rich ($En_{41.5}$ $Fs_{32.8}$ $Wo_{25.7}$, 6 analyses and $En_{47.0}$ $Fs_{34.2}$ $Wo_{18.8}$, 7 analyses). The REE abundances in 24109,74 and 24182,71 are low and exhibit large positive Eu anomalies (Fig. 2). The high REE abundances in 24182,34 compared to 24109,74 and 24182,71 could be attributed to the addition of late-stage Fe-rich pyroxene, which might be high in REE abundances, to the plagioclases even though the amount of pyroxene in this sample is less than those in 24109,74 and 24182,71 as indicated by the FeO and Sc contents in the bulk samples.

References: (1) Barsukov V.L., Tarasov L.S., Dmitriev L.V., Kolesov G.M., Shevaleyevsky I.D. and Garanin A.V. (1977) Proc. Lunar Sci. Conf. 8th, in press; (2) Taylor G.J., Keil K. and Warner R.D. (1977)Geophys. Res. Letts. 4, 207-210; (3) Vaniman D.T. and Papike J.J. (1977) Geophys. Res Letts. (in press);(4) Ryder G., McSween H.Y., Jr. and Marvin U.B. (1977), Basalts from Mare Crisium. Submitted to Moon. (5) Nagle J.C. and Walton W.J.A. (1977) Luna 24 Catalog and Preliminary Description. NASA, Lyndon B. Johnson Space Center; (6) Taylor G.J., Warner R.D., Wentworth S., Keil K. and Sayeed U., (1977) this volume; (7) Laul J.C. and Schmitt R.A. (1972), The Apollo 15 Lunar Samples, pp. 225-228, The Lunar Science Institute, Houston; (8) Laul J.C. and Schmitt R.A. (1973) Proc. Lunar Sci. Conf., 4th, 2 pp. 1349-1367; (9) Ma M.-S., Murali A.V. and Schmitt R.A. (1976) Proc. Lunar Sci., Conf., 7th, 2, pp. 1673-1695; (10) Dowty E., Prinz M. and Keil K. (1973) Proc. Lunar Sci. Conf., 4th 1, pp. 423-444; (11) Laul J.C. and Schmitt R.A. (1975) In Lunar Science VI, p. 489-491. The Lunar Science Institute, Houston; (12) Murali A.V., Ma M.-S., Laul J.C. and Schmitt R.A. (1977) In Lunar Science VIII, pp.700-702. The Lunar Science Institute, Houston.

Chemical and Petrographic Studies

Ma, M.-S. et al.

Table 1. Chemical composition of Luna 24 core fragments from six levels

Sample	Weight mg	TiO_2 (%)	Al_2O_3 (%)	FeO (%)	MgO (%)	CaO (%)	Na_2O (%)	MnO (%)	Cr_2O_3 (%)	Sc (ppm)	V (ppm)	Co (ppm)	La (ppm)	Sm (ppm)	Eu (ppm)	Tb (ppm)	Dy (ppm)	Yb (ppm)	Lu (ppm)	Hf (ppm)	Ta (ppm)	Ni (ppm)	Ir (ppb)	Au (ppb)
Basalts																								
24077,81	0 577	1 0	13.4	17 6	10	12 7	0 30	0.251	0 316	37	149	47	2.4	1 7	0.6	0.40	2.6	1 6	0 23	1 2	0.2	350	823	823
24077,63	9 05>	1.1	12 8	21 1	8	13.5	0 24	0.247	0.240	43	178	38	1 1	1 2	0.6	0.25	1.5	1 0	0 15	0 9	0.1	---	---	---
24109,76	0 710	1.1	11.1	20 8	7	11 5	0 25	0.229	0 246	41	179	37	1.9	1 5	0.6	0.33	2 1	1 3	0.17	1 0	0 1	<50	---	---
24109,78	0 342	1 3	11.6	22 4	7	12 3	0.29	0.258	0 381	47	177	36	2 0	1 9	0 6	0.44	2.8	1 9	0 29	1 1	0 1	80	---	---
24149,29	0.934	1.3	11 4	20.9	8	11 7	0.24	0.246	0 216	42	154	40	1 6	1 3	0 6	0 29	1.7	1 2	0 18	1 1	0.2	<50	---	---
24149,61	0.473	1 1	11.9	19.5	10	11 1	0 26	0.225	0.320	33	129	74	2.5	1 8	0.5	0 40	2 5	1 6	0 24	1 0	0.2	380	823	723
24149,69	0 220	2.3	14.2	15 8	6	11.7	0 55	0.246	0.089	42	131	30	2.1	2.4	0.8	0.51	3 6	2 1	0.30	1 3	0.3	<50	---	---
24174,75	1 289	0 7	17.2	17 7	5	13 4	0 38	0 208	0 067	32	46	32	2 5	1.8	1 0	0 41	2 7	1 7	0.23	1 0	0.1	80	---	---
Pyroxene-rich fragments																								
24182,35	0 210	0.8	2 3	27 0	10	11 1	0.12	0 390	0.153	81	172	46	0 4	0 73	0 2	0.21	(1 8)	1 2	0 22	0 2	0 2	90	---	---
24182,74	0 606	0 6	3 3	26 1	10	10 6	0 094	0 362	0 142	81	175	46	0 6	0 81	0 2	0.21	1.4	1.1	0 18	0 3	0 1	120	---	---
24182,75	0.550	0.6	2.4	28.5	8	11 2	0 11	0.381	0 125	79	139	43	1.9	2 0	0 5	0 53	3 7	2 9	0 44	1 4	0 3	135	---	---
24210,20	0 523	0.8	2.8	24.9	7	14 0	0 082	0 340	0.206	91	212	37	3.2	2 8	0 6	0 67	4.4	2 8	0 39	1.8	0.2	180	---	---
Plagioclase-rich fragments																								
24077,83	1 505	<0.3	31.6	0.9	~1	18 6	0.47	0 013	0 007	1 3	<20	2 2	0 08	0.06	0 6	0 014	---	0 04	0 005	---	---	---	---	---
24149,63	0 312	<0.7	32.4	0.6	<1	19 4	0 76	0 011	0.001	0 5	<40	0.9	0.1	0 06	0 0	0 009	---	0.03	0 004	---	---	---	---	---
Mixed Mineral fragments																								
24109,74	0 207	0 6	21.5	9.0	4	14.5	0.49	0 161	0.087	2 8	79	17	0 2	0 27	0.5	0 07	---	0.4	0 07	0 1	---	---	---	---
24182,34	0 310	0 5	21.7	3.9	6	16 6	0.53	0 139	0 060	7 1	81	4.9	3 8	2 3	1.0	0.51	3 1	1 8	0 26	1 3	0.2	---	---	---
24182,71	0.336	<0.7	24.9	7 8	5	15 9	0.41	0.103	0.139	16	74	16	0.14	0.20	0 4	0.04	0.3	0.2	0.03	---	---	---	---	---
24109,72	0 334	2.0	10.2	24.1	10	8 1	0 33	0 290	0 839	16	151	55	0.1	6.7	1.6	1 3	7.8	4 6	0 65	3.5	0.5	130	---	---

*Estimated errors due to counting statistics are: Al_2O_3, FeO, Na_2O, MnO (~0 1%), Cr_2O_3; Sc, Co, La (>1ppm) and Sm, ±1-5%; CaO, MnO (<0.1%), V, Eu, Tb ±5-10%; TiO_2 (>1%), La (<1ppm) and Lu (>0 1ppm); ±10-15%; TiO_2 (<1%), MgO (~5%), Yb (<0 1ppm), Dy (>1nom), Lu (<0 1ppm), Hf and Ta, ±15-30%; MgO (<5%), Dy (>0.1ppm) and Yb (>1ppm); (<1ppm) and Ni, ±30-50%.

FIG. 1

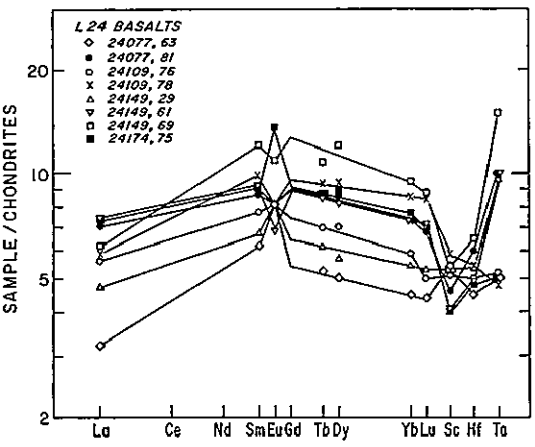

FIG. 2

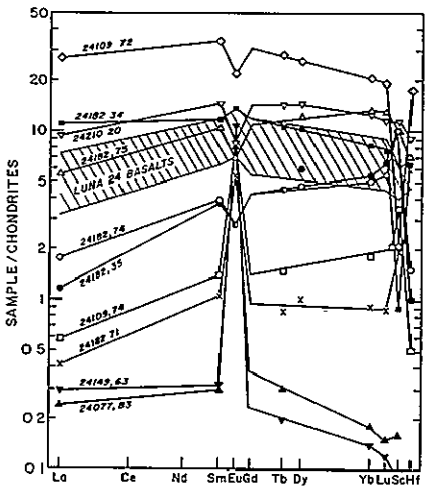

SOME EXOTIC PARTICLES IN THE LUNA 24 CORE SAMPLE.
Ursula B. Marvin, Graham Ryder[1], and Harry Y. McSween, Jr.[2], Center for Astrophysics, 60 Garden Street, Cambridge, MA 02138.

Our survey of 13 thin sections of the Luna 24 soils indicates that over 95% of the particles in the 250-500μm size range are mare-derived crystallines (basalts, gabbros, metabasalts, basaltic mineral fragments) or regolith products (agglutinates, vitric soil breccias, impact melts, vesicular glasses). The overwhelming majority of the crystallines show a chemical affinity with the VLT-Mg-poor ferrobasalts that are characteristic of Mare Crisium. However, we have also identified a few lithic fragments and glasses that are unrelated to that rock suite. These include 2 fragments of olivine vitrophyre, several fragments of anorthositic gabbro, and 1 Ti-rich glass spherule similar to the red-brown Apollo 11 spherules. Such exotic particles, although few in number, provide our only clues to the materials of non-local origin in the Luna 24 core.

Olivine Vitrophyre. Fragments of olivine vitrophyre occur in samples from two layers in the core: 24149,45 and 24174,63. The two fragments are chemically and mineralogically similar but differ in grain size. Both consist of skeletal olivines (Fo_{70-75}) with glassy cores in a glassy matrix containing tiny crystallites of pyroxene and ulvöspinel. Rare grains of troilite and globules of Fe-metal are also present. In the coarser-grained fragment (Figure 1a) the olivine crystallites are up to 200μm long; in the finer-grained one they reach a maximum of 60 μm. The vitrophyres are markedly richer in MgO and poorer in Al_2O_3 and CaO than the local ferrobasalts (see Table 1; and Abstract by Ryder, McSween and Marvin, this Volume). After considering a possible genetic relationship between these two rock types, we conclude there is none; the olivine vitrophyres and the ferrobasalts result from eruptions of separate basaltic magmas.

Ti-rich Glass. A red-brown, nearly opaque spherule, 260μm in diameter, occurs in sample 24149,47 (Figure 1b). The spherule is largely devitrified to crystallites of ilmenite and olivine. The high content of TiO_2 (10.17%; Table 1) makes this spherule unique among the Luna 24 particles we have examined. It matches the composition of the red-brown spherules from the Apollo 11 soils but is 1-2% richer in TiO_2 than the Apollo 17 orange glasses. The Luna 24 spherule may have been projected to Mare Crisium from a great distance; however, we suggest that it is a particle of the dark mantling material that occurs in two patches about 20 km from the landing site.

EXOTIC PARTICLES IN LUNA 24

Marvin et. al.

Anorthositic Gabbro. Six plagioclase-rich crystalline or partially glassy particles with the bulk composition of anorthositic gabbros are present in our thin sections. The texture and composition of the most interesting one are shown in Figure 1c and Table 1. This particle has been shocked to a leafy assemblage of anisotropic crystallites in a glassy groundmass. It is clearly a fragment of highlands rock derived from either an island within Mare Crisium, 35 km from the landing site, or from the rimming mountains 75 km away.

These three types of exotic particles are so fundamentally different from one another that we attach no significance to the fact that they were all found in the same core layer.

Now at: [1]Department of Geology, University of California at Davis, California 95616. [2]Department of Geological Sciences, The University of Tennessee, Knoxville, Tennessee 37916.

EXOTIC PARTICLES IN LUNA 24

Marvin et. al.

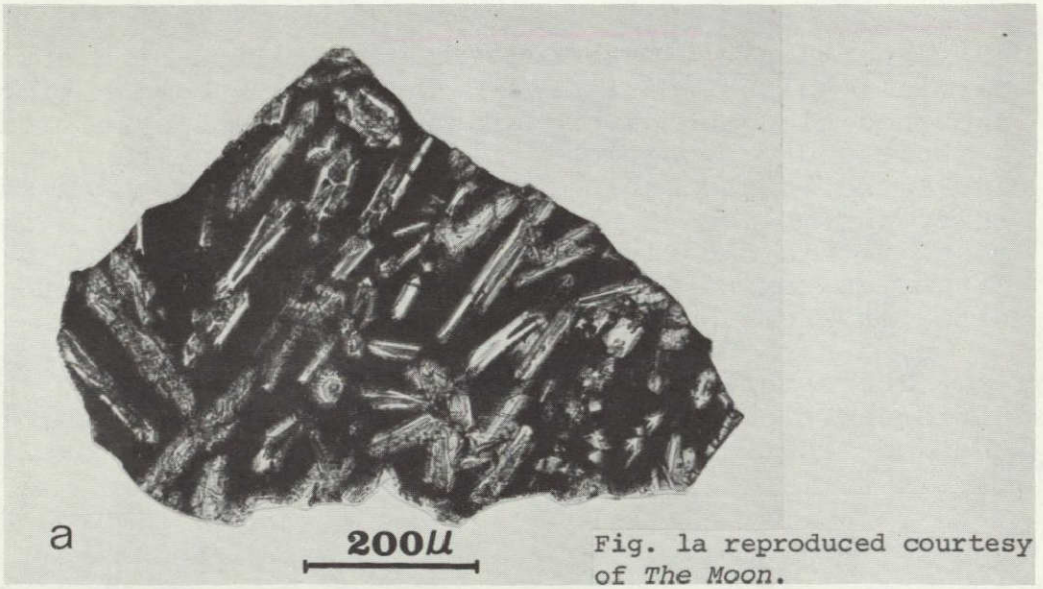

Fig. la reproduced courtesy of *The Moon*.

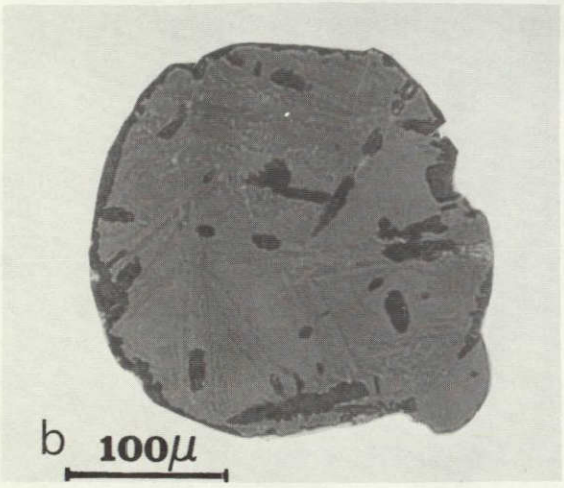

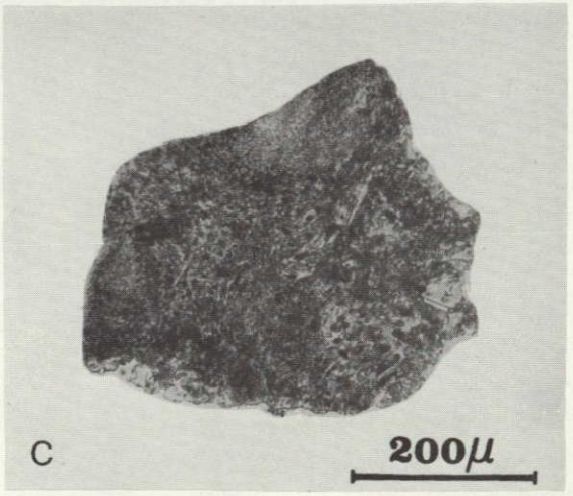

Figure 1. Three exotic particles from Luna 24 sample 24149.
a. Olivine vitrophyre. (Transmitted light.)
b. Devitrified Ti-rich glass spherule. (Reflected light.)
c. Anorthositic gabbro: shock-melted and partially recrystallized. The larger dark specks are cavities, not opaque minerals. (Transmitted light.)

EXOTIC PARTICLES IN LUNA 24

Marvin et. al.

Table 1. Electron microprobe defocused-beam analyses and normative compositions of 3 exotic particles in the Luna 24 core.

	Olivine Vitrophyre (Av. of 19 100 μm anal.)	Red-Brown Spherule (Av. of 3 100 μm anal.)	Anorthositic Gabbro (Av. of 14 100 μm anal.)
SiO_2	45.0	38.05	44.10
TiO_2	1.44	10.17	0.20
Al_2O_3	6.2	6.26	29.28
Cr_2O_3	0.56	0.63	0.04
FeO	19.0	20.66	3.88
MnO	0.25	0.26	0.03
MgO	16.9	13.99	7.57
CaO	7.9	7.41	15.71
Na_2O	0.02	0.35	0.52
K_2O	0.07	0.08	0.10
P_2O_5	0.02	0.02	0.07
BaO		0.04	0.02
Total	97.36	97.92	101.52
Norm wt. %			
Fo	11.1	9.8	12.8
Fa	9.5	6.5	5.1
En	27.2	21.7	0.2
Fs	21.1	13.1	0.1
Wo	9.6	9.1	0.1
Or	0.4	0.5	0.6
Ab	0.1	3.0	4.3
An	17.2	15.6	76.2
Ilm	2.8	19.7	0.4
Chr	0.8	0.9	0.1
Ap	0.1	0.1	0.2

Table 1 reproduced courtesy of *The Moon*.

SOURCES OF HIGHLAND MATERIAL IN MARE CRISIUM REGOLITH. Ted A. Maxwell and Farouk El-Baz, National Air and Space Museum, Smithsonian Institution, Washington, D. C. 20560

Numerous rays originating from Copernican-age craters in the highlands cross the Crisium basin. These rays are accentuated by high-sun elevation Apollo 15 and 17 orbital photographs. Although the ray systems hamper clear definition of geochemical boundaries based on orbital and remote-sensing data, they are a potential source of information regarding the composition of circum-Crisium highlands. Orbital X-ray data, earth-based color difference photographs and spectral data suggest that there are no well-defined contacts within the basin (with the exception of an extensive dark mare unit in the northeast quadrant). However, gradational boundaries have been noted (Pieters et al., 1976; Whitaker, pers. comm., 1977). In addition, crater-counting techniques (Boyce and Johnson, 1977) cannot in all cases resolve different flow units because of the minimum area needed to produce reliable statistics. It is probable that many of these remotely-sensed boundaries (contacts?) are the result of the numerous Copernican ray systems, but it is also possible that the rays obscure any distinct color or flow unit contacts that may be present. For these reasons, it is important to know: (1) the distribution of ray material, (2) the source craters and impacted materials, and (3) orientations of secondary crater clusters that may have been associated with pre-Copernican rays or ejecta. The identification of possible Eratosthenian or early Copernican contributions is significant with regard to studies of the Luna-24 core because younger material in the uppermost part of the core was incompletely sampled (Florensky et al., 1977).

HIGHLAND SOURCES

In addition to Giordano Bruno (Butler and Morrison, 1977), four other Eratosthenian and Copernican craters may have contributed highland material to the Crisium regolith: Langrenus, Taruntius, Proclus and possibly Thales. Based on radial thickness variations of impact crater ejecta (McGetchin et al., 1973), these craters may have contributed up to a third of the total material represented by the core (Table 1). However, Florensky et al. (1977) report that there is a marked deficiency of terra material within the core. Dirty-white to grey feldspar grains comprise only 3% (no. % of particles studied) of the core, and regolith breccias vary from 3 to 50% within segments of the core (Florensky et al., 1977). The failure of the ejecta distribution model to predict highland material abundances within the core is most likely due to repeated impact gardening of the regolith. Consequently, although absolute amounts cannot be calculated, the relative abundance of each crater's ejecta may be useful to sample investigators.

Fragments of highland materials are most likely to be derived from ejecta of the Fecunditatis, Crisium and Serenitatis basins. In addition, there may also be trace amounts of Humboldtianum basin ejecta. A comparison of Luna-16 (Mare Fecunditatis) and Luna-24 highland components would be useful to determine the extent of Langrenus ejecta.

Table 1. Major Eratosthenian and Copernican craters that may be represented in the Luna-24 core sample.

CRATER	DIA. (km)	DEPTH (m)	AGE	DISTANCE FROM LUNA-24 (km)	CONTRIBUTION* (cm)	IMPACTED MATERIAL**
Langrenus	133.4	4200	E/C	673	50	NpNt, Fecunditatis basin ejecta
Fahrenheit	6.3	1400	E	18	30	Im, Crisium mare
Taruntius	55.9	1400	E/C	513	4.4	It, Fecunditatis and Crisium(?) basin ejecta
Picard	22.2	2200	E	227	2	Im, Crisium mare, dark halo
Proclus	27.0	3900	C	457	0.5	IpIh, Serenitatis and Crisium basin ejecta
Peirce	18.4	1900	E	307	trace	Im, Crisium mare, dark halo
Swift	10.8	2000	E	323	"	"
16°N, 50.7°E	9.5	1800	C	352	"	Im, Crisium mare and Yerkes rim material
Greaves	13.3	2500	E?	278	"	Im, Crisium mare; dark halo
13.2°N, 60.2°E	4.4	400	E	58	"	Im, Crisium mare
Giordano Bruno	20.0	--	C	1320	"	NpNt, possible Humboldtianum basin ejecta?
Thales	30.0	--	C	1400	"	possible Humboldtianum basin ejecta?

*Contribution is computed from McGetchin et al. (1973) relationship: $t = 0.14\ R^{.74}\ (r/R)^{-3}$, where t = thickness of ejecta at r distance from crater of radius R (m).

**Geologic map units: Im, Imbrian mare
IpIh, Imbrian or pre-Imbrian hilly terra
It, Imbrian terra, undivided
NpNt, Nectarian or pre-Nectarian terra, undivided

SOURCES OF HIGHLAND MATERIAL

T. A. Maxwell and F. El-Baz

Figure 1. Ray system orientations for Copernican craters surrounding Mare Crisium. Curvature of the lines are great circle routes for ejecta plotted with a stereographic net.

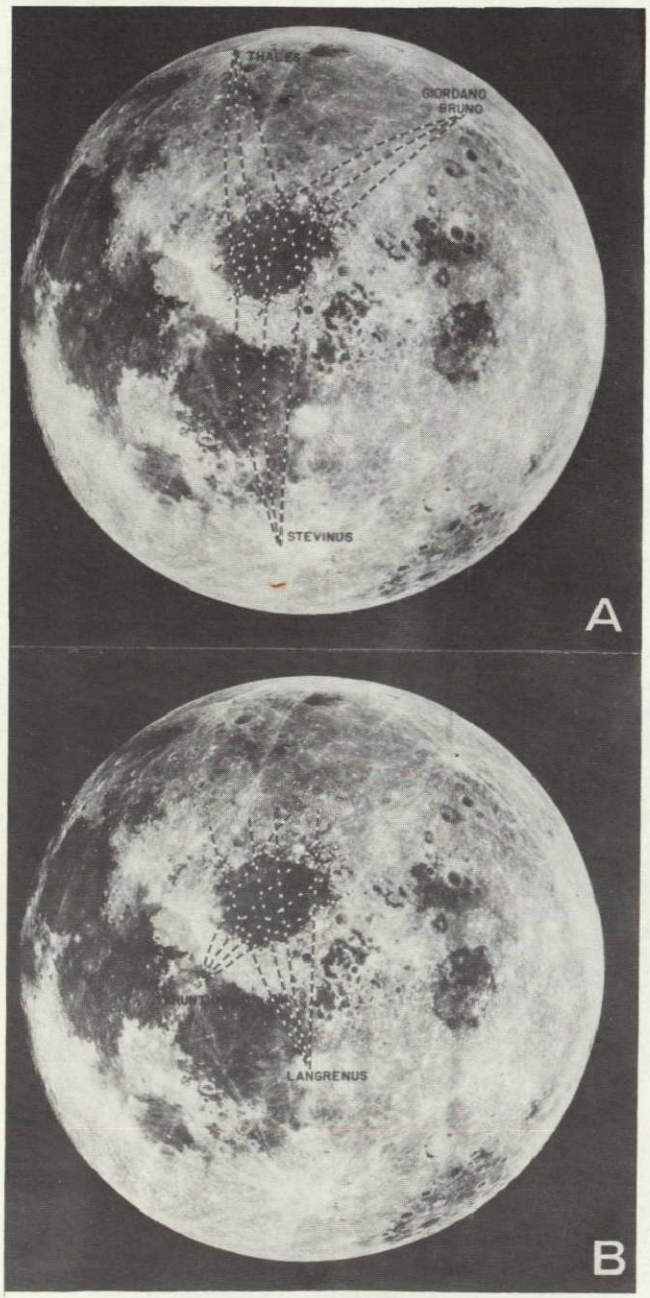

Giordano Bruno, Proclus, Thales and Stevinus (Fig. 1) are the most conspicuous sources for highland ray material, but the presence of ejecta from these craters is highly dependant on the discontinuous nature of the rays, and the exact location of the sample. Based on the spacecraft location according to Lunar Topographic Orthophotomap coordinate system, the sample comes from the border of relatively smooth, dark mare bordering Dorsa Harker and a more heavily cratered patch of light mare colinear with rays from Giordano Bruno. Because the spacecraft landed near the uprange cluster of secondaries (close to the dark mare), it is possible that the sample may completely miss any Bruno secondary material. Furthermore, the core may have incompletely sampled the upper 40 cm, and it is possible that material forming the latest Copernican rays may have been bypassed altogether. For this reason, Langrenus and Taruntius may be much more important contributors of highland material.

MARE SOURCES

Possible sources of mare ejecta originating within the basin are the Eratosthenian craters Fahrenheit, Picard, Peirce, Swift, Greaves and a 4.4 km crater northeast of the landing site. A 9.5 km crater on the east rim of Yerkes may have also contributed trace amounts of both mare and Yerkes rim material. Of these craters, Fahrenheit is the most likely contributor of mare material, but Picard may also be responsible for up to 2 cm of ejecta.

The recognition of contributions from the dark haloed craters Picard, Peirce, Swift and Greaves may be especially important to Luna-24 core studies since it is likely that these

SOURCES OF HIGHLAND MATERIAL

T. A. Maxwell and F. El-Baz

craters sampled a major subsurface basalt type in Crisium. Spectral data indicate that these dark haloes are the result of excavation of a relatively high Ti unit (Pieters et al., 1976). Although published analyses of basalt types indicate a VLT type (Vaniman and Papike, 1977), it is likely that a higher Ti (or Mg; Ryder et al., 1977) basalt type will be identified.

An *extremely* idealistic view of ejecta stratigraphy is shown in Table 2. Although redistribution and gardening must have taken place in the past 1 or 2 billion years, it is significant to note that contributions from the more conspicuous late Copernican craters are likely to be only sporadically represented, if at all. Langrenus, Taruntius and Fahrenheit may be the most important contributors to the Luna-24 sample.

Table 2. HYPOTHETICAL stratigraphic sequence of major Eratosthenian and Copernican crater ejecta

CRATER	DEPTH IN CORE (cm)
Bruno - Proclus	0-1
Thales	0-1
Stevinus	0-1
Langrenus	1-51
Taruntius	51-55
Eratosthenian-Copernican boundary	
Fahrenheit*	55-85
Peirce - Picard	85-87

*Age relations among Fahrenheit, Peirce and Picard are not clear-cut; Fahrenheit is brighter on full-moon photographs, but dark haloes surrounding Peirce and Picard may cause an artificial age distinction.

REFERENCES

Boyce, J. M. and D. A. Johnson, 1977, Lunar Science VIII, Suppl. A, p.6-7.

Butler, P. and D. A. Morrison, 1977, Lunar Science VIII, p. 151-153.

Florensky, C. P. et al., 1977, in press, Proc. 8th Lunar Sci. Conf.

McGetchin, T. R. et al., 1973, Earth Planet. Sci. Lett., 20, p. 226-236.

Pieters, C. et al., 1976, Geophys. Res. Lett., 3, p. 697-700.

Ryder, G. et al., 1977, submitted to The Moon.

Vaniman, D. T. and J. J. Papike, 1977, in press, Geophys. Res. Lett.

Research supported by NASA Grant NSG-7188. Enlargements of Apollo photographs provided by NSSDC.

GRAIN SIZE AND EVOLUTION OF LUNA 24 SOILS

D. S. McKay, A. Basu,[1] G. Waits,[2] U. Clanton, R. Fuhrman,[2] and R. Fruland.
NASA Johnson Space Center, Houston, TX 77058 [1]Lunar Science Inst. [2]Lockheed Corp.

Introduction - We have carried out grain size, petrographic, electron probe, and SEM studies on 6 samples from the Luna 24 core. In this paper we report on the grain size and petrographic data as they relate to soil evolution. Companion papers report on rock types and mineral compositions (1) and on SEM studies of glasses and glass compositions (2). Other complementary studies were performed on separates from our consortium allocation (3,4,5,6).

Grain Size Analysis - We sieved each of our six ~ 50 mg samples through 150 μm, 90 μm, 45 μm, and 20 μm sieves (Table 1). Additionally, we analyzed the grain size below 20 μm with a Coulter counter. Data from the Curator Laboratory (7) was combined with our own data to determine the overall grain size characteristics (Table 2, Figure 1).

The most prominent feature of the grain size distributions is the strong bimodal character of all of these samples. A coarse mode is present at approximately 1 mm and a finer mode occurs around 100 μm. The bimodal character is particularly strong in the uppermost sample 24077. For 4 of the 6 samples the minimum separating the two modal populations occurs between 250 and 500 μm and for the other 2 samples the minimum occurs at coarser sizes. It may be unfortunate that the grain size cutoff used in allocating samples was 250 μm which is close to the minimum between modes.

If the two modes represent two distinct particle populations, they have been at least partially separated by the allocation. For the 6 soils, the coarse mode above 250 μm is based on our average of over 300 particles (mean 344, range 160-625) and is therefore statistically valid. Sample 24210 is apparently polymodal but the coarsest mode is based on a single particle and is therefore not valid. Coulter counter data indicate that about 1% of the mass of the soil is finer than 2 μm.

Variation of mean grain size (Mz) with depth is shown in Figure 2. The soil is coarsest at the top and except for a small reversal, becomes progressively finer grained toward the bottom. This trend can be compared to the trend for the mean grain size of just the <250 um fraction (Table 2, Figure 2). Although somewhat artifical and arbitrary, this mean grain size is more representative of the finer mode. The variations of this parameter with depth are nearly opposite that of Mz for the entire soil. The < 250 μm mean grain size generally increases with depth.

In summary, the Luna 24 samples are all bimodal and the coarse mode dominates the overall grain size characteristics. The sample with the most prominent coarse mode, 24077, is the coarsest-grained overall. However, the fine grained mode of this sample is the finest grained of the six < 250 μm samples.

Modal Data - Table 3 shows the petrographic data for the 90-150 μm size fraction. Some of the original categories (1) have been condensed and others have been eliminated. The "indeterminate" rocks (1) were assumed to be

GRAIN SIZE

D. S. McKay, et al.

basalts. For comparison, a typical Apollo 17 mare soil (71061) is shown. The mineral and lithic fragments appear to be nearly all derived from mare terrain. Highland lithic fragments reach a maximum of ~2%. The glasses contain an appreciable highland component, however (2, 10). Aside from variations in agglutinate content, the 6 samples are rather similar. Sample 24182 has notably more plagioclase; both 24149 and 24210 are enriched in vitric breccia. With the possible exception of agglutinates, no systematic trends with depth are apparent for any component.

Agglutinates and Maturity - The agglutinate content varies with depth (Figure 2). The two uppermost soils are submature and the rest are immature. The agglutinate maturity agrees closely with the maturity determined by the ferromagnetic resonance (FMR) parameter Is/FeO (3). It is noteworthy that the agglutinate content is highest for 24077 and 24109 which are also the coarsest grained. This is opposite the typical relationship in which soils high in agglutinates are fine grained (8). This is because the agglutinates measured in the 90-150 μm fraction (and Is/FeO) are reflecting only the maturity of the fine-grained mode. If only the grain size of the fine-grained mode is considered (as approximated by the 250 μm data), the mean grain size more nearly parallels the agglutinate content with more mature soils being finer grained (Figure 2). This relationship may also be reflected in the track data (6) which indicate that the top 4 samples have predominantely mature feldspar in the 45-90 μm grain size.

The pronounced bimodal grain size distribution of these soils strongly indicates that they are the products of mixing two soils of dissimilar grain size. Furthermore, the unusual relationship between grain size and agglutinate content suggests that these soils are badly out of "internal equilibrium," a state in which the grain size (which reflects the maturity of the entire soil) is closely related to the agglutinate content and Is/FeO (which reflect the maturity of the finer-grained fractions). Based on agglutinate and FMR data, some (11) have suggested that the upper part of the core was reworked progressively downward from the surface. However, reworking would tend to produce a unimodal grain size distribution and would also produce better agreement between mean grain size and agglutinate content (8). We therefore believe that the Luna 24 samples have not been appreciably reworked after the mixing event which created the bimodal distributions. The uppermost sample is the most strongly bimodal and most badly out of "internal equilibrium" and is therefore least likely to be reworked. Consequently it is unlikely that any of the samples have been reworked. The same conclusion was reached (3) based on the FMR profile. Based on bimodal track distribution, (6) suggest that at least the bottom two samples reflect mixing, not reworking.

Variation of Particle Abundances with Grain Size - Table 4 shows the variation of particle abundances normalized to agglutinate-free percentages. Numbers shown are mean values from all 6 Luna 24 samples and represent about 1800 grains in each size fraction. For comparison a typical mare soil from Apollo 17 is also shown (12). An important feature is the slight increase of pyroxene and plagioclase with decreasing particle size. This increase is much less than that of 71061. This suggests that either the source of Luna 24

GRAIN SIZE

D. S. McKay, et al.

pyroxene and plagioclase was much coarser grained so that more minerals were supplied to the coarser grain sizes or that the Luna 24 samples reflect a mixture of a coarse grained source and a finer grained source. In contrast to the pyroxene and plagioclase, the olivine abundance decreases steeply, with decreasing grain size. This is opposite the normal trend in which mineral grains increase with decreasing grain size. This suggests that olivine (and olivine bearing rocks) are greatly concentrated in the coarser grain sizes and are perhaps primarily associated with the coarse-grained mode.

Summary - The unusual bimodal grain size distribution of Luna 24 soils coupled to the anomalous relationship between agglutinates and mean grain are evidence that the soils consist of two populations which have not been strongly blended by reworking. Whether the two populations differ significantly in chemistry and mineralogy remains to be shown but our data indicate that the coarse-grained population may be richer in high Mg olivine and may reflect a large contribution of coarse-grained cumulate rock (1). This coarse-grained population may be ejecta from the crater Farenheit.

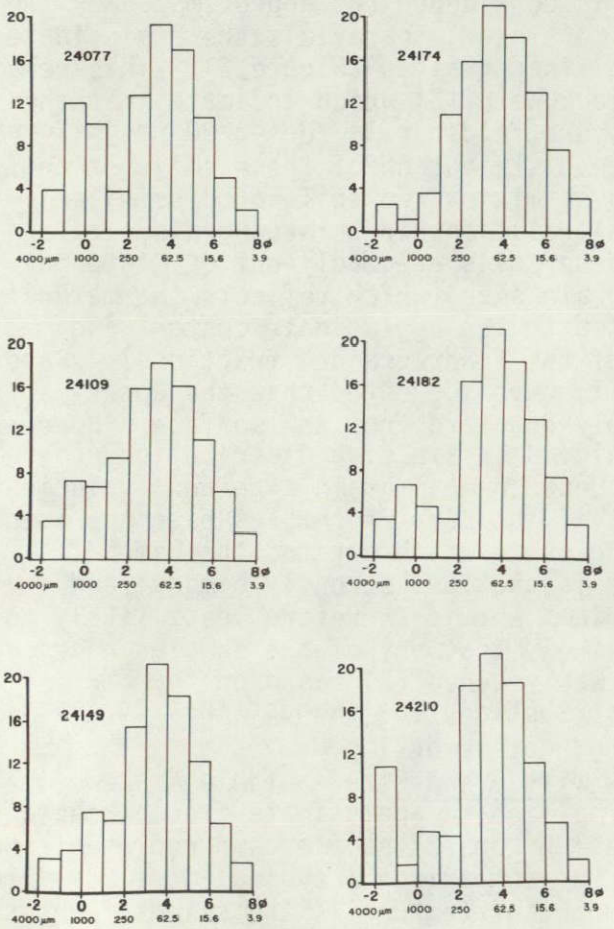

Figure 1

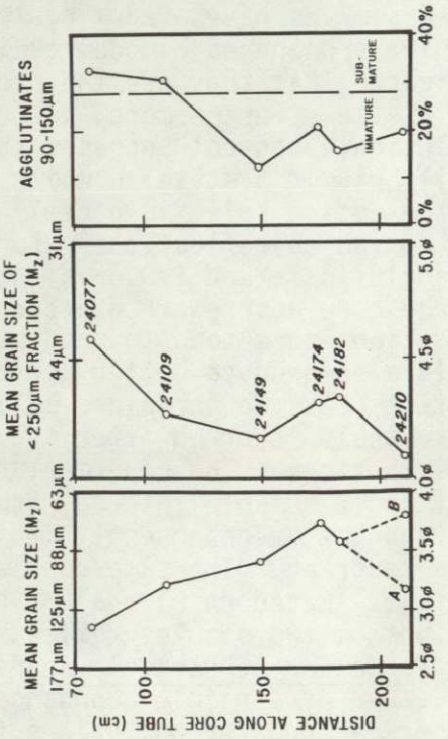

Figure 2

GRAIN SIZE

D. S. McKay, et al.

	150-250 μm	90-150 μm	45-75 μm	20-45 μm	< 20 μm
24077	4.70	6.05	10.22	8.87	10.75
24109	7.82	8.97	12.53	11.59	10.09
24149	8.37	9.45	12.75	11.56	8.66
24174	6.63	8.78	12.20	10.54	9.84
24182	7.11	9.68	13.55	11.95	12.63
24210	7.58	8.32	11.56	9.66	6.82

Table 1 Sieve Weights, in mg.

	Subcentimeter			Sub 250 μm		
	Mz		G_I	Mz		G_I
24077	2.85Ø	139 μm	2.38Ø	4.59Ø	42 μm	1.68Ø
24109	3.21	108	2.35	4.27	52	1.56
24149	3.41	94	2.12	4.17	56	1.50
24174	3.74	75	1.96	4.32	50	1.54
24182	3.59	83	2.24	4.34	49	1.55
24210 (A)	3.47	90	2.45	4.09	59	1.44
24210 (B)	3.79	72	1.70			

Table 2 - Mean Grain Size (Mz) and Standard Deviation (G_I). (A) with large fragment (B) without large fragments.

	150-250 μm	90-150 μm	45-90 μm	20-45 μm
Pyroxene	38.6	39.7	42.3	45.4
Olivine	7.9	6.3	4.5	3.1
Plagioclase	12.1	12.5	16.8	14.1
Olivine-Free Basalts	10.8	12.5	12.2	11.4
Olivine Basalts	4.3	3.3	1.4	1.1
Highland-Derived ANT	1.1	2.2	0.4	0.0
Vitric Breccia	12.0	13.0	11.8	10.0
Melt-Matrix Breccia	2.4	1.8	1.1	0.1
Glass	5.3	5.6	5.8	10.7
	Mare Regolith Sample 71061			
Pyroxene	13.7	28.1	36.1	-
Plagioclase	10.8	23.1	28.3	-
Basalt	43.6	26.2	17.9	-
Vitric Breccia	8.8	5.6	3.5	-

Table 3. Grain Size Variation in Combined Luna 24 Soils. 71061 Shown for Comparison All values in percent.

References: (1) Basu, A. et al. (a), this volume; (2) Basu, A. et al. (b), this volume; (3) Morris, R., this volume; (4) Blanchard, D. et al., this volume; (5) Bogard, D. and Hirsch, W., this volume; (6) Blanford, G. and Wood, G., this volume; (7) Nagle, S. and Walton, W. (1977) Luna 24 Catalog; (8) McKay, D. et al. (1974) Proc. Lunar Sci. 5th, p. 887; (9) McKay, D. et al. (1977) Proc. Lunar Sci. 8th, in press; (10) Simonds, C. et al., this volume; (11) Florensky, C.P. et al. (1977) Proc. Lunar Sci. 8th, in press; (12) Heiken, G. (1975) Rev. Geophys. and Space Phys. 13, p. 567.

LUNA 24 METABASALTS: POSSIBLE EVIDENCE FOR ASSIMILATION OF HIGHLANDS MATERIALS? Harry Y. McSween, Jr., Lawrence A. Taylor and James C. Clark, Dept. of Geological Sci., Univ. of Tennessee, Knoxville TN 37916

Hornfelsic metabasalts comprise a significant portion of the Luna 24 (1) and Luna 16 (2) soil samples. These fragments generally have equigranular textures and consist of fine-grained pyroxene and plagioclase, with scattered olivine, ulvöspinel, and ilmenite (Fig. 1). Constituent minerals are chemically homogeneous and exhibit very restricted compositional ranges. Ryder et al. (1) found that Luna 24 metabasalts are compositionally similar to other Mare Crisium ferrobasalts, and suggested that they formed by contact metamorphism of one flow by another. Chao et al. (3) had previously noted the similarity between hornfelsic basalt fragments found in Apollo 11 soil and samples of foundered crust annealed in terrestrial lava lakes.

Pyroxene analyses in a few metabasalt particles form diffuse clusters (Fig. 2), but most fragments contain pyroxenes with more restricted compositional variation (Fig. 2). These latter pyroxenes are thoroughly equilibrated, even though their apparent Fe/Mg ratios are not constant. We think this trend represents analyses of two pyroxenes (ferroaugite and pigeonite), each of which contains unobserved exsolution lamellae of the other. The measured compositions thus represent a two-component mixture along the tie line, with central compositions less abundant. Similarly MacDonald (4) observed that recrystallized hornfelsic blocks ejected during the 1924 Kilauea explosion contained two pyroxenes rather than the one pigeonite of typical

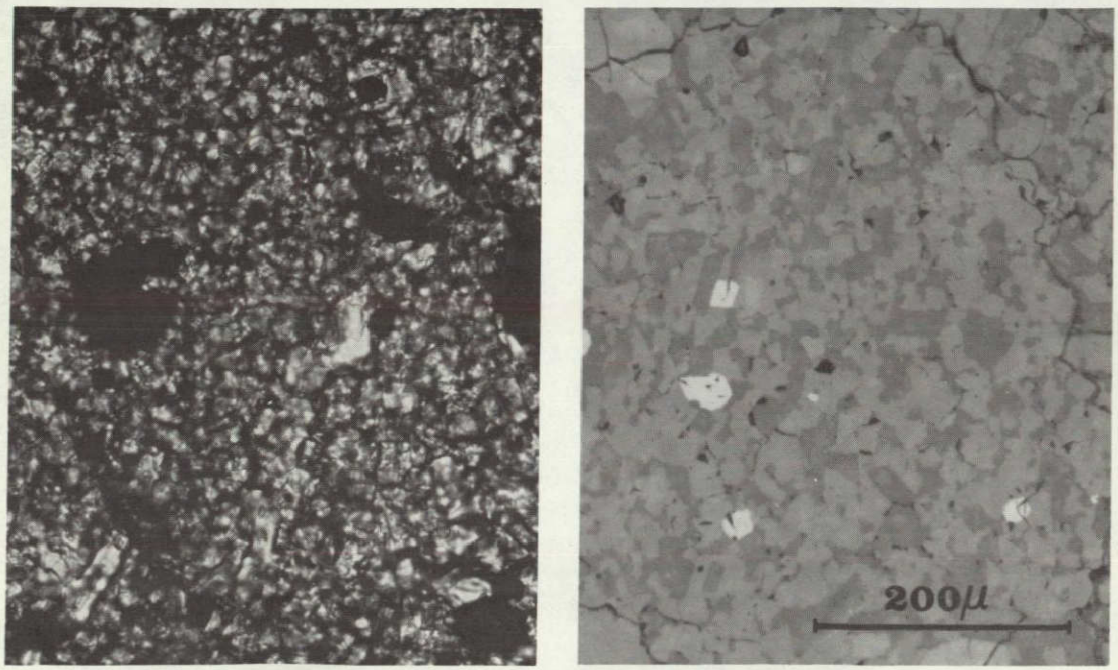

Fig. 1. Metabasalts by transmitted (left) and reflected (right) light.

LUNA 24 METABASALTS

McSween, H.Y. Jr. et al.

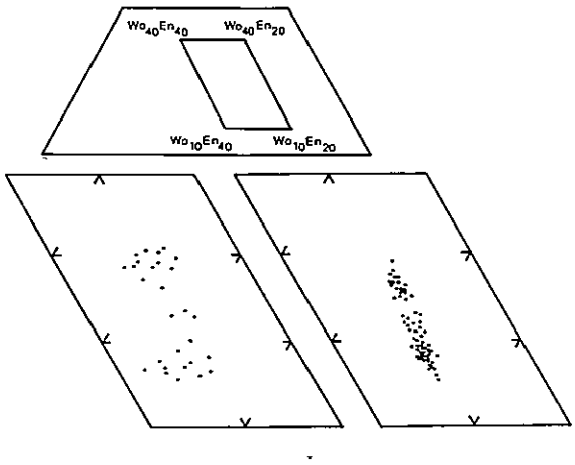

Fig. 2. Pyroxene analyses in two metabasalt particles.

Table 1. Selected Chemical Compositions (DBA) of Luna 24 Metabasalts

Oxides	24174,52 (1)*	24174,52 (2)	24109,40 (4)	24109,40 (5)	24109,40 (6)	24210,44 (1)
Na_2O	0.41	0.38	0.31	0.37	0.44	0.41
CaO	13.8	13 5	13.2	14.5	13.4	15.4
Al_2O_3	13.8	14.9	13.4	16.3	13.9	18.0
MgO	5.84	5.57	5.97	5.03	5.62	4.66
FeO	16.2	16.2	18.4	14.9	17.3	13.1
MnO	0.27	0.25	0.26	0.20	0.25	0.20
Cr_2O_3	0.13	0.10	0.14	0.17	0 22	0.14
TiO_2	0.39	0.36	0.38	0.53	0.68	0.38
SiO_2	47.3	47.0	45.7	47.1	46.3	46.5
Total	98.14	98.26	97.73	99.10	98.11	98.79
Wt.% Norms						
Qtz	0.25	0 06	---	0.54	---	---
Ab	3.53	3.27	2.68	3.16	3.79	3.51
An	36.50	39.70	36.04	43.20	36.56	47.74
Di	28.33	24 25	26.38	24.89	26.64	25.00
Hy	30.44	31.88	27.59	26.94	28.67	22.05
Fo	---	---	1.83	---	0.78	0.76
Fa	---	---	4.54	---	1.91	0.23
Ilm	0.75	0.69	0.74	1.02	1.31	0.73
Cr	0.20	0.15	0.21	0.26	0.33	0.21

* Particle number in the thin section.

Kilauean basalts. The pyroxenes and olivines of Luna 24 metabasalts (1) are more Fe-rich that the corresponding phases in Luna 16 metabasalts (2), reflecting the higher bulk FeO/FeO+MgO of the Luna 24 rocks.

If these metabasalts are contact metamorphosed crusts of basalt flows, their bulk compositions may be representative of the parent magmas. This is especially plausible in view of their very fine grain sizes relative to subophitic basalt fragments. We have analyzed 14 metabasalt fragments by microprobe defocussed beam analysis (DBA), employing necessary correction factors for target inhomogeneity (5). Error analyses (6) indicate statistical sampling uncertainties generally on the order of 5-7% of the oxides present. Our analyses (solid circles) are compared in graphical form with previous published metabasalt analyses (open circles) from (1) in Figs. 3 and 4. The outlined areas in the same figures define the fields of 12 analyzed Mare Crisium subophitic ferrobasalts (1,7,8,this study) of reasonably representative sizes.

Although FeO/FeO+MgO ratios are constant in all the basalts, metabasalts appear to be lower in TiO_2 and higher in Al_2O_3 than are subophitic basalts (Fig. 3). It should be noted that J.G. Taylor et al. (pers. com.) found similar ranges of composition for Luna 24 basalts and metabasalts, but subophitic basalt analyses are plagued by sampling problems. We believe the compositional variability in metabasalts is caused by the addition of plagioclase rather than subtraction of mafic minerals, because (i) the olivine/pyroxene ratio is variable, but samples with high olivine still fall on the olivine + pyroxene vs. plagioclase mixing line (Fig. 4), and (ii) the lower content of TiO_2 in metabasalts (Fig. 3) requires either dilution by plagioclase or early subtraction of Ti-bearing opaque minerals, but ilmenite and ulvöspinel are late-crystallizing phases in Luna 24 basalt mesostasis (1,8).

LUNA 24 METABASALTS

McSween, H.Y. Jr. et al.

Plagioclase enrichment in lava lake crust (prior to solidification or metamorphism) could be accomplished by plagioclase fractionation or assimilation of extraneous plagioclase-rich materials. A flotation mechanism is unlikely because of low density contrast and time constraints, although some mechanism of flow differentiation acting on plagioclase crystals suspended in the erupting magma might be postulated. We prefer the assimilation mechanism, which suggests that metabasalts do not represent liquid compositions, but liquids whose CaO and Al_2O_3 contents have been augmented by incorporation of highlands materials. Mare Crisium subophitic ferrobasalts, which are also high in CaO and Al_2O_3 (1,8), may likewise have been affected by assimilation, though to a lesser degree than the surface crusts of these flows, now represented by metabasalts.

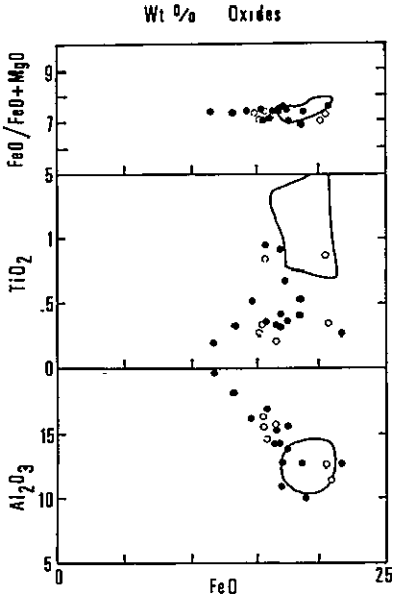

Fig. 3 ←

Fig. 4 →

Metabasalt compositional variations.

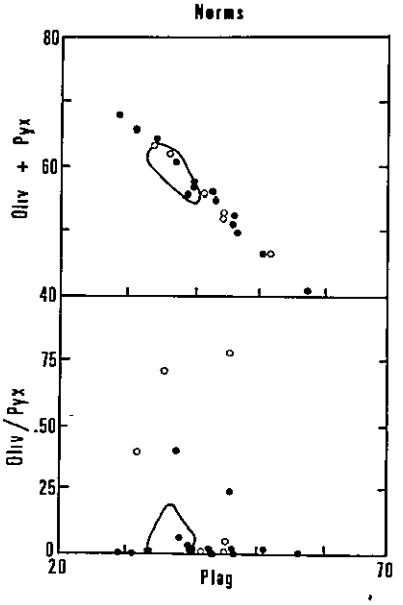

References: (1) Ryder et al. (1977) Basalts from Mare Crisium. The Moon, in press. (2) Kurat et al. (1976) Composition and origin of Luna 16 aluminous mare basalts. Proc. Lunar Sci. Conf. 7th, 1301. (3) Chao et al. (1970) Petrology of unshocked crystalline rocks and evidence of impact metamorphism in Apollo 11 returned lunar sample. Proc. Apollo 11 Lunar Sci. Conf., 287. (4) MacDonald (1944) Unusual features in ejected blocks at Kilauea volcano. Amer. J. Sci. 242, 322. (5) Albee et al. (1977) Source and magnitude of errors in "broad-beam analysis" (DBA) with the electron probe. Lunar Sci. VIII, 7. (6) Bower et al. (1977) Rock compositions by defocussed beam analysis. Abst., 8th Ann. Conf. Microbeam Anal. Soc., Boston. (7) Taylor et al. (1977) Very low-Ti mare basalts. Geophys. Res. Lett. 4, 207. (8) Vaniman and Papike (1977) Ferrobasalts from Mare Crisium: Luna 24. Geophys. Res. Lett., in press.

FMR AND MAGNETIC PROPERTIES OF LUNA 24 SOILS AND >1 mm SOIL PARTICLES

Richard V. Morris, Code SN7, NASA Johnson Space Center, Houston, TX 77058.

Six Luna 24 soils and 25 particles from their >1 mm sieve fractions were studied by ferromagnetic resonance (FMR) and magnetic techniques. The results obtained include FeO and Fe° concentrations and, for the soils, values of the FMR maturity index (I_s/FeO). Except as noted, refer to [1,2] for experimental procedures. The soil studies comprise one segment of a multidisciplinary characterization of the same samples of Luna 24 soil.

Luna 24 Soils

The results for the six <250μm bulk soils are summarized in Table 1. Also given are the concentrations of FeO determined by instrumental neutron activation analysis [3]. The FeO concentration is quite uniform, and the concentrations determined magnetically and by INAA are in very good agreement. However, the FeO concentrations determined by the fused-bead technique are systematically lower and average 17.5 wt.% [4]. The origin of this discrepancy has not been resolved. The FMR linewidths (ΔH) are within the range expected from their FeO concentrations [1]. The values of I_s/FeO, which were calculated using the higher values of FeO, show that the soils are immature to submature.

Table 1. Data on Luna 24 <250 μm bulk soils

Sample	FeO (wt. %) Mag.	FeO (wt. %) Chem.*	ΔH (G)	I_s/FeO (Arb.)	Equiv. wt. % metallic iron Fe^o_{VSM}	Fe^o_{FMR}	Fe^o_I
24077,7	21.0	19.9	787	39.0	0.51	0.32	0.18
24109,14	21.0	20.6	783	31.0	0.46	0.29	0.18
24149,16	20.4	20.3	798	21.0	0.33	0.21	0.14
24174,17	21.0	20.9	790	27.0	0.37	0.18	0.16
24182,12	20.1	20.2	793	19.0	0.30	0.14	0.16
24210,10	19.8	21.1	790	19.0	0.33	0.19	0.12

*Blanchard et al., this volume.

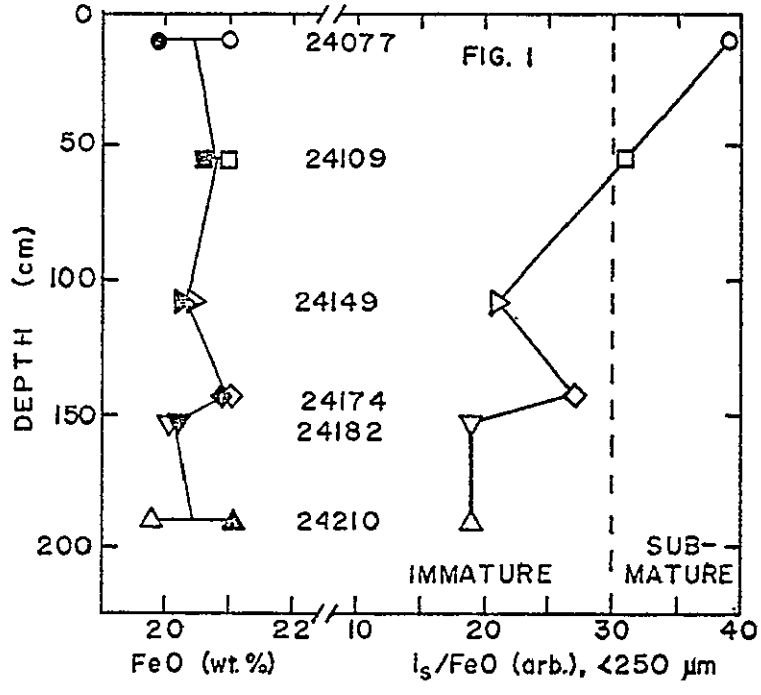

The parameter Fe^o_{VSM} represents the magnetically-determined concentration of metallic iron. Fe^o_{VSM} includes the concentration of metal grains larger than about 20-40 A in diameter[5]. The values of Fe^o_{VSM} for the Luna 24 soils are typical of those observed for other lunar soils [eg, 6,7]. The parameters Fe^o_{FMR} and Fe^o_I will be discussed in the next section.

The depth profiles of FeO and I_s/FeO are shown in Fig. 1. The sample depths are the preferred depths of [8]. The I_s/FeO maturity profile shows a decrease in maturity from the uppermost sample. The agglutinate data of [9] and [10] also show this trend. [10] suggest the decrease is due to reworking, and, in fact, similar trends in other cores have been attributed to in situ reworking of the lunar surface [eg, 11,12]. However, the rate of decrease of

maturity in the Luna 24 core seems too shallow to be attributable to reworking. [9] have reached the same conclusion from analysis of grain size data. Since [13] has found very high track densities in plagioclase crystals from upper 4 soils, these soils must be mixtures of immature and mature components to account for the observed low values of I_s/FeO. Thus it seems reasonable to attribute the decrease in maturity from the surface to a mixing process. Mixing of soils of different maturities is also indicated for the bottom 2 samples since they are characterized by bimodal track distributions [13]. Mixing relationships among the 6 soils is also indicated from the grain size distributions of [9] and the $^{21}Ne_c$ data of [8]. Since mixing characteristics seem to dominate the maturity relationships among the 6 soils, it seems likely that the Luna 24 core was deposited in one event or series of closely spaced events. Slow accumulation of the core is definitely not indicated.

>1 mm Soil Partiles

The results for the >1mm soil particles are summarized in Table 2. The parameter Fe^{o}_{FMR} is the FMR-determined concentration of metallic iron. The procedure used to determine Fe^{o}_{FMR} is described by [14]. Fe^{o}_{FMR} includes the concentration of metallic iron grains between about 40 A and 330 A in diameter and also a contribution from grains somewhat larger than 330 A [15]. As is shown in Fig. 2, a plot of Fe^{o}_{VSM} versus Fe^{o}_{FMR} separates the >1mm particles into 3 distinct groups. Group 1 is characterized by low concentrations of both Fe^{o}_{VSM} and Fe^{o}_{FMR}. Their FMR spectra are dominated by a narrow resonance (lunar soils are dominated by a narrow resonance) and may be due to a small amount of agglutinitic glass on the surfaces of the grains. Group 2 is characterized by high values of Fe^{o}_{VSM} and low values of Fe^{o}_{FMR}. Their FMR spectra are either dominanted by a narrow resonance or contain both narrow and broad resonances. Group 3 is characterized by high values of both Fe^{o}_{VSM} and Fe^{o}_{FMR}. Their FMR spectra are dominated by a narrow resonance. The bulk soils also plot in Group 3, which suggests that the Group 3 particles are derived from soil with minimal heating (ie, low-grade breccias) or are agglutinate particles. This interpretation is supported by the binocular description [16] and by the fact that many of the Group 3 particles crumbled during either handling or analysis in the vibrating sample magnetometer.

Table 2. Data for >1 mm soil particles

Sample	FeO (wt. %)	Fe^{o}_{VSM} (wt. %)	ΔH (Gauss)	Fe^{o}_{FMR} (wt. %)	Group
24077,4	30	0.018	770	0.009	1B
,11	20	0.23	811	0.011	2B
,12	22	0.031	810	0.003	1B
,13	21	0.019	780	0.001	1B
,14	20	0.021	755	0.003	1B
,16	59	1.41	800	0.21	3
,17	7.6*	0.31	810	0.003	2A
,18	28	0.72	800	0.24	3
,19	0.77*	0.027	790	0.004	1A
,21	16.3*	0.70	775	0.26	3
24109,5	---	---	800	0.17	3
,6	22	0.044	802	0.008	1B
,7	22	0.032	777	0.007	1B
,8	22	0.065	800	0.010	1B
,9	25	0.58	745	0.14	3
24149,5	20.3*	0.48	793	0.16	3
24174,5	16.6*	0.028	805	0.006	1B
,6	23	0.057	817	0.012	1B
,7	25	0.064	800	0.016	1B
24182,5	17	0.27	805	0.096	3
,8	7	0.044	800	0.005	1A
,12	23	0.042	765	0.001	1B
24210,5	14	0.41	821	0.013	2B
,6	22	0.33	830	0.006	2B
,50	15	0.47	832	0.009	2B

*Blanchard et al. (this volume). The rest of the FeO values were calculated from the paramagnetic susceptability.

Fig. 3 is a plot of Fe^{o}_{VSM} versus FeO for the rock-like particles, ie, Groups 1 and 2. Where the data were available,

FMR AND MAGNETIC PROPERTIES OF LUNA 24..

Morris R. V.

chemically determined values of FeO were used. For the remaining particles, the magnetically determined values were used. For the >1mm particles, the values of FeO may be substantially in error because an average paramagnetic susceptability for FeO was used in the calculations and because the sample masses were often very small (0.5 to 2 mg). With this crevat in mind, Group 1A is characterized by low FeO content, which is consistent with their binocular description [16]. Group 1B is characterized by higher FeO content. Although many of the Group 1B particles were classified as recrystallized breccias by [16], their high FeO and low Fe^{0}_{VSM} and Fe^{0}_{FMR} contents suggests they are mare basalts. If so, their Fe^{0}_{VSM} contents are comparable to those of the Apollo 12 and 15 mare basalts, but lower than most of the Apollo 17 mare basalts. The Group 2 particles were subdivided according to the nature of their FMR spectra. The FMR spectrum of the sole particle in Group 2A is dominated by a narrow resonance, which may be due to a small amount of adhering agglutinatic glass. The FMR spectra of the Group 2B particles exhibit both a broad and a narrow resonance. The Group 2B particles also have a higher FeO content than the Group 1B particle.

The average value of the FeO and Fe^{0}_{VSM} data for the Group 1 and 2 particles is also plotted in Fig. 3 along with the concentration of initial metal (Fe^{0}_{I}) in the soils. Initial metal is the metal remaining in a soil after the metal acquired during maturation is mathematically removed [14]. The close proximity of the soils and the average value of the rock-like particles suggests the suite of >1mm particles is reasonably representative of the major rock types at the Luna 24 site.

Conclusions

The Luna 24 soils are immature to submature and have a uniform FeO content. It seems likely that the Luna 24 core was deposited in one event or a series of closely spaced events. On the basis of FeO and metallic iron concentrations and FMR spectra, 25 Luna 24 >1mm particles fall into 5 groups.

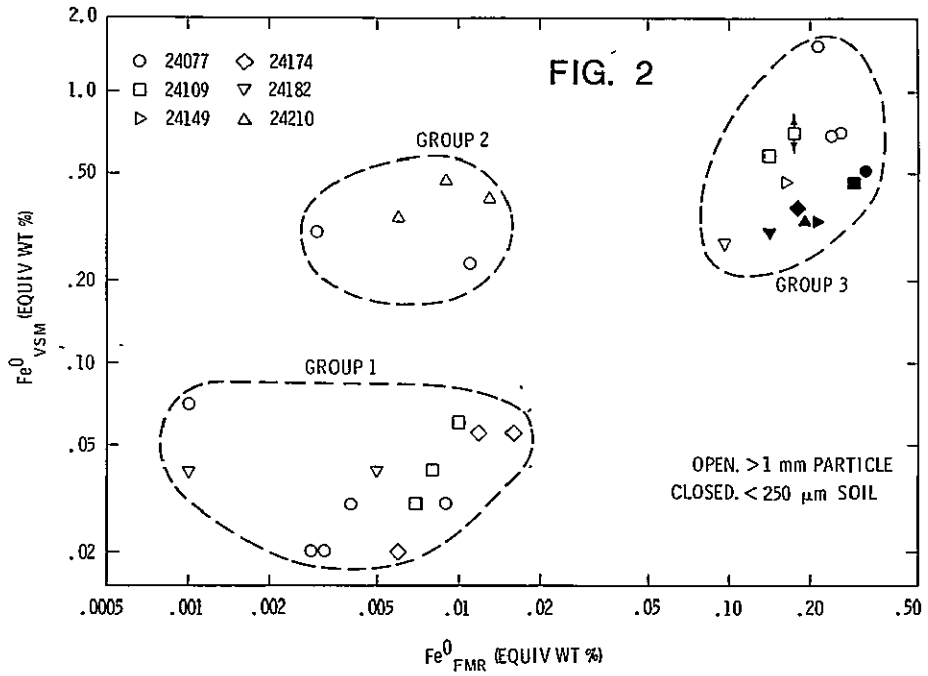

FMR AND MAGNETIC PROPERTIES OF LUNA 24...

Morris R. V.

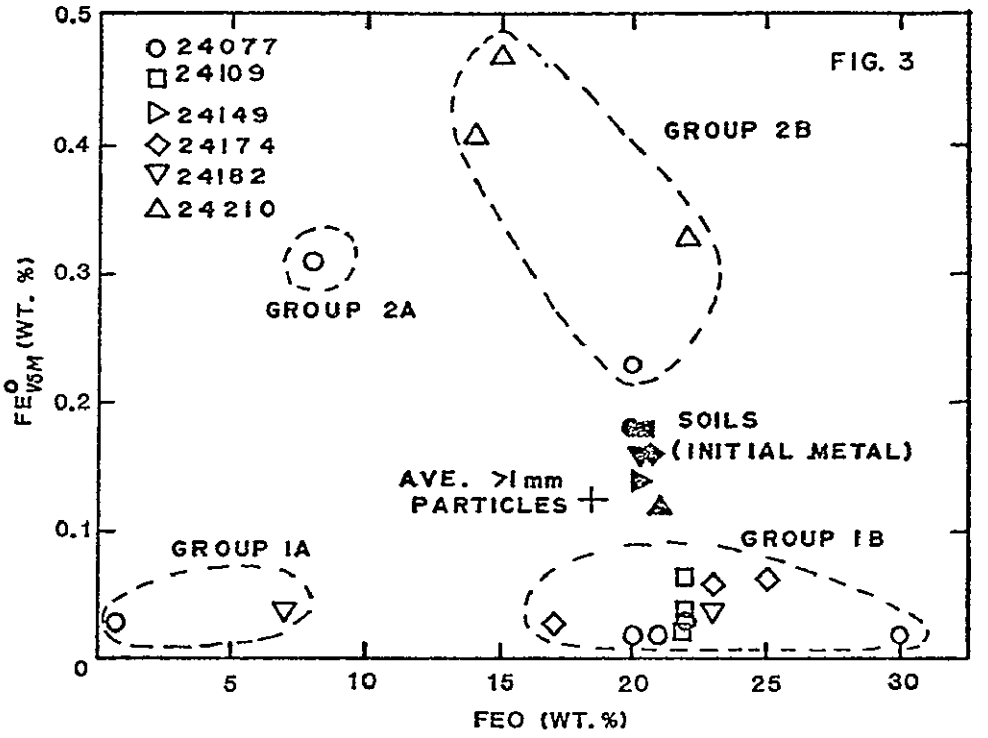

REFERENCES: [1] Morris (1976) P7LSC, 315. [2] Pearce et al. (1973) P4LSC, 3045. [3] Blanchard et al., this vol. [4] Simonds et al., this vol. [5] Pearce and Simonds (1974) JGR, 2953. [6] Pearce et al. (1974) P5LSC, 2815. [7] Cisowski et al. (1974) P5LSC, 2841. [8] Bogard and Hirsch, this vol. [9] McKay et al., this vol. [10] Barsukov (1977) P8LSC, in press. [11]) Heiken et al. (1976)) P7LSC, 98. [12] Morris and Gose (1976) P7LSC, 1. [13] Blanford et al., this vol. [14] Morris, to be submitted. [15] Housley et al. (1976) P7LSC, 13. [16] Nagle and Walton (1977) Luna 24 Catalog.

Geologic Map of the Luna 24 Site

D. A. Morrison and P. Butler, Jr., JSC

We have compiled a geologic map (fig. 1) centered approximately on the Luna 24 sampling site as 12°45'E and 62°12'N (Barsukov et al., 1976) as an aid to interpretation of the area. A brief description of its principal components follows.

Structures: In the vicinity of Luna 24, the mare is divided into 3 subareas consisting of the inner mare, the upper shelf (400-500 m above the inner mare) and the lower shelf (about 300 m above the inner mare). The slopes between these areas are monoclines morphologically, broken by fault scarps, horsts, and grabens. The fault scarps represent normal faults arranged en echelon. Differential movement on closely spaced fault planes produced horst-graben structures. These structures developed in response to tensional stresses.

Fifteen buried craters occur within the map area. Thirteen are concentrated on the hinge line(figs. 1 & 2) corresponding to the first Crisium ring (Olson and Wilhelms, 1974). Since the hinge line probably was a topographic high throughout the mare extrusive phase, flows there would be thinner than elsewhere and craters present less likely to be completely obscured than craters formed on the lower areas of the shelf. If this is the case, then the material filling the buried craters had sources along the hinge line.

The six ridges shown in fig. 1 stand 100-200 m above the local terrain, and are bordered on one or more sides by scarps. Suggestions of flow of material from several of the ridges (e.g., at C) plus their morphology suggests an origin by both volcanic and tectonic processes.

Stratigraphy: Cratering units: Mare ejecta from the crater Fahrenheit of Eratosthenian age may have contributed up to a meter of material to the Luna 24 site (Butler and Morrison, 1977; Barsukov et al., 1977). Rays traced to the young highland crater Giordano Bruno 1300 km to the NE are prominent. However, the probability of Luna 24 having sampled Giordano Bruno material is low (Butler and Morrison, 1977). Numerous, subdued, secondary crater clusters are observable but were not mapped.

Mare units: The most conspicuous mare unit is the dark mantle (figs. 1 & 2) (Olson and Wilhelms, 1974; Butler and Morrison, 1977; Boyce et al., 1977) of apparent pyroclastic origin. The thickest dark mantle deposits occur near the hinge line (fig. 1) overlying the buried craters previously mentioned. The source or sources of dark mantle must be on the hinge line. Downslope mass wasting and dispersal of the dark mantle by impacts are evident. Crater counts (Boyce et al., 1977) suggest an age of 3.75 b.y. for the dark mantle. Its stratigraphic age is ambiguous from photogeology studies because it is not clear if it onlaps or is onlapped by other units on the upper shelf, but it appears to overlap a unit of intermediate albedo (fig. 1). Consequently, the dark mantle may be one of the younger shelf units, as shown by Olson and Wilhelms (1974).

GEOLOGIC MAP

Morrison, D. A., Butler, P., Jr.

The unit underlying the dark mantle is the "dark flow" unit (fig. 1). The "dark flow" unit occurs as a thin (<10 m?) layer visible in the upper part of the scarps (e.g., at B, figs. 1 & 2). Material with the same albedo forms most of the ridges at A (figs. 1 & 2), from which it is mass wasting downslope. On the shelf there is topographic expression suggesting the contacts shown in fig. 1.

A blocky cliff-forming unit is visible in the scarps (e.g., at B, fig. 2) below the "dark flow" unit. Visible boulders suggest a unit more than 10 meters thick. This unit is not apparent in any of the ridges.

There are indications of flows from the ridge at C (fig. 1) south of Fahrenheit. The ridge is en echelon with fault sets. Flows from the ridge appear to have partially obscured the scarp trending south from Fahrenheit. The flows may be contemporaneous with the faulting, as suggested by the small scarps which define the eastern side of the ridge. A similar situation is suggested by possible flow fronts near D (fig. 1), which may indicate flow of volcanics downslope from the ridges at D. Other possible flow fronts are indicated by dashed lines. These flows cannot be traced to a source and the contacts cannot be closed. If they are flows, they are younger than the underlying undifferentiated mare.

Benches were noted in seventeen craters averaging 120 m in diameter, but more accurate measurements will be necessary before an average regolith thickness can be determined.

The stratigraphic column shown in fig. 1 is in order of stratigraphic age. The shelf inner mare slope has been the locus of both volcanic and tectonic activity, the two processes overlapping to some degree. Of the samples returned, the olivine vitrophyre may be a sample of the dark mantle as suggested by Ryder et al. (1977), or the "dark flow" unit. Of course, it may have nothing to do with either one. Rocks with textures of the micro-gabbros returned should be present in the blocky unit present in many scarp fronts.

Barsukov V. L. and Forenski G. P. (1977) The Lunar soil from Mare Crisium: Preliminary data (abstract) in Lunar Science VIII, p. 61-63, The Lunar Science Institute, Houston.

Boyce J. M., Schaber G. G., Dial A. L. (1977) Age of the Luna 24 mare basalts based on crater studies. Nature 265, p. 38-39.

Butler P. Jr. and Morrison D. A. (1977) Geology of the Luna 24 site. Proc. Lunar Sci. Conf. 8, In press.

Olson A. B. and Wilhelms D. E. (1974) Geologic map of the Andarum quadrangle of the Moon, U.S.G.S., Misc. Geol. Inv. map I-837.

Ryder G., McSween H. Y. and Marvin U. B. (1977) Basalts from Mare Crisium, The Moon, In press.

Geologic map Luna 24

Morrison D. A.

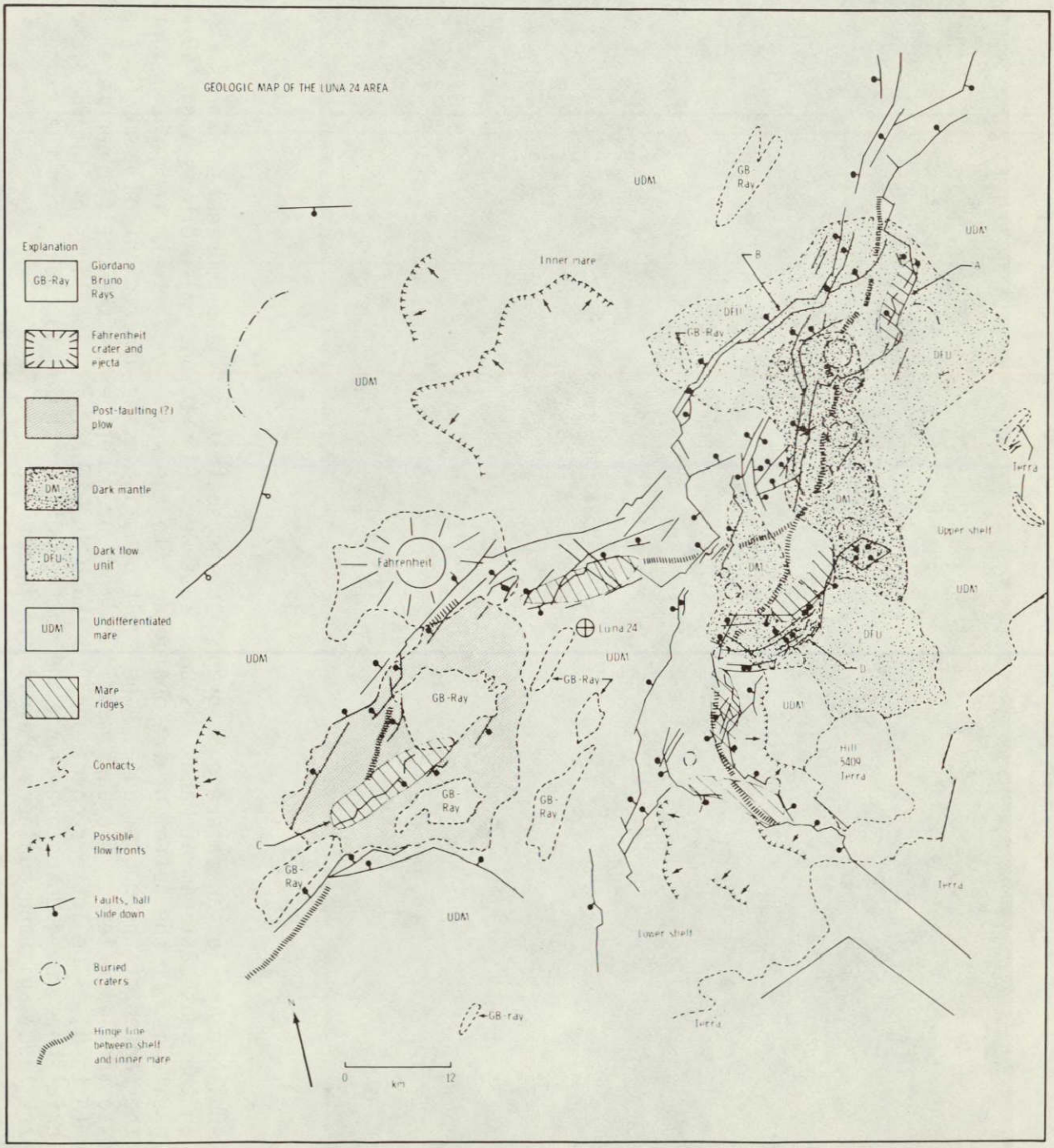

Figure 1: Geologic map of the Luna 24 based on Apollo mapping camera photography.

Figure 2: Oblique Apollo pan camera photograph looking south (from left to right) towards the highlands on the southeast rim of Mare Crisium. East-west (top to bottom) width is about 40 km. The Luna 24 site is off the bottom of the photograph (to the west) about 10 km from the bright crater at the center of the bottom edge. The shelf area is to the upper right of A and D, the inner mare to the lower left. The dark mantle is most prominent along the shelf-inner mare hinge line (A to D). The letters correspond to those in Figure 1. Landslides of intermediate albedo material have moved downslope (down and to the left in the photograph) from the ridge at A. The "dark flow" unit and boulders are visible in the scarp at B.

LUNA 24, CLAST POPULATIONS, J. Stewart Nagle, Northrop Services, Inc., Johnson Space Center, Houston, Texas, 77058

During preliminary examination of LUNA 24 samples presented to the USA, it was noted that different fractions of sand-sized fines (ranging between .09 and 2.0mm) showed distinct and major variations in component abundance. Textural and compositional properties of these components were studied in terms of maturation, as described in (1) to attempt to identify maturing clast populations, and to identify an influx of "new" components in the history of the LUNA 24 core.

The following rock types were identified under the binocular microscope and found to be common enough to study as clast populations. (Details in 2,p. 8-10): plagioclase, pyroxenes, and gabbro were lumped as the crystalline component, but breccias were considered individually, and include melt breccia, aphanitic breccia, recrystallized breccia, soil breccia, as well as agglutinates, devitrified glass and fresh glass chips.

Assumptions and definitions: 1. Clast population groups are defined as all clast populations showing similar size distributions. 2. Newly-introduced clasts will show lower maturity (as defined and illustrated in (1) than those that have matured locally. 3. Crystallines and high-grade breccias cannot have originated in the regolith; their presence can indicate a lower soil maturity than low-grade breccias of intra-regolithic origin. 4. Artifacts of drilling are minimal. 5. Inversion of section is not a factor in samples seen from this core.

Characteristics of samples: All soils but 24177 and 24182 show at least two clast population groups. One population group is relatively mature, with progressively greater abundances of finer sizes; the other is relatively immature with most of the clasts being in the coarser sizes. Particles in nearly all of the relatively immature populations show fresher-appearing surfaces, with rock faces being angular and dust-free.

24210 (fig.1) shows two population groups. All crystalline rocks, agglutinates and devitrified glass show progressively greater abundances of finer grain sizes, and are relatively mature whereas low grade melt breccia, soil breccia, and fresh glass chips have a coarse component and are relatively immature.

In 24182 and 24174, all particle types show only one form of grain-size distribution, indicating only one population group. Additionally these two samples are richer in crystallines and richer in fresh-appearing particles than other samples in the core. (Melt breccia, soil breccia and varities of glass are present, in addition to the crystalline basalts and gabbros.) In addition to being light-colored, 24182 has a great proportion of coarse-sized particles, and is accordingly less mature than 24174, (24170, another sample from the lower-middle portion of the core, may have been a rock that was

fragmented in drilling (3), at any rate, the sample was too small for grain-size analysis, and consisted entirely of fresh gabbro fragments).

24077, 24109, and 24149 are much lower in crystallines and much higher in breccias than 24174 and 24182, and all three of the upper samples show mature and immature populations of clasts. Crystallines, agglutinates, melt breccia and devitrified glass are relatively mature in 24149, with soil breccia, a regolithic component, being the only coarse and immature type. (fig.1, mode 2). 24149 is an unusually cohesive soil and many rock fragments are dust-covered and relatively rounded.

Crystallines, agglutinates, and devitrified glass are again mature in 24109, and soil breccia is coarse and immature. However, two rock types not seen lower - a distinctive, light-colored aphanitic breccia and black-and-white breccia appear in abundance and show an immature size distribution. 24077 also has two clast populations. Size distribution of the more mature component, as seen in crystallines, agglutinates, and melt breccia, is unusual in that there is a maximum at .5 - 1 mm, not in the coarsest or finest sizes.

An immature size distribution, with a maximum in coarsest size, is seen only in a dark, recrystallized breccia not seen lower in the core.

Interpretation: All soils in the LUNA 24 core are either submature or immature, or are fractionally mature, with two clast populations, of differing maturity. Soil in 24210, at the base of the core, is a mixture that includes a mature crystalline-agglutinate-devitrified component, and a less mature component, and a less mature component that is intra-regolithic in origin. 24182 and 24174 contain an abundance of fresh crystallines, with an immature to submature distribution pattern, and show only one clast population. A major distrubance is required to produce such an influx of crystallines and disruption of the clast populations seen at the base of the core. These are the only soils in the core that could be Fahrenheit ejecta, although smaller, bedrock-penetrating local events could also produce the immature to submature soil seen in 24182 and 24174. 24149 is the closer to being a mature soil than any other but even it is fractionally mature, because there is immature soil breccia component. Soil breccia is of intra-regolithic origin, however, and this soil could have been matured in place from 24174. Most of the mature components of 24149 persist upward, but there is an influx of immature, coarse-grained aphanitic breccia and black-and-white breccia in 24109 and dark recrystallized breccia in 24077.

REFERENCES: [1] McKay, Fruland and Heiken (1974) P5 LSC, 887-906. [2] Nagle and Walton. (1977) LUNA 24 Catalog. [3] Barsykov, et. al. (1977) P8 LSC, in press.

Nagle, J. S. LUNA 24 Clast Populations

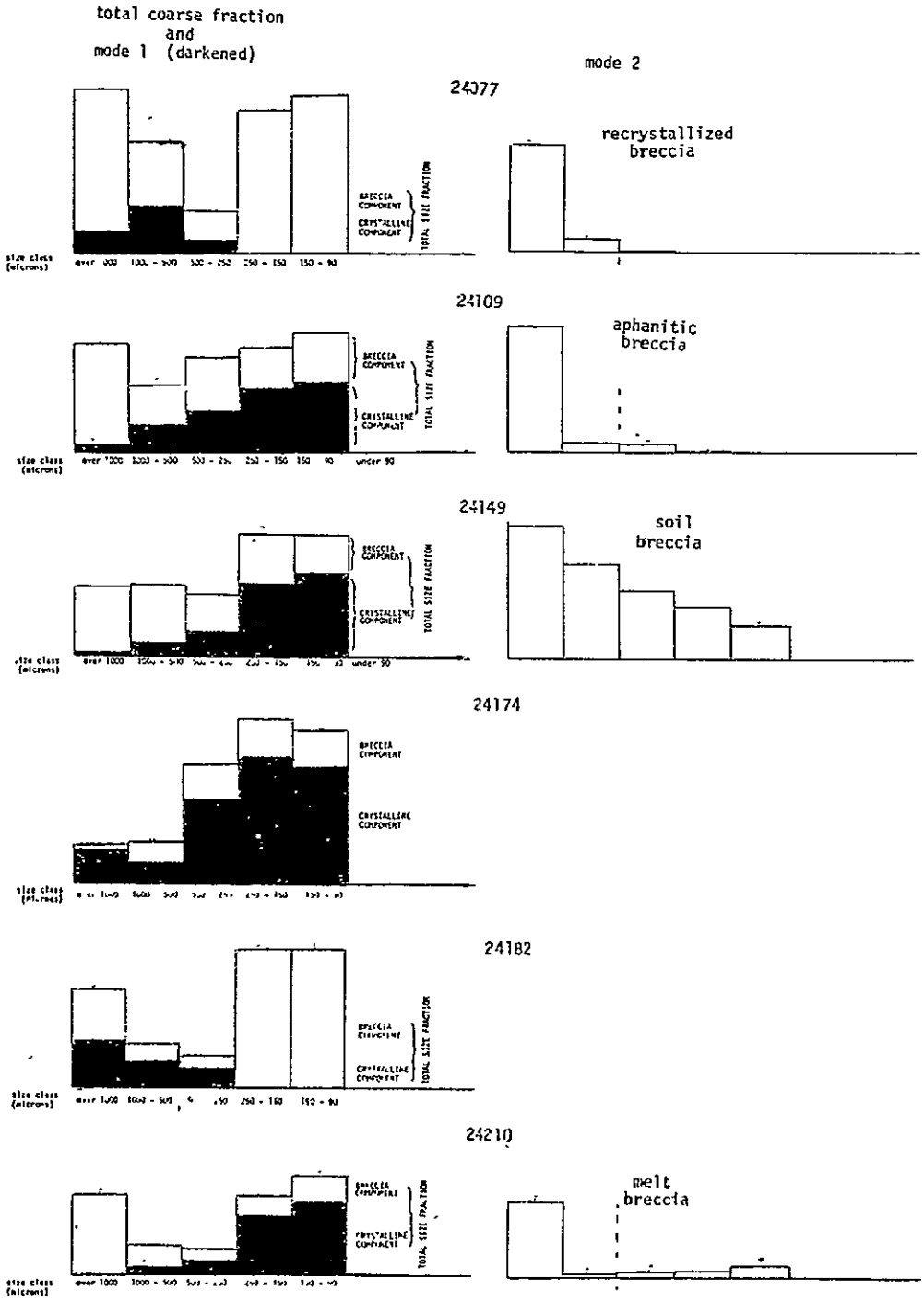

Fig. 1. Size histograms, LUNA 24 core samples. Although only two are shown, they closely reflect all others of their population group.

MAGMA TYPES AT THE LUNA 24 SITE IN MARE CRISIUM. Roger L. Nielsen* and Michael J. Drake**, Lunar and Planetary Laboratory, University of Arizona, Tucson, AZ 85721. *Also Dept. of Geosciences. ** Also Dept. of Planetary Sciences.

INTRODUCTION. We report a microprobe study of 1230 particles contained on six thin sections of Luna 24 core samples. The particles are in the 150-250μm size range. Thin sections studied are, in order of increasing depth in the core: 24077,47; 24109,42; 24149,51; 24174,53; 24182,49; 24210,45. On section 24077,47 all fragments were analyzed quantitatively. On the remaining sections only polymineralic igneous fragments were analyzed quantitatively; other fragment types were characterized utilizing spectra obtained with an energy dispersive Si(Li) detector.

PARTICLE CENSUS. A census of particle types is given in Table 1. Six distinctive types of particles are recognized:

(1) Igneous rocks: lithic fragments with basaltic or gabbroic textures, with crystal sizes of greater than ≃30μm.
(2) Melt rocks: lithic fragments with crystal sizes of less than ≃30μm which appear to have formed from quenched impact melts.
(3) Crystal fragments: fragments composed of a single mineral.
(4) Glass fragments: fragments of homogeneous glass.
(5) Breccias: monomict and polymict.
(6) Agglutinates: fragments of breccias cemented primarily by inhomogeneous glass.

Approximately 11% of all particles were igneous rocks, and to these we shall devote most attention. Of the mineral fragments, 58% were pyroxene, 20% were plagioclase, 20% were olivine, the remainder being composed of ilmenite. As seen in Table 1 distinct differences in the distribution of particle types are observed among the six thin sections studied.

PETROLOGY OF IGNEOUS FRAGMENTS. Pyroxene compositions for Luna 24 igneous rocks are illustrated in Figure 1. Most pyroxenes appear to be of mare basalt origin, and occupy the irregularly shaped envelope. The only exceptions are two Mg-rich pyroxenes designated by open squares. These pyroxenes are compositionally similar to pyroxenes from Luna 20 ANT rocks. An ANT origin for these pyroxenes is also supported by their association with very anorthitic plagioclase (An_{98}). One of the pyroxenes is also associated with a unique (amongst the 1230 particles studied) magnesian ilmenite (MgO = 6.82 wt.%). Single crystals of pyroxene of apparent ANT origin are rare, comprising less than 1% of the pyroxene fragments. Open circles in Figure 1 denote pyroxenes from finer grained basaltic rocks, while closed circles denote pyroxenes from coarser grained gabbroic rocks. The range of compositions overlaps, but gabbroic pyroxenes have a greater degree of Fe-enrichment as one might predict if the parent magma was common to the two textural groups.

Olivine compositions (also shown in Figure 1) display a bimodal distribution, the peaks being centered around ≃Fo_{50} and ≃Fo_{20}. Plagioclase compositions vary from An_{75}-An_{98}. Potassium concentrations in plagioclase are positively correlated with Ab-content but never exceed 0.5 wt.% K_2O, Fe is positively correlated with Ab-content and reaches a maximum concentration of 2 wt.% FeO, while Mg is negatively correlated with Ab-content and never exceeds concentrations of 0.2 wt.% Na_2O.

MAGMA TYPES AT LUNA 24

Nielsen and Drake

Three major oxide phases are present. Aluminian chromites containing 12-16 wt.% Al_2O_3 are found as euhedral crystals in association with the more Mg-rich mare basalt pyroxenes, but were not observed in association with ilmenite or ulvospinel. Ilmenites, usually containing less than 1 wt. % MgO, are associated with the more Fe-rich mare basalt pyroxenes, and often occur in association with troilite, cristobalite, (K,Si)-rich glass, fayalite, and pyroxferroite. Chromian ulvospinels containing up to 8 wt.% Cr_2O_3 are often associated with ilmenite, but tend to occur with mare basalt pyroxenes which are intermediate in composition relative to the most Mg- and most Fe-rich pyroxenes.

DISTINCT MAGMAS SAMPLED AT LUNA 24. Figure 2 is a plot of molar Ti/(Ti+Cr) versus molar Fe/(Fe+Mg) for pyroxenes from Luna 24 igneous rocks. The rationale for this plot is that magmas with grossly different initial compositions will evolve along distinct fractionation paths from lower left to upper right. These fractionation paths are a consequence of pyroxene/melt partition coefficients for Fe and Ti being less than unity and those for Mg and Cr being greater than unity in lunar igneous petrogenesis. Also shown on Figure 2 are envelopes representing the fractionation paths of several other known lunar rock types: ANT rocks, Apollo 15 low-Ti mare basalts, and Apollo 17 VLT (very low titanium) basalts. The field of KREEP basalts is intermediate between and overlaps the ANT and mare basalt fields, but is not included due to the absence of pyroxenes with KREEP characteristics.

Most of the pyroxenes analyzed in this study fall in the field of VLT basalts, but a substantial number of pyroxenes occupy the low-Ti basalt field. Thus there appear to be two grossly distinct mare basalt magma types sampled at Luna 24. Textural and mineralogical differences are not apparent between the two groups. Although aluminian chromite occurs only in the Mg-rich VLT basalts, rocks with such high Mg/(Mg+Fe) ratios are not observed in the low-Ti group. For both groups, ilmenite occurs in samples at the Fe-rich end of the trends, while rare ulvospinel occurs at intermediate Mg/(Mg+Fe) ratios.

The two pyroxenes to which an ANT origin was ascribed above fall into the ANT envelope on Figure 2. A random selection of pyroxenes from breccias is plotted using the same coordinates in Figure 3. This figure suggests that the breccias are derived from local rock types. No pyroxenes corresponding to ANT or KREEP rocks were found in the breccias.

CONCLUSIONS. Three grossly distinct magma types are sampled at the Luna 24 site. The volumetrically minor ANT rocks are almost certainly not indigenous to the site, but were probably derived from the highlands a few tens of kilometers away. The two distinct magma suites, corresponding to a VLT basalt group and a low-Ti basalt group, appear to be the major rock types at the site. Our census suggests that VLT basalts predominate close to the surface at this site. Within each basalt group further, less dramatic, subdivisions of magma type may be possible. For example, the VLT trend could be generated by varying degrees of partial melting of a common source region. Alternatively it may have been generated by near-surface fractional crystallization. However, within each magma group we find no basis in our data to support further subdivision into additional distinct magma types. The absence of KREEP-rich rocks is consistent with orbital γ-ray maps. This work was supported by NASA grant NGR 03-002-388.

MAGMA TYPES AT LUNA 24

Nielsen and Drake

REFERENCES:

Lindstrom M.M., Nielsen R.L., and Drake M.J. (1977) Petrology and geochemistry of lithic fragments separated from the Apollo 15 deep-drill-core. Proc. Lunar Sci. Conf. 8th (in press).

Vaniman D.T., and Papike J.J. (1977) Very low Ti (VLT) basalts: a new mare rock type from the Apollo 17 drill core. Proc. Lunar Sci. Conf. 8th (in press).

TABLE 1. Distribution of fragment types in thin sections from Luna 24 (in % unless otherwise noted).

	GLASS	BRECCIAS	AGGLUTI-NATES	IGNEOUS ROCKS	SINGLE CRYSTALS	MELT ROCKS	TOTAL NUMBER OF FRAGMENTS
24077,47	12	16	21	5	37	8	271
24109,42	7	16	18	10	41	8	256
24149,51	5	14	13	6	57	4	157
24174,53	3	3	6	19	60	9	232
24132,49	3	9	6	10	66	6	155
24210,45	6	18	12	13	40	11	159
TOTAL # OF FRAGMENTS	81	155	165	132	599	98	1230

MAGMA TYPES AT LUNA 24

Nielsen and Drake

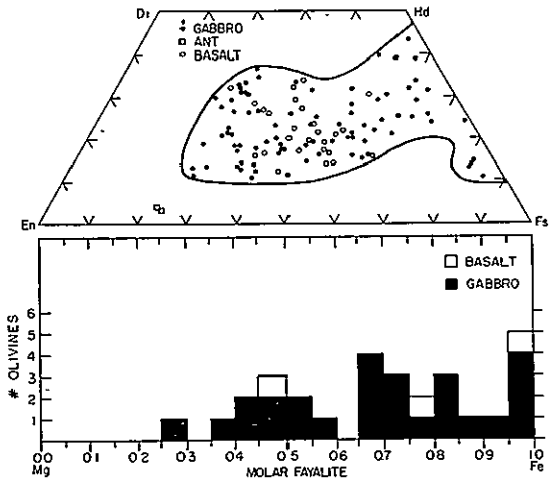

FIGURE 1. Pyroxene and olivine compositions from Luna 24 igneous fragments.

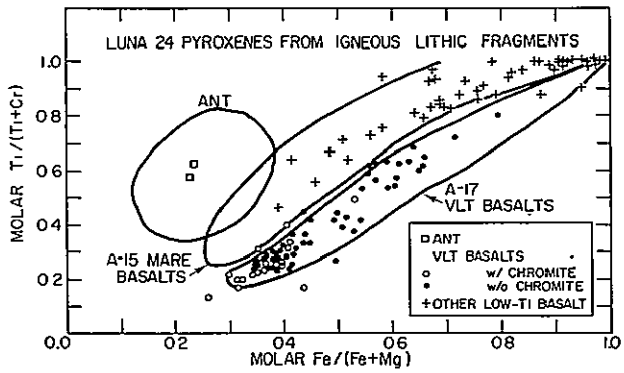

FIGURE 2. Pyroxene compositions from Luna 24 igneous fragments. ANT and Apollo 15 low-Ti basalt envelopes are based on data from Lindstrom et al. (1977) and the literature, Apollo 17 VLT basalt envelope is based on data from Vaniman and Papike (1977).

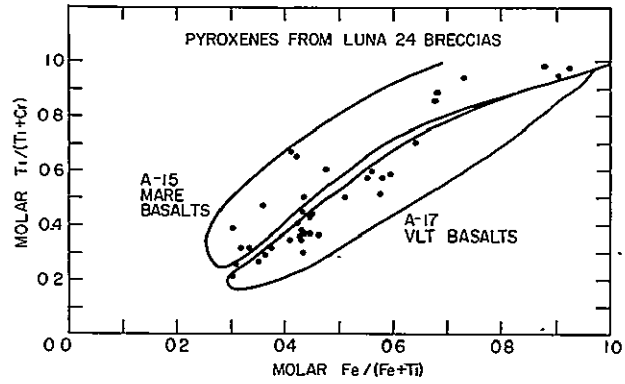

FIGURE 3. Pyroxene compositions from Luna 24 breccias. Envelopes from Figure 2.

GLASS CHEMISTRY AND MAGMA EVOLUTION AT MARE CRISIUM

Marc Norman, R.A. Coish, and Lawrence A. Taylor, Department of Geological Sciences, The University of Tennessee, Knoxville, TN 37916.

The Luna 24 drill core from Mare Crisium contains 4-10 modal % homogeneous glass beads and fragments of various colors. These volcanic glasses are distinct from agglutinitic glasses in that agglutinates are formed by micrometeorite impact on the lunar regolith and tend to reflect the composition of the bulk soil (1). Agglutinitic glass also tends to be inhomogeneous within a single grain. This paper is concerned with the chemical characterization of these homogeneous glasses thought to represent frozen samples of various igneous melts. On the assumption that these glasses represent direct samplings of a lunar magma, it is possible to obtain valuable information on magma evolution at Mare Crisium.

Green, brown, orange, clear, and partially crystallized glasses were recognized, analyzed by EMP, and classified chemically into mare and non-mare components. The mare component, represented by green, brown, and orange glass, accounts for nearly 70% of the fragments studied. The remainder is clear glass reflecting the non-mare, i.e. highlands, component. A very minor component with intermediate chemistry similar to the "Fra Mauro" composition is also present. Partially crystallized (or "devitrified") glasses have chemistries which span the entire range of mare and non-mare compositions.

Within this broad classification, certain preferred compositions were recognized and named accordingly (2). The compositions of these groups are presented in Table 1 and on the CIPW norm plot (3) (Fig. 1). Among the highland glasses, Highland basalt (anorthositic gabbro), gabbroic anorthosite, and plagioclase glass were recognized. Highland basalt is by far the most abundant highland rock type represented by the glasses. A small amount of clear glass too silica deficient to obtain a realistic norm analysis was found. It is similar to the high-alumina, silica-poor (HASP) glass of Naney, et al. (4).

The vast majority of mare glasses are equivalent to a very low Ti, aluminous basalt (5,6,7). Two main groups of mare glasses were recognized corresponding essentially to the brown and green color groups. The brown glass is characterized by its restricted composition, less than 10% normative olivine, and FeO/MgO greater than 2.25. It is chemically identical to the low-Mg sub-ophitic basalts that are the most common rock type in the drill core (5,6). This suggests a genetic relationship between the brown glass and the mare flows that crystallized into sub-ophitic basalts. The green glass is more varied in composition, generally with a

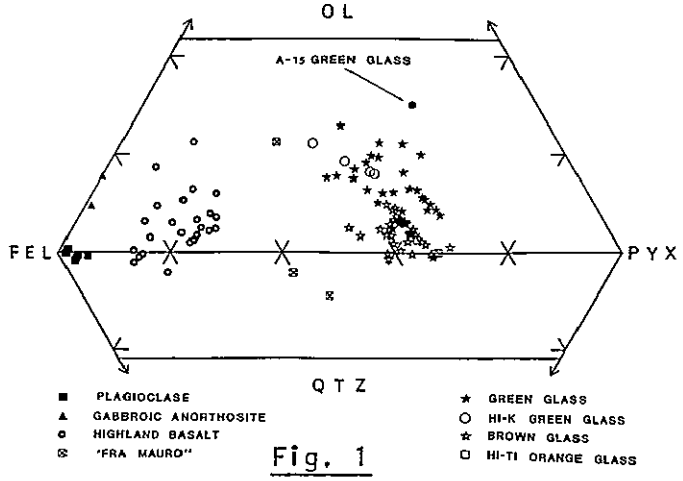

Fig. 1

GLASS CHEMISTRY

Norman, Coish, and Taylor

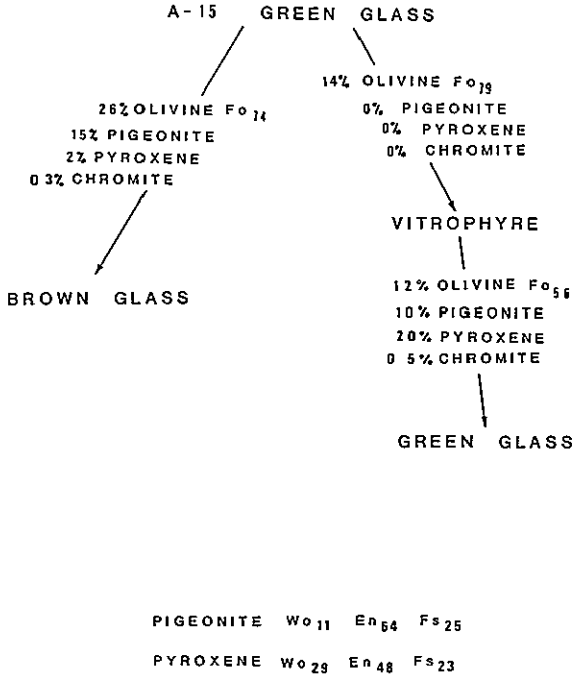

Fig. 2

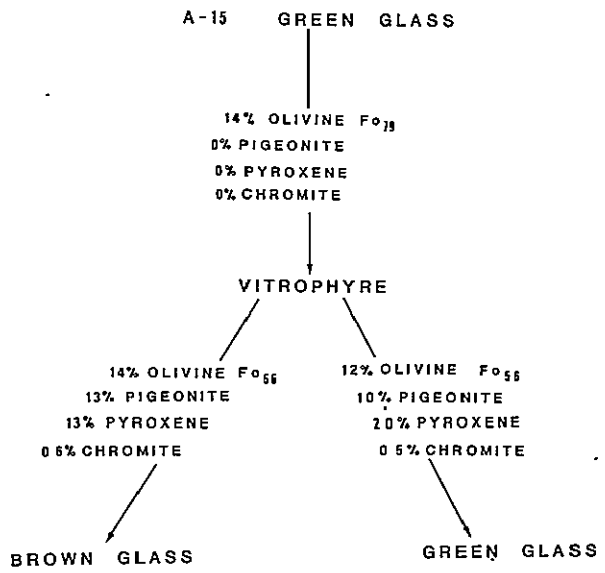

Fig. 3

PIGEONITE Wo_{11} En_{64} Fs_{25}
PYROXENE Wo_{29} En_{48} Fs_{23}

higher normative olivine content (10-27%) and lower FeO/MgO (less than 2.25) than the brown glass.

Other mare glasses representing possible rock types in or near Mare Crisium include a high-K glass that is also somewhat higher in TiO_2 than either the brown or green glass, and fragments containing significantly more TiO_2 than the local material. The high-K glass is green and distinguishable from the other green glasses only by EMP. The high-Ti fragments are easily recognized by their bright orange color.

Given the compositions of these glasses which, for the mare component at least, probably represent frozen magma samples, we are faced with the problem of determining the composition of the parent magma and differentiate products, and of determining whether or not this magma can be related to other glasses of known magmatic origin. Using Wright and Doherty's 1970 mixing program (8), it is possible to quantitatively relate both the Luna 24 green and brown glass, as well as a primitive olivine vitrophyre described in a companion paper (9), to a parent magma having the composition of the Apollo-15 green glass. That the Apollo-15 green glass could be a parent magma is a reasonable assumption in light of the fact that it seems to have a very primitive mafic composition and has been suggested as a possible parent for some other low-Ti mare basalts (7).

As shown in Fig. 2, a model can be constructed such that both the brown glass and the olivine vitrophyre can be related directly to an Apollo-15 type magma. However, this model is weakened somewhat by the fact that no glass having the Apollo-15 composition was found at the Luna 24 site. Therefore, an

GLASS CHEMISTRY

Norman, Coish, and Taylor

TABLE 1. Luna 24 Glass Compositions in the 150 - 250 μm size Fractions.

	Luna 24 Green Glass	Brown Glass	High K Mare Glass	High Ti Mare Gl.	A-15 Green Glass (10)	Highland Basalt Gl.	Gabbroic Anortho.	Plag Glass	Luna 24 "HASP"	"Fra Mauro"
SiO_2	44.96 (0.92)	46.19 (0.61)	44.90 (1.37)	43.13	45.43 (0.63)	45.18 (1.19)	42.07	44.32 (1.25)	38.50 (3.05)	48.00 (2.95)
TiO_2	0.90 (0.20)	0.95 (0.15)	1.42 (0.21)	4.89	0.42 (0.06)	0.34 (0.17)	0.24	0.16 (0.08)	0.31 (0.10)	1.79 (0.28)
Al_2O_3	11.52 (1.66)	12.60 (1.19)	12.24 (1.53)	10.58	7.72 (0.33)	26.68 (2.26)	31.50	33.73 (0.64)	30.43 (2.92)	16.54 (1.64)
Cr_2O_3	0.43 (0.09)	0.25 (0.09)	0.39 (0.08)	0.38	0.43 (0.03)	0.13 (0.06)	0.02	0.01 (0.02)	0.08 (0.03)	0.20 (0.16)
FeO	18.50 (1.23)	19.04 (1.32)	18.61 (1.57)	18.11	19.61 (0.84)	4.98 (1.59)	3.38	0.55 (0.33)	8.81 (6.39)	11.29 (2.17)
MgO	10.52 (1.64)	6.85 (0.67)	8.23 (1.03)	9.55	17.49 (0.54)	6.30 (2.55)	4.45	0.39 (0.41)	6.98 (4.98)	8.10 (2.32)
CaO	10.81 (0.59)	12.32 (0.58)	11.86 (0.43)	10.20	8.34 (0.41)	15.11 (1.05)	17.51	18.37 (0.50)	17.11 (1.82)	11.80 (0.55)
Na_2O	0.27 (0.13)	0.31 (0.09)	0.32 (0.15)	0.13	0.12 (0.05)	0.40 (0.24)	0.05	0.61 (0.35)	0.01 (0.02)	0.57 (0.08)
K_2O	0.02 (0.02)	0.01 (0.01)	0.48 (0.11)	0.04	0.01 (0.01)	0.03 (0.03)	0.00	0.04 (0.04)	0.00 (0.00)	0.35 (0.46)
Total	97.93	98.52	98.45	97.01	99.57	99.15	99.22	98.18	102.23	98.64
FeO/MgO	1.76	2.78	2.26	1.90	1.12	0.79	0.76	1.41	1.26	1.39
CaO/Al_2O_3	0.94	0.98	0.97	0.96	1.08	0.57	0.56	0.55	0.56	0.71
Q	-	-	-	-	-	-	-	0.77		1.65
Or	0.12	0.18	2.88	0.24	0.06	0.18	-	0.24		2.10
Ab	2.33	2.66	2.75	1.13	1.02	3.41	-	5.26		4.89
An	30.73	33.19	31.00	29.02	20.58	71.52	86.44	90.83		42.10
Di	20.01	24.44	24.19	19.21	17.26	3.32	0.69	1.63		14.23
Hy	29.57	33.65	21.96	39.26	30.35	15.34	-	0.94		31.29
Fo	6.29	1.16	5.16	0.46	15.55	3.37	7.68	-		-
Fa	8.50	2.50	8.74	0.53	13.74	2.01	4.42	-		-
Ilm	1.74	1.85	2.74	9.57	0.80	0.65	0.46	0.31		3.45
Chr	0.65	0.38	0.59	0.58	0.64	0.19	0.03	0.02		0.30

alternative model shown in Fig. 3 is preferred. Again using the mixing program, it is possible to derive both the Luna 24 green and brown glass from a magma having the composition of the olivine vitrophyre, which might itself be related to the Apollo-15 composition.

As shown, the olivine vitrophyre can be produced from the Apollo-15 green glass by the simple fractionation of 14% olivine (Fo_{79}). Then, assuming the vitrophyre as a parent magma, the brown glass can be produced by fractionating 14% olivine (Fo_{66}), 13% pigeonite ($Wo_{11}En_{64}Fs_{25}$), 13% pyroxene ($Wo_{29}En_{48}Fs_{23}$), and 0.6% chromite. The Luna 24 green glass can be likewise produced by removing 12% olivine (Fo_{56}), 10% pigeonite, 20% pyroxene, and 0.5% chromite. These mineral compositions are reasonable as they are actual analyses from Luna 24 basalts. In addition, this agrees fairly well with the figures obtained by Coish and Taylor (9) for the fractionation of the sub-ophitic basalts.

From these calculations it can be concluded that although the majority of Luna 24 glasses could be related to a parent magma of the Apollo-15 green glass composition, it is more likely that the primitive olivine vitrophyre actually found at the site represents the primary magma at Mare Crisium.

REFERENCES: (1) Hu and Taylor, 1977, Proc. Lunar Sci. Conf. 8th, in press; (2) Ridley, Reid, Warner, Brown, Gooley, and Donaldson, 1973, Proc. Lunar Sci. 4th; (3) Chao, Best, and Minkin, 1972, Proc. Lunar Sci. Conf. 3rd; (4) Naney, Crowl, and Papike, 1976, Proc. Lunar Sci. Conf. 7th; (5) Ryder, McSween and Marvin, 1977, The Moon, in press; (6) Coish, Hu, and Taylor, 1977, Abstr. A.G.U. Midwest Mtg.; (7) Vaniman and Papike, 1977, Proc. Lunar Sci. Conf. 8th, in press; (8) Wright and Doherty, 1970, Geol. Soc. Am. Bull. 81; (9) Coish and Taylor, 1977, this volume; (10) Reid, Warner, Ridley, and Brown, 1972, Abstr. Meteoritics 7.

CHEMICAL AND SR-ISOTOPIC CHARACTERISTICS OF THE LUNA 24 SAMPLES

L. Nyquist[1], H. Wiesmann[2], B. Bansal[2], J. Wooden[2], G. McKay[3], N. Hubbard[1]. [1]SN/7 NASA Johnson Space Center; [2]Lockheed Electronics Co., Inc.; [3]National Res. Council: Houston, Texas 77058.

Chemical and Sr-isotopic data are reported in Table 1 for five soil samples and one of three lithic fragments allocated for joint study with L. Haskin and D. Blanchard (INAA) and K. Keil (min-pet). From these data and those reported by other authors several important characteristics of the rocks which contribute to the regolith at the Luna 24 site can be inferred.

The major element compositions of our soil samples are rather uniform; in particular, MgO~10% is typical (Fig. 1). Several authors (2,3,4,5) are in agreement that MgO for a major basaltic (gabbroic) component in the Crisium regolith is ~6.5%. The higher MgO content of bulk soils requires the presence of a more magnesian component. Ryder et al. (4) suggest that olivine vitrophyre with MgO~17% is a second basalt composition at the Crisium site. Fig. 1 shows that olivine vitrophyre (OV) lies on a mixing line passing through the lo-Mg basaltic component and the bulk soils (Fragment data in the figure from 2,3,4, and 6 .) This relationship can be seen on other major element plots (not shown) although the presence of ~5% highland basalt (5) is indicated by an Al_2O_3 vs MgO plot.

If the soil composition is dominated by lo-Mg basalt and olivine vitrophyre nearly 1/3 of the bulk soil must be the hi-Mg end member. Alternatively, if the hi-Mg end member has the composition of the hi-Mg VLT glass cluster of Simonds et al. (5) (MgO=10.2%) then this component must totally dominate the soil chemistry.

Ba, REE, and TiO_2 for some Luna 24 soils and pyroxene-rich gabbro fragment 24174,5 (Blanchard et al. (1)) are shown in Fig. 2. Fragment 24174,5 is typical of the lo-Mg basalt (gabbro) (G. Taylor pers. comm.). The REE data require the presence in the soils of at least one additional component with higher REE abundances than the lo-Mg basalts. Recrystallized breccia fragment 24077,17 with REE abundances of ~80x chondritic could represent this component (Blanchard et al. (1)). The FeO content of this fragment is close to that of the LKFM cluster of Simonds et al. (5). REE enrichments accompanied by lower FeO and MgO in bulk soil 24183 (Barsukov et al. (6)), relative to average bulk soil is further evidence of this component.

The amount of LKFM present in the Luna 24 regolith cannot be reliably estimated from available data. The average REE content of the soils (exemplified by 24077 in Fig. 2) can be approximated by a mix of ~5% of 24077,17 and ~95% of 24174,5. This estimate of the LKFM component omits any contributions from other components, especially the hi-Mg component, and seems unreasonably high in view of the low K content of the soil and the relative rarity of LKFM component among the glasses (Simonds et al. (5)) and lithic fragments (Taylor, pers. comm.).

Alternatively one may ignore the contribution of fragments such as 24077,17 and calculate REE for the hi-Mg component of the soil from mass balance. Calculated abundances obtained in this manner assuming a soil composed of 2/3 lo-Mg basalt (24174,5) are shown as the upper pattern in Fig. 2. This calculated pattern is clearly an upper limit for REE in the hi-Mg component. However, it may be significant that this pattern closely resembles that

CHEMICAL AND SR-ISOTOPIC CHARACTERISTICS

Nyquist, L. et al.

of Apollo 15 quartz-normative basalt 15058 and that the TiO_2 content of the olivine vitrophyre (1.4%, Ryder et al. (4)) is close to that of quartz-normative Apollo 15 basalts (~1.8%).

Sr-isotopic data are shown in Fig. 3. "Plagioclase-rich gabbro" fragment 24077,19 was almost pure plagioclase with only two small specks of pyroxene. We believe it to be plagioclase from the lo-Mg gabbro component in the soil. It has an extremely primitive initial $(^{87}Sr/^{86}Sr)_I$ as shown in Fig. 4. If this fragment was produced during the period of mare volcanism from 3.2-3.9 AE ago its $(^{87}Sr/^{86}Sr)_I$ was more primitive than that of any other mare basalt we have studied. This implies a very low Rb/Sr value in the source.

The presence in the soils of a high Rb/Sr component, analogous to the high-REE component, is indicated. We do not as yet have appropriate data to estimate the possible contribution of KREEPy fragments such as 24077,17 to the Rb-Sr inventory of the soils. The Rb-Sr data do not require the presence of a KREEPy component in the soils and are consistent with the alternative hypothesis that a significant fraction of the trace elements in the soils derive from a second mare (hi-Mg) component. As shown in Fig. 3 the bulk soil data are bracketed by values for Apollo 12 and 15 mare basalts. $(^{87}Sr/^{86}Sr)_I$ values for Apollo 12 and 15 basalts bracket calculated values of $(^{87}Sr/^{86}Sr)_I$ for the soils assuming an age of ~3.3 AE (Fig. 4). This would be expected if the Rb-Sr systematics of the soils are dominated by a mare basalt component derived from a source similar to that for other low TiO_2 basalts and extruded approximately contemporaneously with them.

Conclusions: As noted by numerous authors the lo-Mg mare basalt component at the Luna 24 site is quite distinct from mare basalts at other sites. Based on the chemical characteristics of the lo-Mg basalts, and assuming that their source regions formed from the same magma ocean as other mare basalt sources, we infer: (1) The source for lo-Mg basalts was highly fractionated relative to the magma ocean composition. In particular, the Rb/Sr ratio was drastically decreased suggesting also a decrease in the ratio of trivalent REE to Eu. This suggests plagioclase in the source. (2) The low REE abundances and positive Eu anomaly suggest a relatively high percentage of melting of the source such that any plagioclase present was totally exhausted. (3) The positive slope of the heavy REE pattern suggests the presence of opx rather than cpx in the source. (4) The low TiO_2 contents of these basalts are consistent with low REE and a relatively high percentage of melting of the source. The differences between the Luna 24 lo-Mg source and the sources inferred for other mare basalts (e.g. Nyquist et al. (8)) imply heteorgeneities within the lunar mantle. There is evidence that the heterogeneity may be lateral as well as vertical (Hubbard and Vilas (7)). Small scale lateral heterogeneities were suggested by Nyquist et al. (8) for Apollo 12 source regions.

There is strong evidence for the existence of a hi-Mg basaltic component in the Luna 24 regolith. Possible candidates for this component are "olivine vitrophyre" (Ryder et al. (4)), "hi Mg VLT basalt" (Simonds et al. (5)), and "olivine gabbro" (Tarasov et al. (9)). The accurate characterization of the hi-Mg basalt is of particular significance as its inferred REE pattern and Rb-Sr systematics suggests that its source region is similar to that for other low TiO_2 basalts and distinct from that for lo-Mg basalts.

CHEMICAL AND SR-ISOTOPIC CHARACTERISTICS

Nyquist, L. et al.

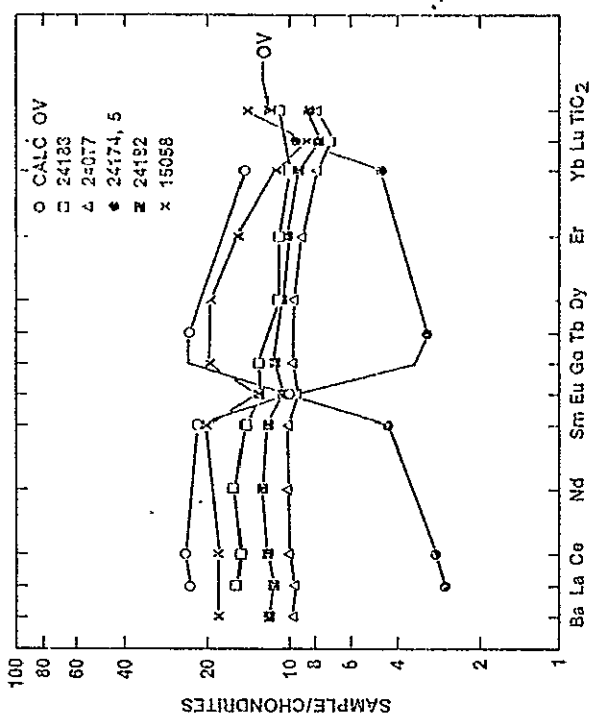

Figure 2

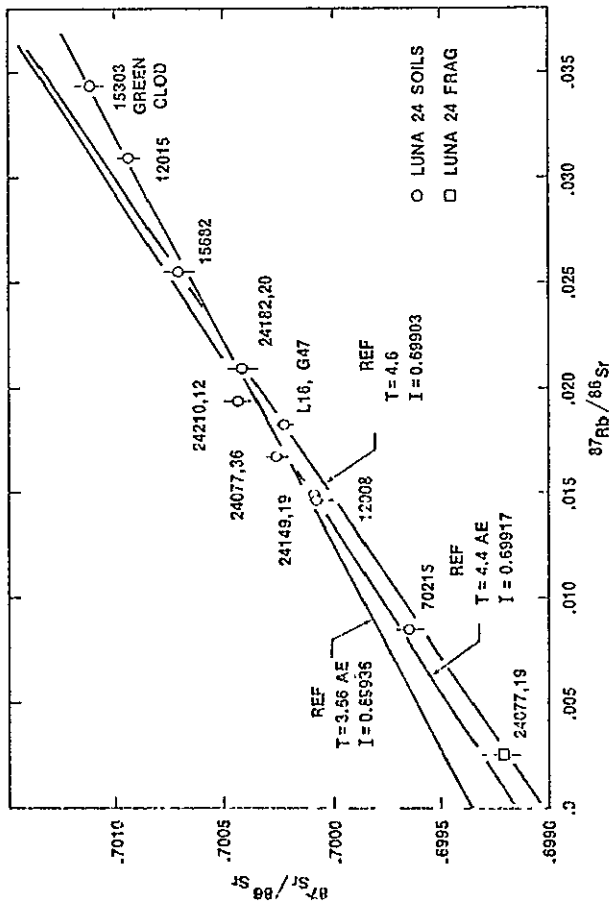

Figure 3

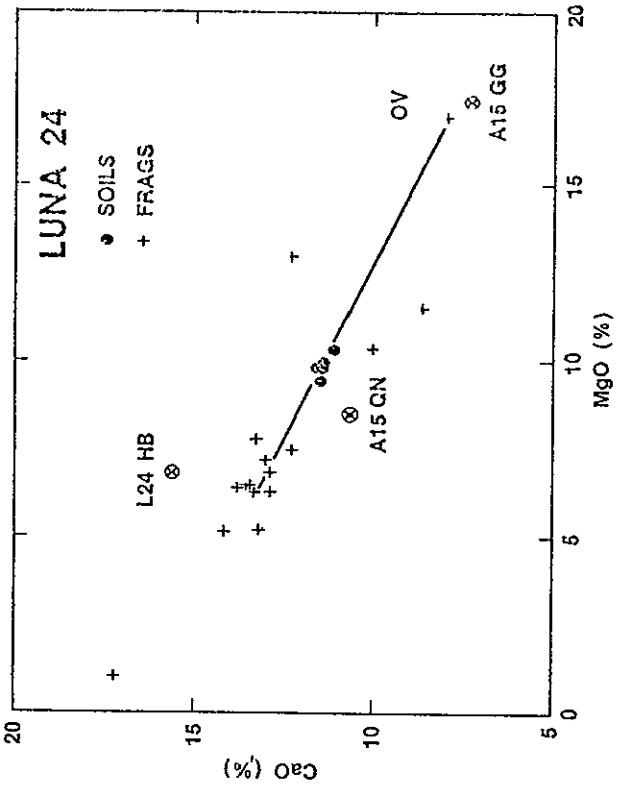

Figure 1

CHEMICAL AND SR-ISOTOPIC CHARACTERISTICS

Nyquist, L. et al.

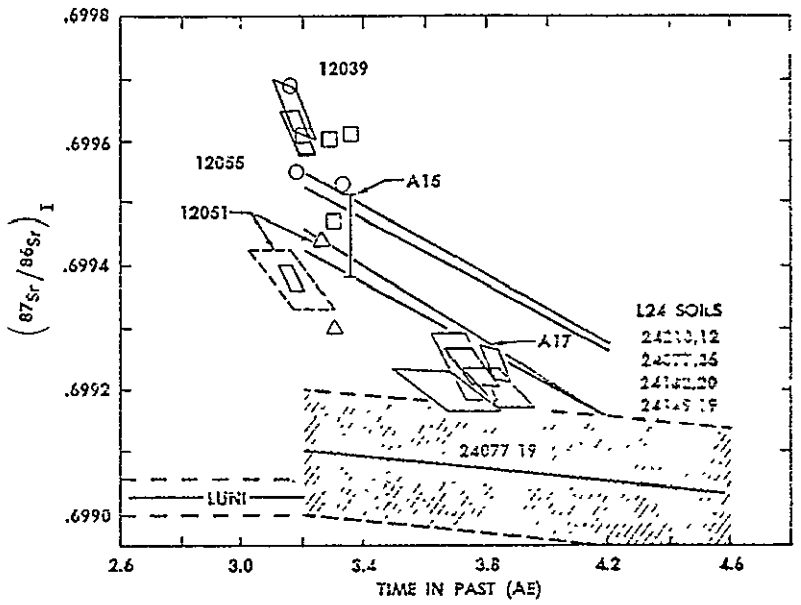

Figure 4

Table 1. Major and Trace Element Analyses of Luna 24 Soils and Fragment 24077,19

Sample #, wt.	24077,36 26mg	24210,12 19mg	24182,20 36mg	24109,17 27mg	24149,9 18mg	24077,19 4mg
Li ppm	5.6	6.0	6.2	5.7	6.0	
K ppm	252	246	294	256	226	
Rb ppm	0.545	0.581	0.699	0.549	0.468	0.145
Sr ppm	94.2	86.9	96.9		90.6	164.4
Ba ppm	37.2	36.3	45.5	37.0		
La ppm	3.09	2.94	3.72	3.11		
Ce ppm	7.99	7.50	9.55	7.64		
Nd ppm	5.74	5.44	7.02			
Sm ppm	1.87	1.78	2.23			
Eu ppm	0.687	0.637	0.738			
Gd ppm	2.47	2.37	2.90			
Dy ppm	2.95	2.88	3.53			
Er ppm	1.85	1.80	2.14			
Yb ppm	1.66	1.65	1.92			
Lu ppm	0.243	0.239	0.273			
U ppm	0.12	0.12				
Zr ppm	44	36	49	38	44	
Mg %	5.67	6.18	5.83	5.83	5.83	
Ca %	8.15	7.83	8.10	8.09	8.17	
Al %	7.20	5.91	6.52	6.36	6.25	
Fe %	14.5	14.9	14.34	14.5	14.8	
Ti %	0.59	0.58	0.65	0.64	0.66	
$Sr^{87/86}$	0.70026±6	0.70043±6	0.70041±7	0.70020±6	0.70009±5	0.69921±10

References

(1) Blanchard D., et al. (1977) This volume.
(2) Taylor G., et al. (1977) Geophys. Res. Lett. 4, 207-210.
(3) Vaniman D. and Papike J. (1977) preprint in press., Geophys. Res. Lett.
(4) Ryder G., et al. (1977) preprint submitted to The Moon.
(5) Simonds C., et al. (1977) This volume.
(6) Barsukov V. L., et al. (1977) in press Proc. 8th Lunar Sci. Conf.
(7) Hubbard N. J. and Vilas F. (1977) This volume.
(8) Nyquist L., et al. (1977) in press Proc. 8th Lunar Sci. Conf.
(9) Tarasov L. S., et al. (1977) in press Proc. 8th Lunar Sci. Conf.
(10) Reference age of 3.66 AE for Luna 24 from G. Allegre et al., 40th Annual Mtg of the Meteoritical Soc., Cambridge, England, 1977.

LUNA 24 90-150 MICRON FRACTION: IMPLICATIONS FOR SAMPLING OF PLANETARY AND ASTEROIDAL REGOLITHS. H. Papp, I. M. Steele and J. V. Smith, Dept. of the Geophysical Sciences, University of Chicago, Chicago, Illinois 60637

One potential method of investigating a planetary or asteroidal regolith is the collection of very small samples from many widespread locations. The 90-150μm fraction of Luna 24 provides us with a test of our ability to recognize key mineralogical features of a sampling site from a minimum of material, mainly using an electron microprobe. The full impact of this study cannot be realized until a later date when all data for Luna 24 have been reported. For the present we report preliminary data and compare these with several other studies obtained in preprint from (1,2,3).

Samples studied are enumerated in Table 1 as well as number and percent of major components. Minor ilmenite, Al-chromite, ulvöspinel, silica, troilite and metal are also present. Most of the ~5,400 grains are monomineralic but occasional plag-pyx-ol fragments show basaltic textures; however, these fragments cannot be considered representative. Compositional data were obtained for most grains using both energy and wavelength dispersive techniques. Emphasis was placed on minor elements (Fe,Mg,K) in plagioclase and major (Fe,Mg,Ca) elements in pyroxene and olivine.

Pyroxene quadrilateral data are shown on Fig. 1 a-l and important features are: 1) all samples have similar compositional ranges regardless of depth in core; 2) the highest mg (=Mg/(Mg+Fe) atomic) value is about 0.72 with only sporadic higher values; 3) low-Ca pyroxenes are absent; 4) the iron enrichment trend is toward hedenbergite; 5) the abundance of intermediate Ca contents indicates a lack of low temperature equilibration. All of these features are characteristic of lunar mare-type basalt; highland rock types usually characterized by more Mg-rich pyroxenes are not present. The Ti/Al atomic ratio correlates with mg as reported in (1) and (3): high mg pyroxenes have Ti/Al < 1/4 and as mg decreases Ti/Al values increase over 1/2 suggesting reduction of Ti^{+4} to Ti^{+3} as crystallization proceeds if the Ti/Al >1/2 is due to the presence of $R^{+2}Ti^{+3}AlSiO_6$ component (4). The maximum mg value (~0.72) of the Luna 24 pyroxenes from our sample is similar to that of mare-type basalts from other missions (5) in contrast to pyroxene distributions reported (1,3) for Luna 24 lithic fragments where the maximum mg is always less than 0.70 and averages ~0.65.

Olivine major element variation is shown in Fig. 1 where mg ranges from a high of 0.78 in all samples to mg near 0.0. The mg range 0.78 to ~0.70 shows a cluster on many of the Fig. 1 plots suggesting early crystallization. This maximum mg value is in marked contrast to high values of 0.64 and 0.58 reported in (1) and (3), respectively, for lithic fragments, and is strong evidence that different material is being sampled in our fine fraction and their lithic clasts. CaO in olivine correlates with mg with values near 0.15 wt.% at mg = 0.75 and increasing to ~0.80 for low mg; these values are consistent with high temperature crystallization (6) as in other mare samples.

Plagioclase major element data (Fig. 2) show a high An content from An_{98} to $\sim An_{80}$ with an average of $\sim An_{93}$ (mol.%). FeO content is high (Fig. 3) and increases with Na; however, the range of FeO values does not agree well with that of other mare samples and tends to lie between the FeO range of Apollo 15 mare and KREEP samples and could indicate complications for a simple classifi-

LUNA 24 90-150 MICRON FRACTION:

Papp, H. et al.

cation based on minor elements (7). Fig. 3 does show, in agreement with the pyroxene data, that plagioclase-rich (ANT) material is not a significant component. Fig. 4 shows MgO vs FeO in plagioclase with a tendency for high-Ca plagioclase (Ab<9 mol %) to have high MgO/FeO relative to low-Ca plagioclase (Ab>16 mol %) indicating a normal trend of increasing Na and decreasing Mg/Fe with crystallization.

Spinels are rare and 7 analyses are shown on Fig. 5a,b. Most are Al-chromites with TiO_2 contents in the range 1.0 to 3.0 wt.% but Cr_2O_3 values are somewhat lower than chromites from Apollo 15 and Luna 20 mare basalts, and most similar to Apollo 12 mare chromites. One ulvöspinel grain is present. Ilmenite is rare and the MgO content (0.2 - 1.0 wt.%) is low suggesting late crystallization (also concluded in (3) based on texture) from a melt with low mg. Similar MgO values were reported (8) for Apollo 15 mare basalt ilmenites. Homogeneous glasses are common with normative plagioclase (anorthite) ranging from ~25 to 75% with some indication of a bimodal distribution (Fig. 6). Troilite is very rare, but one interesting occurrence as elongated, blebby inclusions within Fe-rich olivine (Fa 95.5) was noted; a similar intergrowth was reported in (3).

Using the chemical data and modal abundance for each phase a bulk composition can be derived for the 90-150μm fraction assuming an unfractionated contribution of the parent rock phases. Table 2 presents several estimates of the composition of Luna 24 mare basalt compared with an average Apollo 12 olivine basalt. Our estimate (#4) calculated from the fine fraction is considerably more Mg-rich, as a direct consequence of the more Mg-rich olivines and pyroxenes, than estimates (#2 and #3) derived by modal analysis of basaltic fragments (3). Analysis #1 probably includes a large portion of agglutinates because it represents a bulk fine fraction. Although there is relatively little correspondence among these compositions we emphasize that the most Mg-rich mafic phases are apparently not being sampled in the small basalt clasts and conclusions that the Luna 24 basalt is more Fe-rich than other lunar mare basalts (1) may result from different sample splits. One implication of our data is that Mg-rich olivine fractionated, as previously suggested to relate various low-Ti basalts (3), and is only sampled in the fine fraction. The presence of Mg-rich phases in the surface regolith at the Luna 24 site may indicate that this occurred after extrusion. The lack of Ti-rich phases in the fine fraction supports conclusions that the Luna 24 basalt as sampled has a very low TiO_2 content.

Whether the tiny sample studied better represents the Luna 24 site than does the coarser fraction can only be determined when all Luna 24 data are available and will be discussed at the 9th Lunar Science Conference.

1) Ryder G. et al. (1977) Basalts from Mare Crisium. (Preprint). 2) Barsukov V. L. et al. (1977) The geochemical and petrochemical features of regolith and petrochemical features of regolith and rocks from Mare Crisium (Preprint). 3) Vaniman D. T. and Papike J. J. (1977) Ferrobasalts from Mare Crisium: Luna 24. (Preprint) 4) Bence A. E. and Papike J. J. (1972), PLC 3, 431-469. 5) Papike J. J. et al. (1976), Rev. Geophy. Space Phys., 14, 475-540. 6) Smith, J. V. and Steele I. M. (1976), AM, 61, 1059-1116. 7) Smith, J. V. (1974), AM, 59, 231-243. 8) Nehru C. E., et al. (1975) AM, 59, 1220-1235.

LUNA 24 90-150 MICRON FRACTION:

Papp, H. et al.

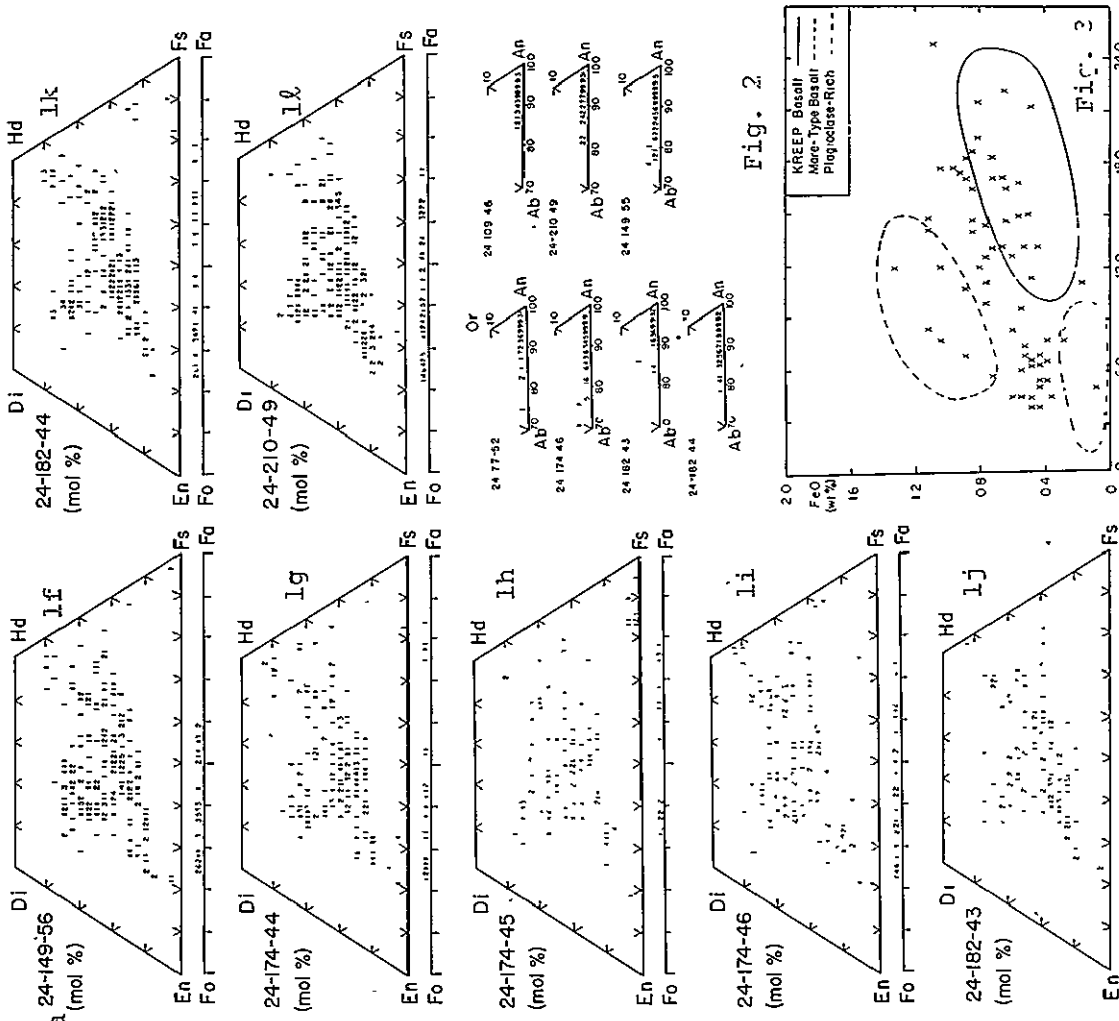

Fig. 1 a-ℓ. Pyroxene and olivine compositions for each 90-150μm sample. Numbers indicate number of analyses at each composition; Fig. 2. Plagioclase compositions for seven 90-150 samples; Fig. 3. FeO in plagioclase vs Ab (mol.%) for several core samples. Outlined areas indicate ranges for different Apollo 15 rock types.

LUNA 24 90-150 MICRON FRACTION:

Papp, H. et al.

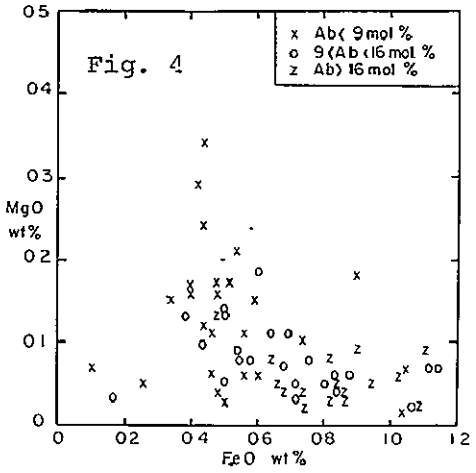

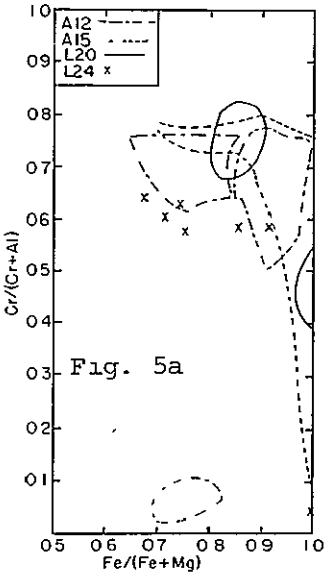

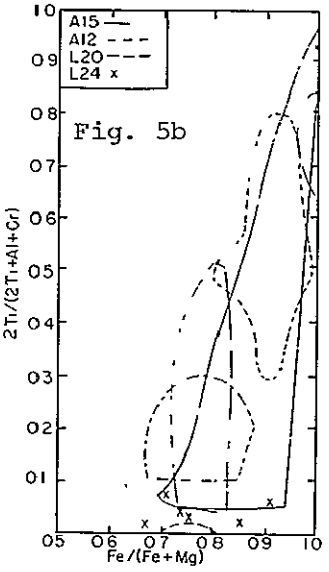

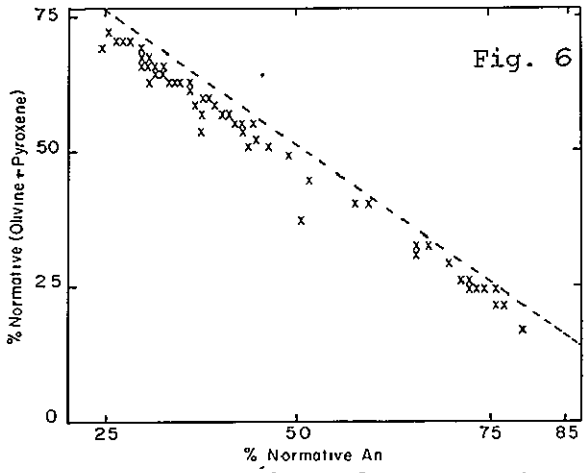

Fig. 4. FeO vs MgO in plagioclase for same samples as Fig. 3. Ab content indicated by different symbols; Fig. 5a-b. Luna 24 spinels compared with ranges for other lunar samples from literature; Fig. 6. Normative An vs olivine + pyroxene in Luna 24 glasses with a tendency for two groups.

Table 1. Samples and % components.

Section	%Pyx	%Plag	%Ol	%Other*
**77-51	41	22	12	25
77-52	36	17	9	38
109-46	38	16	8	38
109-47	35	20	11	34
149-55	42	23	10	25
149-56	49	24	15	12
174-44	38	26	8	28
174-46	41	19	12	28
182-43	50	18	12	20
182-44	56	20	12	12
210-49	38	18	15	29
Mean	43	20	11	26

*Others = ilmenite, spinel, glass, silica, aggultinates.
**First numbers are core depth in cm.

Table 2. Luna 24 Basalt Compositions

	(1)	(2)	(3)	(4)	(5)	(6)
SiO_2	43.5	45.7	45.0	46.8	48.0	44.3
Al_2O_3	15.7	13.8	6.2	9.5	12.9	8.0
CaO	13.2	13.0	7.9	13.2	11.7	8.6
FeO	16.2	19.0	19.0	15.6	16.2	21.1
MgO	8.8	7.1	16.9	14.0	9.6	14.1
MnO	0.2	0.3	0.3	0.2	0.2	0.3
Na_2O	0.4	0.2	0.02	0.1	nd	0.2
Σ	98.0	99.1	95.3	99.4	98.6	96.6
mg	0.56	0.46	0.67	0.67	0.58	0.61

(1) average of 4 <0.074mm bulk samples (2); (2) average of two preferred VLT basalts given in (3); (3) olivine vitrophyre from (7); (4) calculated from mineral data reported here; (5) average glass in this study; (6) average of Apollo 12 olivine basalt (5).

MARE CRISIUM: A SECOND LOOK AT REGIONAL SPECTRAL PROPERTIES.

C. Pieters, NASA Johnson Space Center, Houston, TX 77058 and T. B. McCord, Institute for Astronomy, Univ. of Hawaii, Honolulu, HI 96822

In a previous publication (Pieters, McCord and Adams, GRL, 1976) we discussed the nature of surface units in Mare Crisium that could be inferred from available spectral reflectance data. Some of the main conclusions were: (1) The Luna 24 landing area is a general low-Ti unit. (2) The landing site itself is in a heterogeneous area. (3) The basin contains a different unit (possibly high-Ti) as a much deeper layer. (4) An extensive third unit, low-Ti (<1.5% TiO_2), exists to the north of the landing site.

As further study of Mare Crisium and the Luna 24 samples progressed a number of questions concerning our original conclusions arose: (1) Which of the spectrally identified units (if any) was actually sampled by the Luna 24 core? (2) For low-Ti soils, how accurate is the TiO_2 estimation from spectral measurements of continuum slope? (3) How do the mare units of Mare Crisium compare with other maria?

In order to find answers to these questions telescopic spectral observations were made for small areas in Mare Crisium to be used in conjunction with laboratory measurements of Luna 24 soils (see Adams and Ralph, this volume). A few additional telescopic spectra were obtained in the spectral range .34 to 1.1 μm for comparisons with a previous survey of mare basalts, and new spectra were obtained from .65 to 2.2 μm to examine the nature of the 1 μm (Fe^{+2}) band in lunar soils. Preliminary results confirm the general conclusions above (although we suspect the returned samples may not be representative of the particular surface unit in the Luna 24 area that was studied telescopically -- see Adams and Ralph, this volume). Characterization of the various Mare Crisium units is continuing; these data will be incorporated into a regional study of Mare Crisium (by the FORSE, Head et al., in preparation).

IMPACT FEATURES IN LUNA 16, 20 AND 24 SOILS AND THE MATURATION OF THE LUNAR REGOLITH : G. Poupeau*, J.C. Mandeville°, and M.Christophe Michel-Lévy +

*Centre des Faibles Radioactivités, 91190 Gif/Yvette; °ONERA CERT/DERTS Toulouse, France ; + Laboratoire de Minéralogie-Cristallographie, Université Paris VI.

Impact feature studies were conducted on one level of Luna 16 and 20 cores and 9 levels of the recently come to earth Luna 24 deep core. Shock effect measurements on single crystals (distribution and abundance of impact microcraters and glassy deposits) continue the search program for variations with time of the solar activity and micrometeorite flux and size distribution (1.2). The abundance of glassy agglutinates has been determined in the bulk samples in order to qualify the degree of maturity for the levels studied here. Cosmic ray track results will be presented elsewhere.

GLASSY AGGLUTINATES. The abundance of glassy agglutinates has been determined for Luna 16 and 20 on polished sections; for Luna 24, on the >40 μm grain size powder, using a binocular stereomicroscope. Nine levels from the Luna 24 core, between 82 and 184 cm depth, were studied. Generally, the abundances of glassy agglutinates in these samples do not show large variations in different grain size fraction from 40 to 250 μm. Their abundance were found to vary, between various samples, from ∿ 15 % to 40 %. This stratigraphic column of 1 m therefore is constituted of soil layers presenting apparently various degrees of maturity. The level at 96cm depth (table 9) appears from this point of view intermediate between the mature soil Luna 16 and rather immature soil Luna 20.

IMPACT FEATURES ON SINGLE CRYSTALS. Results are reported in Table 1 for Luna 16, 20 and one level of Luna 24, where they are compared to similar published (2) and unpublished (3) studies on Apollo soils. Search for microcraters and glassy deposits on feldspar crystals (100 μm dia.) follows basically the same procedure as in (1), with only minor modifications (3) in order to improve our detections efficiency.

Luna 16 and 24 present the basic characteristics of mature soils (last line in table 1), with glassy discs (< 2 μm dia.) present on ∿ 90 % of crystals, microcraters present on more than 30 % of crystals, and at least ∿ 10 % of grains with large (> 10^6 cm^{-2}) densities of microcraters (> 0.1 μm dia.). The relatively low percentage of microcratered feldspars in Luna 16 support the hypothesis of the presence of a rather young soil component as previously suggested on the basis of track results (4,5).

In agreement to its much lower glassy agglutinate abundance, Luna 20 has a notably lower abundance of crystals with microcraters. No crystal with large density of microcraters were found. Also, the fractions of crystals with glassy discs (not reported in table 1) in this sample was smaller than in Luna 16 and 24. Track densities at the center of these crystals were reportedly small, of the order of 10^8 cm^{-2}. This soil therefore appears as relatively immature.

IMPACT FEATURES IN LUNA 16

POUPEAU G.

As in Apollo soils, the maximum microcrater density (> 0.1 µm dia.) is of the order of 10^7 cm^{-2} and the cumulative frequency of crater diameter versus crater diameter presents a -2 slope in a Log.Log-diagram, i.e. no change in the micrometeorite mass spectrum was observed.

IMPACT FEATURES AND SOIL MATURATION . The maturity degree of a lunar soil as defined by its bulk properties such as grain size distribution parameters and agglutinates content, solar wind species content, etc., is a function of the residence times of its components within the top few millimeters of the regolith surface. It was therefore expected that the abundance of micro craters on single feldspar crystals in a given soil would be correlated to the degree of maturity of this soil.

It was indeed found that the 3 most immature soils of Table 1 , soils Luna 20, 12033 and 14141, have by far the lowest abundance of micro cratered grains. In soil 12033, not one crystal in 14 studied was found to have microcraters, suggesting that none or very few grains in this soil were ever in the first millimeter of the regolith. This is confirmed by the abnormally low abundance of track-rich grains in this soil, as well as its very low bulk ^{36}Ar content . On the other hand, among the so called "mature" soils, the abundance of microcratered feldspars vary by a factor of about 2, from 30 % to 60 %. Although this large variation could possibly be due to the operational definition of mature soil used here (3), based on McKay et al. (6) soil classification, as well as by our limited statistics, it may also partly result from the fact that at least some of these soils are made of several components with various degrees of maturity. This seems particularly true of our Luna 16 sample (see above).

In a previous paper (1), we considered glassy discs as indicators of very near surface exposure. The fact that there is a tendency for the abundance of feldspars containing glassy discs to increase with increasing maturity of lunar soils confirms a relation between discs and surface micro-impact processes. However, glassy discs are found even in soils (12033) whose crystals are characterized by low track densities indicating that they have never been exposed in the upper millimeter of the lunar regolith. Although a "near surface" process, glassy disc production can apparently occur as the result of impacts penetrating and reorganising the lunar regolith over a depth of a few millimeters.

Adhering micron-size particles and large glassy splashes, whose abundances are not correlated with the degree of maturity of a soil are obviously produced by other processes. For example, the very abundant and atypical glassy deposits on feldspars from soil 12033 seem to correspond to those described by McKay et al.(7)on ropy KREEP glass particles. The origin of this glass might be attributed to some base surge process, as suggested by these authors.

Probably the most significant observation is the fact that soils 67481 and 67601 have the same microcratering characteristics as older, more mature, soils. Both of these soils were collected on the rim of North Ray Crater and were thus emplaced only some 50 m.y. ago. Extensive contamination by

IMPACT FEATURES IN LUNA 16

G. POUPEAU

older regolithic material is excluded by the fact that the rare gas exposure ages for these soils are also 50 m.y . This time therefore represents an upper limit to the time necessary to build up an equilibrium microcrater record in soil grains. From microcrater data, we estimated the maximum exposure time of crystal surfaces to free space to be of the order of 10^4 yrs (1). This order of magnitude estimate, recently confirmed by rare gas analysis on mineral separates (8) is shorter than the estimated surface residence time calculated from the solar flare track density systematics by the SOLMIX code (9). Explanation for the discrepancy is attributed to shielding and/or crystal surface erosion. Evidences for this last phenomena are suggested from optical as well as scanning electron microscopy observations. In this case, an average erosion rate of $\sim 1\mu$ /10^3 yr. is needed to resolve the difference between crystal surface and track exposure ages.

(1) POUPEAU G., WALKER R.M., ZINNER E. and MORRISON D.A., 1975, Proc. 6th Lunar Sci. Conf. 3433-3448.

(2) POUPEAU G. and JOHNSON J., 1976, Lunar Science VII, 709-711.

(3) POUPEAU G. and JOHNSON J., 1976, impub. results.

(4) POUPEAU G., CHETRIT G.C., BERDOT J.L. and PELLAS P., 1973, Geochim. Cosmochim. Acta, 2005-2016.

(5) DRAN J.C., DURAUD J.P., MAURETTE M., DURRIEU L., JOURET C. and LEGRESSUS C., Proc. 3rd Lunar Sci. Conf. 2883-2903.

(6) McKAY D.S., FRULAND R.M. and HEIKEN G., 1974, Proc. 5th Lunar Sci. Conf. , 887-906.

(7) McKAY D.S., MORRISON D.A., CLANTON U.S., LADLE G.H. and LINDSAY J,Fl, 1971, Proc. 2nd Lunar Sci. Conf. , 755-773.

(8) HORN P., BAUR H., DERKSEN U., ETIQUE Ph., FUNK H., SIGNER P. and WIELER R., Vth ECOG, Pise, 5-10 Sept. 1977.

(9) BIBRING J.P., BORG J., BURLINGAME A.L., LANGEVIN Y., MAURETTE M. and VASSENT B., 1975, Proc. 6th Lunar Sci. Conf., 3471-3493.

SOIL SAMPLE	% OF GLASSY AGGLUTINATES		FRACTION (%) of CRYSTALS WITH			NUMBER OF CRYSTALS STUDIED
	50-100µm	100-150	glassy discs < 2 µm	microcraters > 0.2 µm dia.	microcrater* density $> 10^6/cm^2$	
Luna+ 16	41		94	31	9	31
Luna 20	20		-	10	0	20
Luna+ 24	35	35	85	50	17	17
12033			7	0	0	14
14141		5.2	74	14	5	19
67481		23	95	58	12	41
67601		-				
mature soils		40-60	90-100	30-67	11-25	~ 200

+ Depth of samples in cores : Luna 16, 20-22 cm ; Luna 24, 96 cm.

* Larger than 0.1 µm in diameter.

PETROLOGY OF MELT INCLUSIONS IN LUNA 24 SAMPLES. Edwin Roedder, 959 U.S. Geol. Survey, Reston, VA 22092, and Paul W. Weiblen, Dept. Geol. and Geophy., Univ. Minn., Minneapolis, MN 55455.

We have studied the inclusions in nine polished grain mounts (24077,41; 24109,50; 24109,54; 24109,57; 24149,50; 24170,4; 24174,50; 24174,56; 24182,20) by optical petrography, scanning electron microscopy (SEM) with energy-dispersive X-ray analysis, and electron microprobe analysis. All quantitative data reported here are by the last, and were reduced using the methods previously described (1). The specific grains studied are identified by a FOCUS consortium-assigned grain number.

Inclusions in olivine. Most melt inclusions in olivine in these samples have in large part crystallized, including both those from ferrobasalt (2) and the ferrogabbro (3). Analyses of crystallized inclusions are similar to the ferrobasalt (2) but depleted in Mg and Fe, suggesting crystallization of olivine onto the walls after trapping.

Two optically clear, unzoned single crystal olivine grains (24109,50-2 and 24174,50-93) contained a total of five melt inclusions (two at the surface) consisting of ∿1% immiscible sulfide globule, and a colorless homogeneous glass. The bubble/glass and glass/olivine interfaces are featureless under the optical microscope and SEM. The glass in the two exposed inclusions has a very high silica content (87 and 94%) yet the host olivines are intermediate (Fo_{73} and Fo_{51}, Table 1).

The origin of these high-silica melts, how they became trapped in olivine, and the lack of reaction at the interface (Figs. 2-4, 17) are perplexing and unanswered questions; the fact that these melts are so far unique does not minimize these difficulties in any way. The distribution coefficients K'_D for Fe and Mg between melt and crystal for these two melts are high, 0.49 and 1.17, suggesting disequilibrium (4). Four possible mechanisms for the formation of these melts have been considered, none of which seem feasible (4). First, the metastable crystallization of "excess" olivine, either in the magma before trapping or within the inclusion after trapping, could yield the extreme silica enrichment, but petrographic evidence and the lack of compositional zoning in the olivine inclusions walls (Fig. 17) preclude it. Furthermore, this enrichment would require an extreme degree of subliquidus metastable crystallization, to nearly 650°C below the stable liquidus (5). Second, extensive crystallization of Si-free daughter minerals after trapping could yield a similar enrichment, but none are present. Third, as the olivine-inclusion pair falls in the system MgO-FeO-SiO_2 (< 1.7% extraneous material, anal. 3), the inclusions might correspond to the high-Si immiscible melts known in that system (5), but these exist stably only at ∿1700°C, at which the olivine host would be liquid. Fourth, the inclusion might be a variety of the late-stage, immiscible high-silica melts that are common in the mare lavas (6). Inclusions in pyroxene, ilmenite, and plagioclase of the Luna-24 samples, summarized briefly below, do not lend support to this idea.

Inclusions in pyroxene. Many of the Fe-rich intermediate pyroxene grains have two sharp zones, an early clear and almost colorless zone, and a later pinkish and more Fe-rich zone containing many inclusions (Figs. 5 and 6). Most melt inclusions have crystallized at least in part (Figs. 6-7), but the remaining glass is much higher in K and Al than in the inclusions in olivine.

MELT INCLUSIONS

Roedder and Weiblen

We believe this change in the pyroxene marks the onset of silicate immiscibility, as in the Apollo samples (6), and that the inclusions represent in part trapped immiscible blebs of high-K, high-Si liquid.

Inclusions in plagioclase. There are three distinct types. The first presumably represents trapping of a homogeneous melt during rapid skeletal growth of the host (e.g., in 24109,50,19; Fig. 9). Inclusions of this type now consist of a fine-grained crystalline mixture (Figs. 10 and 11); one is now heterogeneous on a larger scale as well (Fig. 10). From their low-K and moderate-Si, they might be considered to be a basaltic melt from which the plagioclase grew, but they are very low in Al_2O_3 (~4%), lower even than one inclusion in olivine. The wedge-shaped feature (Fig. 10) is higher in Si and Ca and lower in Fe than is the other part; these two differ from each very little, but the interface is sharp, possibly suggesting immiscibility. They differ greatly, however, from the "normal" late-stage immiscibility and from the inclusions in olivine.

The second type represents the trapping of late-stage fluids (Fig. 13). It consists of two components in various ratios, a high-Si, high-K glass, and a high-Fe, low-Si fine grained mixture (Fig. 14). These two components represent late-stage immiscible melts, as were found in Apollo mare basalts (6). Few were large enough for analysis (Table 1, nos. 5 and 6). As might be expected, both melts are much richer in iron than those from the Apollo samples, but neither resembles the high-Si inclusions in olivine.

The plagioclase of the gabbro (24170,4) also contains similar inclusions that have crystallized completely. Fe rich pyroxene and silica are major phases in some of these inclusions (Fig. 12); SEM studies on others show, in addition, FeS and phosphates, suggestive of late stage fluids.

The third type of inclusion is best shown in grain 24182,50-19, which consists of a single crystal of plagioclase enclosing a single crystal of high-Fe pyroxene and many minute inclusions (Fig. 15). It is peculiar in that it in turn is cut by a 6-μm-thick diagonal plate of SiO_2 (Fig. 15), and both silica and pyroxene contain opaque blebs and other blebs rich in Ca, Al, and Si, possibly plagioclase (SEM).

The minute inclusions are randomly distributed in two zones in the host plagiclase (Fig. 15). Most are oval, 2-3 μm long, and appear to consist of two phases, a vapor bubble and a material with an index of refraction higher than plagioclase (pyroxene?; Fig. 16). Until compositional (SEM) data are obtained on these inclusions, we can only presume that they are the result of crystallization of melt inclusions, although other origins, such as exsolution from the plagioclase structure, are not excluded, as the total volume percent of such material is small.

Conclusions. Most inclusions in the Luna-24 samples are similar to those from the Apollo samples, but several glass inclusions in olivine were found to have unique compositions, extremely high in silica and low in alumina, and are at present inexplicable in several respects. The compositions differ markedly from all other inclusion types found in these (and the Apollo) samples, including those formed by the process of silicate liquid immiscibility, and there is no evidence of reaction of the siliceous melt with the host olivine. Additional inclusions of this type should be searched for, in order to help resolve some of the problems these two have raised.

MELT INCLUSIONS

Roedder and Weiblen

Figures - (Scale bar dimensions given in μm. Illumination: trans. - transmitted plain light; refl. - reflected plain light; SEM - scanning electron microscope secondary electron image.)
Fig. 1. Olivine single-crystal grain 24109,50-2 (trans.), showing three glass inclusions (see Figs. 2-4). Only "A" is at surface.
Figs. 2-4. Inclusions A-C in Fig. 1 (trans.). The circular zones in the glass are optical artifacts.
Fig. 5. Pyroxene single-crystal grain 24170,4-12 (trans.). Note inclusions in left and right (30 μm SiO_2 at arrow) and inclusion-free center.
Fig. 6. Pyroxene single crystal 24182,50-15 (trans.), showing numerous inclusions. Arrow points to silica (tridymite?) plate.
Fig. 7. Silica crystal (tridymite?) in pyroxene of gabbro in 24170,4-1 (SEM).
Fig. 8. Late-stage melt inclusion in ilmenite of gabbro 24170,4-6 (refl.).
Fig. 9. Melt inclusions in plagioclase of agglutinate grain 24109,50-19 (trans.). Inclusions A and B are at surface (se Figs. 10 and 11).
Fig. 10. Inclusion A from Fig. 9 (SEM), showing finely crystalline texture and two compositions. The bright spot and line at top are artifacts.
Fig. 11. Inclusion B from Fig. 9 (trans.). Note irregular meniscus of bubble from crystallization of melt.
Fig. 12. Interstitial inclusion in plagioclase of gabbro grain 24170,4-6 (SEM), showing major pyroxene (P; MgO 1.95%), silica (S), and other phases.
Fig. 13. Basalt fragment 24077,41-10 (trans.). See arrow for area of Fig. 14.
Fig. 14. Composite inclusion of high-silica melt (S; outlined) and high-iron melt (F), in plagioclase, from center of Fig. 13 (refl.). Bright spot in high-silica melt is an artifact (carbon coating). See Table 1, nos. 5-6.
Fig. 15. Pyroxene crystal (P), containing diagonal lath of silica (S), and embedded in plagioclase single crystal (Pl) containing many minute inclusions (arrows; enlarged in Fig. 16) (trans.).
Fig. 16. Four individual inclusions from plagioclase of Fig. 15 (trans.). Each appears to consist of a pyroxene(?) crystal and a small vapor bubble.
Fig. 17. Electron microprobe traverse across 13-μm high-Si glass inclusion in olivine grain 24174,50-93. Simultaneous 20-sec. counts.

References. (1) Roedder, E., and Weiblen, P.W. (1973) Geoch. Cosmo, Acta, 37, 1031-1052; (2) Vaniman, D.T., and Papike, J.J. (1977) Geop. Res. Lett., (in press); (3) Bence, A.E., Grove, T.L., and Scambos, T. (1977) Geop. Res.

Table 1. Electron microprobe analyses of Luna 24 samples (P.W. Weiblen, analyst).

Anal. no.	1	2	3	4	5	6
Grain no.	24109,50-2		24174,50-93		24077,41-10	
Material	Inc. glass	Host oliv.	Inc. glass	Host oliv.	Hi-Si inc.	Hi-Fe inc.
SiO_2	87.2	36.3	93.8	35.1	71.9	38.2
Al_2O_3	6.84	<0.05	1.51	--	11.2	2.33
FeO	1.27	25.3	2.32	40.2	8.14	46.5
MgO	0.95	38.6	1.61	23.9	<0.5	0.73
CaO	1.76	0.23	0.06	0.23	5.47	6.36
Na_2O	0.9	--	<0.05	--	<0.5	<0.5
K_2O	0.02	--	0.11	--	3.81	0.27
TiO_2	0.36	--	--	--	1.05	6.06
MnO	0.15	--	--	0.25	0.05	--
Cr_2O_3	0.01	--	--	0.04	--	<0.05
Total	99.46	100.43	99.41	99.72	101.62	100.45

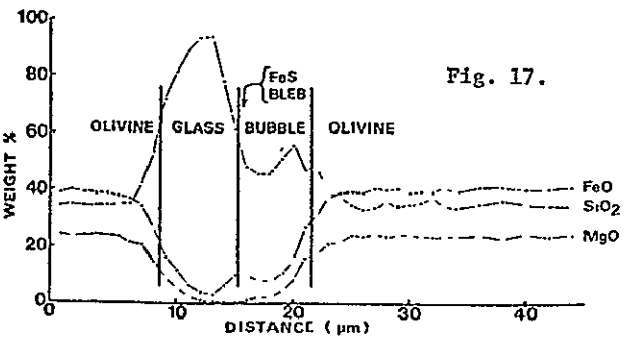

Fig. 17.

Lett., (in press); (4) Roedder, E., and Weiblen, P.W. (1977) Geop. Res. Lett., (in press); (5) Bowen, N.L., and Schairer, J.F. (1935) Am. J. Sci., 29, 151-217; (6) Roedder, E., and Weiblen, P.W. (1970) Proc. Apollo 11 Conf., 801-837.

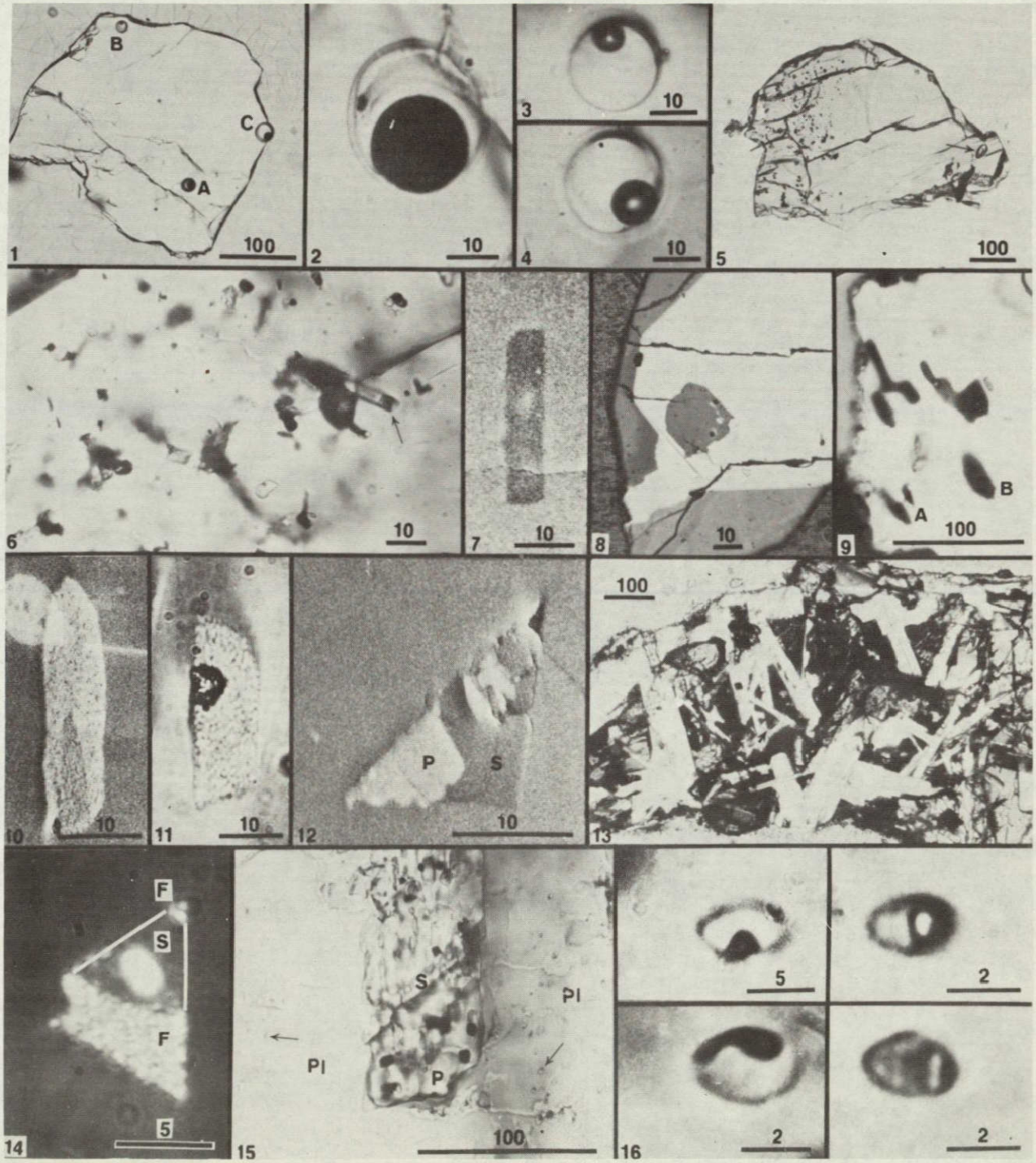

OPTICAL ABSORPTION SPECTRA OF MAJOR MINERALS IN LUNA 24 SAMPLE 24170.
George R. Rossman, Div. of Geol. and Plan. Sci., Calif. Inst. of Tech., Pasadena, Calif. 91125.

Optical absorption spectra of grains of an olivine, a color-zoned pyroxene and a plagioclase were obtained from thin-section grain mounts provided by A. L. Albee (Albee et al., 1977). They were examined as received with a Cary 17I spectrophotometer at 24°C.

The orientation of a yellow olivine crystal (FQM-647) provided both α and γ spectra. The absorption spectrum (Figure 1) is dominated by an absorption band at 1069 nm in γ with shoulder at $\sim$ 1335 nm which arise from Fe^{2+} in the M2 site. Overlapping absorption bands occur in α at $\sim$ 884, 1097 and 1330 nm which arise from Fe^{2+} in both the M1 and M2 sites. The weak absorption bands at visible wavelengths, the most prominent of which are at 624, 497 and $\sim$ 450 nm, arise from spin-forbidden electronic transitions of Fe^{2+}. The spectrum is very similar to that of terrestrial fayalites.

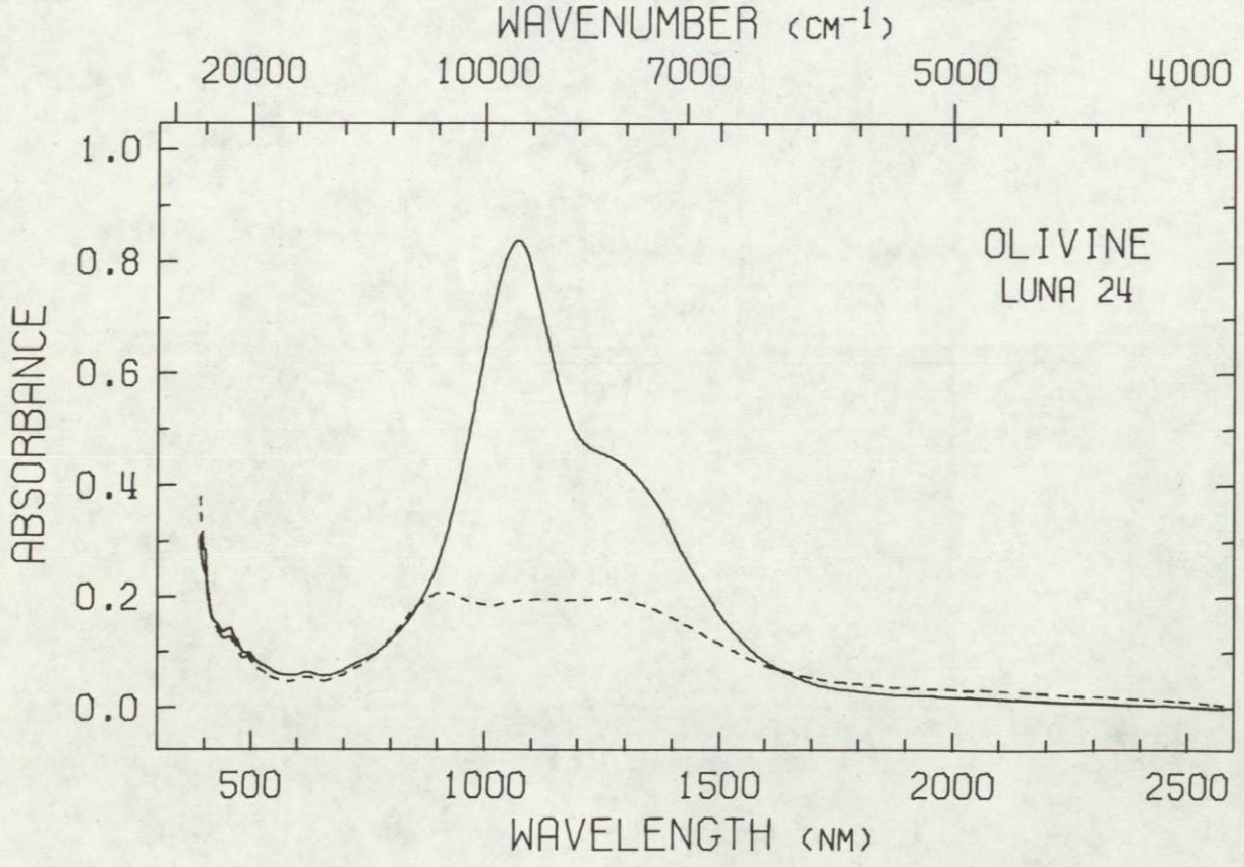

Figure 1. Optical absorption spectrum of the Luna 24 olivine, Fa 76 (γ = solid; α = short dash).

OPTICAL SPECTRA

George R. Rossman

The orientation of the color zoned pyroxene (FQM-649) provided an excellent β spectrum in one direction and a mixture of primarily α with some γ in the other direction. The dominant features (Figure 2) are absorption bands in β at 963 nm and in α at ∿ 2100 nm which originate from Fe^{2+} in the M2 site. Absorption from Fe^{2+} in the M1 site is observed as a shoulder in α at ∿ 1190 nm. A weak, broad Cr^{3+} feature occurs around 640 nm and a sharp, weak Fe^{2+} feature is at 507 nm.

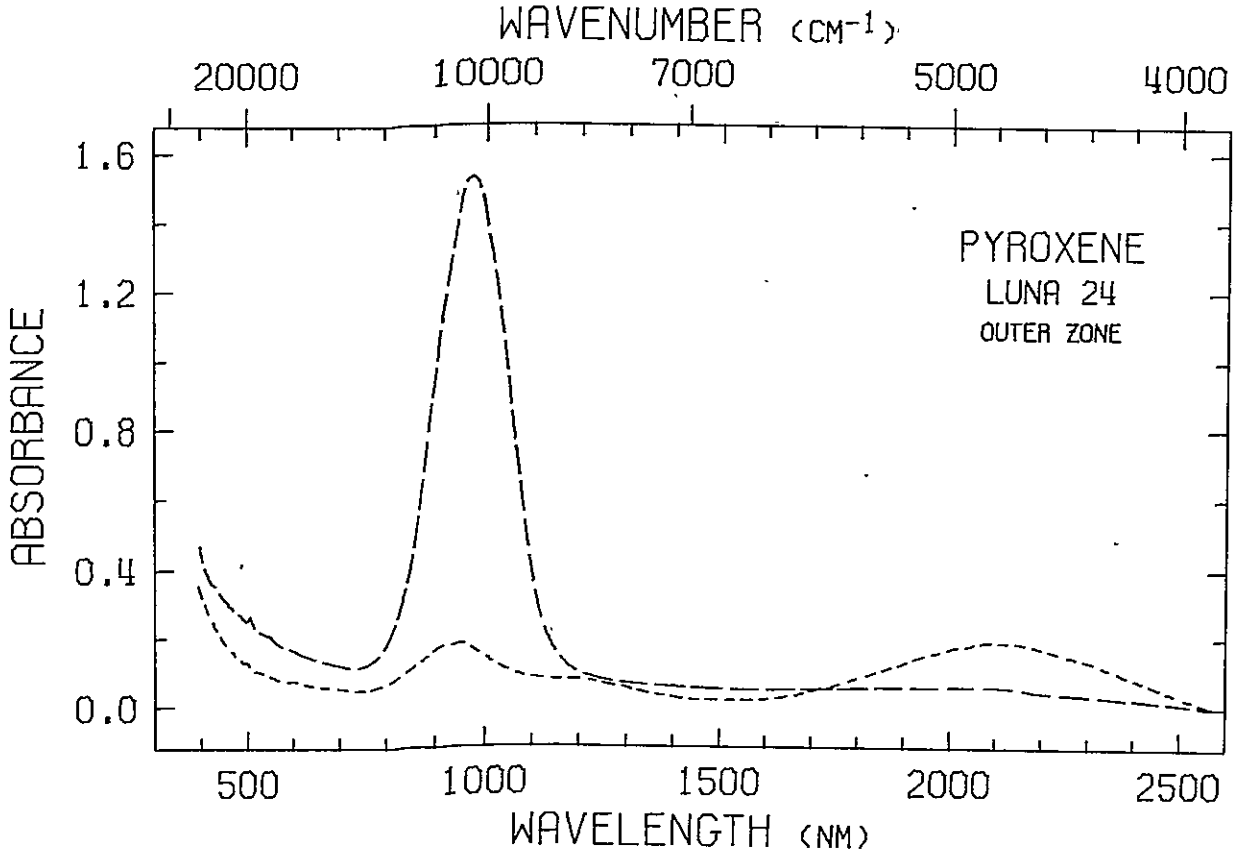

Figure 2. Optical absorption spectrum of the outer zone of Luna 24 pyroxene. The prominent absorption band at 963 nm in β (dashed line) and the broad band near 2100 nm in α (short dash line) are due to Fe^{2+} in the M2 site.

A comparison of the β spectra taken in the central colorless zone and the outer violet-brown zone is shown in Figure 3. The outer zone contains 1.7 times as much Fe^{2+} in the M2 site. Estimates of the average concentrations of Fe^{2+} in the M1 and M2 sites in the two zones can be made from the following assumption: sample thickness 40 μm, ε(M2) = 40 (intensity of M2 band in orthopyroxenes), ε(M1) = 3.5 (typical value for small six-coordinate sites). The results of the calculation are: central zone M1 site 4.3% FeO, M2 site 11.3% FeO; outer zone M1 site 8.8% FeO, M2 site 18.9% FeO. The calculated total FeO, 15.6% central zone, and 27.7% outer zone compare favorably with the electron

microprobe analysis (Table 1). The Cr^{3+} absorption band is more intense in the central zone. The absorption in the 400-600 nm region which rises toward shorter wavelengths is responsible for the color of the outer zone. Similar absorption has been observed in other lunar pyroxenes (Burns et al., 1973).

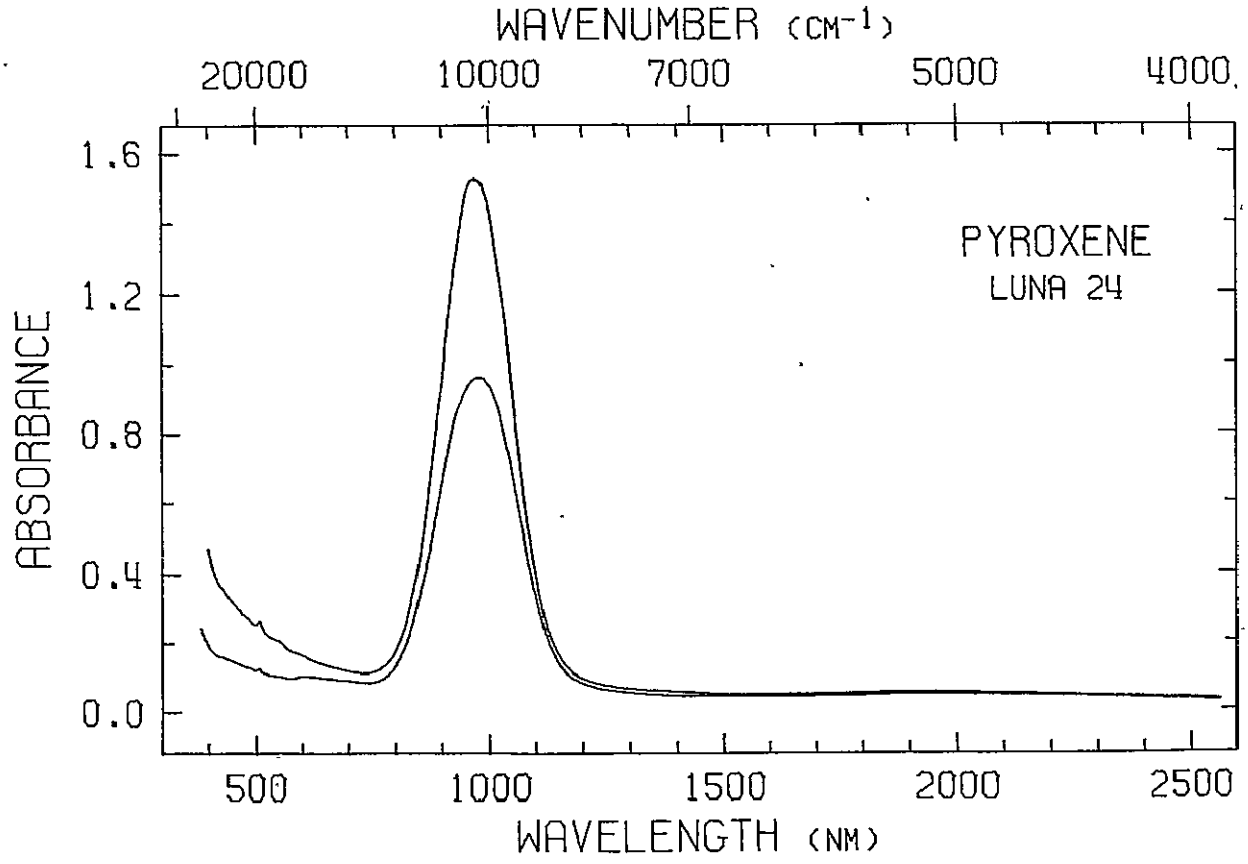

Figure 3. Comparison of the γ optical absorption spectra of the Luna 24 pyroxene, FQM-649, taken in the outer zone and in the central zone. The outer zone contains about 1.7 times as much Fe^{2+} in the M2 site as the central zone.

The orientation of the plagioclase grain was such that no principal direction could be examined. The spectrum showed an absorption band at $\sim$ 1280 nm comparable to other Fe^{2+}-containing lunar plagioclases. (Bell and Mao, 1973).

OPTICAL SPECTRA

George R. Rossman

Table 1. Electron Microprobe Analyses.

	SiO_2	FeO	MgO	CaO	MnO	TiO_2	Al_2O_3	Cr_2O_3	NiO	Na_2O
olivine	32.28	57.46	10.05	0.54	0.62	0.03	0.03	0.01	0.01	--
pyroxene outer zone	48.30	31.02	6.60	12.22	0.42	0.92	1.03	0.09	--	0.00
pyroxene central zone	51.47	15.44	14.95	15.04	0.36	0.34	2.01	0.79	--	0.03

Albee, A. L., A. A. Chodos and R. F. Dymek (1977) Petrology of Luna 24 sample 24170. This volume.

Burns, R. G., D. J. Vaughan, R. M. Abu-Eid and M. Witner (1973) Spectral evidence for Cr^{3+}, Ti^{2+} and Fe^{2+} rather than Cr^{2+} and Fe^{3+} in lunar ferromagnesium silicates. Proc. Fourth Lunar Sci. Conf. Geochim. Cosmochim. Acta, Suppl. 4, Vol. 1, pp. 983-994.

Bell, P. M. and H. K. Mao (1973) Optical and chemical analysis of iron in Luna 20 plagioclase. Geochimica et Cosmochimica Acta, 37, 755-759.

LUNA 24 VLT BASALT: CHARACTER AND ORIGIN. Graham Ryder[1], Harry Y. McSween, Jr.[2], and Ursula B. Marvin, Center for Astrophysics, 60 Garden Street, Cambridge, Massachusetts 02138.

Our studies of thin sections of 250-500 μ-sized particles demonstrate that the Luna 24 core sample is composed primarily of a single variety of very low titanium (VLT), low magnesium, subophitic to ophitic basalt/gabbro*, and its metamorphosed and degraded products (1). These basalts and gabbros were local surface flows in Mare Crisium. A second basalt group, olivine vitrophyric, is much more magnesian, is unrelated, and is very rare. Aspects of the characteristics and origin of the main Luna 24 VLT basalt group is the subject of this abstract.

Variation in composition: We have made bulk composition estimates of the Luna 24 VLT basalts utilizing microprobe defocussed-beam analyses of fine-grained materials [Table 1, Figs. 1, 2, and (1)]. The results agree with those of other workers (2-4). It is not clear that the scatter among the data points represents a real variation in the composition of the Luna 24 VLT basalts, or results from sampling and/or analytical errors: both MgO and the FeO/FeO+MgO ratio remain fairly constant, and the FeO/Al_2O_3 negative correlation could easily result from sampling errors. Nonetheless, with the data at hand, chemical variation among the Luna 24 VLT basalts could be as great as that of any other specific mare basalt subgroup, and may not be as restricted as we (1) and others (3,5) have believed. However, we can find no basis for the subgroups of olivine-basalts, cristobalite basalts, and intermediate 'dolerites' of Tarasov et al. (4) in any chemical sense. We note that one fragment of 24170 is fine-grained and contains 75% plagioclase (6); it is either unrelated to the other Luna 24 VLTs or it represents fractionation amongst them (this may be the particle analyzed by R. Dymek, pers. comm., and if so it has mineral compositions similar to other Luna 24 VLTs). Useful bulk compositions for gabbros are not available; estimates for the gabbros using the mode of 24170 (5) are invalid since the sample was hand-picked (6). Some particles with a medium-grain size (in our samples) consist predominantly of olivine and plagioclase; if these particles represent larger volumes of rock then they must be cumulates and again some fractionation is suggested. We suggest that the total real range of composition of the Luna 24 VLT basalts is similar to that of other specific mare basalt subgroups.

---

*Distinctions without definitions have been made between Luna 24 basalts and gabbros by other authors; we believe that all the samples represent effusive rocks and that basalt would be a better term for all of them. However, we use "gabbro" here for those rocks represented by fragments whose grain size is coarser than the particle size i.e. >0.5 mm, and our distinction may be approximately similar to that of other authors.

Now at: [1]Department of Geology, University of California at Davis, Davis, California 95616. [2]Department of Geological Sciences, The University of Tennessee, Knoxville, Tennessee 37916.

LUNA 24 VLT BASALT...

G. Ryder et al.

Comparison of Luna 24 basalts with other lunar mare groups

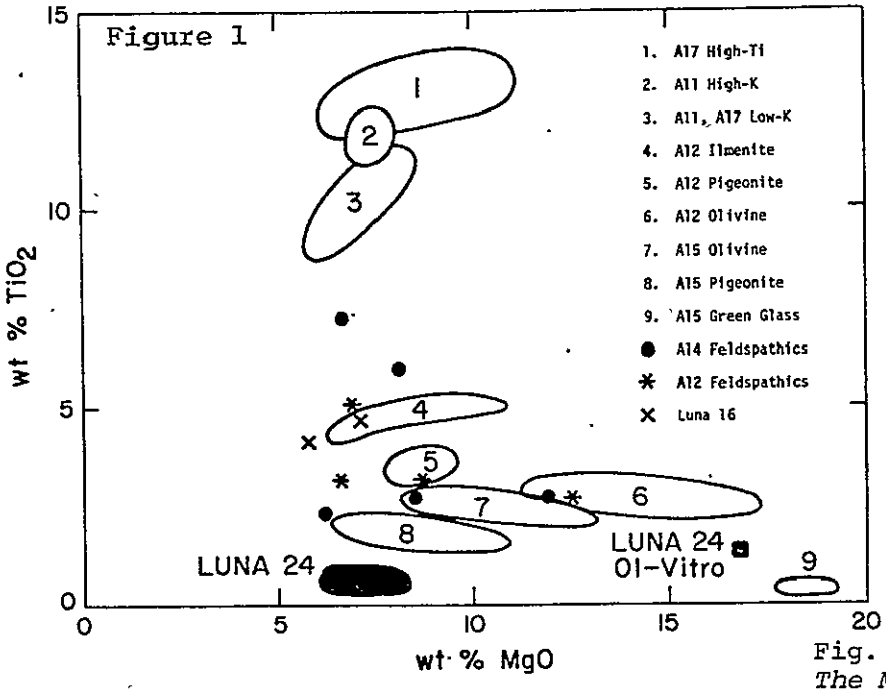

Table 1 (wt. %)
LUNA 24 VLT
BASALT ESTIMATE

SiO_2	46.5
TiO_2	1.00
Al_2O_3	12.5
Cr_2O_3	0.15
FeO	18.0
MnO	0.25
MgO	6.5
CaO	13.5
Na_2O	0.35
K_2O	<0.05
P_2O_5	<0.04
BaO	<0.05

Fig. 1 reproduced courtesy of *The Moon*

Crystallization sequence: Crystallization of the Luna 24 basalts commenced with olivine and/or aluminian chromite, the olivine forming small phenocrysts which enclosed euhedral chromites. The relative positions of pyroxene and plagioclase in the crystallization sequence are in dispute; Bence et al. (5) and others (3,4) believe that pyroxene was a liquidus or near-liquidus phase, and that plagioclase was suppressed. Contrarily, we believe that plagioclase crystallization preceded that of pyroxene (1), although it was not necessarily a liquidus phase. A brown glass whose composition is equivalent to that of Luna 24 VLT basalts contains crystallites of olivine and plagioclase, but not of pyroxene. Our own analyses, and those of Tarasov et al. (4) of the earliest pyroxenes i.e. most Fs-poor, have less than 2% Al_2O_3. Similarly low contents are noted in the gabbro pyroxenes (1, 5). These are lower than in pyroxenes which crystallized prior to plagioclase from other mare basalt melts with much lower bulk Al contents, and indicates that Al activity in the Luna 24 basalts was reduced by the crystallization of plagioclase before pyroxene. Assuming multiple saturation at the liquidus with olivine and pyroxene, Bence et al. (5) calculated that the earliest pyroxenes in the gabbro crystallized from a melt containing 5.5-7.0 mol% Al. However, the Luna 24 VLT basalts (with which the gabbros are assumed to be isochemical) contain at least 8.0 mol% Al. Therefore, notwithstanding the arguments of (5) we assume that these pyroxenes did not crystallize at a multiply saturated liquidus, and that the Al activity in the melt had been reduced by plagioclase preceding pyroxene. Vaniman and Papike (3) find slightly higher Al contents in early pyroxenes, but not so much higher as to invalidate the argument. To us, the evidence suggests distinct

LUNA 24 VLT BASALT...

G. Ryder et al.

Selected compositional variation diagrams

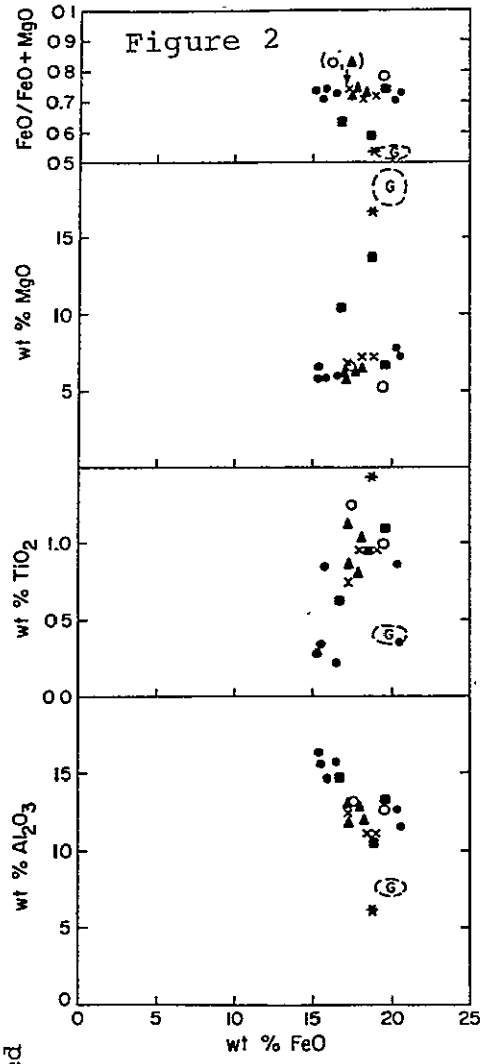

Fig. 2 reproduced courtesy of *The Moon*

temperature intervals between olivine and plagioclase, and subsequently between plagioclase and pyroxene, although we do not know how wide or narrow these intervals may have been.

Relation to other lunar basalts: The chemistry of Luna 24 VLT basalt is distinct from that of any other mare basalt group, particularly in its combination of very low titanium and very low magnesium (Fig. 1). This peculiar chemistry is a result either of advanced crystallization and differentiation of some other mare basalt type, or of independent derivation from a distinct source or process in the lunar interior. For fractional crystallization a conceivable parent must itself be a VLT basalt (1,3). Taylor et al. (2) have performed least-squares calculations which indicate that Luna 16, Luna 24, and Apollo 17 VLTs can all be derived from liquids similar to magnesian Apollo 17 VLTs by fractional crystallization involving the removal of olivine, pyroxene, and chromite. This sequence, supported by (3,5) possibly extends back to compositions similar to Apollo 15 green glass, with magmas differentiating in shallow level holding chambers and being tapped at successive intervals (3). The hypothesis is attractive, especially as some high magnesium glasses and a magnesian olivine vitrophyre are present in the Luna 24 soil (Fig. 2). However, we do not believe this proposed relationship is viable at low pressure, because of the low pressure phase relationships we infer (above) for the Luna 24 VLT basalts i.e. that the liquid was not multiply saturated and that pyroxene crystallization was actually suppressed. Thus the sequence proposed by Taylor et al. (2) while arithmetically viable, could in practise not be realized. Furthermore, the Luna 24 VLTs contain more olivine (>10%) then do the Apollo 17 VLTs (∿5%) with similar cooling histories [although this is not always apparent in the norms of the DBAs], a result not in keeping with the derivation of Luna 24 VLTs by subtraction of predominantly olivine from the Apollo 17 VLT composition. The

LUNA 24 VLT BASALT...

G. Ryder et al.

mineral compositions of Luna 24 VLTs also do not lie on Apollo 17 VLT mineral composition trends e.g. Luna 24 VLT chromites and pyroxenes include varieties with higher Al.

However, the phase relationships of the Luna 24 VLTs would be different at depth. The temperature interval between olivine and pyroxene (a more polymerized mineral) is likely to decrease with depth; the liquid could become multiply saturated and plagioclase even suppressed. In this case a relationship between compositions similar to Apollo 15 green glass and Apollo 17, Luna 16, and Luna 24 VLTs is possible. Experiments could define what "shallow" in "shallow level holding chambers" might be. However, at present we cannot substantiate such a fractionation/differentiation relationship. It it existed, it represents the most extremely differentiated sequence known within a lunar mare basalt group, spanning the range from the most Mg-rich to Mg-poor. We note that not all VLT basalts could belong to this series--the olivine-normative basalts in Boulder 1, Station 2, Apollo 17 (7) are much older, though they are chemically similar to Apollo 17 VLTs [Note that this olivine-normative group is not the KREEP-rich group from the boulder, an error made by Vaniman and Papike (8)]. We suggest that the Luna 24 basalt group was derived independently of other lunar basalts, and does not represent part of a fractionation sequence involving other VLT basalts.

REFERENCES: (1) Ryder, G. et al. (1977) The Moon, in press. (2) Taylor, G. J. et al. (1977) Geophys. Res. Lett. 4, 207-210. (3) Vaniman, D. T., and Papike, J. J. (1977) Geophys. Res. Lett., in press. (4) Tarasov, L. S. et al. (1977) PLSC 8, in press. (5) Bence, A. E., et al. (1977) Geophys. Res. Lett., in press. (6) Nagle, J. S., and Walton, W. J. A. (1977) Luna 24 Catalog, 85 pp. (7) Ryder, G. et al. (1975) The Moon 14, 327-357. (8) Vaniman, D. T., and Papike, J. J. (1977) PLSC 8, in press.

CORRELATION OF TITANIUM IN MARE REGIONS WITH CRUSTAL THICKNESS.
Ernesto Schonfeld, NASA Johnson Space Center, Houston, TX 77058.

Very low titanium mare basalts (VLT) have recently been discovered in the Mare Crisium region (Luna 24)(1,2) and in the central Mare Serenitatis region (3). These mare regions represent areas with very thin crusts (4). Also, high titanium mare basalts, such as those found in Mare Tranquilitatis, represent areas with relatively thick crusts. These facts have stimulated this study: the correlation of titanium in mare regions with crustal thickness. The data used for this study is from lunar samples (5), remote IR reflectance spectra (6,7), remote gamma-ray spectra (8), and estimates for the crustal thickness (4). The result of the correlation between titanium concentration in mare regions and crustal thickness is shown in figure 1. There is a good positive correlation between these two variables. The high titanium, low or intermediate titanium, and the very low titanium (VLT) mare basalts, correspond approximately, respectively, to regions with crustal thickness of about 65, 50 and 25 km.

Some caution should be applied in the interpretation of the correlation shown in figure 1. First, the composition of mare basalts obtained by remote sensing measures mixtures containing about 80% mare basalts. Second, mare basalts flows can sometimes travel considerable distances and, therefore, the composition of the mare basalts might not be related to the cumulate underlying the crust. Third, the composition of a large basin is only approximately uniform. Even with these limitations, the correlation shown in figure 1 is considered to be valid.

Interpretation

The titanium concentration in mare basalts can be related to the degree of differentiation in the following way. If one assumes that the Samarium concentration (LIL element) in mare basalts represents an index of differentiation (the higher the Sm concentration the more differentiated is the mare basalt), then based on the correlation of Sm with Ti in mare basalts (shown in figure 2) the titanium concentration in mare basalts would also be an approximate index of differentiation. Since mare basalts are remelted products of cumulates (9-12), this index of differentiation could apply also to the cumulates underlying the lunar crust.

One possible interpretation of the correlation of titanium in mare regions with crustal thickness is as follows: If one assumes that there is lateral variation in the differentiation process (13-15), then as it has been proposed (15) a thicker crust is more differentiated. Consequently, the cumulates underlying a thick crust, probably would eventually extrude mare basalts into the lunar surface with high titanium concentration (relative to a thin crust).

CORRELATION OF TITANIUM IN MARE REGIONS...

Schonfeld, E.

Another possible qualitative interpretation of the correlation between titanium and crustal thickness is based on current cumulate models for the origin of mare basalts (9-12). In these models the source of mare basalts are stratified cumulates with upward increasing titanium concentrations. The highest titanium concentration cumulates are those underlying the crust. In this interpretation the crustal thickness, source depth, and efficiency factor act as hydrostatic "filters" (16) that control mare basalt flow to the lunar surface. One difficulty with this model is in predicting the proper efficiency factor for each mare basalt flow.

Acknowledgment: The author thanks C.-Y. Shih and M. B. Duke for their useful comments.

REFERENCES: 1) Barsukov V.L. and Florensky C.P., Lunar Science VIII, pp 61-63 (1977). 2) Taylor G.J. et al., Geophys. Res. Lett. 4, 207-210 (1977). 3) Vaniman D.T. and Papike J.J., Lunar Science VIII, pp 952-954 (1977). 4) Bills B.G. and Ferrari A.J., J. Geophys. Res. 82, 1306-1314 (1977). 5) Proc. Lunar Sci. Conf. 1-7 (1970-1976). 6) Pieters C. and McCord T.B., Origin of Mare Basalt Conf., pp 125-129 (1975). 7) Pieters C. and McCord T.B., Proc. LSC 7th, 2677-2690 (1976). 8) Metzger A.E. et al., Proc. LSC 5th, pp 1067-1078 (1974). 9) Philpotts J.A. and Schnetzler C.C., Proc. Apollo 11 LSC, pp 1471-1486 (1970). 10) Taylor S.R. and Jakes P., Proc. LSC 5th, pp 1287-1305 (1974). 11) Walker D. et al., Geochim. Cosmochim. Acta 39, 1219-1235 (1975). 12) Shih. C.-Y. and Schonfeld E., Proc. LSC 7th, pp 1757-1792 (1976). 13) Trombka J.I. et al., Proc. LSC 4th, pp 2847-2853 (1973). 14) Schonfeld E., Lunar Science, pp 846-848 (1977). 15) Schonfeld E., Proc. LSC 8th, in press (1977). 16) Solomon S.C., Proc. LSC 6th, pp 1201-1042 (1975).

Figure Captions

Figure 1. Correlation of crustal thickness with TiO_2 concentration. Numbers 1,2,3,4,5,6,7,10,11,12,13,and 14 correspond, respectively, to Mare Aestum, Fecunditatis, Humorum, Nubium, Nectaris, Procellarum (Ap.12 site), Somniorum, Central Serenitatis, Crisium, Fecunditatis (Luna 16 site), Tranquilitatis, and East of Vaporum.

Figure 2. Sm - TiO_2 systematics of lunar mare basalts. Numbers correspond to Apollo missions. L-16 correspond to Luna 16, and GG correspond to the Apollo 15 green glass composition.

CORRELATION OF TITANIUM IN MARE REGIONS...

Schonfeld E.

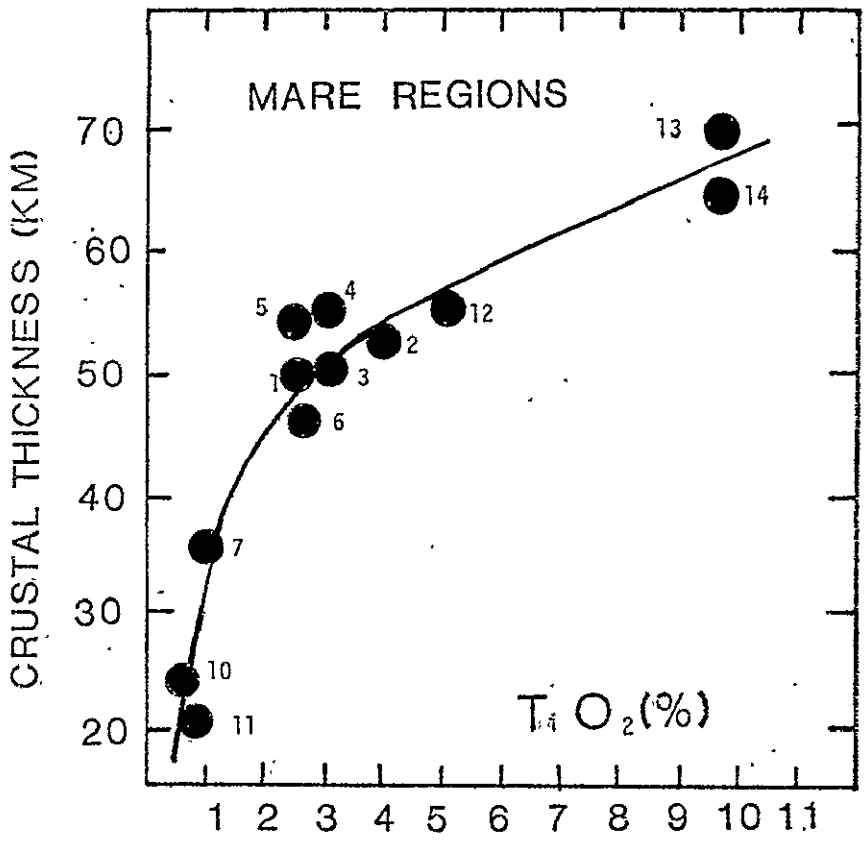

FIGURE 1

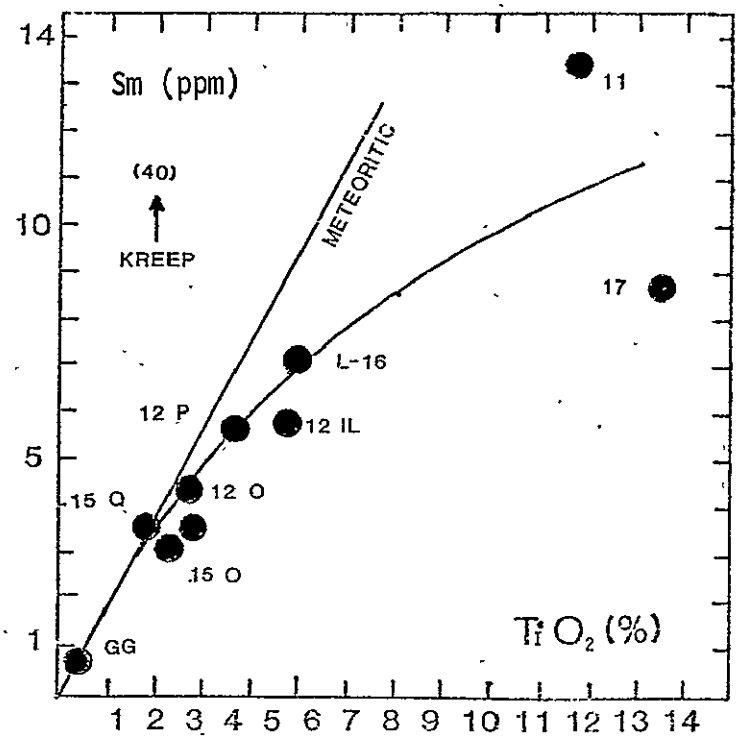

FIGURE 2

CORRELATION BETWEEN GEOCHEMICAL "FEATURES" AND PHOTOGEOLOGICAL FEATURES IN MARE CRISIUM. Ernesto Schonfeld, SN7, NASA Johnson Space Center, Houston, TX 77058 and Michael J. Bielefeld, Computer Sciences Corp., Silver Spring, MD 20910.

The recent Luna 24 mission that brought back a lunar sample from Mare Crisium has stimulated a great deal of interest in this region of the Moon. Very low titanium mare basalts (VLT) have been discovered at the Luna 24 site (1,2) and Apollo 17 landing site (3). There is a suggestion that these mare basalts are related to the high Mg and Mg/Al ratio mare composition called the green glass (2,4). In order to look for this relationship between the very low titanium mare basalts and the green glass composition the measurements of Mg/Si and Al/Si by the orbital chemistry X-ray fluorescence experiment of Adler et al. (5,6) should be very useful. For example, the green glass has a Mg/Al ratio about **two** times higher than the very low-Ti mare basalts or similar mare basalt compositions. The purpose of this paper is to study the Mg/Si, Al/Si and Mg/Al ratio variations in Mare Crisium to show those regions with high Mg/Si and Mg/Al ratios and correlate them with any photogeology features already determined (7-11). By doing this correlation it is hoped that one would better understand mare basalt volcanism in Mare Crisium.

A geochemical "feature" is defined as any region that has a high contrast in chemical composition relative to surrounding areas. Specifically, in this paper we were looking for areas with high Mg/Al and Mg/Si ratios relative to the nearby areas.

Data

An orbital X-ray spectrometer (5) flown in Apollo 15 is the source of geochemical information about the Crisium basin and certain other nearside lunar features (6). Recently, in an effort by the La Jolla Consortium to standardize a variety of lunar geochemical and geophysical data sets, an X-ray data set was processed and arrayed in a 0.25 degree by 0.25 degree format (12, 13) which is the basis for the analysis in this paper. A conversion from measured intensity ratios for the elements Mg, Al, and Si to geochemical concentration ratios was performed by a "ground truth" (lunar sample data) procedure outlined by Bielefeld (14).

Results and Discussion

The comparison between nine geochemical "features" and associated photogeologic features or expressions is shown in Table 1. For comparison the geochemical data for the Luna 24 site and the average Mare Crisium values are inserted in Table 1.

Table 1 illustrates that high MgO and Mg/Al values tend to be associated (4 out of 9 cases) with photogeologic dark mantle deposits (10,11). The most

TABLE 1. COMPARISON OF GEOCHEMICAL FEATURES WITH PHOTOGEOLOGICAL FEATURES.

LATITUDE North	LONGITUDE East	Mg/Al	Al_2O_3* %	MgO* %	PHOTOGEOLOGIC DESCRIPTION OF GEOCHEMICAL FEATURES
13 - 14	52.5-53.5	.63	16.3	8.9	SW of Picard. Could be a flow unit near a ridge (8).
14.2-15	54.7-55.5	.85	14.3	10.6	Picard. Inside and ejecta East portion. Astronaut R. E. Evans described it as layer of dark material (15).See also 16. Mg/Al and Mg/Si ratios match very good dark material area.
13.8-14.2	61.5-62.5	.72	12.1	7.6	Area corresponds to crater materials area (9) and possibly to flow unit (8).
13.8-14.2	60.8-61.2	.72	16.7	10.6	Area corresponds possibly to flow unit (8).
17.4	53.6-54.	.80	16.1	11.2	Area corresponds to Peirce ejecta that is dark mantle material (10).
12.5	57-57.7	.39	14.7	5.1	Low Mg/Al and Mg/Si ratios area near 1st Crisium basin ring.
1.5-2.5	51.2-52.	.88	14.3	11.0	NE mare Fecunditatis. Matches very closely (±6km) an area about 30x30 km of dark mantle material (11).
12.4-12.8	61.6-62.	.70	16.5	10.2	Area near West of landing of Luna 24 site. Corresponds approximately to crater materials area (9).
∿13	∿63	∿.65	∿18.3	∿10.5	Area trending NE from the Luna 24 site. About 50 km long and 20 km wide that is part of 1st Crisium basin ring. The chemical contrast is just medium. This area corresponds partly to a patch of dark mantle (11).
					Other areas (No chemical contrast)
12.75	62.2	.63	17.9	9.9	Luna 24 landing site.
		.61	16.3	8.7	Average Crisium basin (14).

(*) Assumes Si concentration is 21 %.

striking cases are the Crater Picard (east; ref. 15), Pierce ejecta, and the region in NE Fecunditatis. Although the geochemical features are constrained by the data reduction techniques to rectangular regions (about 8 by 8 km), the spatial correspondence between the geochemical and photogeologic features is impressive.

As suggested by Taylor et al. (2) and by Vaniman and Papike (2), the VLT mare basalts might be related to the green glass composition by a differentiation process. The compositions for the geochemical features with MgO and Mg/Al values are intermediate between the VLT composition and the green glass composition, therefore without any additional information, it is difficult to decide if these compositions are mixtures or intermediate products of differentiation (between green glass and VLT). The fact that one observes these intermediate compositions between the green glass and the VLT basalt composition is consistent with the suggestions by Taylor et al. and Vaniman and Papike.

As far as the original locations of these dark mantle deposits, it is possible to speculate based on the observations made of the craters Picard and Peirce. In these cases the dark mantle material is associated with impact craters, suggesting that the Crisium basin in that area is stratified with an underlying basaltic unit that is richer in Mg/Al and Mg/Si ratios.

Acknowledgment: The authors thank D.A. Morrison and J.L. Warner for their useful comments and C. Hardy for typing this paper.

REFERENCES: 1) Barsukov V.L. and Florensky C.P., Lunar Science VIII, pp 61-63 (1977). 2) Taylor G.J. et al., Geophys. Res. Lett. 4, 207-210 (1977). 3) Vaniman D.T. and Papike J.J., Lunar Science VIII, pp 952-954 (1977). 4) Vaniman D.T. and Papike J.J., Geophys. Res. Lett., in press (1977). 5) Adler I. et al., Space Sci. Instr. 1, 305-316 (1972). 6) Adler I. et al., Proc. LSC 3rd, pp 2157-2178 (1972). 7) Butler P. Jr. and Morrison D.A., Lunar Science VIII, 151-153 (1977). 8) Morrison D.A., private comm. (1977). 9) Boyce J.M. et al., Nature 265, 38-39 (1977). 10) Casella C.J. and Binder A.B., USGS I-707 (1972). 11) Olson A.B. and Wilhelms D.E., USGS I-837 (1974). 12) Andre C.G. et al., Science 197, 980-989 (1977). 13) Bielefeld M.J. et al., Proc. LSC 8th, in press (1977). 14) Bielefeld M.J., Proc. LSC 8th, in press (1977). 15) Apollo 17 Prelim. Sci. Rept., NASA SP-330, pp 28-14 (1973). 16) Pieters C. and McCord T.B., Geophys. Res. Lett. 3, 697-700 (1976).

LUNA 24: PETROCHEMICAL POTPOURRI, C. H. Simonds[1], J. L. Warner[2], P. E. McGee[3], A. Cochran[3], and R. W. Brown[3] ([1]Lunar Science Institute; [2]NASA Johnson Space Center; [3]Lockheed Electronics Co., Houston, TX 77058).

Petrologic investigations of six samples of Luna 24 soil suggest:

1. Potassium, and by inference all lithophile trace elements, are depleted in the crust and mantle underlying the Moon's eastern limb relative to the Moon's central nearside.
2. Basalts in southern Mare Crisium are derived from two K and Ti deleted magmas; one almost a factor of two richer in MgO than the other.
3. The soil throughout the Luna 24 core may be modeled as a mixture of immature mare material (compositionally dominated by the higher MgO basalts) and mature highland material.

DATA SETS: All glass spheres and fragments and glass in many agglutinate fragments in the 90-150 μm size fraction of each sample were analyzed using an electron microprobe with a 15 μm spot (Figs. 1-2). From these Figures it is apparent that the agglutinate fragments range continuously from mare to highland compositions; the average composition is given in Table 1. Nonagglutinate data was sorted into compositional clusters (Table 1) utilizing a procedure similar to the dendogram technique used by Higuchi and Morgan (1975). Clusters are named following the terminalogy of previous soil surveys (Reid et al. 1973).

Modal analyses were performed by counting every grain in the thin sections available to our group (Table 2).

Bulk major element analyses of the <250 μm fraction of six samples were obtained using the fused bead procedure of Brown (1977) on replicate 5 mg splits. An average is given in Table 1. The difference between our values for FeO and those reported by Blanchard et al. (1977) is due to a sampling or sample preparation problem.

POTASSIUM DEPLETION: Low lithophile element (Th) contents on the Moon's eastern limb have been measured by the Apollo orbital gamma ray experiment (Parker et al., 1977). This and similar orbital data have led Hubbard and Woloszyn (1977) to suggest that the eastern limb of the Moon is compositionally distinct from the Moon's central nearside.

Whereas the orbital and bulk soil analyses show that the surface soils are depleted, the Luna 24 glass data demonstrates that this depletion is characteristic of both highland and mare constituents. The most K-rich cluster (Low-K Fra Mauro), only 3% of the glasses, is similar in composition to many impact-melt rocks of Apollo 16 and 17, except that K_2O in the glasses is depleted by a factor of 6. The three major clusters all contain <0.05 % K_2O. Figure 3 demonstrates that the potassium depletion displayed by Luna 24 is shared by Luna 16 and 20, and to a lesser extent by Apollo 11, 16 and 17. Not only are the Luna soils depleted in K_2O, but Figure 3 indicates that a K-rich constituent is missing. This depletion in trace elements in the basaltic constituents of the Luna 24 soil is supported by trace element and Rb-Sr data of Blanchard et al. (1977) and Nyquist et al. (1977).

Because both mare and highland glasses at Luna 16, 20 and 24 are depleted in potassium and other trace lithophile elements, and the sources of mare and highland materials are apparently genetically linked, we suggest that the entire crust and at least some of the mantle that underlies the eastern limb of the Moon is depleted. This implies that there are major lateral heterogeneities

LUNA 24: PETROCHEMICAL POTPOURRI

Simonds C. H. et al.

in the Moon's crust and mantle that have survived for 4.6 A.E.

MARE BASALTS: Two different mare basalt compositional clusters, a low MgO and high MgO one, have been defined. Both contain less TiO_2 (ca. 1.0 wt. %) than has been reported from individual mare basalt rock samples collected at Apollo landing sites, however, the chemically similar Apollo 15 green glasses have even lower TiO_2 contents (ca. 0.4 wt. %, Reid et al., 1972). The mare glasses are compositionally similar, but not identical, to the "very low TiO_2" basalts discovered at Apollo 17 by Vaniman and Papike (1977a) and Taylor et al. (1977). The low MgO (6.5 wt. %) group is compositionally well defined and consists of spherulitic to dendritic textured devitrified glass fragments. The high MgO (ca. 10 wt. %) group is compositionally more diffuse and consists of pale green glass spheres and fragments. The low MgO group is identified with the bulk of the basaltic lithic fragments discovered in the Luna 24 soil by Vaniman and Papike (1977b), Taylor et al. (1977), and Ryder et al. (1977). The high MgO group is not correlated with any lithic fragments thus far identified, but its composition does approach the very MgO-enriched olivine vitrophyre fragment described by Ryder et al. (1977). Both mare basalt groups are believed to represent, at least in part, volcanic magmas rather than impact-formed melts (see below).

Both mare basalt groups have olivine on the liquidus at low pressures. On Figure 1 we have sketched olivine fractionation lines using olivine compositions determined by Ryder et al. (Fo_{75} for the high MgO group and Fo_{61} for the low MgO group). It is apparent that simple olivine fractionation cannot derive one basalt type from the other.

SIGNIFICANCE OF THE COMPOSITIONAL CLUSTERS: Compositional clusters among the glasses in a lunar soil may form by volcanic activity or impact fusion. Volcanic glasses have homogeneous compositions, no inclusions, spherical shapes (at least for low viscosity mafic compositions), and low trace siderophile element contents (Heiken et al., 1974). Impact-fused glasses have schlieren and clasts, are compositionally heterogeneous on the μm to mm scale, and enriched trace siderophile element contents (Simonds et al., 1976). Note that on the scale of a few grams, impact melts are quite homogeneous.

The small compositional scatter among the devitrified glasses and the internal homogeneity and regular shapes of the pale green glass spheres suggest that these two glass groups represent volcanic liquids. The bulk of the green glass fragments display a wide compositional range and are probably impact produced. Preservation of the compositional cluster probably results from impacts into the local terraine which must have been fairly pure.

The highland basalt cluster, consisting of colorless glass fragments, has been observed in samples collected at every lunar landing site (Warner et al., 1972). Its schlieren and other compositional heterogeneities suggest that these glasses are impact fused. The ubiquity of the Highland Basalt cluster and its similarity to the highland composition measured from orbit suggest that it is the grand compositional average of the lunar highland crust surrounding each landing site.

MAKEUP OF LUNA 24 SOIL: The Luna 24 soil does not have a simple history of in situ cominution of a mare basalt terraine as evidenced by the discrepency between the bulk soil analysis, the average glass analysis, and the average agglutinate analysis (Table 1). Three modal observations help resolve the

LUNA 24: PETROCHEMICAL POTPOURRI

Simonds C. H. et al.

discrepancies: (1) the glasses, including the agglutinates, do not constitute a major portion of the soil; thus they could be a transported component. (2) The modal abundance of the glasses has a positive correlation with the modal abundance of agglutinates suggesting that the highland glasses and agglutinates may have been transported together. (3) The discrepancies among the average analyses is such that the agglutinates are more highland-rich than the bulk soil, and the glasses are more highland-rich than the agglutinates.

If the soil is modeled as a two-component mixture of immature mare soil (with few glasses) and mature highland soil (with many glasses) the glass and agglutinate average analyses will be biased toward highland compositions as is observed.

A secondary effect which biases the glass and agglutinate average analyses toward highland compositions is that highly aluminous highland material will remain glass under cooling rates that will yield crystalline rocks for the high iron mare material (Handwerker et al., 1977). Note that many of our "glasses" are in fact of devitrified fragments that are nearly holocrystalline.

TABLE 1. LUNA 24 CHEMICAL DATA.

	Average Soil	Average Glass 226 points	Average agglutinate 71 points	Highland basalt cluster 67 points	Feldspar cluster 8 points	Low K Fra Mauro cluster 5 points	Low Mg mare cluster 23 points	High Mg mare cluster 42 points
SiO_2	47.79	45.46±1.73	45.62±1.44	45.02±1.41	44.44±3.36	48.36±0.71	46.26±0.71	45.08±1.85
TiO_2	1.05	0.68±0.39	0.83±0.27	0.29±0.15	0.13±0.20	1.38±0.24	0.98±0.09	0.96±0.26
Al_2O_3	11.15	18.93±7.55	15.62±5.68	26.44±2.67	34.41±2.17	19.07±0.44	12.98±0.73	12.60±2.23
Cr_2O_3	0.45	0.24±0.18	0.32±0.16	0.11±0.04	0.00±0.02	0.12±0.05	0.23±0.05	0.40±0.08
FeO	17.51	12.61±7.05	15.87±5.15	5.02±1.67	1.42±2.23	8.66±1.08	20.00±1.03	18.36±1.87
MnO	0.28	0.18±0.11	0.23±0.09	0.06±0.03	0.00±0.02	0.10±0.02	0.28±0.01	0.26±0.02
MgO	9.84	7.96±2.81	8.50±2.07	7.23±2.40	0.61±0.96	8.38±2.49	6.47±0.32	10.21±1.08
CaO	11.10	13.47±2.35	12.53±1.54	15.44±1.43	18.74±1.79	12.58±0.78	12.73±0.29	11.43±1.44
Na_2O	0.28	0.29±0.22	0.31±0.16	0.24±0.17	0.78±0.53	0.37±0.25	0.29±0.06	0.18±0.10
K_2O	0.03	0.06±0.04	0.07±0.11	0.05±0.04	0.06±0.04	0.09±0.02	0.04±0.01	0.04±0.01
P_2O_5	0.06	0.03±0.03	0.04±0.03	0.02±0.03	0.00±0.01	0.03±0.04	0.03±0.01	0.02±0.01
S		0.12±0.13	0.12±0.17	0.04±0.06	0.00±0.02	0.01±0.04	0.19±0.05	0.11±0.08
Total	99.54	100.05	100.13	99.96	100.59	99.15	100.48	99.65

REFERENCES:

Blanchard D.P., Haskin L.A., Brannon J.C. and Aaboe E. (1977), this volume.
Brown R.W. (1977) Geochim. Cosmochim. Acta 41, 435-438.
Handwerker C.A., Onorato P.I.K. and Uhlmann D.R. (1977) this volume.
Heiken G., McKay D.S. and Brown R.W. (1974) Geochim. Cosmochim. Acta 38, 1703-1718.
Higuchi H. and Morgan J.W. (1975) Proc. Lunar Sci. Conf. 6th, 1625-1651.
Hubbard N.J. and Woloszyn D. (1977) Proc. Lunar Sci. Conf. 8th, in press.
Nyquist L., Wiesmann H., Bansal B., Wooden J., McKay G. and Hubbard N. (1977) this volume.
Parker R.E., Haines E.L., and Metzger A.E. (1977) Lunar Science VIII, 756-758.
Reid A.M., Warner J.L., Ridley W.I. and Brown R.W. (1972) Meteoritics 7, 395-415.
Reid A.M., Warner J.L., Ridley W.I. and Brown R.W. (1973) Geochim. Cosmochim. Acta 37, 1011-1030.
Ryder G., McSween H.Y. and Marvin U.B. (1977) The Moon, in press.
Simonds C.H., Warner J.L. and Phinney W.C. (1976) Am. Mineral. 61, 569-577.
Taylor G.J., Keil K. and Warner R.D. (1977) Geophys. Res. Lett. 4, 207-210.
Vaniman D.T. and Papike J.J. (1977a) Proc. Lunar Sci. Conf. 8th, in press.
Vaniman D.T. and Papike J.J. (1977b) Geophys. Res. Lett., in press.
Warner J.L., Reid A.M., Ridley W.I. and Brown R.W. (1972) Earth Planet Sci. Lett. 17, 7-12.

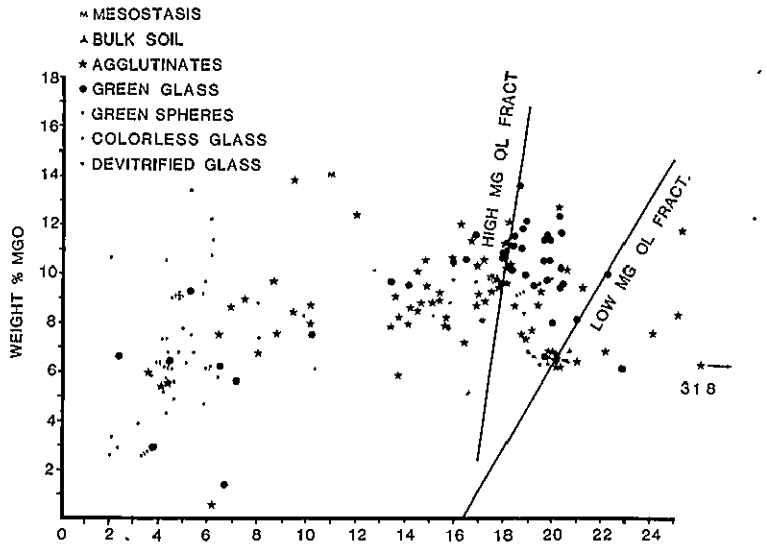

FIGURE 1

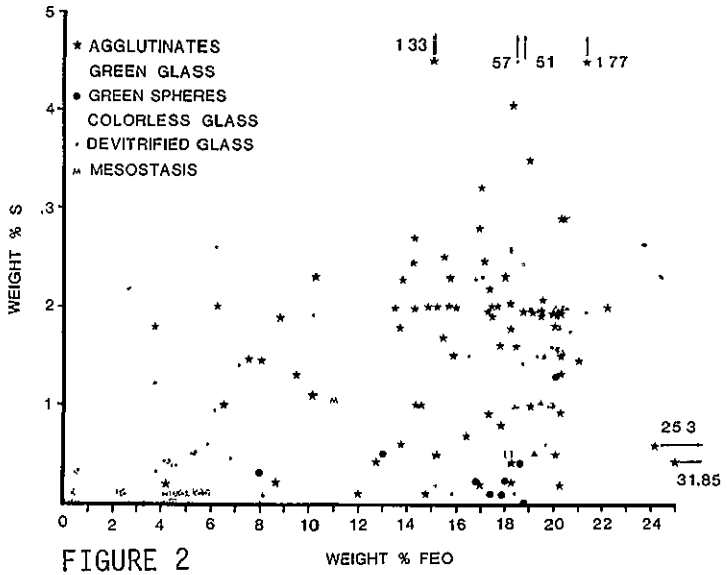

FIGURE 2

TABLE 2. LUNA 24 MODAL DATA FOR 90-150 μm SIZE FRACTION

	24077, 49&50	24109, 44&45	24149, 53&54	24174, 42&43	24182, 41&42	24210, 47
Component			Volume Percent			
Glass spheres	.71	.54	.32	.19	0	.46
Glass fragments	3.26	3.90	2.16	1.66	2.47	1.86
Devitrified glasses	2.34	2.64	1.19	1.07	1.76	3.96
Heterogeneous glasses	1.53	1.64	1.40	1.17	.70	1.63
Agglutinates	24.71	17.59	10.17	8.90	6.00	10.72
Plagioclase	10.62	11.33	9.09	18.88	20.84	12.58
Pyroxene plus Olivine	21.44	24.93	28.67	26.99	30.14	23.07
Basalts	11.03	10.94	13.96	14.28	14.13	17.48
Crystalline matrix breccias	5.40	2.81	3.02	3.51	5.18	5.58
Vitric matrix breccias	17.97	23.14	28.67	22.99	18.49	22.14
Others	.91	.46	.86	.29	.23	.46
Total	99.92	99.92	99.51	99.93	99.94	99.94
Plagioclase/Mafic mineral	.50	.45	.32	.70	.69	.55
Total grains	979	1279	924	1022	849	429

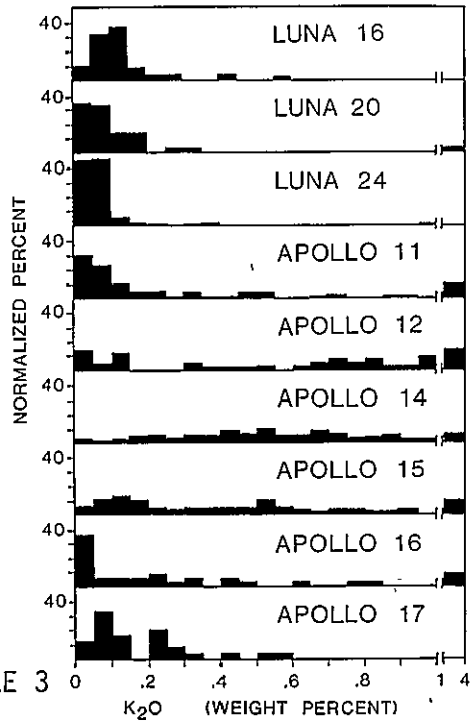

FIGURE 3

PRELIMINARY RESULTS OF PALAEOINTENSITY MEASUREMENTS ON LUNA 24 SAMPLES. A.Stephenson, D.W.Collinson and S.K.Runcorn, Institute of Lunar and Planetary Sciences, School of Physics, The University of Newcastle upon Tyne, Newcastle upon Tyne NE1 7RU, England.

Measurements of the NRM of 47 samples as well as susceptibility and other remanence measurements were carried out. Because most of the samples were to be used for other purposes and were sealed in pyrex tubes it was considered impracticable to attempt to remove each sample from its tube for measurement especially as the average weight of sample was only about 1 mg. To estimate the NRM therefore the tube was rotated about its vertical long axis in a digico magnetometer with a specially adapted sensor of small dimensions to increase the sensitivity. Using this arrangement the minimum detectable moment was about 5×10^{-7} G cm^3. Each sample was placed in an arbitrary orientation in its tube and because of its irregularities and the constrictions at the sealed ends of the tube, the samples did not move relative to their tubes when these were rotated about their vertical axes of symmetry. Thus only the horizontal components of magnetization of each sample was measured. In unfavourable cases therefore when any magnetization happened by chance to be vertically orientated, no magnetization would be detected.

Only 3 of the 47 samples possessed a detectable NRM by this method. These were described as a weakly sintered clod, a shock anorthosite and an agglutinate, respectively. The agglutinate sample, however, had inadvertently been fused into the end of the tube during the sealing process so that its magnetization was undoubtedly a TRM acquired on cooling in the earth's field. Its temperature on heating was probably in excess of the Curie point of iron (770°C). The NRM of the anorthosite was halved by application of a peak alternating field of 30 Oe and was therefore considered to be magnetically too soft to be a reliable indicator of the original NRM.

The sintered clod had an NRM however which was much more stable, there being very little change in intensity on application of a 30 Oe field.

All three samples were then given an ARM in a direct field of 1.8 Oe on which was superimposed an AF field of peak value 1000 Oe along the same axis as the 1.8 Oe field. The usual tumbling could not be employed. Assuming that the original NRM is a TRM acquired in a field h_p and that TRM is 1.34 times stronger than ARM in the same steady field (1), the palaeointensity h_p was estimated for the sintered clod to be 0.3 Oe. Applying the same argument to the inadvertently heated agglutinate sample gives a 'palaeointensity' of 0.4 Oe which is similar to the earth's field at the place where the samples were sealed and therefore provides an unexpected but convenient check that the above method is reasonable. A palaeointensity value of 0.3 Oe for the sintered clod, which could obviously be subject to considerable errors by the above method, is typical of values obtained for lunar rocks of age 3.6 AE(2).

References

(1) Stephenson, A. and Collinson, D.W. 1974. E.P.S.L. 23, 220-228.
(2) Stephenson, A., Collinson, D.W. and Runcorn, S.K. 1974. Proc.Lunar Sci. Conf. 5th, 2859-2871.

Ar^{39}-Ar^{40} PATTERN AND LIGHT NOBLE GAS SYSTEMATICS OF TWO MM-SIZED ROCK FRAGMENTS FROM MARE CRISIUM

A. Stettler, Physikalisches Institut, University of Bern, Sidlerstrasse 5, 3012 Bern, Switzerland, and

F. Albarède, Laboratoire Géochimie Cosmochimie (LA 196), Institut de Physique du Globe, Universités de Paris 6 - 7, 2 Place Jussieu, Paris 5, France

Start and duration of lunar mare filling are important clues for the early thermal history of the lunar mantle, the theory of mascon formation and the anchoring of an absolute time scale to the relative ages of unsampled lunar areas or planetary surfaces as determined by photogeology. The global mare filling activity apparently lastened from 3.92 AE to 3.00 AE ago and characteristic time intervals seem to be associated with the different maria. The sample return of the automatic space probe Luna 24 provided now the possibility to extend the field of mare flooding chronology to the basin of Mare Crisium.

Since its first application the Ar^{39}-Ar^{40} dating technique has undergone a considerable development and at present Ar^{40}-resetting age, Ar^{38}-Ar^{37} exposure age, Ar^{40}/Ar^{36} trapped ratio, K, Ca, Cl, Fe, Ti and some REE concentrations as well as the argon diffusion behavior of an extraterrestrial sample can be inferred from an Ar^{39}-Ar^{40} analysis. In this work we present a further extension of the method including the information contained in the isotopic composition of He and Ne released during the stepwise heating experiments.

Two fragments, L24A and L24B were taken from sample 24096.1 in USSR unit II, located at 96 cm below the top of the core. L24A was a lithic fragment of low-Ti (LT) or very low-Ti (VLT) basalt type, which had low trapped gas concentrations and which yielded therefore a reliable crystallization and exposure age. L24B, a glass rich agglutinate with also LT or VLT composition and bearing much more trapped gas, was suitable to determine the trapped composition. The petrological nature of both fragments will be described in detail elsewhere [1].

Argon

The Ar^{39}-Ar^{40} systematics of the two fragments has already been published [2]. We confine us therefore to a brief summary of the results. Fig. 1 shows the Ar^{39}-Ar^{40} and K/Ca release patterns for L24A wherefrom a cristallization age of 3.65 ± 0.12 AE has been inferred. The Ar^{38}-Ar^{37}

evolution indicates only minor loss of spallogenic Ar^{38} and a reliable exposure age of 660 my could be calculated.

Helium and neon

All isotopes of He and Ne are produced in various proportions by fast and epithermal neutrons during irradiation. Calibration experiments with high-purity salts and minerals suggest that He^4 and He^3 originate most likely in reactions of the type (n, α), (n, He^3) on targets heavier than Mg. The Ne isotopes on the other hand are built up specifically by reactions on F, Na and Mg: Ne^{20} mainly from F and Na, Ne^{21} entirely from Mg, Ne^{22} from Mg and to a lesser extent from Na. The reactions and their measured yields will be discussed in detail elsewhere [3]. Depending on the complexity of the neon mixture in a given sample it is possible to calculate F, Na and Mg contents and the spallogenic (sp) and trapped (tr) Ne composition. Similarly the amount of He^3_{sp} can be estimated. The Ne results of the two fragments are displayed in Fig. 2 using a three-isotope plot. The relative position of the data points enables us to calculate three important parameters: (a) assuming the low temperature points of L24A (up to 750 °C) and all data points of L24B to lie on mixing lines between Ne_{tr} and Ne_{sp} we find $(Ne^{20}/Ne^{22})_{tr} = 13.0 \pm 0.4$ and 13.05 ± 0.20 respectively; (b) as indicated by arrows in Fig. 2 we assume the data points ($T > 750$° C) of L24A to be displaced from the Ne_{tr}-Ne_{sp} line due to Ne^{21} produced by neutrons on Mg. Calculating $Ne^{21}(Mg)$ and using the corresponding production rate [3] we obtain a Mg content of 3.00 ± 0.15 %; (c) correction of Ne^{21}_{tr} and $Ne^{21}(Mg)$ gives Ne^{21}_{sp} and using our Mg content, an average Al and Si content [4], and the appropriate spallation production rates [5] we infer a Ne^{21} exposure age of 620 my which, compared with the Ar^{38}-Ar^{37} age indicates a slight Ne^{21} diffusion loss after excavation from greater depth. Diffusion calculations which consider also the low temperature drop of the Ar^{38}-Ar^{37} curve [2] and the He^3 spallation age of 370 my show that solar heating over 660 my at the very lunar surface might in fact account for the observed diffusion loss.

Summary

We consider the parallel measurement of He and Ne in an Ar^{39}-Ar^{40} analysis as a worthwhile completion providing Mg (and eventually Na and F) concentrations, He^3 and Ne^{21} spallation ages and the trapped gas composition. The respective results of L24A and L24B are summarized in Tables 1 and 2. Apparently the Ar^{39}-Ar^{40} age of 3.65 ± 0.12 AE marks a period of lava extrusion in the basin of Mare Crisium. This agrees well with the corresponding age predicted from photogeology for the Luna 24 landing site [7]. VLT basalts which are expected to be a widespread mare component [8] are chemically very similar to Apollo 15 green glasses for which two Ar^{39}-Ar^{40}

solidification ages of 3.38 AE [9] and 3.79 AE [10] have been reported so far. In fact our age of 3.65 ± 0.12 AE falls well within this range but the apparent uncertainties preclude a chronological confirmation of any petrogenetic relationship.

References

[1] M. Christophe-Michel-Lévy, in preparation. [2] A. Stettler and F. Albarède (1977), submitted to Earth Planet. Sci. Lett. [3] A. Stettler and P. Bochsler, in preparation. [4] G. Ryder et al. (1977), Center for Astrophysics, preprint No. 775. [5] P. Eberhardt et al., Geochim. Cosmochim. Acta 38 (1974) 97. [6] C.J. Allègre et al. (1977), abstract, Met. Soc. Meeting, Cambridge, UK. [7] J.M. Boyce et al. Nature 265 (1977) 38. [8] C. Pieters and T.B. Mc Cord, Proc. Lun. Sci. Conf. 7th, Vol. 3 (1976) 2677. [9] F.A. Podosek and J.C. Huneke, Earth Planet. Sci. Lett. 19 (1973) 413. [10] L. Husain, in The Apollo 15 samples, Lun. Sci. Inst. (1972) 374.

	$T_e(Ar^{38}/Ar^{37})$	$T_e(Ne^{21})$	$T_e(He^3)$	K	Ca	Mg	Fe	Ti
	my			ppm	%			
L 24 A	660 ±130	620 ±150	370 ± 70	175 ±10	8.3 ±.4	3.00 ±.15	17.25 ± .30	≤0.62
L 24 B	500 ±200		85 ± 25	320 ±15	9.1 ±.5		17.60 ± .30	≤0.58

Table 1: Exposure ages and chemistry of L 24 A and L 24 B as inferred from γ-counting (Fe, Ti) and from the light rare-gas composition. L 24 B contained too much trapped Ne to decipher a reliable Mg content and Ne^{21} exposure age. Ti has to be considered as an upper limit due to possible interferences from Ca and Pt.

Sample	Weight (mg)	He^4	Ne^{20}	Ar^{36}	He^4/Ne^{20}	Ne^{20}/Ar^{36}	Ar^{40}/Ar^{36}	Ar^{36}/Ar^{38}	Ne^{20}/Ne^{22}
		10^{-8} cc STP/g							
L 24 A	9.4	36'500 ±2'500	1'030 ± 60	184 ±16	35.5 ±3.5	5.6 ±.7	0 3 ±.3		13 00 ±.40
L 24 B	1.9	640'000 ±60'000	37'500 ±1'800	17'500 ± 900	17.1 ±1.9	2.15 ±.15	0.40 ±.05	5.34 ±.02	13.05 ±.20

Table 2. Composition of trapped gases in L 24 A and L 24 B Ar data are taken from [1]. Neutron induced He and Ne and radiogenic He^4 (assuming U = 0.126 ppm, Th = 0 43 ppm [6], age 3.6 AE) have been corrected.

Ar^{39}-Ar^{40} pattern and light noble gases

Stettler A., et al.

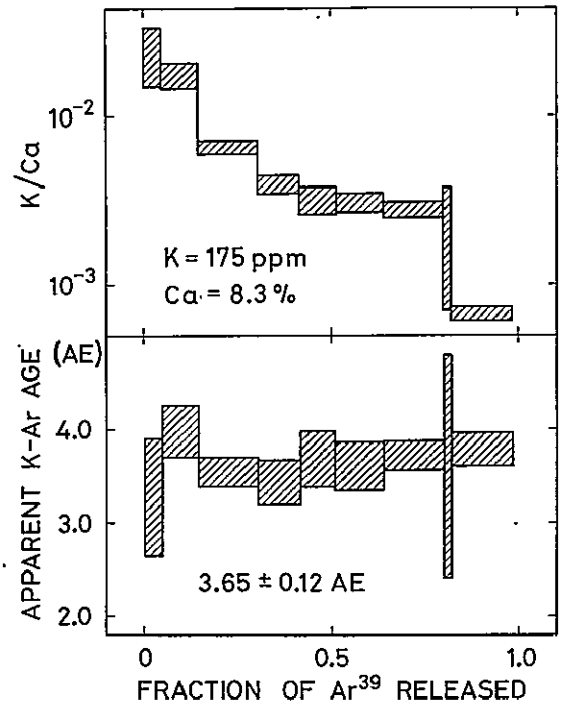

Fig. 1: Ar^{39}-Ar^{40} and K/Ca patterns of lithic fragment L24A.

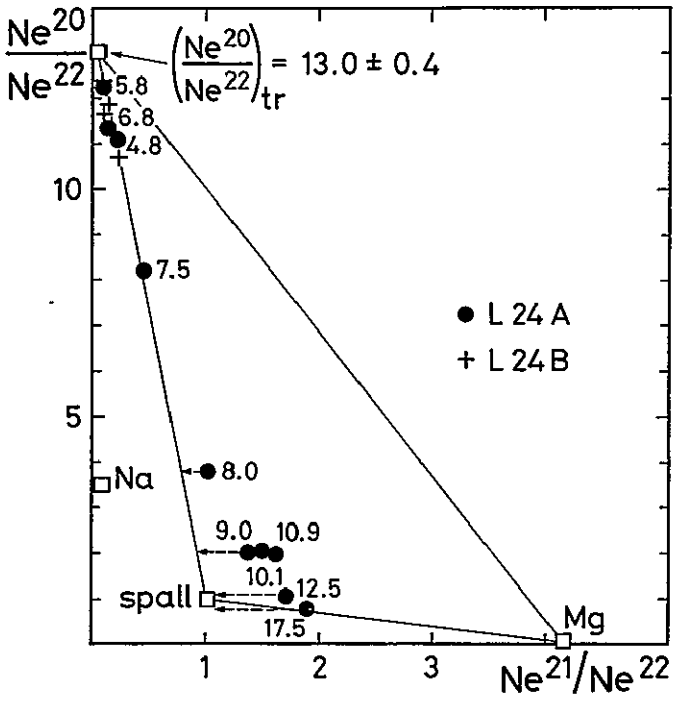

Fig. 2: Three-isotope plot for Ne. Open squares mark the isotopic composition of pure components. The square corresponding to neutron induced Ne from Na might be shifted towards the abscissa along a Ne (air) -Ne(Na) mixing line. Numbers give release temperatures in 100 °C.

PRIMITIVE PB IN LUNA 24 MICROGABBRO 24170

Mitsunobu Tatsumoto and Daniel M. Unruh
U. S. Geological Survey, MS 963, Box 25046, Denver, Colo.

Uranium, thorium, and lead concentrations and lead isotopic compositions have been determined on "whole-rock" and mineral separates from Luna 24 sample, 24170. Although our 12 mg sample of 24170 consists predominantly of ~1 mm fragments (most are monomineralic) and not a single fragment of rock, it is presumed that this material originally represented a specimen of a single coarse-grained ophitic VLT basalt (or gabbro) which was broken up during the coring process (1). Mineral separates, weighing about 0.5-2 mg, of plagioclase (not yet analyzed) light - colored pyroxene (yel-brn), dark-colored pyroxene (dark brown), and opaques (containing also some dark pyroxene) were hand-picked from the material without prior crushing of the material. Our "whole-rock" (WR) consists of several polymineralic fragments. Prior to dissolution, all samples were washed in doubly-distilled acetone for five minutes and rinsed twice with quadruply-distilled H_2O. In addition, the whole-rock (WR) sample was leached for ten minutes with cold 2N HCl. Both the leach (WR-L) and residue (WR-R) fractions were analyzed. The data for the leach and residue fractions were also recombined and are designated by " WR" in the table and figures.

In order to more precisely analyze such small samples, a ^{205}Pb enriched tracer has been employed instead of our previous ^{208}Pb tracer. Since ^{205}Pb is not a naturally occurring isotope, the use of a relatively pure ^{205}Pb tracer allows us to determine both the Pb concentration and Pb isotopic composition from a single analysis, thus eliminating the necessity for making powder - splits or aliquots from solutions. A similar spike has also been employed by the Caltech group (2).

The U, Th, and Pb concentrations and Pb isotopic compositions of the various separates are shown in Table 1, and the Pb data are plotted on a $^{207}Pb/^{204}Pb$ vs. $^{206}Pb/^{204}Pb$ plot in figure 1. The most striking feature is the non-radiogenic character of the Pb data compared to other lunar samples. The non-radiogenicity of WR-L, WR-R, and PXL may be a result of unaccounted for laboratory contamination, as increasing the Pb blank by a factor of two or three will produce $^{206}Pb/^{204}Pb$ ratios of ≳100, but the PXD and OP data can not be explained in this manner, unless the blank is increased by about an order of magnitude. One should also notice that a tie-line connecting PXL, PXD, OP, and ΣWR in figure 1 passes slightly below our blank composition (MT="modern terrestrial"Pb). It is possible that the samples were contaminated with modern terrestrial Pb of a slightly different composition than that of our blank (from the coring device?), but the acetone and H O-washing should have removed any pre-analysis, terrestrial contamination. Furthermore, if signifi-

PRIMITIVE PB IN LUNA 24 MICROGABBRO 24170

M. Tatsumoto and D. M. Unruh

cant Pb contamination were present, we would expect the HCl-leach data to be less radiogenic than the residue, whereas it appears to be more radiogenic (compare WR-L and WR-R in fig. 1). It is also conceivable that the sample was "contaminated" with meteorite Pb on the lunar surface, but at this point such an interpretation would be pure speculation since the Pb isotopic composition of the contaminating meteorite Pb can not be determined.

The simplest interpretation is that the parental material of the Luna 24 micro-gabbro evolved in a lower $^{238}U/^{204}Pb$ ($=\mu$) environment than did those of most Apollo basalts. The non-radiogenic character is compared with that of the orange soil Pb (2) in fig. 1. The orange soil Pb has a larger $^{207}Pb/^{204}Pb$ value but a smaller $^{206}Pb/^{204}Pb$ value than the Luna 24 micro gabbro (the initial $^{238}U/^{204}Pb$ of the orange soil was higher than that of the micro gabbro). The Pb of the Luna 24 micro gabbro is also less radiogenic than those of soils from Luna 16 (4), 20 (5), and 24 (3). The chemical composition of Luna 24 basalt is close to that of Apollo 15 green glass (6) which is the most primitive composition yet found on the moon and is considered to represent deep lunar mantle material ($\gtrsim$400 km). If the non-radiogenic Pb isotopic composition is indigeneous to the rock, the Luna 24 rocks probably represent primitive lunar mantle material.

A tie-line (broken line in fig. 1) connecting PXL (light-colored pyroxene), PXD (dark-colored pyroxene), OP (opaques) and ΣWR (WR-L + WR-R) yields a slope which corresponds to an age of 3.75 $\pm$ 0.09 (2σ) b.y. (10^9 yrs). This age is in reasonably good agreement with the 3.66 $\pm$ 0.12 b.y. Ar-Ar plateau age (3), thus suggesting that the U-Pb system has been closed since crystallization, ~3.7 by ago.

The U-Pb data, however, indicate that there has been some post-crystallizational open system behavior. The U-Pb data plotted on concordia (not shown) do not yield a linear array. A tie-line connecting PXL, PXD, and ΣWR intersects concordia at ~4.7 and 0.7 b.y. when no initial Pb correction is made, and at ~4.2 and 0.4 b.y. when the data are corrected for Canyon Diablo troilite Pb as the initial Pb. The OP data plot distinctly away from this trend, whereas U-Pb data from Luna 24 soils (3, and Allegre, pers. comm.) lie quite close to the 4.7-0.7 b.y. trend. The apparent lower intercepts are quite close to the 0.6 b.y. Ar-Ar exposure age (3). If these 0.4-0.7 b.y. ages represent a real disturbance to the U-Pb system, then the apparent agreement between the Pb-Pb and Ar-Ar ages may be fortuitous. Alternatively, if a very recent disturbance ($\lesssim$0.1 b.y.) has affected the U-Pb system, the disturbance may not be reflected in the Pb-Pb data, in which case the tie-line in fig. 1 may represent a real isochron. However, there is no sound geologic evidence for a severe recent thermal event. Analysis of plagioclaise is still in progress, and the interpretation of the significance of the apparent 3.7 b.y. age must await these results.

PRIM. PB IN LUNA 24 MICROGABBRO 24170

M. Tatsumoto and D. M. Unruh

References

(1) Barsukov et al. (1977) Lunar Science VIII, 67.
(2) Tera and Wasserburg (1976) Lunar Science VII, 858. Tatsumoto et al. (1973) EOS 54, 614.
(3) Allegre et al. (1977), Program for the fourth annual meeting of the Meteoritical Society, Cambridge.
(4) Tera and Wasserburg (1972) Earth Plan. Sci. Lett. 13, 457.
(5) Tera and Wasserburg (1972) Earth Plan. Sci. Lett. 17, 52. Tatsumoto (1973) Geochim. Cosmochim. Acta 37, 1079.
(6) Vaniman and Papike (1977) Geophys. Res. Lett., in press.

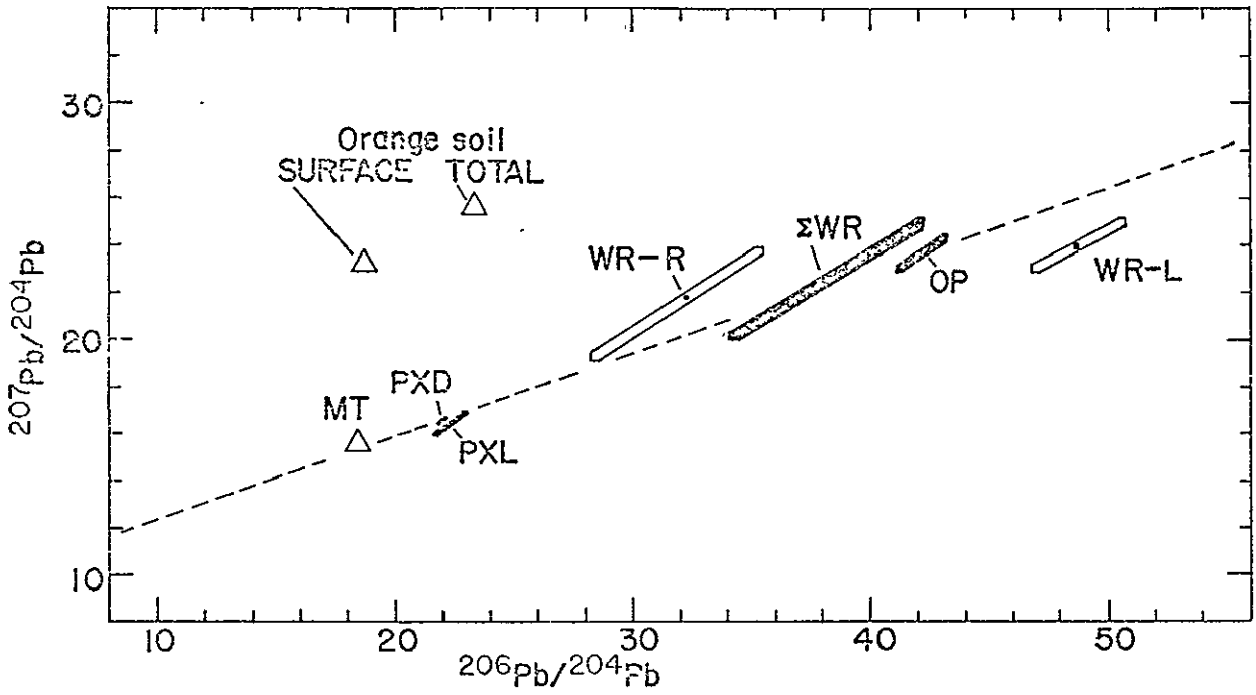

Figure 1. ^{207}Pb-^{206}Pb plot for 24170. The data define an apparent 3.75±0.09 b.y. age. Shown for comparison are data from orange soil 74220.

M. Tatsumoto and D. M. Unruh

TABLE 1. U, Th and Pb concentrations; Pb isotopic compositions and single-stage Model Ages for Luna 24 sample, 24170.

[1] Sample	WT(mg)	Blank (ng)	PPM U	PPM Th	PPM Pb	$\frac{^{238}U}{^{204}Pb}$	$\frac{^{232}Th}{^{238}U}$	$\%^{204}Pb_{BL}$ [2]	$\frac{^{206}Pb}{^{204}Pb}$ [3]	$\frac{^{207}Pb}{^{206}Pb}$ [3]	$\frac{^{208}Pb}{^{206}Pb}$ [3]	$\frac{^{206}Pb}{^{238}U}$	Model Ages In 10^9 yr. $\frac{^{207}Pb}{^{235}U}$	$\frac{^{207}Pb}{^{206}Pb}$	$\frac{^{208}Pb}{^{232}Th}$
PXD	0.9733	0.040	0.052	0.217	1.19	3.07	4.30	3.67	22.2±0.1	0.7453±.0021	1.856±0 0045	10.62	5.73	4.20	12.83
PXL	1.8556	0.040	0.005	0.014	0.051	7.3	2.88	32.4	22.0±0.5	0.760±0.013	1.89±0.03	6.53	4.89	4.27	9.33
OP	0.7793	0.052	0.220	0.584	0.739	31.5	2.75	13.0	42.2±0.9	0.5619±.0055	1.324±0.014	4.61	4.15	3.94	5.38
WR-L	(0.6962)	0.021	0.121	0.420	0.095	169	3.60	40.5	48.7±2.0	0.4922±.0091	1.636±0.012	1.35	2.54	3.70	1.60
WR-R	0.6962	0.052	0.057	0.054	0.018	44	0.98	47.6	32.3±3.2	0.672±0.027	1.28±0.10	2.70	3.66	4.23	4.96
ΣWR [4]	0.6962	-	0.178	0.474	0.203	88	2.75	45.3	38.1±3.8	0.590±.026	1.44±.11	1.82	3.04	4.00	1.99

1 PXD = Dark pyroxene, PXL = Light pyroxene, OP = opaque, WR-L = 2N HCl leach of "whole-rock", WR-R = Residue after leaching

2 $\%^{204}Pb_{BL} = \frac{^{204}Pb_{Blank}}{^{204}Pb_{Blank}+^{204}Pb_{Sample}} \times 100$

3 Uncertainties primarily correspond to a blank uncertainty of 0.015ng for PXD, PXL, WR-R and OP and a blank uncertainty of 0.005 ng for WR-L.

4 ΣWR = recombination of WR-L and WR-R

CHEMICAL DISTINCTIONS AMONG VERY LOW-TI MARE BASALTS. G.J. Taylor, R.D. Warner and K. Keil, Dept. of Geology and Inst. of Meteoritics, Univ. of New Mexico, Albuquerque, New Mexico 87131

Very low-Ti (VLT) mare basalts are distinguished from other mare basalts by low TiO_2 contents (< 1 wt.%). They were first recognized in the Apollo 17 deep drill core (1, 2), but they are also present in other Apollo 17 samples: VLT basalts occur as clasts in soil breccias 78568 and 78547 and Boulder 1, Station 2 breccia 72235 (3); green glassy rock 78526 has the bulk composition of a VLT basalt. VLT basalts are the dominant lithology in Luna 24 soils (4-6), and, though uncommon, also occur in Luna 16 soils (7, 2). This paper summarizes what we know about the bulk compositions of VLT mare basalts and related materials, points out differences among them, and discusses possible genetic relationships.

Bulk compositions of VLT basalts are listed in Tables 1-3 and plotted in Figs. 1-3. Most of the analyses were done in our laboratory by the broad beam microprobe technique. The data were corrected by the nomative procedure described by Bower et al (8). (The analyses reported previously by us (2) are superseded by those in Tables 1-3.) The data in Tables 1-3 suggest that there are at least three types of VLT mare basalt: 1) Apollo 17 (valley floor); 2) Apollo 17 Boulder 1, Station 2; and 3) Luna 16. Luna 24 might constitute a fourth group (see below).

Apollo 17 VLT basalts (Tables 1 and 2) are characterized by low Na_2O and K_2O contents, generally low Fe/(Fe+Mg) ratios (usually < 0.5), and high CaO/Al_2O_3 ratios (usually $\geq$ 0.9). There are exceptions to these rules: 70009, 295-L1 (Table 2, Column 3) has higher Fe/(Fe+Mg) and 70004, 485-L1 (Table 2, column 4) has a low CaO/Al_2O_3 ratio (perhaps due to poor sampling). Analyses of the Apollo 17 suite form fairly clear, coherent chemical trends: As MgO decreases, Al_2O_3 increases (Fig. 1) and Cr_2O_3 decreases (Fig. 2). A reasonable interpretation of these trends is that these rocks are related by fractional crystallization of an Mg-rich silicate (olivine, low-Ca pyroxene) and chromite. The most magnesian of the Apollo 17 VLT basalts (the vitrophyric ones listed in Table 1) contain the appropriate phases as phenocrysts. However, the apparent relationship between MgO and TiO_2 (Fig. 3) is not consistent with such a simple model: As MgO decreases so does TiO_2, which implies fractionation of a Ti-rich phase. However, no appropriate Ti-rich phase precipitates until very late during the crystallization of any VLT basalt. This rules out a simple relationship via fractional crystallization of Apollo 17 VLT basalts. An alternative idea is that they are related by partial melting. However, the trend of increasing MgO, with increasing TiO_2 also argues against this notion: progressively greater degrees of melting ought to produce magmas with increasing MgO and decreasing Fe/(Fe+Mg), as observed, but also decreasing TiO_2, unless the source contains an especially refractory Ti-bearing phase.

We previously suggested that Luna 24 basalts might have formed by fractional crystallization (2). Specifically, we proposed that rock 78526 could have fractionated olivine, pigeonite, and chromite to produce Luna 24 basalts. That idea now seems untenable. Using our revised composition of 78526 and the average Luna 24 fine-grained basalt (4) we made least-

VLT MARE BASALTS

G.J. Taylor et al

squares mixing calculations (Table 4). Although the calculated Luna 24 basalt composition is too high in FeO and too low in CaO, the main problem is that the calculated Luna 24 basalt contains too much TiO_2. To circumvent this problem, we tested whether Apollo 17 vitrophyric lithic fragments lower in TiO_2 than 78526 might represent suitable parent magmas. The results (Table 4) are more satisfactory for TiO_2, though SiO_2 and FeO are too high in the calculated basalt. We also tested whether less magnesian Apollo 17 VLT basalts could fractionate to form the Luna 24 basalts. The calculations (Table 4) result in SiO_2 contents that are much higher than those in the Luna 24 basalts. In all these calculations, the real Luna 24 basalts contain significantly more Na_2O than the calculated ones. Perhaps this indicates that the Luna 24 VLT basalts are fundamentally different from the Apollo 17 VLT basalts.

Luna 16 VLT basalt 313-15 (Table 3) is characterized by higher Na_2O and K_2O than Apollo 17 VLT basalts. It is otherwise very similar. Note that the P_2O_5 content is low and CaO/Al_2O_3 is high; this is not a lithic fragment from a KREEP basalt.

Apollo 17, Boulder 1, Station-2 VLT basalts have high K_2O contents, like the Luna 16 VLT basalt, but have Na_2O contents similar to Apollo 17 VLT basalts from the valley floor. They also have low FeO and Fe/(Fe+Mg). Two of the four have CaO/Al_2O_3 ratios in the normal mare basaltic range, but the other two have CaO/Al_2O_3 values closer to those observed in nonmare, rather than mare rocks. On the other hand, P_2O_5 levels are quite low, suggesting that they are not KREEP basalts. Clearly, more work must be done on these samples, particularly since they occur in a highland breccia.

Many lunar glasses have affinities to mare basalts and have low TiO_2 contents. We have plotted these glasses in Fig. 4 (data from the literature and our laboratory). There is a clear trend of decreasing MgO with increasing Al_2O_3; the lithic fragments also fall on this trend. This suggests that there is a general genetic relationship among these very low-Ti, mare-like substances. Perhaps they represent varying degrees of partial melting of similar source regions in the Moon. The differences we observe among the VLT basalts might be due to minor differences in the composition of the source regions, assimilation reactions, or fractional crystallization.

References

1) Vaniman, D. and Papike, J. (1977) Proc. Lunar Sci. Conf. 8th, in press; 2) Taylor G.J., Warner, R., and Keil, K. (1977) Geophys. Res. Lett. 4, 207-210; 3) Ryder G., et al (1975) The Moon 14, 327-357; 4) Taylor, G.J., et al, (1977) this volume; 5) Ryder G., et al (1977) The Moon, in press; 6) Vaniman, D. and Papike, J. (1977) Geophys. Res. Lett., in press; 7) Green, J.A. et al (1972) Sp. Publ. No. 5, UNM Inst. of Meteoritics. 8) Bower, J.F. et al (1977) Abstracts of the VIII International Conf. on X-ray Optics and Microanalysis, in press.

VLT MARE BASALTS

G.J. Taylor et al.

Table 1. Compositions (wt.%) of Apollo 17 vitrophyric (glassy) VLT mare basalts.

	1	2	3	4	5	6	7
SiO_2	47 5	48.5	48.8	47 5	48 0	48 8	47.0
TiO_2	0 95	0.70	0 57	0.62	0.57	0.69	0.67
Al_2O_3	10.9	11.8	12 1	10 9	11.6	10.0	10.4
Cr_2O_3	0.88	0 66	0 67	0.62	0 55	0.69	0 87
FeO	17 8	18 2	18 2	17 6	17 5	17 9	18 9
MnO	0 27	0 29	0.30	0.21	0 22	0.30	0.30
MgO	11.5	10.6	11.1	11.0	10.5	11.8	13.9
CaO	9.8	10.3	10 3	11.0	10.7	9.4	9.3
Na_2O	0.16	0 12	0 12	0.26	0.18	0 06	0.09
K_2O	0.02	<0 02	<0.02	0 05	0 05	0 02	0.02
P_2O_5	<0.02	<0 02	<0.02	<0 02	0.02	—	—
Total	99 78	101.18	102.18	99.76	99.89	99.7	101.1
Fe/(Fe+Mg)	47	49	48	.47	48	.46	43
CaO/Al_2O_3	90	.87	.85	1.01	92	.93	90

1) 78526 (average of two analyses reported by Laul et al (1973) and Murali et al (1977), with SiO_2 determined by broad-beam, 2) 70008,367-G1, 3) 70007,321-G1; 4) 78548,3-B, 5) 78548,3-C, 70007, 328 (Vaniman and Papike, 1977), 6) 70008, 362 (Vaniman and Papike, 1977).

Table 2. Bulk compositions (wt %) of Apollo 17 and Luna 24 VLT mare basaltic lithic fragments.

	1	2	3	4	5	6	7	8
SiO_2	50 7	50.5	48 4	48 1	48.0	48.7	48.1	46.7
TiO_2	0 56	0 36	0 73	1.0	0.29	0.50	0.36	0.69
Al_2O_3	10.8	11 8	12.7	15 1	12.5	11.4	11.2	14 0
Cr_2O_3	0 47	0 35	0 27	0 32	0 53	0.60	0.60	0 28
FeO	16 4	16.2	18 0	14.4	17 4	19.0	18.2	17 1
MnO	0 30	0 32	0.34	0.26	0 36	0.26	0.26	0.28
MgO	11 6	10 0	7 0	9 1	10 5	9 4	11.0	6.6
CaO	10.0	11 5	12 9	12 3	11.0	10.2	10.2	13 2
Na_2O	0 10	0.11	0.16	0.23	0.16	0.15	0.15	0.31
K_2O	<0.02	0 02	0.03	0 06	0.04	0.04	0.01	0.04
P_2O_5	<0.02	<0 02	<0 02	0 03	0.04	—	—	0.02
Total	100.93	101 16	100.53	100 90	100.82	100 2	100.1	99.22
Fe/(Fe+Mg)	.44	.48	.59	.47	.48	.55	.48	.59
CaO/Al_2O_3	.93	97	1.02	.81	88	.89	90	.94

1) 70007,325-L1, 2) 70007,333-L1, 3) 70009,295-L1; 4) 70004,485-L1, 5) 78568,1-1, 6) 70008,370 (Vaniman and Papike, 1977), 7) 70007,328 (Vaniman and Papike, 1977), 8) Luna 24, average of 30 fine-grained basaltic lithic fragments (Taylor et al., 1977b)

Table 3. Bulk compositions (wt.%) of Luna 16 and Apollo 17 Boulder 1, Station 2 VLT mare basaltic lithic fragments. Analyses 3-5 are averages of broad-beam microprobe analyses done in our laboratory and reported by Ryder et al (1977)

	1	2	3	4	5
SiO_2	47.5	45 2	45.5	46.7	46.5
TiO_2	0 35	0 53	0 26	0 38	0 70
Al_2O_3	12 7	13.8	15.3	11 8	10 9
Cr_2O_3	0 32	0 63	0 68	0 33	0.88
FeO	15.8	15.1	13.1	15.5	17 4
MnO	0 27	0.20	0.23	0.28	0.28
MgO	10.2	10.4	10.3	12.4	13 5
CaO	11 9	10.7	11.3	10.3	9.9
Na_2O	0.60	0 19	0.14	0 20	0.15
K_2O	0.20	0 10	0 11	0.26	0.10
P_2O_5	0 05	0.03	0.03	0.02	<0.02
Total	99 89	96.88	96.95	98.17	100.31
Fe/(Fe+Mg)	.47	.45	.42	41	.42
CaO/Al_2O_3	94	.78	.74	.87	.91

1) Luna 16, 313-15, 2) 72235,59-1, 3) 72235,59-2, 4) 72235,59-3, 5) 72235,59-4.

Table 4 Data used in and results of petrologic mixing calculations

	Data								Results			
	1	2	3	4	5	6	7	8	9	10	11	12
SiO_2	53 6	37 3	38 9		47 5	48 0	50 6	46 7	47 1	47 0	47 8	49 6
TiO_2	0 12	—	—	0 66	0 95	0 57	0 46	0 69	1 26	1 25	0 76	0 57
Al_2O_3	0 92	—	—	15 3	10 9	11 6	11 5	14 0	14 4	14 2	14 5	14 6
Cr_2O_3	0 53	0.35	0 15	58 5	0 88	0 55	0 41	0 29	0 32	0 11	0 30	0 38
FeO	15 8	28 3	20 4	27 2	17 8	17 5	16 1	17 1	17 6	18 1	17 0	16 5
MgO	24 7	33 4	40 6	0 53	11.5	10 5	10 8	6 6	6 4	6 4	6 6	6 4
CaO	3 1	0 25	0 25	6 1	9 8	10 7	10 8	13 2	12 4	12 3	12 8	13 2
Na_2O	—	—	—	—	0 16	0 18	0 20	0 31	0 22	0 22	0 23	0 15
Fe/(Fe+Mg)	26	32	22	.97	47	45	46	59	61	61	60	59

1) Low Ca pyroxene in 78526 2) olivine in 78526 3) calculated liquidus olivine for 78526 (Kp=0 33), plus Cr_2O_3 and CaO from column 2 4) chromite in 78526 5) 78526 6) average of 4 Apollo 17 glassy lithic fragments 7) average of 2 Apollo 17 VLT lithic fragments 8) Average Luna 24 fine grained basalt 9) 78526 (col 5) - 20 8% col 1 + 81 col 2-11 col 4=Luna 24 basalt (col. 8) 10) 78526 (col 5) - 21 4% col 1-3 5% col 3-1 4% col 4= Luna 24 basalt (col. 8). 11) col 6-17 9% col. 1 - 3 5% col 2 + 1 6% col 3= Luna 24 basalt (col 8) 12) Col 7 24 2% col 1= Luna 24 basalt (col 8)

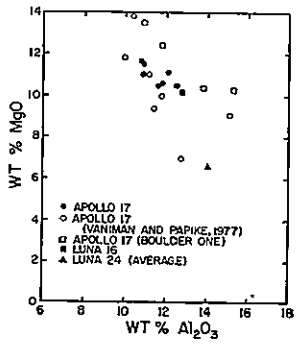

Fig. 1

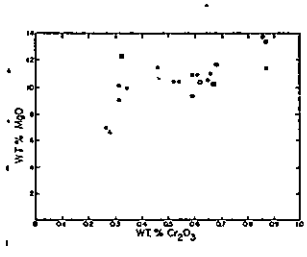

Fig. 2

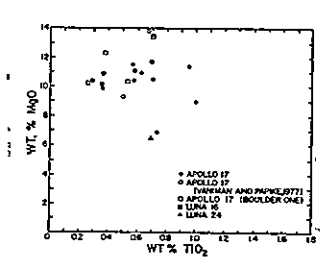

Fig. 3

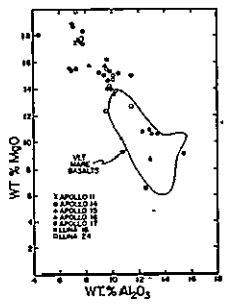

Fig. 4

THE LUNA 24 REGOLITH: LITHOLOGIC ABUNDANCES IN THE 250-500 μm SIZE FRACTION, AND COMPOSITIONS OF AGGLUTINATES AND NONMARE LITHIC FRAGMENTS AND GLASSES. G.J. Taylor, R. Warner, S. Wentworth, and K. Keil, Dept. of Geology and Inst. of Meteoritics, Univ. of New Mexico, Albuquerque, New Mexico 87131

We have classified the 700 soil particles on the 13 sections (250-500 μm size range) allocated to us from 6 Luna 24 soils. The results are given in Table 1. Although the number of fragments in any given sample is too small for rigorous statistical treatment, several observations are pertinent. First, the abundance of nonmare lithic fragments is low. The soil appears to be derived from predominantly mare lithologies with a very small contribution from nonmare sources. Second, the dominant mare lithology is coarse basalt, which is represented by identifiable lithic fragments and by monomineralic fragments. (Compositions of the monomineralic fragments (1) suggest that almost all of them are derived from mare basalts.) Third, in all but one case (24077), the abundance of vitric soil breccias exceeds that of agglutinates. Our results are consistent with those reported by Ryder et al (2).

We determined the compositions of glassy areas in agglutinates. Of the 80 agglutinates identified in the six soils, only 13 had glassy, clast-free areas large enough (> 10 μm across) to allow accurate microprobe analysis. The analyses of those 13 agglutinates are given in Table 2. We cannot make a statistical analysis based on only 13 analyses, but we note two things: First, although the compositions are generally consistent with formation of these agglutinates in a soil composed predominantly of VLT mare basalts, the agglutinates are generally richer in TiO_2 and MgO than the average Luna 24 fine-grained basalt. This suggests that a basalt somewhat richer in TiO_2 and MgO is present at the Luna 24 site. Two homogeneous glasses have appropriate compositions (1). The MgO content of these agglutinates (hence of the Luna 24 soil) may also have been enhanced by the presence of olivine-rich rocks similar in composition to Apollo 15 green glass (1). Second, all four agglutinates in 24109 contain significantly more K_2O (~0.1 wt.%) than the others. Except for one of these four, however, their P_2O_5 levels are normal. This seems to rule out an appreciable contribution from KREEPy lithologies. This conclusion is supported by rare earth contents of the Luna 24 soils, which indicate that there is little, if any, contribution from KREEP rocks (3). It is not clear why the K_2O contents are higher in the four agglutinates from 24109.

We have also determined the compositions of nonmare lithic fragments, aphanitic fragments, and glasses. We have listed the results in Table 3. The compositions of the lithic fragments were determined by broad beam microprobe analysis; the data were corrected by the normative procedure pioneered by Bower et al (4). Both ANT and KREEPy (low-K Fra Mauro basalt) compositions are represented among the analyses in Table 3; a few are ambiguous. Curiously, none of the lithic fragments listed in Table 3 have textures typical of ANT or KREEP rocks. Instead, they are all impact melts. In fact, of the eight nonmare lithic fragments on our sections, only one had a typical texture: an apparent granulitic ANT fragment that was too

small for bulk analysis. It appears that nonmare rocks are represented in the Luna 24 soil by shock melts of one sort or another.

References

1) Taylor et al (1977) Petrology and chemistry of Luna 24 mare basalts and basaltic glasses, this volume.
2) Ryder et al (1977) Basalts from Mare Crisium, The Moon, in press.
3) Ma, M.-S. and Schmitt, R. (1977), this volume.
4) Bower, J.F., et al (1977) Abstracts of the VIII Internatl. Conf. on X-ray optics and Microanalysis, in press.

Table 1. Relative proportions of rocks, minerals, and glasses in the 250-500 μm size range in six Luna 24 soils.

	24077	24109	24149	24182	24174	24210
No. of particles	109	176	75	22	273	45
Agglutinates	23.9	16.5	1.3		7.7	6.7
Soil Breccias	10.1	21.0	48.0	9.1	12.8	22.2
Aphanitic frags	2.8	2.3	4.0		3.7	4.4
Glasses						
colored	4.6	1.1	—	—	—	2.2
colorless	—	0.6	—	—	0.7	—
Mare Basalts						
coarse-grained	7.3	8.0	5.3	18.2	12.4	—
fine-grained	9.2	8.5	8.0	9.1	7.0	8.9
metabasalts	2.8	—	2.7	13.6	4.0	—
Nonmare lithic frags.	0.9	0.6	—	4.5	1.1	6.7
Other lithic frags.	2.8	1.7	—	—	1.1	8.9
Mineral Fragments						
plagioclase	8.3	9.1	6.7	13.6	11.4	15.6
pyroxene	24.8	25.6	21.3	22.7	30.0	17.8
olivine	2.8	4.5	2.7	9.1	7.7	6.7
other	—	0.6	—	—	0.4	—
Total	100.3	100.1	100.0	99.9	100.0	100.1

LITHOLOGIC ABUNDANCES.....

G.J. Taylor et al.

Table 2. Compositions (wt.%) of glassy areas in agglutinates in Luna 24 soils.

	24077							24109					
	1	2	3	4	5	6	7	8	9	10	11	12	13
SiO_2	45.2	44.8	43.8	44.2	44.2	43.5	44.1	43.6	39.2	44.7	44.3	46.6	46.1
TiO_2	0.85	0.66	2.84	0.72	1.33	1.36	0.83	0.87	3.9	0.60	0.92	0.77	0.96
Al_2O_3	12.8	14.6	11.0	16.9	11.0	14.0	13.4	11.3	12.8	23.0	17.3	9.1	11.9
Cr_2O_3	0.40	0.31	0.36	0.29	0.43	0.38	0.48	0.38	0.39	0.21	0.22	0.43	0.33
FeO	18.2	17.6	20.8	16.0	20.6	19.5	18.5	21.0	22.4	10.5	14.6	20.2	20.1
MnO	0.23	0.17	0.25	0.18	0.25	0.34	0.36	0.35	0.30	0.18	0.22	0.19	0.15
MgO	10.3	9.9	9.7	8.9	10.3	10.2	10.0	9.3	8.6	5.8	8.8	11.2	8.7
CaO	12.3	11.6	10.9	12.8	11.0	11.3	11.6	11.3	10.5	15.2	13.5	11.0	11.2
Na_2O	0.19	0.23	0.20	0.21	0.26	0.17	0.15	0.18	0.25	0.24	0.25	0.13	0.19
K_2O	0.04	0.05	0.05	0.04	0.04	0.03	0.03	0.10	0.11	0.09	0.13	0.04	0.04
P_2O_5	<0.02	0.03	0.03	0.04	0.04	0.03	0.04	0.02	0.12	0.03	0.06	0.02	0.02
Total	100.52	99.95	99.93	100.28	99.45	100.81	99.49	98.40	98.57	100.55	100.30	99.68	99.69

1) 24077,43-33; 2) 24077,43-41; 3) 24077,43-25; 4) 24077,43-16; 5) 24077,40-2; 6) 24077,40-14; 7) 24077,40-19, 8) 24109,55-2; 9) 24109,55-27; 10) 24109,60-8; 11) 24109,60-53; 12) 24149,42-8; 13) 24174,59-4.

Table 3. Compositions (wt.%) of nonmare lithic fragments, aphanitic particles, and glasses in Luna 24 soils.

	Lithic Fragments							Aphanites			Glasses		
	1	2	3	4	5	6	7	8	9	10	11	12	13
SiO_2	44.0	44.0	44.0	45.8	44.4	43.8	45.2	43.4	46.0	45.6	47.2	45.9	45.6
TiO_2	0.08	0.23	0.19	0.19	0.58	0.21	0.56	0.18	1.22	1.66	0.29	0.09	0.68
Al_2O_3	28.9	28.6	22.9	23.0	24.1	25.0	22.6	32.0	20.3	16.8	24.2	30.6	26.3
Cr_2O_3	0.02	0.10	0.17	0.15	0.19	0.06	0.08	<0.02	0.13	0.34	0.14	0.07	0.10
FeO	5.1	4.3	6.7	5.7	9.0	4.5	10.6	3.0	7.9	13.8	5.2	3.6	6.0
MnO	0.09	0.06	0.10	0.16	0.08	0.04	0.14	0.04	0.10	0.19	0.08	<0.02	<0.02
MgO	5.6	4.8	10.6	11.8	4.4	8.7	3.1	3.1	11.0	9.2	8.2	2.8	6.7
CaO	15.6	16.1	13.7	12.4	15.6	14.8	15.2	17.8	12.1	12.0	13.4	16.8	14.8
Na_2O	0.41	0.34	0.45	0.60	0.34	0.30	0.59	0.16	0.64	0.55	0.83	0.36	0.26
K_2O	0.03	0.05	0.06	0.07	0.05	0.11	0.11	0.02	0.28	0.18	0.12	0.03	0.03
P_2O_5	<0.02	0.02	<0.02	<0.02	<0.02	0.07	0.12	<0.02	0.17	0.13	<0.02	<0.02	<0.02
Total	99.8	98.4	98.9	99.8	99.0	97.8	98.2	99.8	99.8	100.4	99.7	100.3	100.5
Fe/(Fe+Mg)	.34	.33	.26	.21	.53	.22	.66	.35	.29	.46	.26	.42	.34
CaO/Al_2O_3	.54	.56	.60	.54	.65	.59	.67	.56	.60	.71	.55	.55	.56

1) 24109,60-45; 2) 24174,58-41; 3) 24210,43-45; 4) 24174,58-44; 5) 24174,60-65; 6) 24210,43-20; 7) 24174,65-19; 8) 24149,43-25; 9) 24077,43-30; 10) 24077,43-31; 11) 24149,42-26 (colorless); 12) 24174,60-64 (colorless); 13) 24210,43-7 (colorless).

PETROLOGY AND CHEMISTRY OF LUNA 24 MARE BASALTS AND BASALTIC GLASSES. G.J. Taylor, R. Warner, S. Wentworth, K. Keil and U. Sayeed, Dept. of Geology and Inst. of Meteoritics, Univ. of New Mexico, Albuquerque, New Mexico 87131

In this paper, we describe the petrology of Luna 24 basalts, with emphasis on their bulk compositions. The basalts fall into three main categories: 1) Fine-grained basalts, with ophitic to subophitic textures, and crystal sizes smaller than ∿ 100 μm. 2) Coarse-grained basalts, which have grain sizes larger than 250 μm. These were referred to as "gabbros" by Barsukov (1). The finer-grained members of this group seem to have ophitic or subophitic textures, but we could not discern the texture for fragments with grain sizes larger than ∿ 500 μm. Monomineralic fragments are probably from coarse basalts. 3) Metabasalts, are fine-grained (crystals are smaller than 25 μm) and have granulitic textures and equilibrated mineral compositions. A fourth type of rock also occurs. It is more mafic than the basalts and richer in olivine. The texture of three fragments ranges from glassy with olivine microphenocrysts to basaltic to granular.

We determined the bulk compositions of 30 fine-grained basalts, 7 metabasalts, and 3 olivine-rich lithic fragments by broad-beam microprobe analysis. The analyses were corrected by the method outlined by Bower et al (2). The results are given in Table 1 and shown in Figs. 1 and 2. (We also estimated the bulk composition of the coarse basalts; see below). The lines in Fig. 1 (fine-grained basalts) and Fig. 2 (metabasalts) start at the average composition (Table 1) and extend toward the average pyroxene or plagioclase compositions (Table 2). The tendency for the plotted points to string out along these lines suggests that the range of compositions observed is due to sampling, not to variations in magma compositions. Consequently, we listed only the averages of our analyses of fine-grained basalts and metabasalts in Table 1. Two points are obvious from a study of these two average compositions: First, the two rock types have nearly identical compositions, except for a discrepancy in FeO. Second, the Luna 24 basalts have higher Al_2O_3 and lower TiO_2 and MgO than other mare basalts. They are most similar to Apollo 17 VLT mare basalts, but have lower MgO contents. We discuss the chemical relationships among the known samples of VLT mare basalts in a separate abstract (3).

Pyroxene compositions are illustrated in Figs. 3 and 4 and olivine compositions are shown in Fig. 5. Average compositions are given in Table 2. These data show the following: First, the metabasalts have the most distinctive pyroxene and olivine compositions; they have obviously been metamorphosed. Second, the fine-grained basalts and coarse basalt 24170 have nearly identical pyroxene compositions. This suggests that they are similar in bulk composition. Third, coarse basalt lithic fragments have similar pyroxene compositions as 24170, though their olivines are richer in MgO. Fourth, monomineralic pyroxene and olivines extend to more magnesian values than either coarse basalt 24170, coarse basalt lithic fragments, or fine-grained basalts. The average pyroxene and olivine compositions given in Table 2 for monomineralic fragments exclude analyses with $>En_{70}$ or $>Fo_{70}$. These magnesian phases may be derived from the olivine-rich rocks

or from nonmare lithologies. Fifth, in all cases (except metabasalts), as Fe/(Fe+Mg) increases in pyroxene, Ti increases (Fig. 4). This is typical for magmas with low TiO_2 contents. Sixth, the details of pyroxene compositional trends have been described by Vaniman and Papike (4) and Ryder et al (5); our results are similar.

We estimated the modal and bulk chemical composition of the coarse basalt by assuming that there is only one magma from which all the coarse basalts crystallized and that the combined mode of the mineral fragments and coarse basalt lithic fragments approximates the mode of the coarse basalt lithology. Table 3 lists the abundances of monomineralic grains (column A), the mode of the coarse basalt lithic fragments (column B), and the weighted average of the two (column C). We suggest that column C is a good estimate of the average modal composition of the coarse basalt. Its bulk composition can be estimated from this mode and the average mineral compositions (Table 2). There are two logical choices for the average mineral composition: the monomineralic fragments and 24170. We used the monomineralic fragments because 24170 was hand-picked and, therefore, may not be a random sample. Our estimated bulk composition is given in Table 1, column 3. Compared to the fine-grained basalts and the metabasalts, it contains less Al_2O_3, more MgO, and has lower Fe/(Fe+Mg). The important point is that the rock is apparently a VLT mare basalt; pyroxene compositions support this conclusion (Fig. 4).

The olivine-rich lithic fragments are clearly distinct from the L-24 mare basalts. They are much richer in MgO, and poorer in Al_2O_3 and CaO. Their compositions most closely resemble the Apollo 15 green glass. (Ryder et al (5) report one analysis of an olivine vitrophyre. Its composition is very similar, except for higher TiO_2, 1.4 wt.%).

Our sections contained only seven homogeneous glass fragments of mare affinity; their compositions are given in Table 4. One (column 1) is similar to the Apollo 15 green glass, four (columns 2-5) have VLT mare basaltic compositions (though they are generally more similar to Apollo 17 VLT's than Luna 24), and two (columns 6 and 7) have higher TiO_2 contents than VLT mare basalts.

References

1) Barsukov, V.L. (1977) Proc. Lunar Sci. Conf 8th, in press. 2) Bower, J.F. et al (1977) Abstracts of the VIII International Conf. on X-ray Optics and Microanalysis, in press. 3) Taylor, G.J. et al (1977) Chemical distinctions among VLT mare basalts, this volume. 4) Vaniman, D.T. and Papike, J.J. (1977) Geophys. Res. Lett, in press. 5) Ryder, G., et al (1977) The Moon, in press.

LUNA 24 MARE BASALTS .....

G.J. Taylor et al.

Table 1. Bulk compositions (wt.%) of Luna 24 mare lithologies.

	1	2	3	4	5	6
SiO_2	46 7	46.4	47 1	45.4	43 1	44.2
TiO_2	0 69	0.79	0 6	0.66	0.15	0.62
Al_2O_3	14.0	13 7	10 7	8.9	6.9	7.7
Cr_2O_3	0.28	0.20	0.2	0.21	0.65	0 53
FeO	17.1	18 5	20.0	19.2	20.1	21.6
MnO	0.28	0.30	—	0.37	0.25	0 43
MgO	6.6	6.5	9.0	15.4	20.8	18.2
CaO	13.2	13.3	11.8	8.9	6.9	7 0
Na_2O	0.31	0.28	0.25	0 20	0 12	0 15
K_2O	0 04	0.04	—	0 05	0 03	0 05
P_2O_5	0.02	<0.02	—	<0 02	<0.02	0.03
Total	99 22	100.01	99.65	99 29	99 00	100.51
Fe/(Fe+Mg)	59	61	55	41	.35	40
CaO/Al_2O_3	94	97	1.1	1 0	1.0	91

1) Average of 30 broad-beam analyses of Luna 24 fine-grained basalts
2) Average of 7 broad-beam analyses of Luna 24 metabasalts
3) Coarse-grained basaltic lithology; calculated from modal data and average mineral compositions (see text).
4) Olivine-rich, microporphyritic lithic fragment 24149, 42-18
5) Olivine-rich, granular lithic fragment 24174, 65-7.
6) Olivine vitrophyre 24174, 59-12.

Table 2 Average mineral compositions (wt %) in coarse basalt 24170, monomineralic fragments (MINO), and fine-grained basalts (FG) MESO refers to mesostasis in coarse basalts Its composition was determined by broad beam analysis ILM is ilmenite in 24170 N is the number of analyses

	Pyroxene				Olivine				Plagioclase			
	24170	MINO	FG		24170	MINO	FG		24170	MINO	MESO	ILM
N	72	136	104		20	27	12		20	30	3	2
SiO_2	50 8	50 4	49 4		31 6	33 5	33 3		45 1	46 0	49 3	—
TiO_2	0 58	0 57	0 58		—	—	—		—	—	0 45	52 5
Al_2O_3	1 26	1 30	1 65		—	—	—		35 2	34 6	0 30	—
Cr_2O_3	0 33	0 37	0 41		—	—	—		—	—	<0 03	0 20
FeO	24 2	23 5	26 0		58 3	49 1	49 3		0 52	0 81	42 1	46 8
MnO	0 46	0 38	0 37		—	—	—		—	—	0 68	—
MgO	11 1	12 6	11 6		9 0	15 5	16 6		<0 05	0 05	1 4	0 6
CaO	12 5	11 2	10 6		0 49	0 43	0 44		19 0	18 6	6 2	—
Na_2O	—	—	—		—	—	—		0 69	0 86	<0 03	—
K_2O	—	—	—		—	—	—		0 03	0 03	0 06	—
Total	101 25	100 12	100 61		99 39	98 33	99 64		100 54	100 75	100 47	100 1
En	33 0	3[illegible] 1	34 1	Fo	21 6	35 7	37 5	An	96 2	95 2		
Fs	40 3	38 9	41 2	Fa	78 4	64 3	62 5	Ab	3 7	4 7		
Wo	26 7	21 8	22 4					Or	0 1	0 1		

Table 3. Estimated average modal composition (vol.%) of coarse-grained basalts in Luna 24 soils.

	A	B	C
Plagioclase	23.8	54.9	28.7
Pyroxene	61.4	33.9 (41.1	57.0
Olivine	13.1	7.2)	12.2
Opaques	0.3	1.9	0.6
Silica	0.3	1.9	0.6
Mesostasis	1.0	0.1	0.9
	99.9	99.9	100.0

A. Computed from abundances of 298 monomineralic fragments in 5 soils.

B. Mode of 52 coarse-grained basalt lithic fragments. Pyroxene and olivine in same ratio as column A.

C. Columns A and B combined, weighted according to the abundances of monomineralic fragments and coarse basalt lithic fragments in 5 soils. Uses olivine/pyroxene ratio from column A.

Table 4 Compositions (wt.%) of homogeneous glasses of mare affinity in Luna 24 soils.

	1	2	3	4	5	6	7
SiO_2	43.6	45 2	44.8	44 8	45.7	44 2	44.4
TiO_2	0 88	0.97	0.99	0.99	1.00	1.33	1.70
Al_2O_3	7.8	9.6	11.4	13'5	12.5	11.0	11.6
Cr_2O_3	0.32	0.39	0.35	0 40	0.22	0.43	0 41
FeO	22.8	21 0	18.6	18.9	20.9	20.6	21 2
MnO	0.18	0.23	0.26	0.19	0.25	0.25	0 21
MgO	17.7	12.3	12.7	8 2	6.6	10.3	8.4
CaO	7 2	10.0	9.8	12 1	12.9	11 0	11.0
Na_2O	0 38	0 16	0.24	0 06	0 21	0.26	0 27
K_2O	0 05	0 03	0.04	0.03	0.09	0.04	0.04
P_2O_5	0.04	0 02	0.05	<0 02	0.02	0.04	0.06
Total	100.95	99.90	99.23	99.17	100.39	99.45	99.29
Fe/(Fe+Mg)	.42	.49	.45	.56	.64	.53	59
CaO/Al_2O_3	92	1 04	.86	.90	1 03	1 00	.95

1) 24077,43-34 (pale yellow), 2) 24077,43-2 (pale yellow), 3) 24077,43-42 (greenish yellow), 4) 24210,43-31 (pale yellow), 5) 24109,53-17 (red-brown); 6) 24077,40-2 (pale yellow), 7) 24077,43-5 (pale yellow).

LUNA 24 MARE BASALTS.....

G.J. Taylor et al.

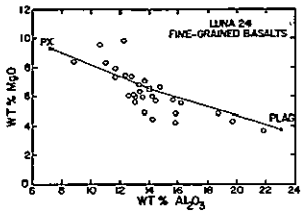

Fig. 1

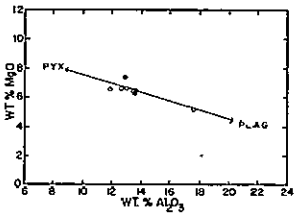

Fig. 2

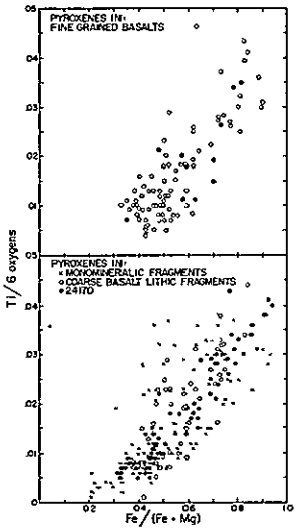

Fig. 4

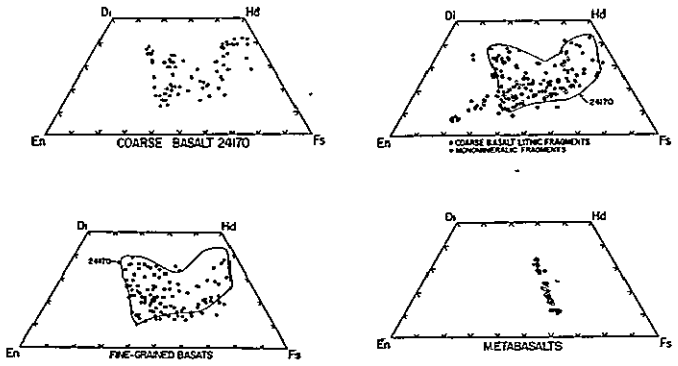

Fig. 3

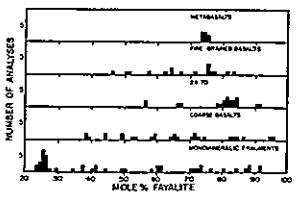

Fig. 5

COOLING RATES OF LUNA 24 SUB-OPHITIC BASALTS

Lawrence A. Taylor¢, P.I.K. Onorato*, D.R. Uhlmann*, and R.A. Coish¢; ¢ = Dept. of Geol. Sci., The Univ. of Tenn., Knoxville, Tn 37916; * = Dept. of Mat. Sci. & Engr., M.I.T., Cambridge, Mass. 02139.

It has been shown that the rate at which a magma cools significantly affects the textures and mineral chemistries of the solidified rock (1,2,3). In the recent past, much attention has been directed toward finding methods of estimating the cooling rates of lunar basalts. Lunar researchers have approached this problem from two aspects, one textural and the other chemical. First, variations in the crystal morphology and texture of olivine and plagioclase have been calibrated to obtain cooling rates of lunar basalts (e.g. 2,4,5). Secondly, cooling rates have been determined by modeling: a) the kinetics of the reequilibration of Zr partitioning between ilmenite and ulvöspinel (6) and b) the Fe^{2+} and Mg^{2+} diffusion in olivine during cooling (7).

In this study, cooling rates of Luna 24 sub-ophitic basalts have been calculated using both the Zr partitioning method (6) and a refinement of the olivine diffusion technique (7).

SAMPLE - 24077,68 is a sub-ophitic basalt fragment approximately 1 mm by 1.2 mm and was chosen for application of the cooling rate indicators because it is a representative of the most common basalt type at Mare Crisium (8). The fragment consists of phenocrysts (o.6 by 0.4 mm) of olivine and microphenocrysts of olivine and pyroxene set in a matrix of plagioclase laths (0.15 mm long) partially enclosed by pyroxenes. Accessory minerals include minor chromite-ulvöspinel and ilmenite. Like all other Luna 24 sub-ophitic basalts, this fragment has mineral compositions which suggest that it crystallized from a liquid with a high Fe/Fe + Mg ratio. Early formed olivines have Fo 58-60 compositions and later smaller olivines have Fo 20-25 contents; pyroxenes range from $Wo_{13}En_{51}Fs_{35}$ to $Wo_{24}En_{23}Fs_{53}$. The texture of 24077,68 consisting of these medium-grained minerals indicate that this assemblage may represent a "relatively" slowly cooled lunar rock.

OLIVINE COOLING SPEEDOMETER - Recently, Taylor et al. (7) reported on a method for estimating the cooling rate from a compositional profile in olivine. A major limitation of that kinetic model was due to a lack of data on the "as-solidified profile", of olivine due to primary crystallization. A step function based on mass balance considerations was assumed, and this resulted in minimum cooling rate estimates. Our present analysis takes specific account of the partial equilibrium which occurs during solidification and is based on an initial Fo profile across the olivine grain. That is, the "as-solidified profile" is now calculated as an important sophistification of the overall kinetic model of the cooling process.

In estimating the initial Fo profile of the olivine, the following assumptions are made: 1) Growth starts at some temperature slightly below the liquidus; in the present case, at 1200°C; 2) An olivine grain grows in a small spherical volume (radius = 570 μm) of a well-stirred melt; 3) The composition of the olivine solidifying at any time is in equilibrium with the melt; 4) Diffusion in the olivine may take place during solidification; 5) Olivine is the only major FeMg phase crystallizing; and 6) The modal % of olivine, an

average Fo content, and an approximate bulk composition of the melt can be used to calculate the amount of MgO and FeO for use in the crystallization of the olivine.

In order to calculate the initial olivine profile, the melt composition for a typical sub-ophitic basalt is estimated at 18.5% FeO and 6.0% MgO (9). Olivine makes up about 10 modal % of the solidified rock (10) with an average Fo content of about 45%; this restricts the amount of MgO and FeO available for total olivine crystallization. The partition relation of Roeder and Emslie (11) is:

$$\log \frac{C^{ol}_{FeO}}{C^{liq}_{FeO}} \frac{C^{liq}_{MgO}}{C^{ol}_{MgO}} = \frac{171}{T} - 0.63$$

This results in an initial olivine core of about Fo 65 at 1200°C - a not unreasonable value based on the reported olivine compositions of Vaniman & Papike (9) and Ryder et al. (10). The growth rate of the olivine grain is a function of temperature and is estimated from the nucleation and growth measurements of Bianco & Taylor (3) as about 4×10^{-7} cm sec^{-1} at 1200°C and for purposes of the present analyses, an isotropic growth is assumed. The diffusion coefficient has been shown by the detailed investigation of Buening & Buseck (12) to be a function of: 1) Temperature, 2) Composition, 3) oxygen fugacity, and 4) crystallographic direction. All of these factors have been taken into account. The oxygen fugacity was assumed to be about 0.5 log atm below the iron/wustite buffer curve. A diffusion equation in spherical coordinates was used, and during growth, the number of spatial increments was increased at every step in time, with the size of the additional increment equal to the change in radius during that time period. During solidification, boundary conditions are:

$$\frac{\partial C}{\partial r}(0,t) = 0; \quad C(R,t) = C_{eq}$$

where C_{eq} is that given by the partition relation. The liquid composition is changed to account for the spherical shell of volume dv that has solidified during a period dt as well as any diffusion at the boundary (13):

$$dX^{liq}_{Mg} = -dvC_{eq}/V_{liq} - D(R,t)/V_{liq} \left(\frac{\partial C}{\partial r}\right)_{r=R} Sdt$$

where V_{liq} is the volume of liquid remaining and S is the surface area of the grain. The second term and, in general, diffusion during solidification are found to be negligible below about 1200°C. The concentration profile upon solidification is shown in Fig. 1.

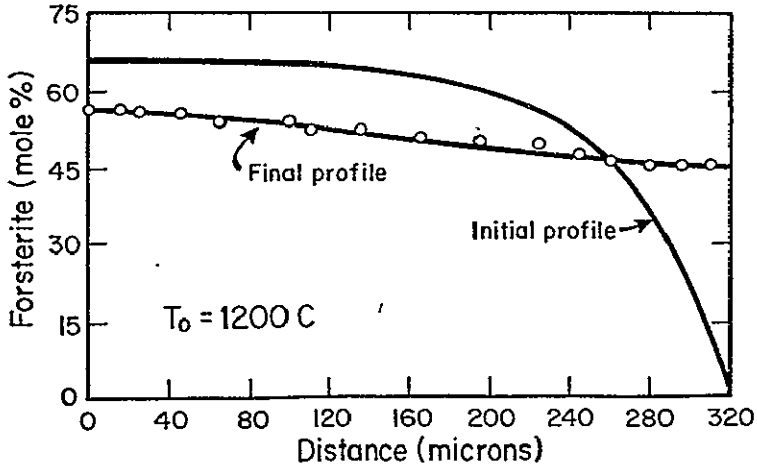

Fig. 1. The calculated "as-solidified profile" (initial profile) and the computer-fitted final profile for 5°C/day cooling rate in relation to the EMP-measured profile (open circles) of olivine in 24077, 68.

The generation of the initial

COOLING RATES

Taylor et al.

olivine profile can be summarized: the olivine is allowed to grow to a small extent, its composition dictated by the Roeder-Emslie equation (11). The growth is stopped, a new composition calculated for the liquid, and growth reinstated with a slightly less Fo composition to the olivine, again dictated by the Roeder-Emslie equation, reiteration, etc.

After solidification of the olivine is complete, the olivine is assumed to be an isolated system - i.e., no flux exists across the crystal-liquid interface. Hence, the outer boundary condition is changed to: $\frac{\partial C}{\partial r}(R,t) = 0$ The analysis proceeds as in the previous modeling (7), and cooling is continued until the Fo profile no longer changes significantly with time. It was found that cooling from 1200°C, of a melt with 18.5% FeO and 6.0% MgO, at a linear rate of 5°C/day results in a Fo profile which precisely matches the measured profile in the c crystallographic direction (Fig. 1).

The errors which could affect the accuracy of the predicted cooling rate are primarily associated with the diffusion coefficient. The diffusion coefficient is fastest in the c direction, so any deviation from this direction in the measured sample would tend to lower the predicted cooling rate. If convection in the liquid is not sufficient for a complete mixing, growth may be diffusion-controlled, resulting in a change in the initial profile and possibly more diffusion during solidification.

ZR COOLING SPEEDOMETER - Taylor et al.(6) determined the kinetics of the re-equilibration of the partitioning of Zr between coexisting ilmenite and ulvöspinel. As long as the criteria for the application of this partitioning method are met, it can be used to estimate the cooling rates of certain lunar rocks.

The Luna 24 sub-ophitic basalts contain only sparse assemblages of coexisting ilmenite and ulvöspinel. In most cases, the ilmenite is <15 μm wide such that it does not react as an "infinite" volume with respect to the large (e.g. 100 μm) ulvöspinel. The absolute amounts of Zr in both phases are low (usually <0.20% in ilmenite) such that the Zr compositions as determined by EMP have large precision errors associated with them. The Zr partitioning between ilmenite and ulvöspinel for 24077,48 is 1.64 with a 1σ of 0.23. Using the kinetic model of Taylor et al.(6), this results in a characteristic temperature of 887°C. In turn, this temperature indicates a linear cooling rate of 2.2°C/day. However, the lack of precision in the Zr determinations translates into an uncertainty in the cooling rate estimate of at least 3-5 times.

CONCLUSION - Using both the Fe-Mg diffusion in olivine and the Zr partitioning in ilmenite/ulvöspinel, the cooling rates of Luna 24 sub-ophitic basalts are estimated to be on the order of 2-5°C/day.

REFERENCES - (1) Lofgren et al., 1974, PLSC 5th; (2) Walker et al., 1976, GSA Bull.87; (3) Bianco & Taylor, 1977, PLSC 8th; (4) Donaldson, 1976, Contr. Min. Pet. 57; (5) Lofgren et al., 1975, PLSC 6th; (6) Taylor et al., 1975; PLSC 6th; (7) Taylor et al., 1977, PLSC 8th; (8) Coish & Taylor, 1977, this volume; (9) Ryder et al., 1977, Moon; (10) Vaniman & Papike, 1977, Geophys. Res. Lett; (11) Roeder & Emslie, 1970, Contr. Min. Pet. 29; (12) Buening & Buseck,1973, J.G.R. 78; (13) Brody & Fleming, 1966, Trans. AIME 236.

LUNA 24 FERROBASALT: PETROLOGY AND COMPARISONS WITH OTHER MARE BASALT TYPES; D. T. Vaniman and J. J. Papike, Dept. of Earth and Space Sciences, State University of New York, Stony Brook, N. Y. 11794

INTRODUCTION

Fragments of mare ferrobasalt within the LUNA 24 drill core are low in TiO_2 ($\sim$ 1.0 wt.%) and Fe-rich [Mg/(Mg+Fe) = Mg' = 0.3-0.4]. LUNA 24 mare rocks and very low Ti (VLT) mare basalt at Apollo 17* form a distinctive mare type. In this report we summarize modal and microprobe data for LUNA 24 basalt and brown glasses of similar composition, and make comparisons to other members of the total mare basalt suite. This is part of a consortium effort by A. E. Bence, J. Friel, J. Goldstein, T. L. Grove, S. Haggerty, J. Head, J. J. Papike, E. Roedder, D. T. Vaniman, and P. Weiblen united under the acronym of FOCUS (Friends of Crisium Unmanned Sampling).

PETROGRAPHY

We have analyzed ferrobasalt fragments at depth intervals of 77, 109, 174 and 210 cm in the LUNA 24 drill core, and ferrobasalt glasses at depths of 109 and 182 cm. Ferrogabbros (grain size $\gtrsim$ 0.4 mm) also occur in the drill core; this rock type is equivalent to the ferrobasalt [1]. A few (< 10%) of the ferrobasalt fragments have been recrystallized, with annealed grain boundaries but non-poikilitic texture. Mineral zoning trends are prominent in most ferrobasalts, but the recrystallized ferrobasalts have re-equilibrated with fixed mineral compositions (Fig. 1b, 2b). The drill core also contains brown ferrobasalt glasses. Some of these glasses have a breccia texture of glass fragments within a glass matrix, and in some fragments patchy areas of micropoikilitic texture occur. Both the recrystallized ferrobasalt and the brown ferrobasalt glasses are impact-modified rock types, but in bulk composition they are similar to the unaffected ferrobasalt (Table 1).

MINERALOGY OF CRYSTALLINE FERROBASALTS

Pyroxene. Pyroxene grains in the ferrobasalt fragments are zoned from initial Ca-rich ($Wo_{37}En_{41}Fs_{22}$) or Ca-poor compositions ($Wo_{12}En_{52}Fs_{36}$) through a point of low Ca content ($Wo_{25}En_{25}Fs_{50}$) and then either rise in Ca content to $Wo_{35}En_{5}Fs_{60}$, or zone directly to a final ferropyroxene composition of $Wo_{20}En_{5}Fs_{75}$ (Fig. 1a). These zoning trends are compressed in the recrystallized ferrobasalts, which have pyroxenes that span the pyroxene solvus at an Mg/(Fe+Mg) ratio of $\sim$ 0.35 (Fig. 1b).

Ti/Al zonation is prominent in the unrecrystallized ferrobasalts but restricted in the recrystallized ferrobasalts (Fig. 2a,b). Zoned pyroxenes are initially low in Ti:Al ratio ($\sim$ 1:10) and attain higher Ti:Al ratios with subsequent Fe enrichment. Al content is highest (Al_2O_3 = 3-4%) in the Ca-rich pyroxenes. The Ti:Al zonation trend is similar to that of the Apollo 17 VLT basalt [8].

Olivine. Olivine is abundant ($\sim$ 10%) in the LUNA 24 ferrobasalts and it is zoned from Fo_{58} to Fo_5 in most ferrobasalt fragments. However, recrystallized ferrobasalts have a restricted olivine composition of Fo_{25} (Fig. 1). Using the most magnesian olivine (Fo_{58}) and the Mg-Fe K_D of 0.33 [ref. 2] determined for low-Ti basalts, the calculated Mg/(Mg+Fe) ratio of coexisting liquid is 0.31. This is close to the bulk compositions of LUNA 24 basalts in

*Mg' = 0.5-0.6; TiO_2 $\sim$ 0.5%: [6,7,8].

LUNA 24 FERROBASALT

Vaniman, D. T. et al

Table 1. Both olivine and pyroxene are intergrown with euhedral feldspar laths, indicating simultaneous growth of olivine, pyroxene and feldspar. We note that ferrobasalt olivine zonation is continuous from Fo_{58} to Fo_5 (Fig. 1a). Papike et al. (1976) report that olivine of Fo_{70}-Fo_{90} is rare in mare basalts; the lack of olivine in this compositional range is presumably due to reaction with basalt liquid to form pyroxene. Apparently this reaction did not take place in the quickly cooled, Fe-rich LUNA 24 basalts.

Feldspars. As with pyroxene and olivine, feldspars of unrecrystallized ferrobasalt preserve a zonation (Ab_3An_{97} to $Ab_{11}An_{88}Or_1$) that is restricted in the recrystallized basalts ($\sim Ab_7An_{93}$). The range of feldspar composition in the LUNA 24 ferrobasalt is comparable to the feldspar range in Apollo 12 and Apollo 15 low-Ti basalts [3]. This range is broader and more Na-rich than in the Apollo 17 VLT basalt (Ab_3An_{97} to Ab_7An_{93}).

Opaque minerals and silica. Zonation trends in LUNA 24 spinels are similar to the spinel trends in the Apollo 17 VLT basalt [8], beginning with chromian spinel and zoning toward ulvöspinel with progressive crystallization. Ulvöspinel co-precipitates with late-stage ilmenite. In the recrystallized ferrobasalts, subhedral crystals of ulvöspinel occur with ilmenite. Silica is a minor phase in most ferrobasalts, appearing as intergrain crystals. Free silica does not occur in the recrystallized basalt fragments; it is apparently lost by reaction with olivine in the recrystallization process.

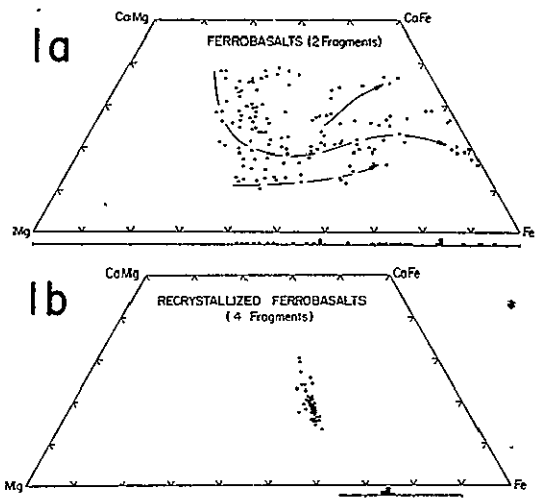

LUNA 24 FERROBASALT AND THE MARE BASALT SUITE

On the basis of mineralogy and modal composition, the LUNA 24 ferrobasalt is most similar to Apollo 17 VLT and feldspathic mare basalts. LUNA 24 ferrobasalt and Apollo 17 VLT basalt are similar in spinel composition and in their Ti-poor pyroxene zonation trends. Major differences between these two mare types occur in the extreme Fe enrichment of LUNA 24 olivine, in the Ca-rich compositions of some initial LUNA 24 pyroxenes, and in the more sodic LUNA 24 feldspars. These differences can be attributed to the more Ca, Al, Fe-rich and more alkaline nature of the LUNA 24 basalt compared to the Apollo 17 VLT basalt. The total CaO and Al_2O_3 content of LUNA 24 basalt is $\sim$ 27% by weight, compared to $\sim$ 14 to 24% in most other mare basalts except the feldspathic basalts (e.g., 14053 and 14063, $\sim$ 26%). This close approach to feldspathic basalt composition is reflected in the relatively high content of modal plagioclase in LUNA 24 ferrobasalt ($\sim$ 38%, Table 2), and in

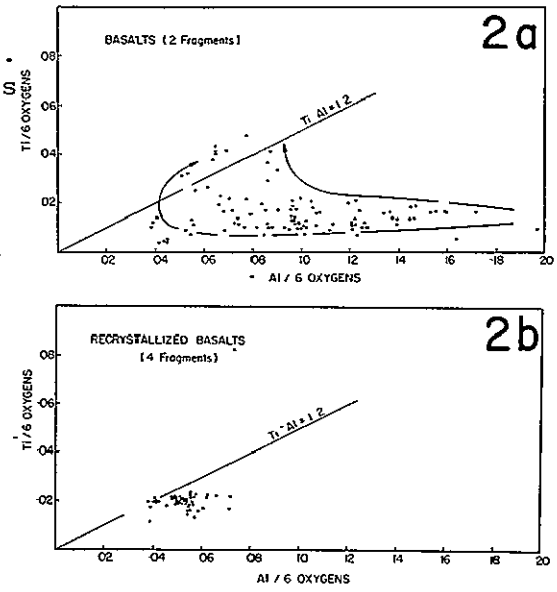

LUNA 24 FERROBASALT

Vaniman, D. T. et al.

a Wo-En-Fs pyroxene zonation trend that is similar to feldspathic basalts [3].

In feldspar content the LUNA 24 ferrobasalt is most similar to feldspathic basalt 14053 and feldspathic basalts of LUNA 16, but in its low opaque content the ferrobasalt is more similar to the Apollo 17 VLT basalt. The ferrobasalt and the ferrogabbro [1] have a higher content of modal olivine than other mare basalts, except for A-12 olivine basalt. A strong case can be made for olivine accumulation in the Apollo 12 olivine basalts [4], but crystal accumulation cannot account for the high concentration of the late-stage olivine in LUNA 24 ferrobasalt. (But note that the effects of recrystallization greatly alter the abundance of pyroxene, feldspar and olivine in the LUNA 24 basalts: Table 2.)

Figures 3-8 summarize the gross differences in major-element chemistry of mare basalt types. The ratio Mg/(Mg+Fe), or Mg', is plotted on the abscissa of each diagram as a fractionation index. On the basis of these plots, the oxides on the ordinate can be ranked by their ability to separate major mare basalt groups: Cr_2O_3 vs. Mg' (Fig. 3) is a poor discriminant of mare rock types. Characteristic values of Cr content do not distinguish the different mare basalts at any given Mg' value, though Cr varies directly with Mg'. Feldspathic basalt 14063 is notably low in Cr content, and the Apollo 15 emerald-green glass is low in Cr_2O_3, though green glass at the Apollo 14 site may have > 0.7% Cr_2O_3 [5]. CaO, Al_2O_3 and K_2O vs. Mg' (Figs. 4-6) are capable of discriminating LUNA 24 and Apollo 17 VLT basalts from other mare basalts. The Apollo 17, LUNA 24 and Apollo 14 feldspathic basalts are higher in CaO and Al_2O_3 content. The other low-Ti (A-12, A-15) and high-Ti (A-11, A-17) mare basalts plot as a single group in these diagrams. The plot of K_2O vs. Mg' (Fig. 6) shows LUNA 24-Apollo 17 VLT as a distinctive low-alkali group, beneath the low-Ti/high-Ti basalt series. The feldspathic mare basalts (Apollo 14 and LUNA 16) are even higher in K_2O content. The Apollo 11 high-K basalts stand apart with $\sim$ 0.3 wt.% K_2O. Na_2O and TiO_2 vs. Mg' (Figs. 7, 8) separate the very low Ti, low Ti, and high Ti basalt groups. The more Ti-rich basalt groups tend to be higher in Na content (Fig. 7). 14063 is an exceptionally Na-rich feldspathic basalt.

Plots of TiO_2 vs. other components give the greatest separation of different mare basalt groups. Figure 8 provides a sharp distinction between the LUNA 24-Apollo 17 VLT group, the low-Ti mare group, and the high-Ti mare group. However, there may well be mare basalts which form a continuum between these groups. The Apollo 15 low-Ti basalts tend to fall between the Apollo 12 low-Ti basalts and the LUNA 24-Apollo 17 VLT basalts. It is well known that the high-Ti and low-Ti trends tend to converge with increased fractionation, but the presence of a mare basalt that falls between these two trends (14063) is not as well known. The number of such basalts may well increase as small basalt fragments in the soils are examined more closely.

References

[1] *Bence, et al., 1977, GRL, in press;* [2] *Lipin, 1976, Lunar Sci. VII, p. 495-497;* [3] *Papike et al., 1976, Rev. Geo. & Sp. Phys., 14, p. 475-540;* [4] *Rhodes et al., 1977, Lunar Sci. VIII, p. 804-806;* [5] *Stolper, 1974, "Lunar Ultramafic Glasses", unpub. B. A. thesis, Harvard, 178 pp.* [6] *Taylor et al., 1977, GRL 4, 207-210;* [7] *Vaniman and Papike, 1977, Lunar Sci VIII, p. 952-954;* [8] *Vaniman and Papike, 1977, PLSC 8th, in press.*

LUNA 24 FERROBASALT

Vaniman, D. T. et al.

T 1 Chemical Compositions of Luna 24 Ferrobasalts and Recrystallized Ferrobasalts (obtained by Modal Recombination of Mineral Analyses) and Compositions of Luna 24 Brown Mare Glass.

	Ferrobasalts		Recrystallized ferrobasalts		Brown mare glasses	
	24109,52 frag. 18	24077,41 frag. 21	24109,51 frag. 11	24109,51 frag. 35	24182,25 frag. 1	24109,52 frag. 7
SiO_2	45.2	46.2	46.7	46.8	47.08	46.90
TiO_2	0.89	0.83	0.65	1.00	0.75	1.02
Al_2O_3	13.8	13.9	12.2	13.5	12.68	12.41
Cr_2O_3	0.19	0.30	0.23	0.29	0.28	0.28
FeO	20.5	17.5	21.7	20.4	19.65	20.62
MnO	0.27	0.30	0.34	0.23	0.27	0.24
MgO	6.35	7.77	7.09	6.71	6.51	6.66
CaO	12.7	13.2	11.1	10.8	13.03	12.24
Na_2O	0.24	0.20	0.29	0.35	0.25	0.14
K_2O	0.01	---	0.02	0.01	0.02	0.01
	100.2	100.2	100.3	101.0	100.52	100.54
$Mg/(Mg+Fe)$	0.36	0.44	0.37	0.37	0.37	0.37
CaO/Al_2O_3	0.92	0.95	0.91	0.87	1.03	0.99

T 2 Summary Modal Data* for the Mare Basalts

	Opaques	Pyroxene	Feldspar	Olivine
A-17 very high Ti	24.4	47.7	23.4	4.6
A-11 high K	20.6	57.5	21.7	0.1
A-17 low K	15.1	51.6	33.3	---
A-11 low K	14.6	50.9	32.2	2.3
A-12 ilmenite	9.3	61.1	25.9	3.6
A-12 pigeonite	9.1	68.4	21.1	1.4
A-12 olivine	7.1	53.5	19.2	20.2
L-16	7.1	51.5	41.2	0.1
A-15 olivine	5.5	63.3	24.1	7.0
A-15 pigeonite	3.7	62.5	33.8	---
14053	3.2	53.8	43.0	---
L-24 ferrobasalt	1.8	48.6	39.1	10.4
L-24 Recrystallized Ferrobasalt	1.4	60.2	34.2	4.2
A-17 "VLT"	1.0	61.7	31.9	5.4

* *Normalized to 100% for the four phases considered. Ordered from top to bottom in terms of decreasing modal content of opaques.*

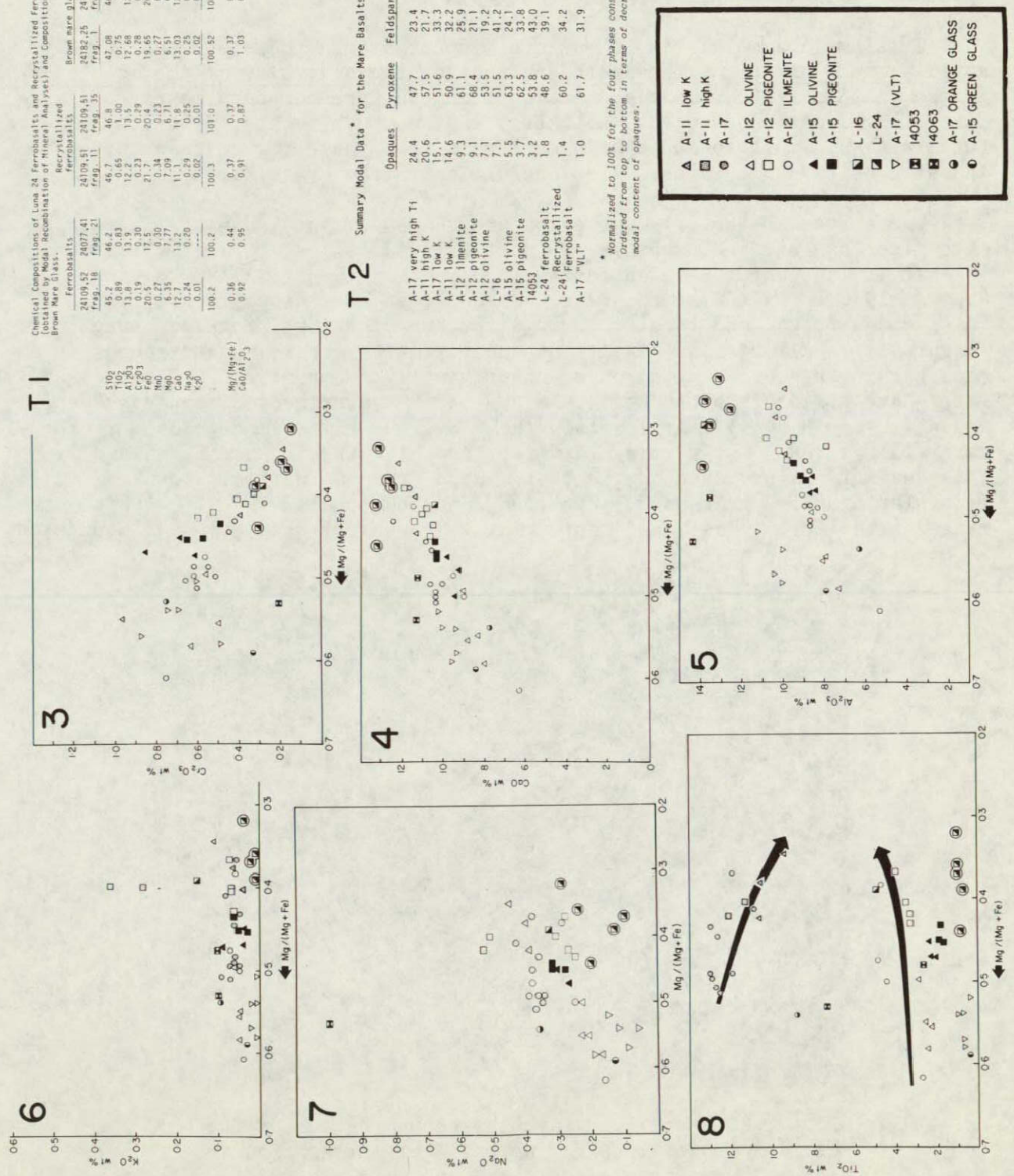

THE CRISIUM BASIN AND ADJACENT TERRA. Don E. Wilhelms, U.S. Geological Survey, Menlo Park, Calif.; and Farouk El-Baz, National Air and Space Museum, Smithsonian Institution, Wash., D.C.

Crisium is a multi-ringed basin of impact origin that has considerably modified much of the northeastern quadrant of the near side of the moon. The terrae in this region, as elsewhere on the moon, are composed mostly of basin rims, their continuous ejecta blankets, and secondary crater deposits. The Luna 24 sample must include basin materials from these terrae transported to the site as rays of Eratosthenian and/or Copernican craters.

The terrae in the Crisium region are shaped by the basin itself, six or more older basins, and probably two post-Crisium basins. Crisium is anomalous in that it is elongated in an east-west direction (Stuart-Alexander and Howard, 1970). On the north, west and south, its main topographic rim is massive and rugged and is divided into two sub-rings by irregular troughs (Figure 1). Salients and re-entrants nearly match across these troughs in a manner that suggests separation of an originally coherent rim. The two sub-rings have diameters of about 540 km and 680 km (averaged between east-west and north-south axes). At least on the west, the rim segment closer to the mare fill is lower, suggesting that the separation was caused by inward slump. This dual rim is breached on the east. Here, the basin rim is low and irregular, and its peaks and short arcs cannot be traced readily with the two rings of the north, west, and south rims. The eastern rim may have foundered

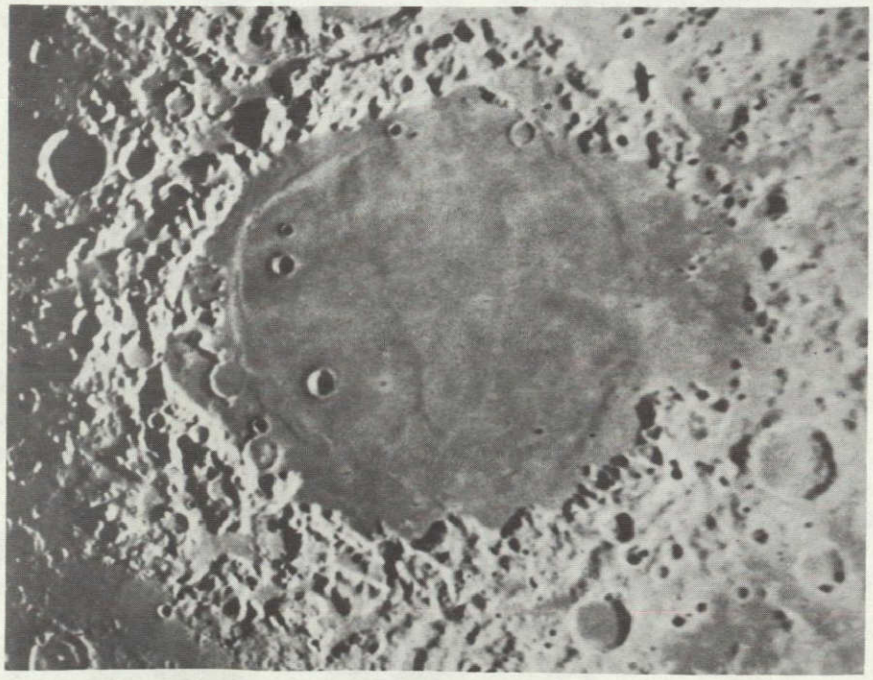

Figure 1. Rectified earth-based photograph of the Crisium basin illustrating east-west elongation and incomplete east rim (Hartmann and Kuiper, 1977).

CRISIUM BASIN AND ADJACENT TERRA

D. E. Wilhelms and F. El-Baz

(Wilhelms, 1973), may be poorly developed (because it lay under the oblique trajectory of the basin-forming bolide analogous to missle craters at White Sands, New Mexico; Moore, 1976), or may be a subsidiary crater produced by a twin impact. A shelf and protruding islands in the mare may represent an interior ring, and conspicuous arcs about 500 km north, west, and southeast of the basin center lie outside the topographic basin rim (Hartmann and Kuiper, 1962; Wilhelms and McCauley, 1971; Casella and Binder, 1972; Wilhelms, 1973; Olson and Wilhelms, 1974; DeHon and Waskom, 1976; Wilhelms and El-Baz, 1976, Wilhelms and others, 1977). The exterior arcs might also be the products of an oblique impact from the east.

Although well-developed in some sectors, the Crisium continuous ejecta and secondary craters are difficult to map because of poor or uneven photographic coverage. South and southeast of Mare Spumans and Mare Undarum, secondary crater chains are abundant and much of the exposed terra material probably is ejecta from these secondaries. Crisium ejecta may have pitted the floor of the Smythii basin, 1000 km to the southeast. This photogeologic interpretation is supported by x-ray fluorescence data, which indicate that Al/Si ratios in the southern floor of Smythii are similar to those west of Smythii, and lower than those of the terra east of it (Andre and others, 1977). East of Crisium, continuous ejecta extends at least 300 km to Mare Marginis, and continuous and secondary ejecta may form part of a thick mantling deposit of Nectarian age (El-Baz and Wilhelms, 1975; Wilhelms and El-Baz, 1976) that extends at least 900 km farther east. Continuous ejecta and secondary craters also occur north of the basin, but their extent beyond about 500 km from the rim is uncertain because of overlap with similar basin ejecta and secondary craters of Humboldtianum. The extent of ejecta west of Crisium is uncertain because of burial by younger materials.

Older basins whose interior materials, rings, and ejecta constitute the substrate for Crisium include Smythii, Marginis, Humboldtianum, Fecunditatis, probably Nectaris, presumably the poorly defined Tranquillitatis to the west (Figure 2), and possibly other basins whose rings have been severely modified. The western rim of the Marginis basin lies only 150 km east of Crisium (Wilhelms and El-Baz, 1976) and may have influenced its shape. The northeast rim of the Fecunditatis basin, probably covered by some Nectaris material, underlies the southwest flank of Crisium. Humboldtianum, centered 1400 km north-northeast of Crisium, has a figure-8 ring pattern that suggests a twin impact (Lucchitta, 1977). Its age relative to Crisium is not completely clear, but it seems to be older based on superposition relations with the apparently post-Humboldtianum, pre-Crisium crater Zeno. This appears to be supported by crater densities; 30 Nectarian-age craters > 20 km in diameter per 10^6 km^2 are superimposed on identified Crisium materials and 33 craters on Humboldtianum materials. The area of these craters (within the rim crest) covers 6.6% of the area of Crisium versus 14% for Humboldtianum.

CRISIUM BASIN AND ADJACENT TERRA

D. E. Wilhelms and F. El-Baz

Figure 2. A view of the moon centered at the Crisium region. All features that are mentioned in the text are labeled (AS11-44-6667).

CRISIUM BASIN AND ADJACENT TERRA

D. E. Wilhelms and F. El-Baz

Post-Crisium basins that have influenced the region are Imbrium and possibly Serenitatis. Imbrium secondary craters and their ejecta cover much of the southwestern (Olson and Wilhelms, 1974) and western flanks of Crisium and are scattered elsewhere. Relations with Serenitatis are less clear. Serenitatis appears very old because of deep burial by mare material and cover by Imbrium ejecta, but tenuous superposition relations between secondaries of Crisium and Serenitatis suggest that the latter is the younger. Some of the large basin secondaries superposed on the rim of Crisium could be from Serenitatis, and thus some Serenitatis ejecta could be present over much of the Crisium basin.

References

Andre, C. G. and others, 1977, Chemical character of the partly flooded Smythii basin based on Al/Si orbital x-ray data: Proc. Lunar Sci. Conf. 8th, in press.

Casella, C. J. and Binder, A. B., 1972, Geologic map of the Cleomedes quadrangle of the Moon: U.S. Geol. Survey Map I-707.

DeHon, R. A., and Waskom, J. D., 1976, Geologic structure of the eastern mare basins: Proc. Lunar Sci. Conf. 7th, p. 2729-2746.

El-Baz, Farouk and Wilhelms, D. E., 1975, Photogeological, geophysical, and geochemical data on the east side of the Moon: Proc. Lunar Sci. Conf. 6th, p. 2721-2738.

Hartmann, W. K., and Kuiper, G. P., 1962, Concentric structures surrounding lunar basins: Arizona Univ. Lunar and Planetary Lab. Commun., v. 1, no. 12, p. 51-66.

Lucchitta, B. K., 1977, Geologic map of the north side of the Moon: U.S. Geol. Survey Map I-1062 (in press).

Moore, H. J., 1976, Missle impact craters (White Sands, New Mexico) and applications to lunar research: U.S. Geol. Survey Prof. Pap. 812-B,47p.

Olson, A. B., and Wilhelms, D. E., 1974, Geologic map of the Mare Undarum quadrangle of the Moon: U.S. Geol. Survey Map I-837.

Stuart-Alexander, D. E., and Howard, K. A., 1970, Lunar maria and circular basins--A review: Icarus, v. 12, no. 3, p. 440-456.

Wilhelms, D. E., 1973, Geologic map of the northern Crisium region: Apollo 17 Prelim. Sci. Rept., NASA SP-330, p. 29-29 to 29-34.

Wilhelms, D. E., and El-Baz, Farouk, 1976, Geologic map of the East Side of the Moon: U.S. Geol. Survey Map I-948.

Wilhelms, D. E., and McCauley, J. F., 1971, Geologic map of the near side of the Moon: U.S. Geol. Survey Map I-703.

Wilhelms, D. E., Hodges, C. A., and Pike, R. J., 1977, Nested-crater model of lunar ringed basins: Impacts and Explosion Cratering, Pergamon Press, (in press).

CRATER MORPHOLOGY AND SUBSURFACE LAYERING IN MARE CRISIUM

R.W. Wolfe, National Air and Space Museum, Washington, DC 20560

There is evidence from earth-based spectral reflectance studies[1] and orbital X-ray fluorescence data[2] that the Eratosthenian crater Picard may have excavated basaltic material that is compositionally different from the basalt nearer the surface of Mare Crisium. The depth of Picard beneath the general level of the mare surface is 1700 meters. The crater is extensively modified by slumping and the transient cavity was considerably deeper. Therefore, Picard must have excavated some material from deeper than 1700 meters beneath the surface of Mare Crisium.

Data from the Apollo Lunar Sounder Experiment (ALSE) indicate a subsurface radar reflector at a mean depth of 1400 meters below the Mare Crisium surface. This depth is a function of the assumed dielectric constant for the subsurface materials. The reflector is interpreted as a basin-wide interface[3], presumably between mare fill and the basin floor or between different mare basalt units. An isopach map of mare fill in southern Mare Crisium shows thicknesses greater than 1500 meters near the Eratosthenian crater Peirce[4], which lies on the ALSE profile. This may indicate that the subsurface radar reflector is an interface between different basalt layers, rather than the mare fill-basin floor contact.

It has been shown that the morphology of experimental impact craters in layered media is related to the nature of the substrate and to its depth.[5] Where the crater diameter is less than 6.5 times the thickness of the surface layer, normal (bowl-shaped) craters are formed; for diameters 6.5 to 11 times the thickness, flat-bottomed craters are formed; and craters with diameters exceeding 11 times the thickness of the surface layer have a concentric geometry. This relationship between crater morphology, thickness of the surface layer (depth of the substrate), and crater diameter has been applied to the study of natural craters. Thicknesses of regolith in the lunar maria have been determined from the morphologies of fresh impact craters less than a few hundred meters in diameter.[5] The influence of a substrate has also been cited as responsible in part for the break in slope of the depth-diameter curve for lunar craters.[6]

Let us assume that this same relationship will apply for large impact craters (greater than 5 kilometers diameter) and that the morphology of the craters will be influenced by a substrate that may not be too different from the surface layer (such as a basalt of somewhat different composition). The study of post-mare impact craters, then, may provide evidence of subsurface layering in Mare Crisium independent from the ALSE interpretation.

LAYERING IN MARE CRISIUM

R. W. Wolfe

There are only a few post-mare craters greater than 5 kilometers diameter in Mare Crisium. They are:

NAME	DIAMETER (km)	MORPHOLOGY
Fahrenheit	6.4	normal
Swift	10.5	flat-bottomed
Cleomedes F	12.5	flat-bottomed
Greaves	13.4-15.0	flat-bottomed
Peirce	19.0	concentric
Picard	23.5	concentric

Craters with a normal geometry define the minimum depth to the substrate and those with a concentric geometry, the maximum depth. Flat-bottomed craters define a range between which the interface lies (Figure 1). If a single subsurface layer at a constant depth is assumed for Mare Crisium, the relationship between diameter and morphology of these craters places that depth between 1200 and 1600 meters. This range is consistent with the ALSE interpretations.[3]

What is the nature of this subsurface layer? None of the post-mare craters in Mare Crisium has excavated any discernable terra material[2], i.e., basin floor. For example, the ejecta of Picard has a high Ti[1] and Mg[2] content and is, therefore, basaltic. Consequently, it appears that the subsurface layer in Mare Crisium, which influenced the geometry of impact craters and was detected by ALSE, is an older mare basalt that is probably compositionally different from the near-surface material.

References

1. Pieters, C., McCord, T. B., and Adams, J. B., 1976, Geophys. Res. Let., 3, p. 697-700.
2. Andre, C. G., Wolfe, R. W., Adler, I., 1977, L.S.I. Conf. on Luna 24.
3. May, T. W., Peeples, W. J., Maxwell, T., Sill, W. R., Ward, S. H., Phillips, R. J., Jordan, R. L., and Abbott, E. A., 1976, Lunar Sci. VII, p. 540-542.
4. DeHon, R. A. and Waskom, J. D., 1976, Proc. Lunar Sci. Conf. 7th, p. 2729-2746.
5. Quaide, W. L. and Oberbeck, V. R., 1968, J. Geophys. Res., 73, p. 5247-5270.
6. Head, J. W., 1976, Proc. Lunar Sci. Conf. 7th, p. 2913-2929.

LAYERING IN MARE CRISIUM

R. W. Wolfe

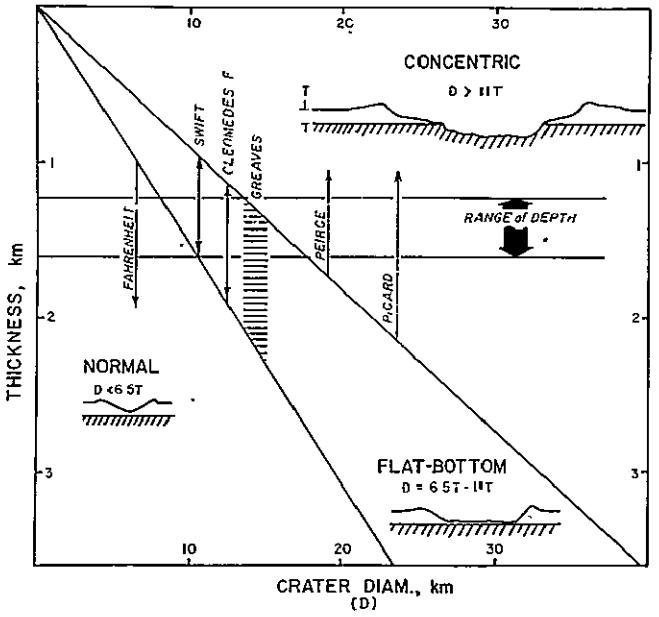

Figure 1. Thickness of the surface layer as a function of crater diameter and morphology. Profiles are from reference 6.

TOPIC INDEX*

Topic I

MARE CRISIUM AND THE LUNA 24 LANDING SITE: REGIONAL GEOLOGY, GEOCHEMISTRY, AND GEOPHYSICS

Topic II

PETROLOGY, MINERAL CHEMISTRY, AND COOLING HISTORIES OF THE LITHIC FRAGMENTS IN LUNA 24 SAMPLES

*Pagination refers to first page of paper in which author is cited

Topic III

CHEMISTRY, ISOTOPIC STUDIES AND GEOCHRONOLOGY OF LUNA 24 SAMPLES

Topic IV

REGOLITH STUDIES OF THE LUNA 24 SOIL SAMPLES

SUBJECT INDEX*

*Pagination refers to first page of paper in which subject is cited

AUTHOR INDEX*

*Pagination refers to first page of paper in which subject is cited

NOTES